

New Silepins – Structure and Reactivity

Jinyu Liu

Vollständiger Abdruck der von der TUM School of Natural Sciences der Technischen Universität München zur Erlangung einer
Doktorin der Naturwissenschaften (Dr. rer. nat.)
genehmigten Dissertation.

Vorsitz: Prof. Dr. Tom Nilges

Prüfende der Dissertation:

1. Prof. Dr. Dr. h.c. Bernhard Rieger
2. Prof. Dr. Shigeyoshi Inoue

Die Dissertation wurde am 14.10.2024 bei der Technischen Universität München eingereicht und durch die TUM School of Natural Sciences am 27.11.2024 angenommen.

' You may be disappointed if you fail,

but you are doomed if you don't try. '

Beverly Sills

Die vorliegende Arbeit wurde von Feb 2020 bis Okt 2024 am WACKER Lehrstuhl für Makromolekulare Chemie der Technische Universität München unter Betreuung von Prof. Dr. Dr. h.c. Bernhard Rieger angefertigt.

Acknowledgments

Mein besonderer Dank gilt Herrn Prof. Bernhard Rieger, meinem Doktorvater, für die Aufnahme in seinen Lehrstuhl, sowohl für die Masterabschlussarbeit als auch für die anschließende Promotion. Er brachte mir somit das besondere Vertrauen entgegen, ein anspruchsvolles Projekt in der anorganischen Grundlagenforschung durchzuführen. Mir wurden viele Freiheiten geboten, und dennoch wurde ich gestützt durch vielfältige Diskussionen und Anregungen, welche sowohl meine fachliche als auch persönliche Entwicklung signifikant gefördert haben.

Darüber hinaus möchte ich Herr Prof. Inoue, mein Mentor, für seinen wertvollen Input in allen fachlichen Bereichen meines Projekts und die daraus entstandenen Publikationen danken. Dadurch konnte ich mein Wissen und Verständnis der anorganischen Chemie erweitern.

Großen Dank möchte ich an Carsten und Frau Bauer aussprechen, die uns Doktoranden stets geholfen haben und immer hinter uns standen. Sie kümmerten sich hervorragend um die Organisation des gesamten Lehrstuhls, was nicht selbstverständlich ist. Diesbezüglich möchte ich auch Katja danken, die mir immer bei Beschaffung der benötigten Labormaterialien zur Seite gestanden ist.

Mein Dank gilt allen aktuellen und ehemaligen Doktoranden des AK Rieger, die mich durch ihre fundierten Kenntnisse der Polymerchemie und Analytik unterstützt haben. Auch alle meine Studenten, die ich im Synthesepraktikum, Forschungspraktika und Bachelorarbeit betreut habe, haben mir wertvolle Erfahrungen für die Zukunft beschert.

In den Jahren im „Si-Institut“ sorgten meine - mittlerweile ehemaligen - Laborkollegen, Andreas Saurwein, Matthias Nobis, Teresa Eisner, Ramona Baiertl und Florian Tschernuth immer für eine ausgesprochen gute Arbeitsatmosphäre, was ich sehr geschätzt habe. Dabei möchte ich insbesondere Andi danken, der mit mir bereits im Bachelorstudium diversen Praktika absolviert hat und mit dem ich viele gute fachliche als auch persönliche Gespräche führen konnte.

Des Weiteren möchte ich meine Wertschätzung und meinen Dank gegenüber dem den Mitarbeitern des AK Inoue ausdrücken, welche mich als eines ihrer Mitglied angesehen haben und mir während zahllosen offiziellen aber auch privaten Anlässen viele großartige Erinnerungen beschert haben. Dabei möchte ich vor allem Fiona, Moritz, Yueer, Andi H. und Lukas erwähnen, mit denen ich auch gerne außerhalb der Uni verabredet habe. Sie sorgten immer für eine heitere Stimmung - auch während den manchmal etwas ermüdenden Laboralltag.

Zuletzt bedanke ich mich bei meinen Eltern für die anhaltende Unterstützung während meines Studiums und bei meiner Schwester, die immer für mich da ist. Nicht zu vergessen ist natürlich Martin, der seit dem Masterstudium an meiner Seite ist, mich motiviert und mich in allen Bereichen meines Lebens unterstützt. Ich danke dir für alles, was du für mich getan hast!

Publication List

Publications included in this Thesis

J. Y. Liu, T. Eisner, S. Inoue, B. Rieger

European Journal of Inorganic Chemistry – **2024**, 27, e202300568

Titel: “Isolation of a New Silepin with an Imine Ligand Based on Cyclic Alkyl Amino Carbene”

DOI: doi.org/10.1002/ejic.202300568

J. Y. Liu, S. Inoue, B. Rieger

European Journal of Inorganic Chemistry – **2024**, 27, e202400045

Titel: “Isolation and Reactivity of Silepins with a Sterically Demanding Silyl Ligand”

DOI: doi.org/10.1002/ejic.202400045

Publications beyond the Scope of this Work

M. E. Doleschal, A. Kostenko, J. Y. Liu, S. Inoue

Chemical Communication – **2024**

Titel: “Silicon-Aryl Cooperative Activation of Ammonia”

DOI: 10.1039/D4CC04617J

M. E. Doleschal, A. Kostenko, J. Y. Liu, S. Inoue

Nature Chemistry – **2024**

Titel: “Isolation of an NHC-stabilized heavier nitrile and its conversion into an isonitrile analogue”

DOI: 10.1038/s41557-024-01618-6

T. M. Lenz, I. Chiorescu, F. E. Napoli, J. Y. Liu, B. Rieger

Angewandte Chemie International Edition – **2024**, e202406848

Titel: “Aluminum Alkyl Induced Isomerization of Group IV meso Metallocene Complexes”

DOI: doi.org/10.1002/anie.202406848

M. M. Kleybolte, L. Zainer, J. Y. Liu, P. N. Stockmann, M. Winnacker,

Macromolecular Rapid Communications – **2022**, 43, e2200185

Titel: “(+)-Limonene-Lactam: Synthesis of a Sustainable Monomer for Ring-Opening Polymerization to Novel, Biobased Polyamides”

DOI: doi.org/10.1002/marc.202200185

Abstract

The pursuit of sustainable and environmentally friendly processes in the chemical industry brought forward the concept of main group-mediated catalysis. Due to the low abundance and thus inherent high cost of transition metals, one of the primary objectives of interest is the replacement of the ubiquitous TM-containing catalysts in various industrial applications by greener alternatives based on main group elements. In this regard, the element silicon represents a remarkable candidate owing to its rich resources and general low toxicity. Literature reports have demonstrated a particular reminiscence of isolable, low-valent silicon compounds to transition metal complexes. Amongst them, some acyclic silylenes undergo a unique intramolecular insertion, giving silacycloheptatriene (“silepin”) moieties showing a reversibility between Si(II) and Si(IV). These findings open up new fields of research regarding potential metal-free catalysis, which illustrates the major focus of this doctoral thesis: Investigations of novel silepin species based on acyclic silylenes.

The first step is to synthesize new silepin species due to limited reports in the literature. For this purpose, an imine ligand based on *CycAAC* is first synthesized and subsequently converted with potassium hypersilanide (KSiTMS₃) to simultaneously introduce the silyl ligand and reduce the precursor to the respective silylene. The isolated product is observed to undergo intramolecular insertion, leading to a silepin structure, revealed with X-ray crystallography. The “*CycAAC* silepin” is able to oxidatively cleave a series of small molecules. Especially in the presence of ethylene, a migratory insertion is determined. DFT calculations showed enhanced stability compared to literature known silepins with a comparably larger HOMO-LUMO gap, demonstrating the importance of substituent effect in such species.

Furthermore, the stabilizing silyl ligand is varied in the next step from the previously applied hypersilyl (–SiTMS₃) to bis(trimethylsilyl)triphenylsilyl silyl (–SiTMS₂SiPh₃) group. Combined with either the *DippNHC*- or *CycAAC*-based imine ligand, two new silepins could be synthesized. Both silepin structures show an unusual intramolecular sp²C-H bond insertion at elevated temperatures supported

by SC-XRD analysis. Their electronic and steric properties were compared relatively to structurally similar compounds, which shed light on the impact of simple ligand modifications in silepins based on acyclic silylenes.

Zusammenfassung

Das Streben nach nachhaltigen und umweltfreundlichen Prozessen in der chemischen Industrie hat das innovative Konzept der „Hauptgruppenelement-basierten Katalyse“ hervorgebracht. Begründet durch das geringe natürliche Vorkommen und der damit verbundenen hohen Kosten von Übergangsmetallen (ÜM), ist dabei das primäre Ziel, ÜM-haltige Katalysatoren für verschiedene industrielle Anwendungen durch umweltfreundlichere, auf Hauptgruppenelementen basierende Alternativen zu ersetzen.

In dieser Hinsicht ist das Element Silicium ein vielversprechender Kandidat, da enorme Mengen verfügbar sind und das Element gesundheitlich unbedenklich ist. Bisherige Forschung hat gezeigt, dass isolierbare, niedervalente Siliciumverbindungen, wie beispielsweise Disilene und Silylene, eine besondere Ähnlichkeit mit Übergangsmetallkomplexen aufweisen. Einige azyklische Silylene können zusätzlich eine einzigartige, intramolekulare Insertion durchführen, wobei sich ein Silacycloheptatrien („Silepin“) als Produkt bildet. Bemerkenswert ist, dass zwischen den jeweiligen Si(II) und Si(IV) Spezies ein reversibles chemisches Gleichgewicht herrscht. Diese Erkenntnisse eröffnen neue Forschungsfelder für eine potenziell metallfreie Katalyse, was den Schwerpunkt dieser Doktorarbeit darstellt: Die Untersuchung neuartiger Silepinspezies auf der Basis azyklischer Silylene.

Der primäre Schritt besteht darin, neue Silepinspezies zu synthetisieren, da es nur wenige Beispiele in der Literatur gibt. Zu diesem Zweck wird zunächst ein Iminligand auf ^{Cyc}AAc-Basis synthetisiert und anschließend mit Kaliumhypersilanid (KSiTMS₃) umgesetzt, um gleichzeitig den Silylliganden einzuführen und das Edukt zum entsprechenden azyklischen Silylen zu reduzieren. Bei dem isolierten Produkt wird eine intramolekulare Insertion beobachtet, die zur Bildung eines Silepins führt. Das sogenannte „^{Cyc}AAc-Silepin“ ist in der Lage, eine Reihe von kleinen Molekülen oxidativ zu spalten. Hervorzuheben ist, dass in Gegenwart von Ethylen eine Insertion des aktivierten C2-Fragments festgestellt wurde. DFT-Berechnungen zeigen eine vergleichsweise große HOMO-LUMO-Lücke und damit eine erhöhte

Stabilität im Vergleich zu literaturbekannten Silepinen. Dies unterstreicht die Bedeutung des Substituenteneffekts in solchen Spezies.

Darüber hinaus wird der stabilisierende Silylligand von der zuvor verwendeten Hypersilyl- ($-\text{SiTMS}_3$) zur Bis(trimethylsilyl)triphenylsilyl-silylgruppe ($-\text{SiTMS}_2\text{SiPh}_3$) modifiziert. In Kombination mit dem DippNHC - oder CycAAC -basierten Iminliganden konnten zwei neue Silepine synthetisiert werden. Beide Silepinstrukturen zeigen eine ungewöhnliche intramolekulare $\text{sp}^2\text{C-H}$ -Bindungsinsertion bei erhöhten Temperaturen, was durch SC-XRD Analysen bestätigt wird. Ihre elektronischen und sterischen Eigenschaften werden mit strukturell ähnlichen Verbindungen verglichen, und die Auswirkungen einfacher Ligandenmodifikationen in Silepinen auf der Basis azyklischer Silylene näher betrachtet.

List of Abbreviations

Ad	adamantyl
Bu	butyl
cAAC	cyclic alkyl amino carbene
Cp*	pentamethylcyclopentadienyl
Cy	cyclohexyl
Dipp	2,6-diisopropyl phenyl
E	Element
e.g.	latin exempli gratia: "for example"
Et	Ethyl
<i>et al.</i>	latin et alii: "and others"
HOMO	highest occupied molecular orbital
hypersilyl	tris(trimethylsilyl)silyl
<i>i</i>	<i>iso</i>
L	ligand
LUMO	lowest unoccupied molecular orbital
Me	methyl
Mes	2,4,6-trimethylphenyl
MG-Si	metallurgical grade silicon
NacNac	β -diketiminato
NHC	N-heterocyclic carbene
NHI	N-heterocyclic imine
Nu ⁻	nucleophile
<i>o</i>	ortho
PGE	platinum group metal
Pr	propyl
r.t.	room temperature
SC-XRD	single crystal X-ray diffractometry
SG-Si	solar grade silicon
silepin	sila-2,4,6-cycloheptatriene
<i>t</i>	<i>tert</i>
Tb	2,4,6-tris[bis(trimethylsilyl)methyl]phenyl
Tip	2,4,6-triisopropyl phenyl
TM	transition metal
TMS	trimethyl silyl
$\Delta E_{s,t}$	singlet-triplet energy separation

Table of Contents

1.	Introduction	13
1.1	Heavier Main Group Elements as Transition Metals	13
1.1.1	Main Group Multiple Bonds: The Beginning	14
1.1.2	Ge/Sn Multiple Bonds: Synthesis and Application as Molecular Catalyst.....	17
1.1.3	Tetrylenes: An Overview	20
1.1.4	Ge(II)- and Sn(II)-containing compounds as Molecular Catalysts: A Highlight.....	22
1.2	The Element Silicon	25
1.2.1	Si-Si Multiple Bond: Synthesis and Reactivity	28
1.2.2	Isolation and Reactivity of Silylenes	32
1.2.3	“Silepins” – Novel Structures of Acyclic Silylenes	39
2.	Scope of This Work	43
3.	Isolation of a New Silepin with an Imine Ligand Based on Cyclic Alkyl Amino Carbene	45
4.	Isolation and Reactivity of Silepins with a Sterically Demanding Silyl Ligand.....	52
5.	Summary and Outlook.....	60
6.	Appendix	64
6.1	Supporting Information for Chapter 3	65
6.2	Supporting Information for Chapter 4.....	109
6.3	Licenses.....	150
7.	References	161

1. Introduction

To date, the synthesis of a vast variety of organic and industrial-relevant compounds via catalysis involving transition metals is well-established and constantly evolving. It is estimated that around 90% of the chemicals are obtained from catalytic processes of some kind.^[1] Besides the significance in academia, transition metal (TM) catalysis has proven its value in the chemical industry: As one of the 12 green chemistry principles, the application of catalysis significantly reduces waste streams, cycle times, and volume requirements, thus simplifying the synthetic processes in chemical manufacturing.^[2] Pivotal reaction processes thereby include metathesis, cross-coupling, asymmetric hydrogenation, and oxidation.^[3] A complete catalytic cycle consists of oxidative addition, transmetallation, and subsequent reductive elimination alongside the backformation of the catalyst. Due to the additional *d*-orbitals of *d*-block elements and thus coordinative flexibility, transition metals possess variable oxidative states and are therefore able to engage in addition and elimination reactions of small molecules. Some of the most applied TM catalysts are based on platinum-group metals (PGE) and include platinum, palladium, rhodium, ruthenium, iridium, and osmium.^[4] Besides their function as catalyst centers, PGEs found widespread applications in various fields, e.g., the electronic, jewelry, and medical industries. However, PGEs are among the most valuable naturally occurring elements due to their extremely low abundance, which is estimated to be 0.0004 ppm to 0.005 ppm and comprise less than 2 wt% of the earth's crust.^[5] The imbalance between the supply and demand of PGEs, therefore, contributes greatly to a high price volatility. Consequently, the search for more abundant alternatives to transition metals unfolded in the past, whereby heavier main group elements expressed outstanding properties and characteristics reminiscent of *d*-block metals when put in the right environment.

1.1 Heavier Main Group Elements as Transition Metals

The rising idea of utilizing heavier group elements as possible catalyst centers emerged in the first decade of the 21st century after successful isolations of seemingly unstable main group species. These new compounds highlighted the

fundamental differences between light and heavier *p*-block elements, which were hitherto presumed to be similar to each other in their electronics and properties. The spectrum of these species covered one or more unusual features at that time, e.g., multiple bonds between the same main group element (Al, Si, P and their congeners)^[6], stable low valency, and thus the accessibility to open coordination sites^[7,8] and, lastly, main group centers bearing unpaired electrons, some even found in singlet states.^[9] Extensive studies on these elements and their derivatives were performed subsequently, and a common characteristic is shared between them: A small energy separation between the frontier orbitals. Thus, scientists often observe a reactivity of such species towards small molecules, e.g. dihydrogen, ammonia, and ethylene, which were only known for transition metal complexes during that time.^[10] The electronic and bonding properties of novel low coordinated and/or low valent compounds are discussed and highlighted in the following chapters due to their substantial impact on the scientific field of main group chemistry.

1.1.1 Main Group Multiple Bonds: The Beginning

The difference in the core electronics between the first and second row in the periodic system is mainly shown in the covalent radii, e.g. 0.76 Å for C and 1.11 Å for Si, which majorly influences the coordination spaces around the particular element due to the increasement of size.^[11] Early main group complexes such as $[\text{Al}(\text{OH}_2)_6]^{3+}$, $[\text{SiF}_6]^{2-}$ and PCl_5 do not show transition metal-like behavior as in coordinational flexibility or reactivity towards small molecules in an oxidative/reductive manner, which are critical features for potential catalytic applications. Typical transition metal complexes additionally display a small energy separation between the frontier orbitals, thus possessing a small HOMO-LUMO gap (≤ 4 eV), that is, the energetic gap between the highest occupied molecular orbital and the lowest unoccupied molecular orbital. In the process of synthesizing main group curiosities bearing multiple bonds, scientists have progressively obtained species resembling transition metal complexes in their properties and behavior. The crucial aspect in the isolation of heavier main group multiple bonds is the application of large substituents in order to prevent the association of such compounds into oligo- or polymers due to the large radii of the heavier congeners. The beginning of the low

Introduction

valent main group chemistry lays in the last quarter of the 20th century: While aiming for the heavier analogs of carbenes ($:\text{MR}_2$, $\text{M} = \text{Ge}, \text{Sn}$, $\text{R} = \text{CH}(\text{TMS})_2$), which will be discussed in a later chapter, *Lappert et al.* obtained intensely colored product solutions. However, the respective products display a dimeric structure in the solid state, as shown in Figure 1.^[12]

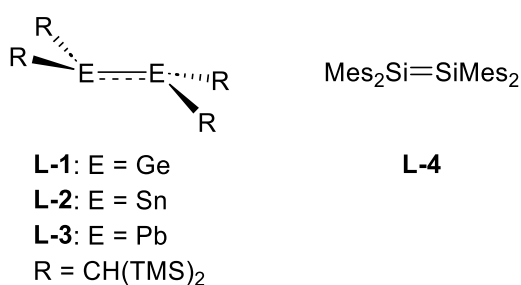


Figure 1: Structure of heavier ethylene analogs, R = CH(TMS)₂.

X-ray structure analysis revealed that the E–E distances in **L-1** (2.347 Å) and **L-2** (2.768 Å) do not have a double bond nature bonding and are just slightly shorter than regular single bonds between the elements, unlike their lighter congener, carbon. Thus, *Lappert* described the bonding properties in two ways: a) Two weak donor-acceptor bonds; b) One single bond with an electron pair sitting on either side resulting in two resonance structures as shown in Figure 2.

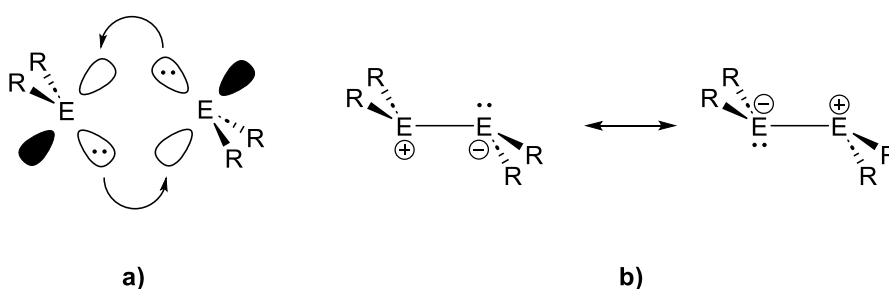


Figure 2: Bonding properties described by *Lappert*, E = Ge, Sn, Pb.

Subsequently, *West et al.* isolated the first ever room-temperature stable silicon analog of ethylene, the tetramesityldisilene (**L-4**), by photolysis of 2,2-bis(Mesityl) hexamethyl trisilane in hexane, which highlights a landmark in the field of low valent main group chemistry.^[13] The structure can be determined as a quasi-planar double bond with a very short Si=Si bond, when compared to a Si–Si single bond (2.34 Å)^[14], of roughly 2.16 Å. Lead analogs, e.g., **L-3**, were to follow at the end of the 90s.

Introduction

Interestingly, in contrast to **L-1** and **L-2**, **L-3** is found to have a *trans*-bend structure with a very long Pb–Pb single bond of 4.129 Å, which can barely be considered a covalent bond.^[15] Thus, with an increase in atom size from carbon to lead, the double bond character gradually decreases, resulting in two quasi-non-bonded, electron-rich metal centers with one lone pair on each atom, respectively. Additionally, proceeding down group XIV, a geometrical distortion can be determined from the linear structure of a C=C double bond to the previously mentioned *trans*-bend Pb–Pb single bond. An additional analysis of molecular orbitals in the heavier group XIV multiple bonded species can explain the observed alteration in geometry. Extensive studies revealed a symmetry-allowed mixing of an unoccupied non-bonding or anti-bonding orbital with a bonding orbital, most likely the HOMO.^[16] This results in the development of a non-bonding character of the bonding orbital, usually the π -orbital, bearing a lone pair, which consequently leads to a second-order Jahn Teller effect, causing the change in the molecular shape.^[17] Furthermore, the “inert electron pair effect” in heavy main group metal atoms, e.g., Pb, also contributes to the *trans*-bend structure: After hybridization of the *s*- and *p*-orbitals, the lone pair occupies an inert orbital in the ligand atmosphere. Though the lone pair itself might not be chemically active due to the high *s* character of the molecular orbital, it is undoubtedly stereo-chemically active under a variety of criteria. Factors favoring this behavior include the presence of small ligands and the low coordination number of the central atom.^[18] In addition, the degree of orbital mixing is simultaneously inversely related to the HOMO-LUMO gap and is maximized in heavier group XIV elements, thus allowing a close approach (< 4 eV) of the orbitals reminiscent of transition metals in their characteristics. Similar considerations regarding the bonding properties and molecular shape can also analogously be made for neighboring group XIII and group XV elements. Overall, multiple bond characters containing conventional σ - and π -bonds are generally found in the lighter main group elements.^[10]

1.1.2 Ge/Sn Multiple Bonds: Synthesis and Application as Molecular Catalyst

Group XIV elements have been vastly studied by scientists in the past decades and are arguably the most investigated multiple bonds, mainly due to the ubiquity of their lighter carbon congener.^[19] The isolation of heavier homologs and novel bonding motifs bearing Ge/Sn/Pb has been proven to be challenging. *Lapperts* isolation of digermenes and stannenes in 1976 displayed instability in solvents at ambient temperatures in great contrast to the extensively robust C=C double bond.^[20] Ever since then, a broad spectrum of “authentic” multiple-bond compounds bearing germanium and tin centers have been isolated and characterized to date. The in-depth reactivity studies displayed their high potential in the field of catalysis. Lead, on the other hand, is overall observed to form “double” bonds with very long Pb–Pb distances comparable with single bonds, which will not be further discussed in this chapter. The preparation of stable digermenes (Ge=Ge double bond) usually follows one of the four general synthetic routes: a) Dimerization of germynes; b) Reductive dehalogenation of 1,1-dihalogermanes; c) Photolysis of cyclotrigermanes; d) 1,2-addition or cycloaddition (CA) of digermynes. Similar synthesis methods can be applied to isolate stable distannenes: a) Dimerization of stannylenes; b) Photolysis of cyclotristannanes; c) Redistribution of ligands between homoleptic stannylenes (R₂Sn:, R'₂Sn:) to heteroleptic stannylenes (RR'Sn:) and subsequent dimerization.^[21] Dimetallynes are usually prepared analogously *via* reductive dehalogenation or consecutive dimerization.^[19]

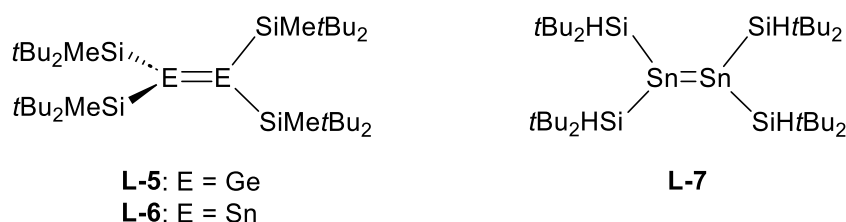


Figure 3: Selected early examples of double bond species bearing Ge and Sn centers.^[22–25]

Sekiguchi et al. observed a highly twisted double bond between germanium (**L-5**) and tin center (**L-6**). Their synthesis route followed the reductive dehalogenation to isolate a digermene capable of maintaining its structural integrity even in solutions.

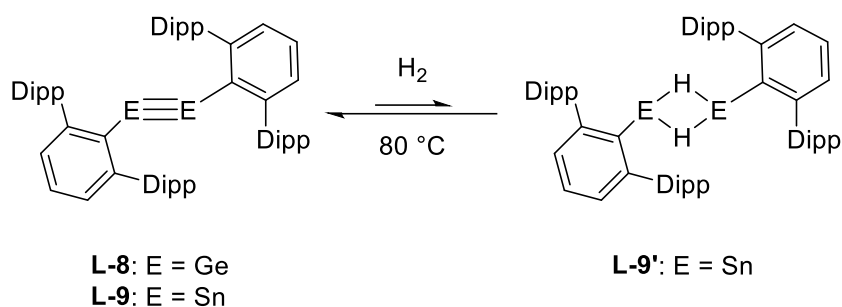
Introduction

The straightforward reduction *via* potassium graphite with the respective 1,1-dichlorogermane precursor yielded a highly twisted structure as shown in Figure 3.^[23,24] Distannenes were known for a long time for the unavoidable double bond breaking in solution despite being structurally characterized as double bonds in the crystalline state. In 2006, *Sekiguchi* and coworkers further applied the di-*t*-butylmethyl silyl ligand to isolate the first ever stable distannene **L-6** even in solvent *via* reduction of the 1,1-dichloro tin precursor.^[22] A series of E=E (E = Ge, Sn) double bond species were since then isolated and characterized, whereby it is worthy of mentioning compound **L-7** with an especially unusual molecular structure: Being completely planar, **L-7** portrays the first structurally direct analog of a C=C double bond. As discussed before, the typical formation of a planar double bond consisting of two triplet carbenes is not found in tetrylenes. Instead, the bonding properties are rather described as a donor-acceptor interaction in distannenes, resulting in a weak Sn··Sn bond. *Apeloig et al.* conducted a thermolysis of tris(di-*t*-butyl-hydridosilyl)stannane to obtain the respective stannylene as an intermediate, which subsequently dimerizes to **L-7**. However, the transient stannylene is trappable as ^{Me}NHC adduct or [1+4] cycloaddition product with 2,3-dimethylbuta-1,3-diene exhibiting typical characteristics of stannylene species in their reactivity.^[25]

Heavier alkyne analogs were in simultaneous development as the alkene congeners and have been pivotal in emphasizing the potential of heavier main group elements as transition metal centers, whereby a series of prominent reactivities towards small molecules could be determined. In this regard, *Power et al.* reported the first H₂ activation by a digermynes (**L-8**) readily at room temperature, yielding a mixture of digermenes and digermanes, which led to the conclusion that firstly, an addition of dihydrogen to other unsaturated group XIV compounds may also be possible and secondly, the addition might be reversible.^[26] Indeed, the same group could observe a reversible coordination of H₂ by distannyne **L-9** in 2018, about a decade later, bearing the same structural motif as its germanium derivative.^[27] Structure **L-9** is found to be in equilibrium with **L-9'** in the presence of dihydrogen. The calculated

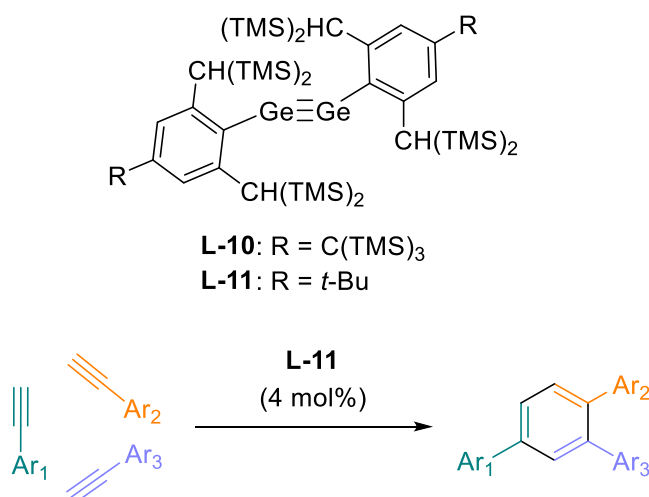
Introduction

equilibrium constant and the Gibbs free energy, however, strongly favor the Sn(II) hydride form **L-9'**.



Scheme 1: Structure of digermynes and distannynes isolated by *Power et al.*^[26,27]

A few more examples of heavier ethylene analogs, such as **L-10** and **L-11**, were to follow, showing interesting reactivities towards acetylene and alkyne derivatives forming 1,2-digermylenes.^[28] Additionally, digermine **L-11** is reported to act as a precatalyst in the cyclotrimerization of aryl-substituted acetylenes to the respective 1,2,4-triaryl benzenes.^[29] The highlight of this reactivity not only lies in the C-C bond formation but also in the absolute regioselectivity of the aryl groups, which represents the importance of main group multiple bond compounds in the catalysis.



Scheme 2: Reaction path of the digermine catalyzed cyclotrimerization of arylacetylenes.^[29]

1.1.3 Tetrylenes: An Overview

Tetrylenes, being heavier analogs of carbenes, are low-valent, electron-deficient species with one lone pair and an empty p -orbital. They usually display E^n and E^{n+2} (e = element) oxidation states as a result of the inert pair effect. The preferred electronic ground state furthermore changes from triplet to singlet state proceeding down the group XIV (Figure 4). This phenomenon is mainly caused by the singlet-triplet energy separations: While being negative for $H_2C(II)$ (estimated $\Delta E_{s,t} = -14.0$ kcal/mol), the value increases descending down group XIV to 16.7 (for H_2Si), 21.8 (for $H_2Ge(II)$), 24.8 (for $H_2Sn(II)$), 34.8 (for $H_2Pb(II)$) kcal/mol respectively, based on theoretical calculations.^[7] Silylenes, e.g. the silicon congener of carbenes, thus has singlet as the preferred ground state whereby two electrons are in the sp^2 orbital (lone pair orbital) while the energetically higher p -orbital remains vacant. The lone pair orbital additionally possesses an extensively high s character due to the increasing energy of hybridization from carbon to lead mainly coming from the higher effective nuclear charge and the lower tendency for s - and p -orbital overlap, which is, on the other hand, introduced by increasing energy separation and diverging spatial extension of both molecular orbitals. Worth mentioning is also the fact that the relative stability of the low-valent and low-coordinated species R_2E : (R = alkyl/aryl) to their corresponding dimeric structure $R_2E=ER_2$ increases down the column and is maximized at Pb.

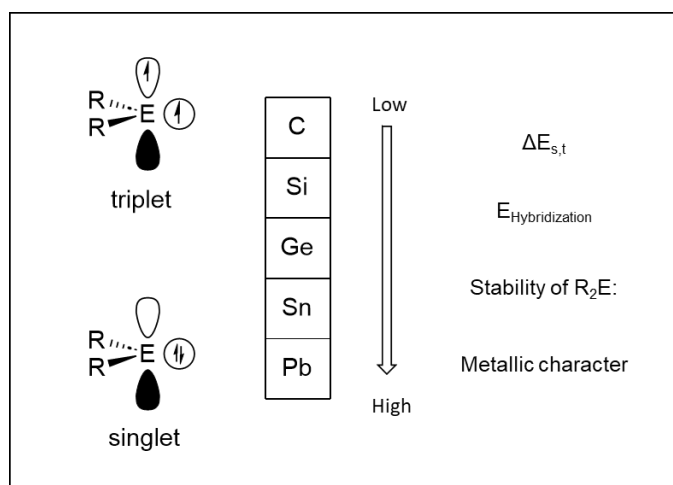


Figure 4: Group XIV general electronic properties and representation of the frontier orbitals.

Introduction

Though plumblylenes are supposed to be stable as such, some compounds are observed to be thermally unstable and undergo disproportionation reactions due to the lack of electronic or steric stabilization.^[30] Even though the lone pair orbital stays extensively inert, resulting from its high *s* character, the vacant *p*-orbitals, as mentioned above, are highly reactive and are therefore assumed to introduce the high instability due to the unfulfilled octet rule. Thus, in order to prevent reactivities amongst themselves and towards other molecules, the stabilization of heavier low valent group XIV compounds is achieved in two major ways, respectively: the thermodynamic and the kinetic method.^[7] Overall, the application of π -donating moieties, such as N, O, P, or Cp* containing ligands, is utilized in the thermodynamic stabilization of methallylenes. The lone pair of the hetero atom can donate electron density into the empty *p*-orbital, increasing the energy level of the LUMO by reducing its electrophilicity. Simultaneously, the σ -accepting properties of such ligands can withdraw electron density from the tetrylene center thus lowering its HOMO leading to a comparably larger HOMO-LUMO gap.^[31]



E = Si, Ge, Sn, Pb
L = N, O, P, Cp* containing ligand

Figure 5: Schematic representation of thermodynamic stabilization of methallylenes by electron-donating ligands.

The other crucial aspect is the usage of sterically bulky ligands in order to kinetically prevent the coordination of nucleophiles as well as dimerization or polymerization reactions of tetrylene centers. A vast variety of such ligands were developed in the progress and will be further discussed in upcoming highlighted methallylenes.

Introduction

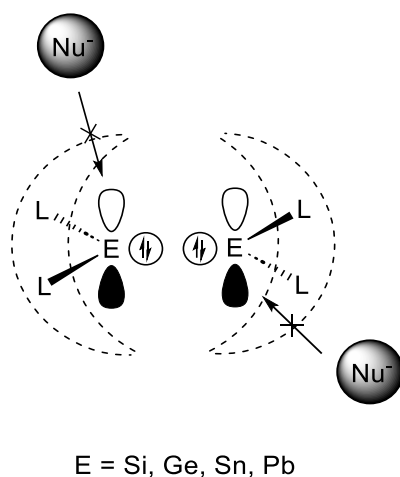


Figure 6: Schematic representation of kinetic stabilization of methallylenes by bulky ligands.

Though tetrylene species theoretically have free coordination sites, and their electronic constitution does resemble transition metals, the application of such compounds as molecular catalysts has yet to achieve the variety of precious metals. Nonetheless, some interesting reactivities have been observed over the past two decades and should be highlighted.

1.1.4 Ge(II)- and Sn(II)-containing compounds as Molecular Catalysts: A Highlight

As mentioned above, the application of group XIV elements as catalyst centers has been an emerging field in the main group chemistry. The narrow HOMO-LUMO gap enables reactivities of tetrylene centers found in the first step of catalytic cycles: Oxidative addition of dihydrogen, ethylene, or carbon dioxide. A wide variety of examples are reported in literature till today^[32], whereby a few compounds could successfully convert the activated small molecules in a catalytical manner. Reversibility, thus, is the key feature in focus regarding catalytic activities of tetrylenes and will be highlighted in selected compounds in the next paragraph.

Introduction

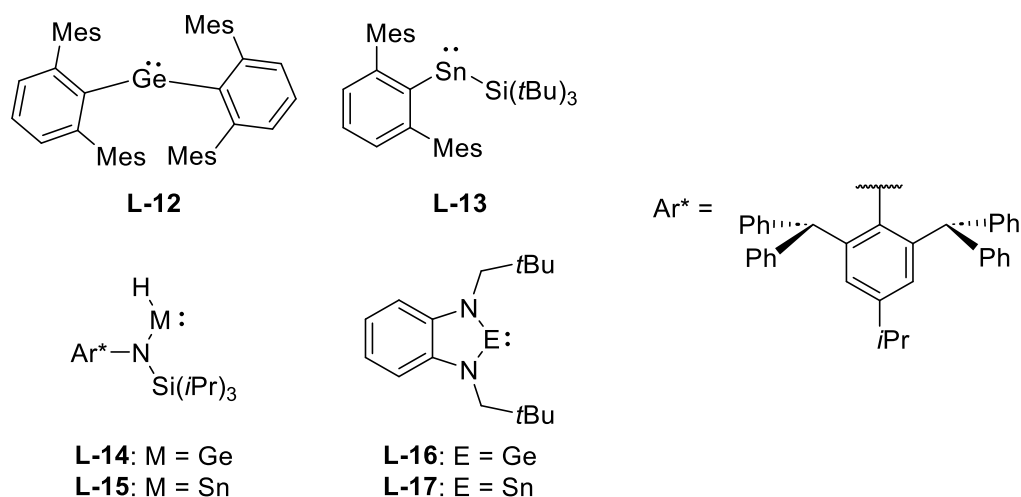
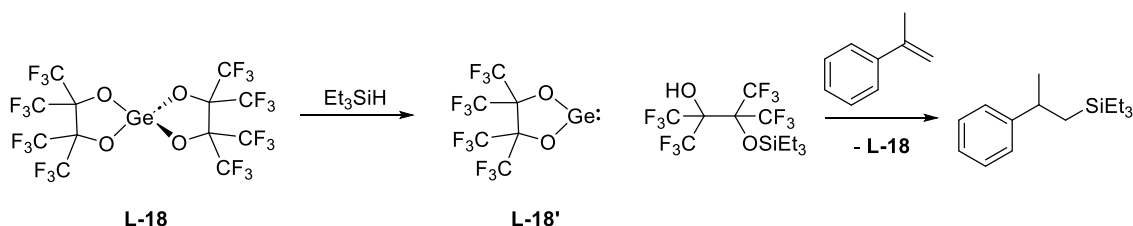


Figure 7: Structure of selected literature reported tetrylenes.

Germylene **L-12** is shown to activate P_4 readily at room temperature. The release of the coordinated fragment takes place in the presence of UV light after only 30 minutes.^[33] The reversible activation of P_4 is also reported for the heteroleptic stannylene **L-13**, which is isolated by treating the respective chloro-precursor with one equivalent of $NaSi(tBu)_3$.^[34] The release of the P_4 fragment, similar to germylene **L-12**, is UV-induced. However, in contrast to **L-12**, a quantitative back-formation of **L-13** could not be achieved. Nonetheless, this example illustrates the first reversible P-P bond activation by a low-valent tin compound. The efficient catalytic activity of a bulky, acyclic germylene (**L-14**) and stannylene (**L-15**) was demonstrated by *Jones et al.* Both two coordinated hydrido tetrylenes are able to perform efficient catalytic hydroboration of carbonyl compounds with HBpin (pin = pinacolato), whereby the tin-based catalyst solely requires a loading of 0.5 mol% to achieve turnover frequencies over 600 h^{-1} in some cases.^[35] Furthermore, **L-14** and **L-15** can reduce molecular CO_2 to “methanol equivalents” ($MeOBR_2$).^[36] Other versatile reactivities within both compounds are found with further investigations, including regioselective hydrometallations of cyclic and acyclic alkenes, as well as dimerization to the respective oxo-bridged species in the presence of molecular oxygen.^[37] Additionally, a reversible hydrogermylation of cyclohexene could be determined with **L-14**. The mechanism most likely involves a β -hydride elimination of the coordinated cycloalkyl moiety regenerating cyclohexene and the hydrido-germylene. Cyclic germylenes and stannylenes have also been reported to exhibit

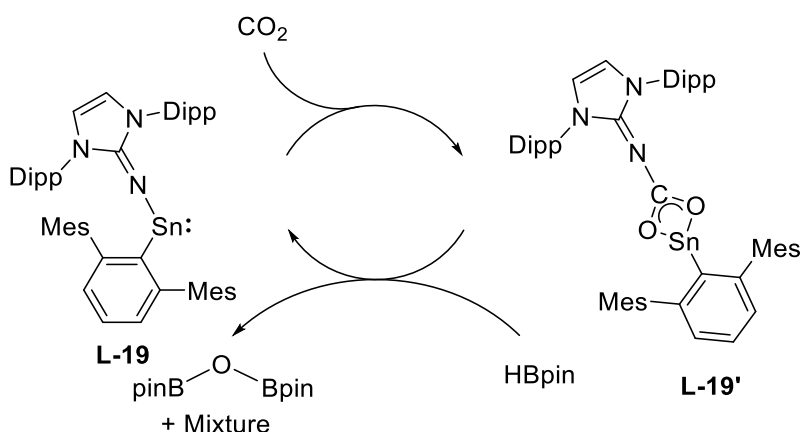
Introduction

activities as single-site catalysts. *Khan et al.* determined the catalytic properties of **L-16** and **L-17** about two decades later after their isolation and characterization.^[38] The application of both compounds in the cyanosilylation and hydroboration of aldehydes transforms a broad spectrum of substrates to the respective products in a catalytical way.^[39] However, the typical oxidative addition, usually found in catalytical cycles, to the tetrelene center is not included in the proposed mechanism. Instead, the nitrogen/oxygen atom of the TMSCN/HBpin coordinates to the low valent center to initiate the reaction.



Scheme 3: Catalytic hydrosilylation of α -methylstyrene with triethylsilane in the presence of the Lewis super acid.

Furthermore, *Inoue et al.* reported a germanium-centered *Lewis* superacid (**L-18**) in 2024.^[40] The structure showed a reverse temperature dependency: At -35°C , **L-18** is able to catalytically hydrosilylate α -methylstyrene in the presence of triethylsilane with a conversion up to 98% at a catalyst loading of only 5 mol%. DFT calculations revealed the germylene species **L-18'** as the active catalyst during the reaction (Scheme 3).



Scheme 4: Catalytic cycle of the reduction of CO_2 with compound **L-19**.

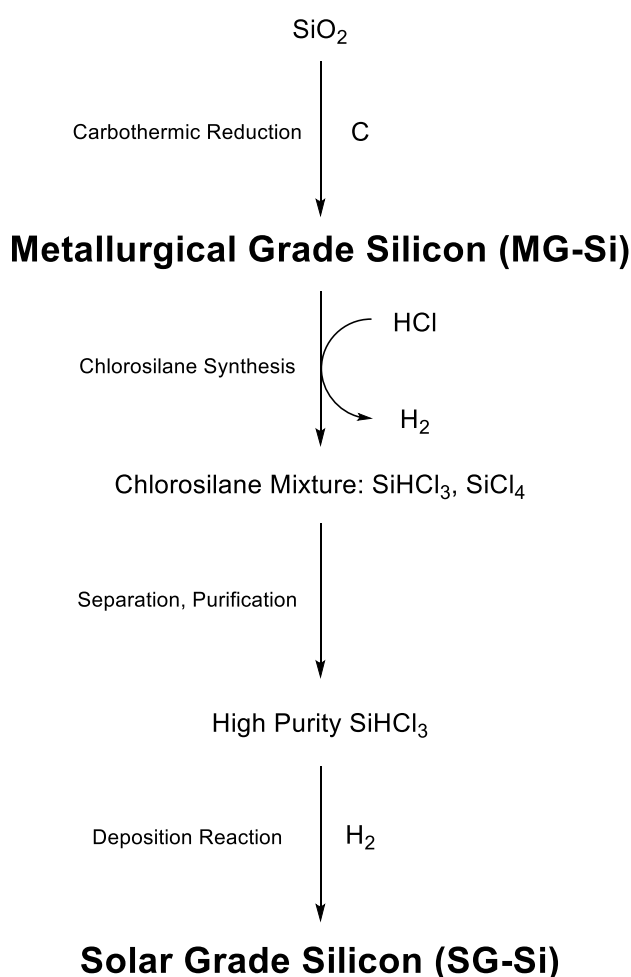
The aryl(imino) stannylene **L-19** can activate CO₂ and reduce it in the presence of HBpin (pin = pinacolato) in a catalytic way.^[41] Simultaneously, the reaction offers a variety of specific products compared to conventional tetrylene-catalyzed CO₂ reductions. The mechanism involves the insertion of CO₂ into the N-Sn bond, yielding a tin-carbamate moiety (Scheme 4) thus highlighting the first ligand-assisted activation and catalytic conversion of carbon dioxide by an NHI-stabilized stannylene. Even though the reversibility of the oxidative addition and, thus, conversion of some small molecules are detected in certain tetrylene species, it remains a challenging aspect to tune the electronic and steric properties of such compounds. Additionally, in regard to potential large industrial applications, the toxicological aspects of Ge and Sn have to be considered. Even though germanium-based compounds are considered rather low risk^[42], organo-tin compounds are hazardous to human health^[43]. Therefore, their lighter congener raised special interest due to its natural abundance and non-toxicity: the element silicon.

1.2 The Element Silicon

The pursuit to replace inherent scarce and thus expensive transition metal-based catalysts brought forward concepts of a silicon-mediated catalysis. Besides being the element of interest for main-group chemists, silicon has demonstrated its wide-ranging and irreplaceable utility in the industry. The group XIV element silicon, discovered by Jöns Jacob Berzelius in 1824, is the second most abundant element in our earth's crust, making up to 27.7% by mass, and comes in the form of oxides, as in sand, quartz, or flint, and silicates, as in granite and clay. Refining silicon is thus a process of great importance. Thereby, the manufacturing of hyper-pure silicon follows two different stages, beginning with the production of metallurgical grade silicon: In an electrode arc furnace, silica (SiO₂), the dioxide form of silicon, reacts with carbon in the form of coal and charcoal at temperatures up to 2000 °C forming metallurgical grade silicon (MG-Si) with a purity of 98-99% and carbon dioxide. The impurities of roughly 1-2% mainly consist of carbon, alkali-earth (B and P of > 50-100 ppm), and transition metals, the latter causing deep levels in band gaps. MG-Si is, therefore, not suitable for electronic and photovoltaic applications.^[44] The process behind the manufacturing of MG-Si to polycrystalline silicon, also known as

Introduction

solar grade silicon (SG-Si), mainly consists of two conventional routes: 1) *Siemens* process and 2) “Fluidized bed reactor” process by *Union Carbide*.^[45] The obtained MG-Si is oxidized to trichlorosilane and tetrachlorosilane in the presence of hydrogen chloride, whereby only trichlorosilane is isolated and undergoes further deposition reaction with dihydrogen to form SG-Si (Scheme 5). The major difference between both processes is that the *Siemens* method operates under less harsh conditions with reduced efficiency compared to the procedure developed by *Union Carbide*. The obtained SG-Si can be further manufactured to monocrystalline silicon in the next step *via* the *Czochralski* method.^[46]

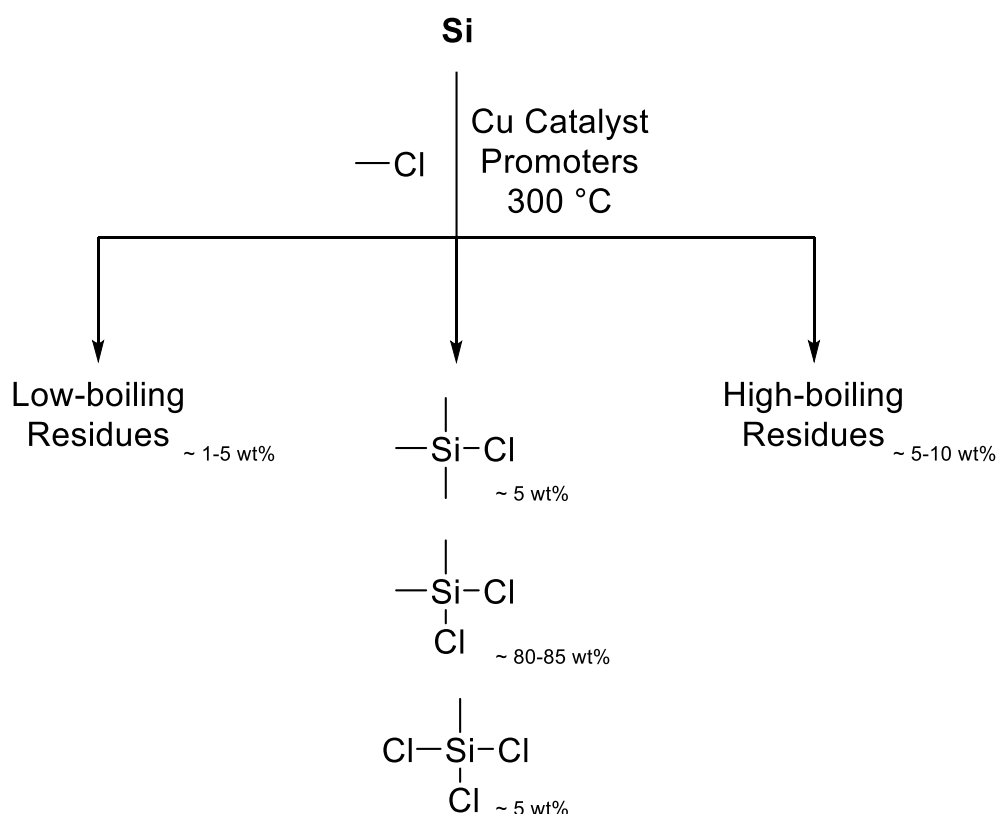


Scheme 5: Processing pathway of silica to solar grade silicon.

Another industrial application of importance demonstrated the so-called “*Müller-Rochow*” process providing methyl chlorosilanes (Scheme 6). Thereby, methyl chloride is added to powdered Si in the presence of a copper-based catalyst and

Introduction

promoters, such as Zn, Sn, and P.^[47] The process itself has a certain degree of complexity due to the large number of side products generated during the synthesis. A selective formation of the desired product, Me_2SiCl_2 , can be extensively achieved by selecting suitable catalysts and promoters to reduce the amount of low-boiling (e.g. SiMe_4 , SiCl_4) and high-boiling (e.g. $\text{Si}_2\text{Me}_2\text{Cl}_2$) residues.^[48]



Scheme 6: Schematic depiction of the Müller Rochow process.

Methyl chlorosilanes are the essential starting materials for the production of silicones (polysiloxanes). This class of high-performance polymers consists of an alternating Si-O backbone bearing a variety of side groups and comes in the forms of oil, grease, rubber, resin, etc.^[49] The outstanding physical and chemical properties of these polymers include high durability, flexibility, and adhesion, as well as resistance to radiation, heat, and discharge, which quickly led to a vast application in the construction, electronic, medical, and transportation industries.

The non-toxic nature and high abundance make silicon one of the most useful elements to mankind with versatile applications in computers, microelectronics, glass production, cosmetic industries, and many areas of manufacturing.^[50] Alongside its heavier congeners (Ge, Sn, Pb), the element silicon has thus raised special attention with the development of main group multiple bonds and low valent species. Chemists all over the world reported the transition metal-like behavior of such Si-containing compounds under mild conditions, which undoubtedly opens up new alternatives to transition metal catalysts. A wide variety of novel compounds have been isolated to date, bringing new insights into the depth of silicon chemistry, which will be further elaborated on in the next chapters.

1.2.1 Si-Si Multiple Bond: Synthesis and Reactivity

Ever since the first room-temperature stable disilene^[13] and silaethene^[51], being separately reported in the same year, silicon-containing multiple bonds have received special attention regarding the diverse aspects of their synthesis, bonding characteristics, spectroscopic properties, and reactivity.^[52] As discussed in an earlier part, theoretical and practical studies accumulated distinctions between low-coordinated Si-containing compounds and their carbon congeners in their bonding, structure, and resulting chemistry. A series of novel thermally stable homo- and heteronuclear silicon compounds containing double or triple bonds were isolated and elucidated to date^[53], whereby this chapter will be focusing majorly on the disilene and disilynes. The general synthesis route towards both species is similar to their heavier congeners (Ge, Sn), including one of these ways: a) Reduction of 1,2-dihalodisilanes; b) Dimerization of silylenes; c) Metathesis reaction involving lithium disilene or dilithiosilane. All novel synthetic strategies allowed the isolation and characterization of various Si-Si multiple bonds showing to activate small molecules in an oxidative manner, including dihydrogen, ammonia, oxygen, carbon dioxide, and carbon monoxide, which are all industry-relevant building blocks.

Introduction

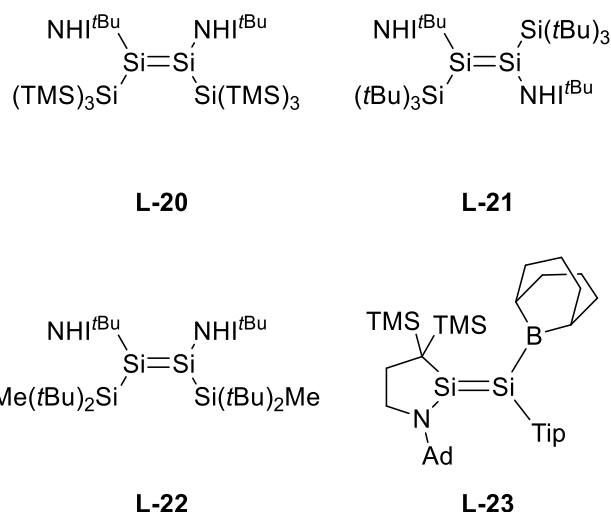


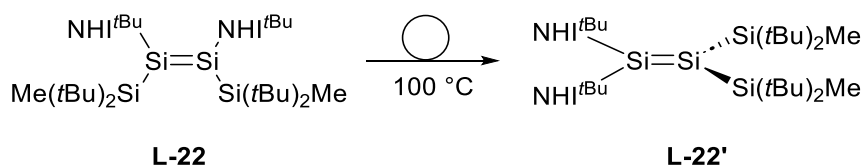
Figure 8: Structure of selected isolated disilenes. Tip = 2,4,6-triisopropyl phenyl.

The isolation of **L-20**, a diiminodisilyldisilene, follows a synthesis route featuring a reduction and subsequent substitution of the respective *t*BuNHI-SiBr₃ precursor with potassium hypersilanide (KSiTMS₃). **L-20** displays a highly twisted structure with a bonding character of an extensively weakened double donor-acceptor bond. Its unique electronic and structural properties allow an *anti*-addition of dihydrogen under ambient temperatures within minutes, demonstrating the first example of an H₂ activation by a Si-containing multiple bond.^[54] Furthermore, in the presence of ammonia, two different products could be selectively achieved by thermodynamic control, respectively: The *trans*-1,2-adduct and the aminosilane as the formal silylene addition product. DFT studies suggest a mechanism similar to the H₂ addition. A few other examples of disilenes activating NH₃ have since been reported and elaborated.^[55] **L-20** is also shown to form various silacycles with O₂, CO₂, and N₂O.^[56]

Due to the limited thermal stability of **L-20** and its inefficient synthesis, attempts to isolate more stable derivatives were further pursued. Herein, **L-21** and **L-22** were reported in 2021 in a detailed study of such disilenes.^[57] It is assumed that the hypersilyl group might be causing thermal decomposition due to its tendency to undergo rearrangement.^[58] Thus, the hypersilyl substituent is modified to tri(*tert* butyl)silyl (-Si^tBu₃) group. The syntheses were carried out analogously to **L-20** in the preparation and yielded the respective *E* isomer as the sole product. **L-21** is

Introduction

observed to be stable as a solid and in benzene at room temperature, unlike the previously mentioned **L-20**. Despite the increased stability, **L-21** still undergoes unselective decomposition at temperatures above 50 °C. Subsequently, another ligand modification attempt was made by replacing one *tert*-butyl group of the silyl ligand in **L-21** with a methyl group. The synthesis of the respective disilene **L-22** led to a mixture of *E* and *Z* isomers with the equilibrium shifted to the *Z* isomer, which displayed high stability as solid and in benzene up to 90 °C and undergoes irreversible rearrangement at 100 °C to **L-22'** (Scheme 7).



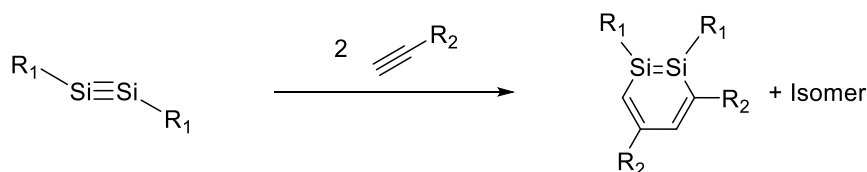
Scheme 7: Rearrangement of **L-22** above 100 degrees Celsius.

Reactivity-wise, **L-22** expresses typical behavior for low-coordinated Si compounds. In the presence of diphenylacetylene, **L-22** forms the respective silirene as the product of a [1+2] cycloaddition. Moreover, **L-22** can also selectively activate dihydrogen in an *anti*-addition type of way. The versatility in the reactivity of **L-22** also involved one-electron oxidation to the respective radical cation, the activation of P₄ and oxidation by molecular oxygen and nitrous oxide demonstrates that the choice of suitable ligands in the stabilization can simultaneously also lead to new, advancing reactivities of disilenes.

Iwamoto et al. reported the first “push and pull” disilene **L-23** bearing amino and boryl-containing structural motifs.^[59] The isolation of **L-23** starts with the reduction of a cyclic alkyl amino silylene (cAASi) and TipSiCl₃ (Tip = 2,4,6-triisopropyl phenyl) in the presence of KC₈ and subsequent addition of B-chloro-9-borabicyclo[3.3.1]nonane. The Si=Si double bond shows interactions with both substituents in the spectroscopic analyses. Additionally, **L-23** cleaves the strong bond of dihydrogen, forming the corresponding trihydridosilane and hydroborane. The addition of other small molecules onto Si=Si bonds, e.g., CO or the previously mentioned CO₂ and N₂O, are also described in the literature, whereby a series of

Introduction

diverse products are characterized bearing bridged oxygen atom(s) between both Si centers.^[60]



L-24: $R_1 = \text{Si}i\text{Pr}(\text{CHTMS}_2)_2$

L-25: $R_1 = 2,6\text{-bis}(\text{CHTMS}_2)\text{-4-CTMS}_3\text{-C}_6\text{H}_2$

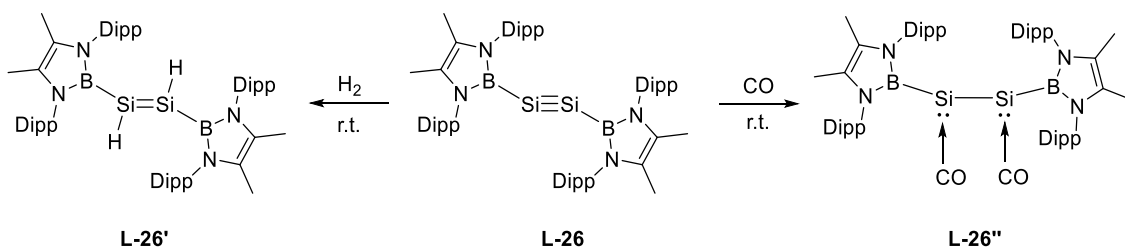
L-24': $R_1 = \text{Si}i\text{Pr}(\text{CHTMS}_2)_2$

L-25': $R_1 = 2,6\text{-bis}(\text{CHTMS}_2)\text{-4-CTMS}_3\text{-C}_6\text{H}_2$

Scheme 8: Cycloaddition of disilynes and alkynes forming 1,2-disilabenzenes.

When combined with their lighter carbon congener (alkenes or alkynes), [2+2] cycloaddition and subsequent rearrangement are often reported in Si-containing multiple bonds, whereby the latter, multi-step reactivity is found in disilynes.^[61,62] Regarding this matter, disilynes **L-24** and **L-25** were reported to react with acetylene derivative to 1,2-disilabenzene **L-24'** and **L-25'** as one of two regioisomers representing a new route to synthesize disilabenzenes.^[61,63]

Cui et al. isolated the disilyne **L-26** by the reduction of *N*-heterocyclic boryl (NHB) ligand stabilized tribromosilane in the presence of elemental lithium in diethyl ether. An interesting, simultaneous benzylic C–H bond insertion of one silicon atom and a silyrane formation of the other silicon atom with the C=C double bond of one single toluene molecule is found. This type of cycloaddition of toluene has not been reported so far, highlighting the unusual electronic and steric properties of the NHB-stabilized disilyne. The high reactivity of disilyne **L-26** is moreover demonstrated in its capability to cleave the strong and non-polar bond of dihydrogen forming the respective disilene **L-26'**.^[64]



Scheme 9: Reactivity of disilyne **L-26** towards small molecules.

In addition, **L-26** displays a double coordination of two carbon monoxide molecules forming a unique 1,2-dicarbonyl-disilane moiety in **L-26**".^[65] Subsequent DFT calculations could reveal noticeable backbonding from the lone pairs sitting in the empty *p*-orbitals of the silicon atom to the π^* -orbitals of the CO molecule. Moreover, the respective "activated" CO molecules can be released in the presence of water/methanol or iodomethane. Not only is the coordination of CO resulting in a CO complex a scarce finding among low coordinated silicon-containing compounds, which will be further discussed in the next chapter, but the demonstrated backbonding in **L-26**" by DFT and SC-XRD analyses also illustrates distinct resemblances to classic transition metal CO complexes.

1.2.2 Isolation and Reactivity of Silylenes

Silylenes are neutral, low-valent, and low-coordinated silicon-containing compounds with the silicon center in the oxidative state of +II. Due to their intrinsic unsaturated nature, silylenes are usually unstable intermediates that decompose when exposed to air and ambient temperatures. However, contemporary and innovative synthesis routes involving previously mentioned stabilization methods for tetrylenes could be applied to successfully isolate cyclic and acyclic silylenes. Their diverse bonding nature, structure, and physical properties enabled unique reactivities toward small molecules reminiscent of transition metal complexes.

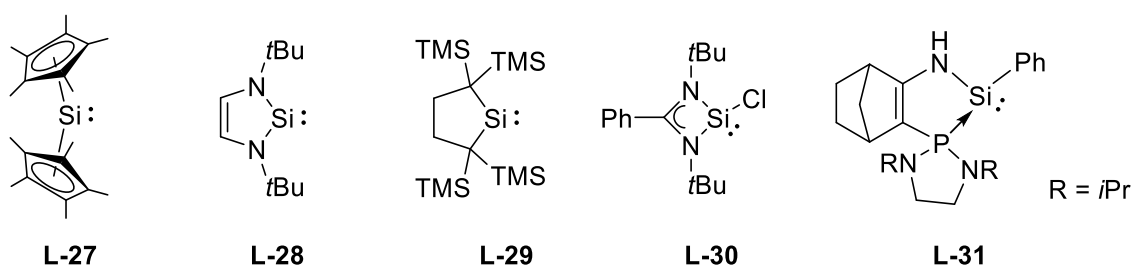


Figure 9: Structure of the first silylene by *Jutzi et al.* and diverse cyclic silylenes.

The first isolable silylene **L-27** by *Jutzi et al.* was achieved by the reduction of the respective dibromo precursor with potassium anthracene in the late 20th century.^[66] Diverse cyclic silylenes (Figure 9) were to follow subsequently, whereby various ligands were applied to effectively stabilize the silylene atom. Among them, π -donation of adjacent hetero atom (**L-28**, **L-29**, **L-30**), sterical stabilization of

Introduction

bidentate ligands (**L-30**), or a combination of both (**L-31**) are proven to be advantageous.^[67] Acyclic dicoordinated silylenes (Figure 10), on the other hand, were first discovered after the first decade of the 21st century.

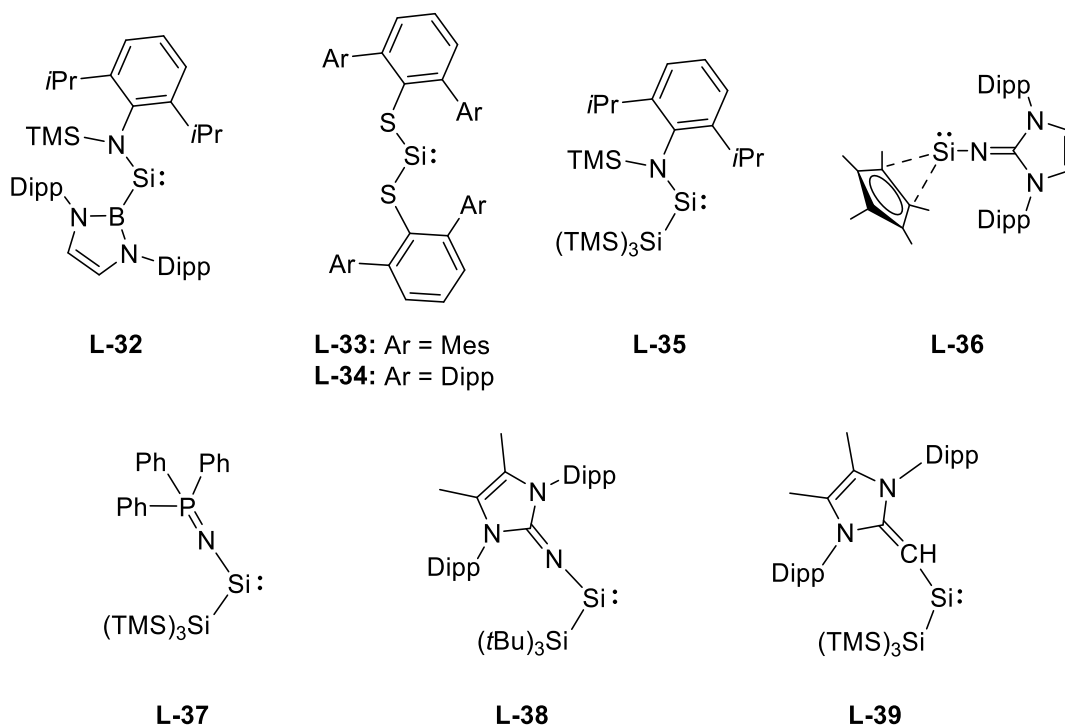


Figure 10: Structure of selected acyclic, dicoordinated silylenes.

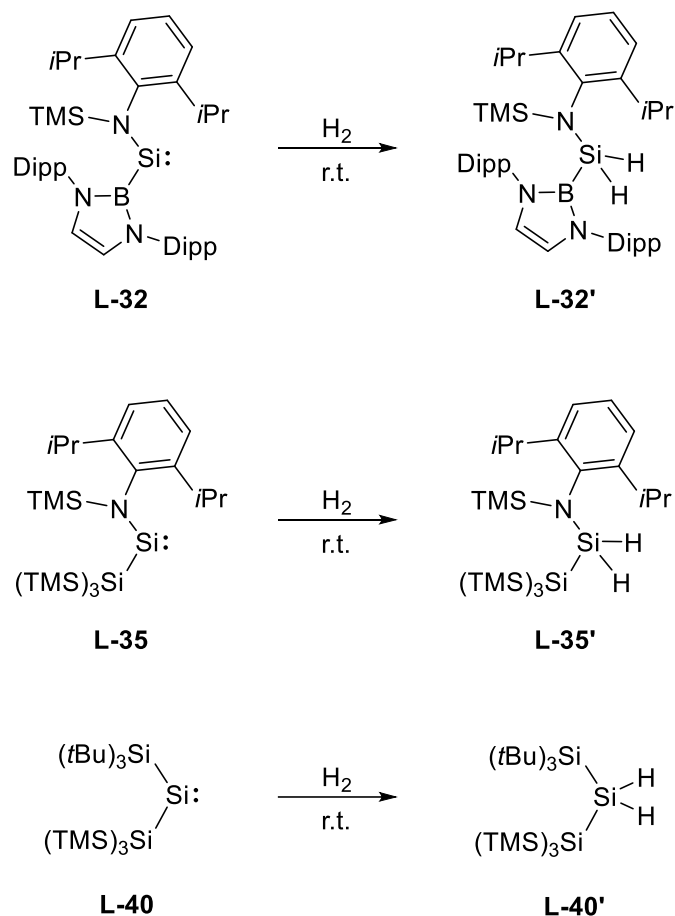
The synthesis of the acyclic, heteroleptic silylene **L-32** followed the substitution and reduction of the respective tribromo silicon precursor in the presence of two equivalents of the lithium boryl species in order to simultaneously introduce the boryl ligand and to reduce the Si(IV) to Si(II).^[68] The structure of the homoleptic silylene **L-33**, on the other hand, is obtained by the reduction of the dibromo precursor with *Jones's* complex (IMesMg)₂ after the introduction of both sulfur ligands in two separate steps.^[69] For the sterically more demanding version (**L-34**), the dibromo precursor is reduced in the presence of Mg with catalytical amount of anthracene.^[70] Subsequently, the strategic application of KSiTMS₃, an anionic reagent with sufficient nucleophilicity, strong reducing properties, and great sterical bulkiness, could enable a one-pot synthesis of silyl silylene **L-35**.^[71] *Inoue et al.* utilized an *N*-heterocyclic imine (NHI) for the first time in the stabilization of an acyclic silylene (**L-36**) with several mesomeric structures, among them a zwitterionic silylene amide species, highlighting the multiple bond characteristics

Introduction

between the nitrogen and the silicon atom.^[72] Altering the NHC moiety of the NHI ligand to a sterically less demanding phosphine group in silylene **L-37** resulted in a transient acyclic silylene, which can only be trapped in the presence of cyclohexene as a silirane species.^[73] Addition of two methyl groups to the NHC backbone of the imine ligand in combination with the application of the hypersilyl group ($-\text{SiTMS}_3$) yielded silylene **L-38**, which is of particular importance and will be discussed more in detail in the next chapter. The structurally similar vinyl silylsilylene **L-39** by *Rivard et al.* expresses extended thermal stability while possessing a high reactivity towards small molecules.^[74]

Following the synthesis of diverse silylenes, their reactivity towards small molecules was extensively investigated, and their reminiscence of PGE complexes was quickly discovered: Due to their amphiphilic nature, silylenes can engage in small molecule activation in an oxidative manner, thus expressing a series of interesting behavior towards σ - and π -bonds. Thereby, acyclic silylenes are especially regarded as promising species as “greener” alternatives of transition metal-based catalysts due to their oxidative flexibility, small HOMO-LUMO gap, and open coordination site. As an example, silyl silylene **L-32** is capable of oxidatively cleaving the strong and nonpolar σ -bond of dihydrogen (Scheme 10) giving dihydrosilane **L-32'**. A likewise reactivity is also found in the structurally similar silylene **L-35** bearing the hypersilyl instead of the boryl ligand with a narrow HOMO-LUMO gap of ~ 2 eV.

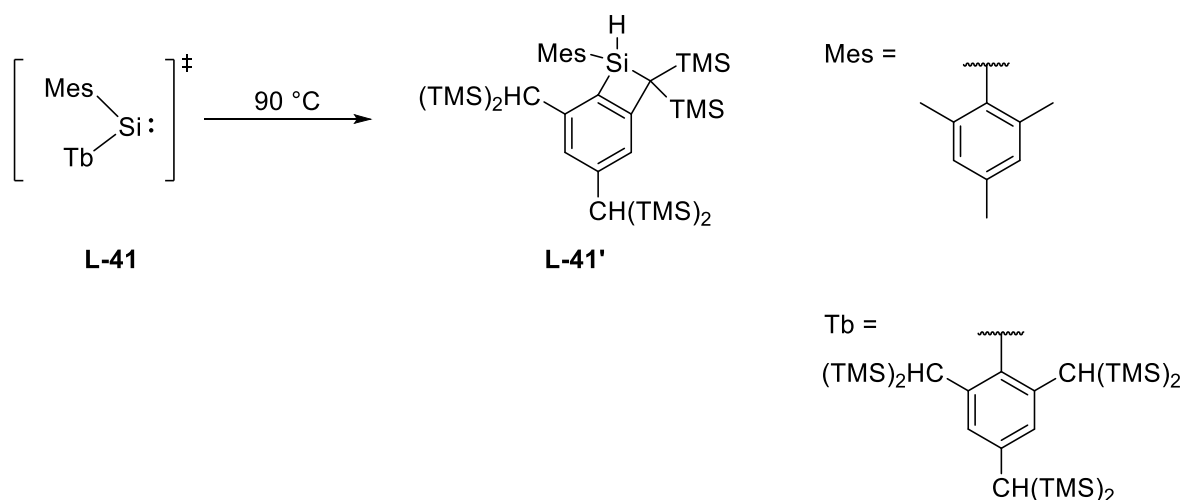
Introduction



Scheme 10: Oxidative addition of dihydrogen to acyclic silylenes.

Moreover, bis(silyl)silylene **L-40**, which is in equilibrium with its tetrasilyldisilene isomer, is also reported to activate dihydrogen in an oxidative addition.^[75] Other diverse reactivities are additionally found within these low valent species: Besides cleaving H₂ bond, it is reported that benzylic C–H bond insertion can be achieved, illustrating an interesting approach to simultaneously build a Si–C and a Si–H bond. The formation of Si–H_{benzylic} by an acyclic silylene was first reported by *Okazaki et al.* in 1993.^[76] The process follows an intramolecular insertion of the silylene atom in intermediate **L-41** after thermolysis of the corresponding *cis* or *trans* disilene, forming the benzosilacyclobutane species **L-41'**.

Introduction



Scheme 11: Intramolecular insertion of the silylene atom of the intermediate into a C-H bond. Tb = 2,4,6-tris[bis(trimethylsilyl)methyl]phenyl.

Similar intramolecular insertions are also reported for acyclic silylenes **L-32**, **L-35**, and **L-38** with their respective hydrosilane product **L-32''**, **L-35''**, and **L-38''**.

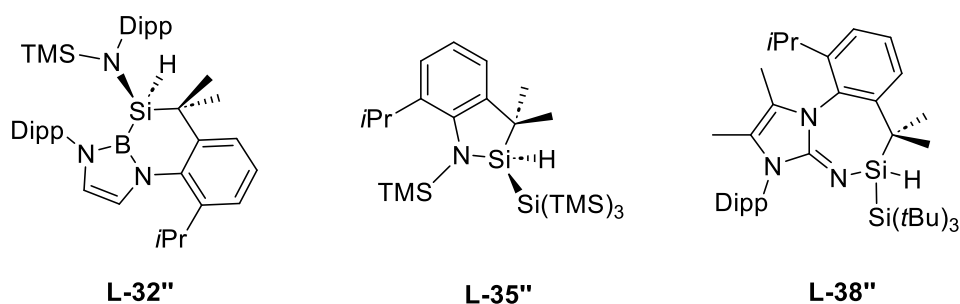
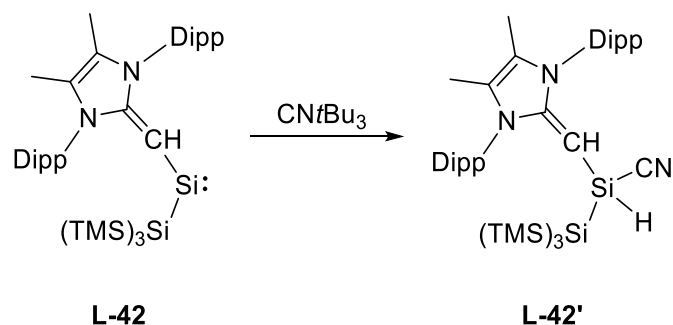


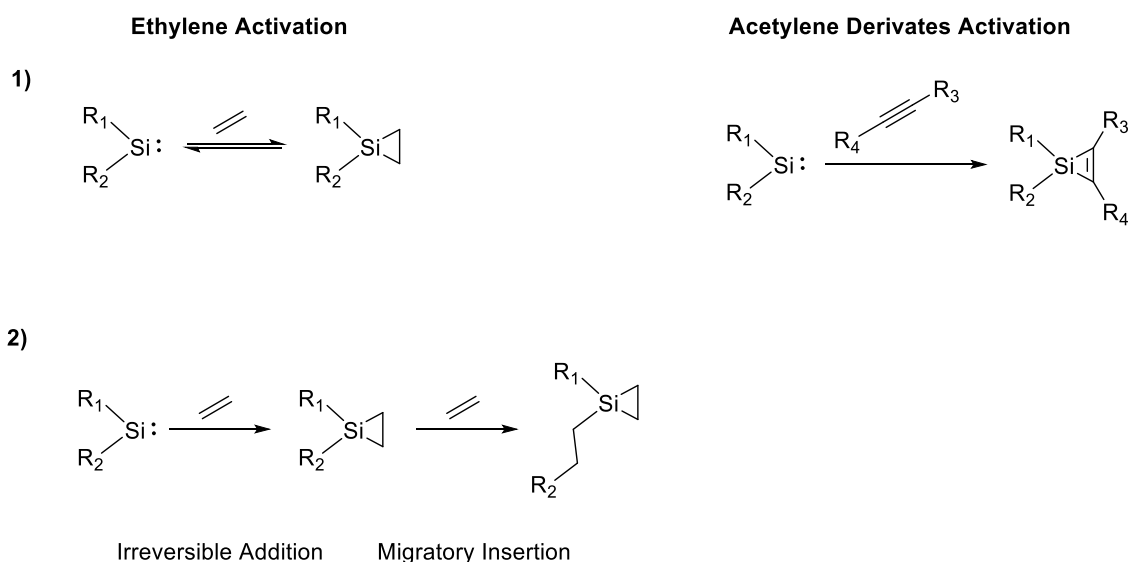
Figure 11: Structure of the respective intramolecular insertion product.

Intermolecular insertion into C-H bonds, on the other hand, is not reported to date. However, vinyl silylsilylene **L-42** is able to cleave and thus activate the primary C-H bond in CN*t*Bu₃, forming a silicon carbonitrile bond (Si-CN) and a Si-H bond.^[74]



Scheme 12: Addition of tertbutyl isonitrile to acyclic silylene **L-42**.

The reactivity of acyclic silylenes towards unsaturated compounds has also been reported extensively to date. The main mechanism is assumed to involve a concerted cycloaddition step involving the n and vacant $3p\pi$ orbitals of the silylene and the π and π^* orbitals of the substrate. In the presence of C–C multiple bonds, the respective silirane or silirene is formed. Regarding cycloadditions with ethylene, different types of activation of the C=C double bond are reported in the literature: Reversible (Scheme 13, route **1**) and irreversible activation (Scheme 13, route **2**), the latter occasionally combined with migratory insertion of the ethylene fragment.



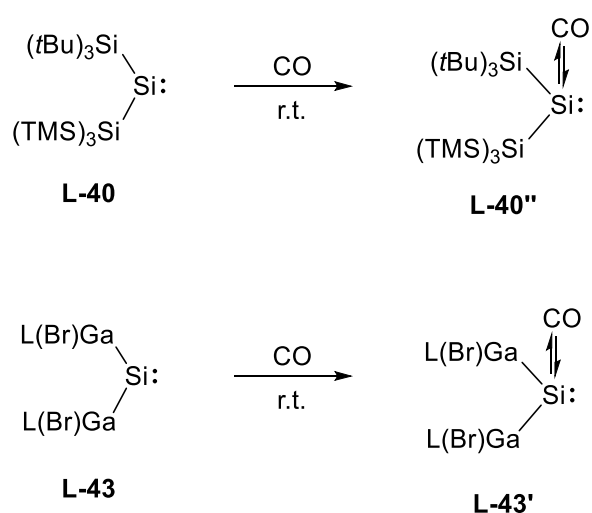
Scheme 13: Different types of π -bond activation by acyclic silylenes.

Among all acyclic silylenes, solely compound **L-33** and **L-34** can reversibly coordinate ethylene, which can be arguably considered as a type of “side-on complexation” by a silylene center reminiscent of transition metals.^[77] Simple, irreversible addition of ethylene without followed-up insertion is, e.g., reported for the already mentioned compound **L-40**. Migratory insertion after forming the respective silirane species was first found in silylsilylene **L-35**. Thereby, the silirane structure forms readily at room temperature. When elevating the reaction temperature to 60 °C, the “coordinated” ethylene fragment is inserted into the Si–Si bond of the silyl ligand, and one more fragment of ethylene can be activated by the silylene atom, which was tracked with deuterated ethylene (C_2D_4) in an NMR

Introduction

spectroscopic experiment.^[78] A likewise reactivity is also reported for silirane **L-37** by *Inoue* and *Rieger et al.*, whereby the cyclohexyl ring is released during the process. Despite the coordination of a second ethylene fragment, follow-up migratory insertions are not observed in silylene species. Cycloaddition of acetylene and derivatives to silylene **L-34** and **L-35** forms the respective silirene functionality and is, so far, an irreversible process.

A key reactivity of silylenes to point out is their behavior towards the C1 building block, carbon monoxide (CO), illustrating a currently evolving finding especially reminiscent of *d*-block metals. Ever since the discovery of $\text{PtCl}_2(\text{CO})_2$ in 1868, transition metal carbonyl complexes have captured widespread interest not only in academia but also in the industry.^[79] These species found wide-ranging applications across industrial processes and organic syntheses due to their conveniences compared to pure, highly toxic CO gas.^[80] The sole drawbacks are the non-abundant and thus expensive transition metals, and their complexes also cause harm to the environment, owing to their toxicity. The question of sustainability has to be greatly considered in chemical research. As a result, special attention was attracted by the silylene-carbonyl complex of the readily mentioned silylated acyclic silylene **L-40** and homoleptic, Ga-coordinated **L-43**.



Scheme 14: Formation of CO complexes by acyclic silylenes. L = NacNac.

The metal-free silicon-carbonyl complexes **L-40''** and **L-43'** were reported independently from each other in 2020 and flag two landmark compounds in the

low-valent silicon chemistry. Structure **L-40**, being in equilibrium with its disilene form as mentioned previously, can coordinate CO and release it quantitatively in the presence of 2,6-dimethyl phenyl isocyanide, the stronger σ -donor compared to CO, forming a silylene-isocyanide species.^[81] The exchange of valence isoelectronic ligands is typically found in *d*-block metal complexes, highlighting the transition-metal mimicry of **L-40**.^[82] Compound **L-43'** shows similar ligand exchange and additional H₂ bond cleavage, amongst other reactivities, demonstrating the versatility of silylene-carbonyl complexes.^[83]

The past decades have brought forward novel low-valent silicon species stabilized by a variety of ligands, which express groundbreaking reactivities towards small molecules, amongst them important building blocks in synthetic chemistry. However, the reversibility of the oxidative addition still remains a big challenge for silicon-containing compounds in general. While germanium and tin are considered more promising candidates in mimicking transition metal catalysts due to their increased tendencies to form oxidative states of +II, they come with their own disadvantages, such as the toxicity of the organo tin compounds. Nonetheless, reversibility was detected in silylenes to a certain degree, which will be highlighted in the next chapter.

1.2.3 “Silepins” – Novel Structures of Acyclic Silylenes

Silacyclo-2,4,6-heptatrienes (i.e., “Silepins”) are conventionally 7-membered, unsaturated, organic ring molecules bearing one Si atom and are the heavier analogs of cyclo-1,3,5-heptatrienes (Figure 12).

Introduction

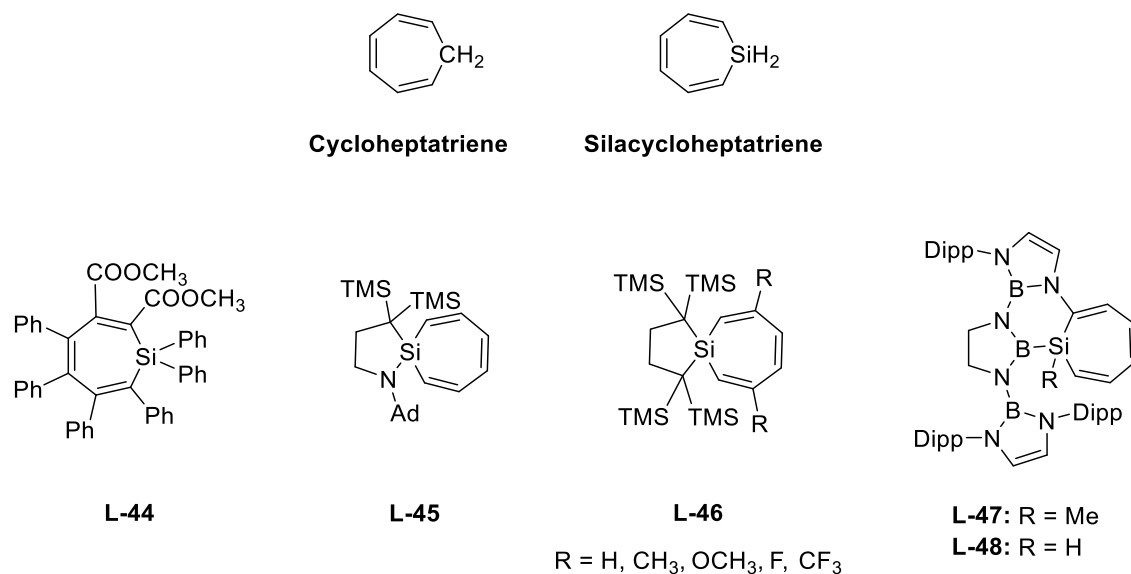
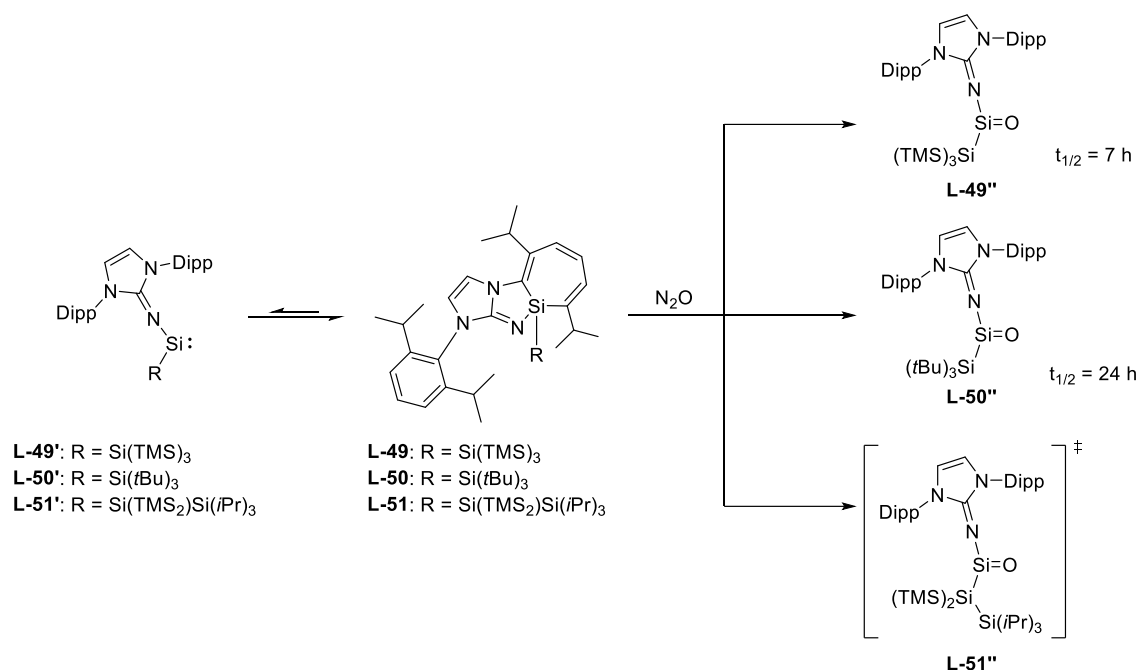


Figure 12: Structure of different silepin species.

Silepins have been elusive for a long time in the first half of the 20th century until the accessibility to modern synthetic methods. To date, there have been a few silepin species isolated^[84], amongst them novel structures based on acyclic silylenes. *Rieger* and *Inoue et al.* demonstrated this new type of silepins in 2017: The unique species displays a Si(II) and Si(IV) interaction. After adding two equivalents of potassium hypersilanide to DippNHC-SiBr_3 , the respective green acyclic silylene **L-49'** formed as expected, whereby the color quickly changed to yellow at room temperature. SC-XRD analysis revealed a silacycloheptatriene moiety (**L-49**) resulting from the intramolecular insertion of the silylene atom into its aromatic framework.^[85] They further demonstrated the silylene-like behavior of this new species: **L-49** can oxidatively cleave dihydrogen, carbon dioxide, and ethylene and thus acts as a “masked” silylene. In 2019, *Cui et al.* reported the ring-expansion products **L-47** and **L-48** obtained *via* salt metathesis of the corresponding lithium precursor, illustrating a distinct different synthesis approach.^[86]

Introduction



Scheme 15: Structure of different isolated silepins and their reactivity towards N₂O.

Subsequent research regarding this new type of silicon-containing compound was conducted by *Rieger and Inoue et al.* (Scheme 15): The silyl ligand attached to the central silicon atom in **L-49** were modified to –Si(*t*Bu)₃ (**L-50**) and –Si(TMS)₂Si(*i*Pr)₃ (**L-51**). Comparing the formed, three coordinated silanone products (Si=O) of **L-49** and **L-50** after exposure to N₂O, the species bearing the tri-*tert*-butyl silyl group (**L-50''**) expressed a prolonged half-life time of 24 hours, while the structural analog bearing the hypersilyl group (**L-49''**) has a half-life time of 7 h.^[87] Silepin **L-51** quickly rearranges to the respective oxygen-bridged cyclo disiloxane with two equivalents of N₂O. The transient silanone **L-51''** is proposed to be the first intermediate in the rearrangement.^[88] The drastic differences between the silanone structures are solely created by the silyl ligand modification: The seemingly minor changes influence the electronic and steric properties of the silylene atom and, therefore, its reactivity. The substituent effect also shows in the equilibrium of the “open” silylene and the “closed” silepin form: **L-49** and **L-50** stay as silepins at ambient temperatures while **L-51** displays a r.t. observable interconversion between both forms. Furthermore, adding two methyl groups to the NHC backbone in **L-50** while simultaneously keeping the tri-*tert*-butyl silyl ligand as it is, the

Introduction

respective silylene center in readily mentioned **L-38** does not display any intramolecular insertions and stays in the “open” form.

The interplay between Si(II) and Si(IV) in silepins based on acyclic silylenes opens up new fields of research regarding catalytic applications of silicon-containing compounds. The reversibility of the oxidative states of the silicon center illustrates a great potential for a backformation of the silepin after the transfer of activated small molecules to a receiving substrate. Regarding this, reactivity studies mentioned above have outlined the application of different ligands in order to tune the electronic and steric properties of the silylene atom in silepins, which may favor a potential backformation. It is readily shown that the applied imine- and silyl ligands have a significant impact on the reactivity of the resulting silylene atom, which has not been extensively investigated for silepins yet. This work is therefore dedicated to gaining insight into the substitution effect and resulting reactivity of these silicon species called silepins and the pursuit of a silicon-mediated catalysis.

2. Scope of This Work

To date, low valent main group chemistry delivered a series of novel compounds bearing Ge, Sn, and Pb centers showing intriguing properties amongst them species capable of full catalytic cycles. Even though groundbreaking chemistry was detected in low valent and low coordinated silicon to some extent, a full catalytic cycle remains a scarce finding. Silylenes, reminiscent of transition metal complexes in their reactivity and properties, have been widely investigated by scientists in the past decades. When put in the right environment, the silylene atom is capable of undergoing oxidative addition towards small molecules and thus “activating” them, similar to transition metal centers. The extensive research brought forward a unique silicon-containing species, the so-called “silepins”. Being the intramolecular insertion product of the respective “open” silylene structure, the “closed” silepin form acts like a masked silylene reactivity-wise. As reported in the literature, the equilibrium between both forms is so far largely influenced by silyl ligand variations.

Therefore, the major aim of this work is to synthesize new silepin species based on acyclic silylenes. To achieve this challenge, the selection of the respective ligands is a crucial step: The substituent has to simultaneously stabilize the low-valent silicon center and allow a silepin formation. The readily applied NHI, being an excellent π -donating ligand in general, can also be applied in this case to thermodynamically stabilize the silylene center. In the first task of this work, the ^{Dipp}NHC moiety in the NHI will be modified to a ^{Cyc}cAAC (Figure 13). Cyclic alkyl amino carbenes have improved π -accepting and σ -donating properties compared to conventional NHCs and are thus widely applied in the stabilization of main group and transition metal complexes ever since their isolation. Additionally, cAACs possess a Dipp group in their base structure, which is fundamental for the aimed intramolecular insertion and subsequent silepin formation. The cyclohexyl group in ^{Cyc}cAAC, moreover, can act as a “flexible” bulk in the final product, allowing new steric features around the

Scope of This Work

silicon center. The hypersilyl ligand ($-\text{SiTMS}_3$) is kept the same for easier comparison of the formed silepins to literature.

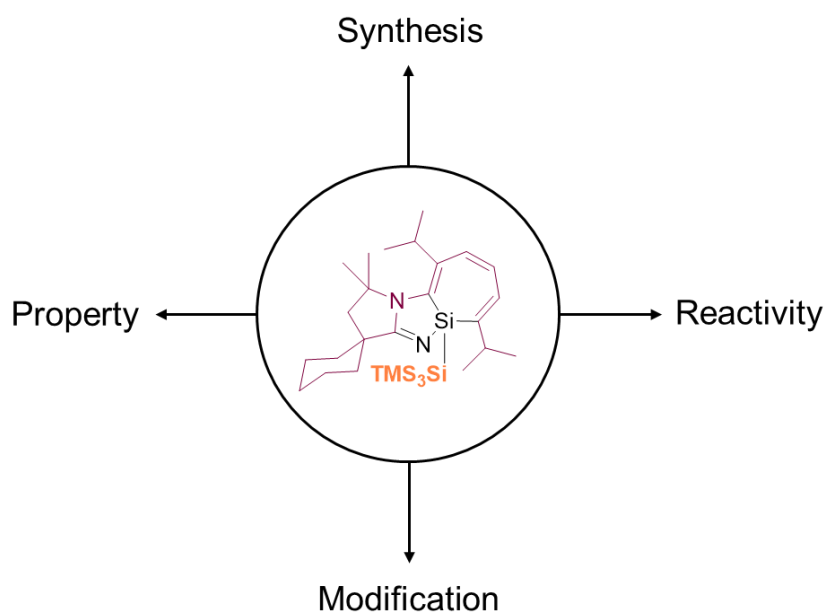


Figure 13: Aimed structure of the new silepin and subsequent investigations.

After the isolation, the new silepin structure should be subsequently investigated regarding its reactivity towards small molecules. Further comparison to literature-known compounds should conclude the effects of the imine ligand modification.

The influence of silyl ligand variation, on the other hand, is further researched in the second task of the thesis. The original hypersilyl ($-\text{SiTMS}_3$) is swapped to a sterically demanding bistrimethylsilyl-triphenylsilyl silyl group ($-\text{SiTMS}_2\text{SiPh}_3$) bearing aromatic moieties, which should additionally change the overall electronic properties of the stabilizing silyl ligand. The desired ligand, $\text{KSiTMS}_2\text{SiPh}_3$, should be isolated with literature-known procedures and applied in combination with either *Dipp*NHC- or *CycAAC*-based imine ligand to effectively stabilize the resulting silylene product. Upon successful syntheses and intramolecular insertions, all newly obtained silepins should be compared relatively to each other regarding their chemical and physical properties in order to draw conclusions on the substituent effects in such molecules.

3. Isolation of a New Silepin with an Imine Ligand Based on Cyclic Alkyl Amino Carbene

Titel: "Isolation of a New Silepin with an Imine Ligand Based on Cyclic Alkyl Amino Carbene"

Status: Research Article, first published online October 20th, 2023

Journal: European Journal of Inorganic Chemistry

Publisher: Wiley-VCH

DOI: 10.1002/ejic.202300568

Authors: Jin Yu Liu, Teresa Eisner, Shigeyoshi Inoue and Bernhard Rieger

Note: J.Y. Liu planned and executed all experiments, conducted the SC-XRD measurements, and wrote the manuscript. T. Eisner performed the theoretical studies. Prof. S. Inoue contributed valuable mental input. All work was performed under the supervision of Prof. B. Rieger.

Content: After the isolation of the first silepin based on acyclic silylene, as mentioned in the upper part of this work, further investigations of these novel compounds were carried out due to their interplay between the "open" Si(II) form (silylene) and their "closed" Si(IV) form (silepin). We isolated a new silepin with an imine ligand based on a cyclohexyl cyclic alkyl amino carbene (^{Cyc}AAAC) instead of the previously applied diisopropylphenyl *N*-heterocyclic carbene (^{Dipp}NHC). The new species showed an enhanced stability in its "closed" silepin conformation, which, however, is able to open up to its "open" silylene form in the presence of a suitable small molecule as its counterpart. Thus, the oxidative addition of CO₂, silanes, and olefins was observed. Moreover, DFT studies showed that the HOMO-LUMO gap of the respective silylene form is greater than its predecessor bearing the imine ligand containing ^{Dipp}NHC, demonstrating the importance of substituents in these types of species. Single crystal XRD could furthermore prove the successful isolation of all new compounds.

Isolation of a New Silepin with an Imine Ligand Based on Cyclic Alkyl Amino Carbene

Jin Yu Liu,^[a] Teresa Eisner,^[b] Shigeyoshi Inoue,^[b] and Bernhard Rieger^{*[a]}

To date, there are solely a handful of silacycloheptatriene structures (silepins) based on acyclic silylenes described in the literature. The unique property of such compounds is the interconversion between their silepin and silylene forms, which has raised great interest due to their potential catalytic applications. Herein, we want to report a new silyl substituted

silepin with an implemented Cy-CAAC moiety, presumably enhancing the stability of the respective low-valent species. In this work, we will demonstrate the synthesis and facile purification of a newly isolated silepin with an imine ligand based on a cyclic alkyl amino carbene as well as its typical silylene-like behavior towards small molecules.

Introduction

Extraordinary advances have been made in the past decades regarding the chemistry of low-valent silicon compounds. With the isolation of the first-ever room temperature stable divalent silicon species (A) by *Jutzi et al.* (Figure 1),^[1] silylenes received particular interest from main group chemists due to their amphiphilic character: As a result of their extensively reduced tendencies to hybridize, the lone pair orbital (HOMO) of silylenes possesses a high *s* character and can act as an electron density donor while the vacant *p*-orbitals (LUMO) can functionalize as electron density acceptor.^[2] This phenomenon is reminiscent of frontier orbitals of *d*-block metals, thus allowing silylenes to mimic the reactivity of complexes bearing a transition metal center.^[3] Extensive syntheses and studies of acyclic silylenes demonstrated their unique properties due to narrow HOMO-LUMO gaps and open coordination sites enabling easy accessibility of the frontier orbitals.^[4] Sterical flexibility furthermore allows facile coordination of small

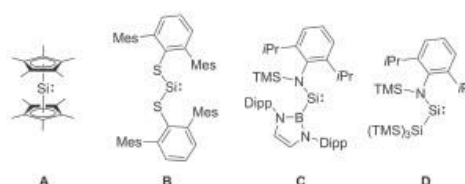


Figure 1. Selected examples of acyclic silylenes (Dipp = Diisopropyl phenyl, TMS = trimethylsilyl).

molecules to the Si(II) center, thus enhancing the reactivity towards oxidative addition.^[5] The first ever stable acyclic silylenes under ambient temperatures, B and C, were separately reported in 2012.^[6] One year later, *Aldridge et al.* reported another room-temperature stable silyl silylene (D) with a hypersilyl group instead of the previously applied boron carbenoid ligand in C.^[7]

The divalent silicon atom in C and D is observed to insert into one of the methine C–H bonds of the diisopropyl phenyl moiety at elevated temperatures, forming the respective heterocyclic ring (Figure 2). In both cases, the intramolecular C–H bond cleavage was found to be an irreversible process.

Similar intramolecular insertion of silylene atoms was reported in 2017. *Rieger and Inoue et al.* have isolated an acyclic iminosilylsilylene (E), which undergoes an insertion into the C=C bond of its own aromatic ligand framework, forming a

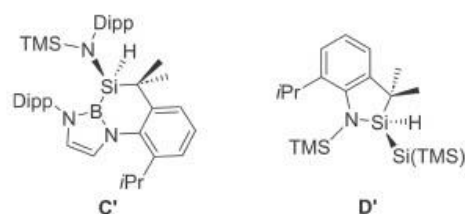


Figure 2. Intramolecular C–H insertion product of C and D, respectively.

[a] J. Y. Liu, Prof. Dr. B. Rieger
Department of Chemistry
School of Natural Sciences
Wacker Chair of Macromolecular Chemistry
Lichtenbergstraße 4
85748 Garching bei München (Germany)
E-mail: rieger@tum.de
Homepage: <http://www.ch.nat.tum.de/makro/startseite/>

[b] T. Eisner, Prof. Dr. S. Inoue
Department of Chemistry
School of Natural Sciences
Institute for Silicon Chemistry
Technical University of Munich Technical University of Munich
Lichtenbergstraße 4
85748 Garching bei München (Germany)

Supporting information for this article is available on the WWW under <https://doi.org/10.1002/ejic.202300568>

© 2023 The Authors. European Journal of Inorganic Chemistry published by Wiley-VCH GmbH. This is an open access article under the terms of the Creative Commons Attribution Non-Commercial NoDerivs License, which permits use and distribution in any medium, provided the original work is properly cited, the use is non-commercial and no modifications or adaptations are made.

Isolation of a New Silepin with an Imine Ligand Based on Cyclic Alkyl Amino Carbene

silepin (sila-cycloheptatriene) at room temperature (Figure 3).^{8d} Silepin E acts like a “masked” acyclic silylene and shows characteristic silylene-like behavior, e.g., oxidative addition of small molecules such as dihydrogen, CO₂, and ethylene. This illustrates the first reversible intramolecular insertion of a silylene center. Related compounds, such as F and G, were consecutively investigated by Rieger’s and Inoue’s group, whereby the latter demonstrated a room-temperature observable equilibrium between the respective silepin (G) and silylene species (G’), highlighting the importance of substituent effects on the reactivity of silepins.^{8d} In 2019, Cui *et al.* isolated two more silacycloheptatriene species by an electrophilic substitution of an anionic silanocaradienyllithium structure with MeOTf and NEt₃Cl yielding H and I, whereby the silicon center can be released from its silepin form by adding an NHC.¹⁰ Even though other examples of compounds bearing a silacycloheptatriene moiety were isolated, e.g., J and K, their reactivity is not as thoroughly investigated as the ones mentioned, and no reversibility was determined to our knowledge.^{10,11}

The intramolecular formation of silepin rings is assumed to improve the respective species’ stability while maintaining an acyclic silylene’s reactivity. In this work, we want to further investigate ligand influences on the silicon center by applying a cyclic alkyl amino carbene (cAAC) based imine ligand to isolate the respective low-valent silicon compound. Due to their improved σ -donating and π -accepting abilities compared to NHCs, cAACs have received vast attention ever since their isolation and are widely applied in the field of small molecule activation and the stabilization of reactive main group and transition metal complexes.¹² Hence, we want to present a synthetic route to a new silepin with a modified imine ligand bearing a Cy-cAAC moiety, capable of activating small molecules as a “masked” silylene despite the enhanced stability compared to contemporary reported structures as suggested by DFT calculations.

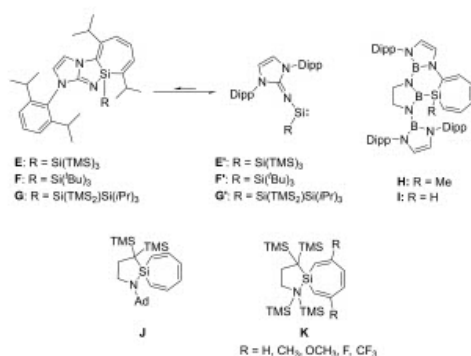
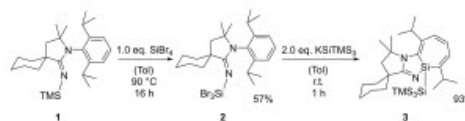


Figure 3. Structures of selected silacycloheptatriene species.

Results and Discussion

The syntheses to the respective imine ligand precursor (1) were carried out according to the procedures reported by Braunschweig *et al.* (Scheme 1),¹³ whereby silicon tetrabromide was added in a following step yielding 2.¹⁴ The final product, silepin 3, is isolated by substitution and a subsequent reduction with two equivalents of potassium hypersilanide (KSITMS₃). As stated by our group, the side product (BrSiTMS₃) of the final step could not be separated from silepin E. However, we found an easy method to purify the new silepin 3: The bromide species can be extensively removed by washing the mixture with acetonitrile. We assume that this method couldn’t be applied to silepin E due to the sigma donation of MeCN inducing an adduct formation leading to the undesired open silylene form of E.

After the purification, the formation of the desired silepin 3 is firstly analyzed by NMR spectroscopy: ¹H NMR spectrum shows asymmetrical aromatic proton shifts of the Dipp group around 6.3 to 6.6 ppm, which is likewise found in reported structures (E–G) hinting a successful intramolecular insertion of the silicon atom into its aromatic ligand framework. The ²⁹Si NMR spectrum displays the characteristic silepin silicon atom (Si1, Figure 4) signal at 17.6 ppm. This shift is remarkably similar to the known species (e.g. 16.1 ppm for E), supporting our findings. The high field shifted signal at –135.7 ppm is typical for the electron-rich hypersilyl silicon atom (Si2, Figure 4). Single crystal XRD analysis could confirm the silacycloheptatriene



Scheme 1. Final steps of the synthetic pathway to 3.

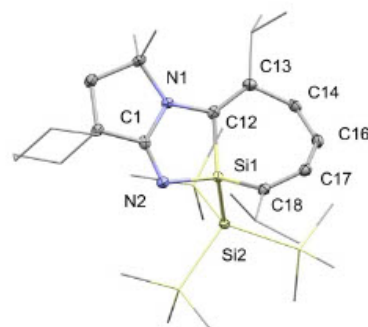


Figure 4. Molecular structure of compound 3 with ellipsoids set at the 50% probability level. Hydrogen atoms are omitted for clarity. Part of the Cy-cAAC moiety and the TMS groups are simplified as wireframes. Selected bond lengths: Si1–C12 1.895(2) Å, Si1–C18 1.863(2) Å, Si1–N2 1.754(2) Å, Si1–Si2 2.355(1) Å, N2–C1 1.278(2) Å. Selected angles: C12–Si1–C18 106.86°, N2–Si1–C18 111.83°, Si1–C12–C13 123.91°, Si1–C18–C17 115.66°.

Isolation of a New Silepin with an Imine Ligand Based on Cyclic Alkyl Amino Carbene

structure of **3**. The seven-membered silepin ring, as suggested by selected bond lengths and angles, is found to be in a "folded" conformation with a C12-Si1-C18 angle of 106.86° which is roughly in accordance with silepin E (105.3°) as reported by our group in 2017.

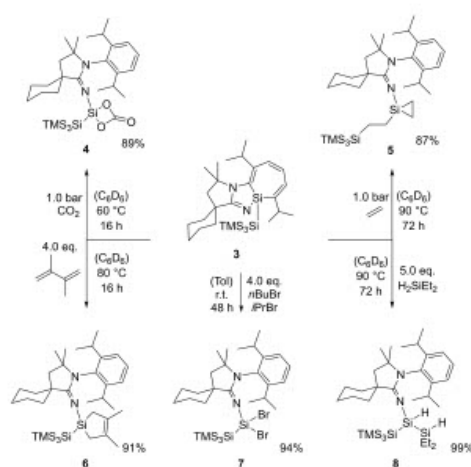
Due to its related structure motives to literature known silepins E–G, we were convinced of its direct usage as an acyclic silylene. As a matter of fact, **3** is found to react in a similar fashion towards small molecules as common acyclic silylenes: In the presence of a suitable reactant, **3** is capable of cleaving covalent bonds thus oxidatively activating small molecules, as shown in Scheme 2.

Over the past decades, the binding of CO₂ by metal-free compounds has raised the particular interest of main-group chemists. *Jutzl et al.* were the first to describe the formation of

the silicon biscarbonato complex **L** (Figure 5).^[5] Monomeric coordinating carbonato groups are a scarce occurrence with silylenes, and only a few are described in the literature to the present day, e. g., in **M**, **N** by *Tacke et al.*^[16] and **O**, **P**, **Q** by *Inoue and co-workers*. Silepin **3**, mechanistically analogous to *Jutzl's* descriptions, can convert one equivalent of CO₂ to CO while forming the respective silanone as the intermediate, which subsequently reacts with one additional equivalent of CO₂ to **4**. The formation of the Si(IV) carbonato moiety was confirmed with SC-XRD analysis. Furthermore, we observed an ethylene insertion into the Si-Si bond at room temperature after 30 days, forming silirane **5** (Figure 6). This process can be significantly accelerated by elevating the temperatures to 90 degrees Celsius. Comparable structures (**S**, **T**) were recently reported in the literature.^[17] Such reactivity of acyclic silylenes towards ethylene was extensively studied by our group beforehand: The formation of **R** is spectroscopically proven with deuterated ethylene, whereby a migratory insertion mechanism could be determined.^[18] A likewise reaction is assumed with silepin **3**. Not only are there hardly any examples of such compounds in the field of low-valent silicon chemistry reported, but the respective molecular depiction is even more scarce. To our best knowledge, the only literature-known crystal structure of ethylene insertion products is the one of compound **R**. In our case, we could isolate single crystals suitable for SC-XRD analysis in pentane.

Interestingly, silepin **3** does not show insertion of any kind towards 2,3-Dimethyl-1,3-butadiene. Instead, we could determine the silacyclopentene **6** as the product of a [4+1] cycloaddition reaction. Analogous reactivity is reported and investigated by our group before with silylsilylene **D**, which, again, underlines the silylene-like reactivity of Cy-cAAC imine-based silepin **3**.

Regarding the reactivity towards C–X bonds, we added isopropyl bromide and *n*-butyl bromide to **3** in two separate



Scheme 2. Reactivity of Cy-cAAC silepin **3** towards various small molecules.

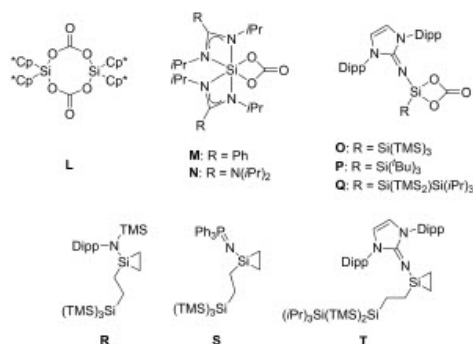


Figure 5. Selected literature known silicon carbonato and silirane compounds.

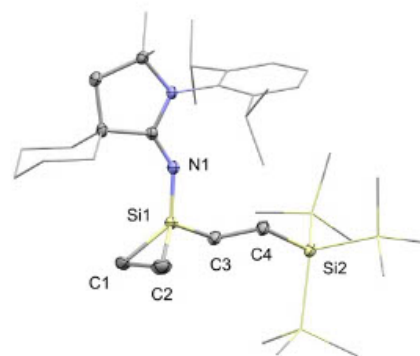


Figure 6. Molecular structure of silirane **5** with ellipsoids set at the 50% probability level. Hydrogen atoms are omitted for clarity. Part of the Cy-cAAC moiety and the TMS groups are simplified as wireframes. Selected bond length: Si1-C1 1.867(1) Å, Si1-C2 1.831(2) Å, Si1-C3 1.861(1) Å, Si2-C4 1.907(1) Å, C1-C2 1.607(2) Å, C3-C4 1.543(2) Å.

attempts. A complete conversion could be achieved readily at room temperature after 20 hours. However, ^1H and ^{29}Si NMR suggested an identical product in both attempts. Additional SC-XRD analysis supported the assumed outcome of the reaction: Instead of an oxidative addition of the alkyl bromides cleaving the C–Br bond, we found a full bromination of silepin **3** to the respective dibromo species **7**. Herein, we assume a mechanism involving radicals due to the enhanced stability of bromine radicals. Additionally, to C–X bonds, we were especially interested in the oxidative addition of silanes due to potential applications in hydrosilylation as an industrial usage. Therefore, as the simplest representative, diethyl silane was applied as a model compound for investigations. A successful conversion to **8** could be determined, resulting in two Si–H bonds potentially able to react with double bonds. We applied a variety of substrates bearing C=C bonds as well as aldehydes, ketones, and imines. Unfortunately, decomposition or inactivity was determined as the reaction outcome, leading to the assumption that a transfer from such Si(IV) species is not feasible.

Despite being a “masked” silylene, **3** is inert towards the strong and nonpolar bond of dihydrogen compared to silepin **E** or reported silylenes **C** and **D** with related structure motifs, which suggests an overall improved stabilization of the Si1 atom in **3** after our application of a Cy-cAAC containing imine ligand. This phenomenon is assumed to be affected by the increased silepin silylene interconversion energy barrier in molecule **3** compared to structures **E/E'** and **G/G'**. This observation and the calculated HOMO-LUMO gap of 3.188 eV supported our theory that the ligand modification from an NHC- to a Cy-cAAC-containing imine moiety led to enhanced stability of the resulting silepin **3**, which underlines the significance of substituent effects on low-valent silicon species.

The calculated HOMO-LUMO gap of 3.188 eV is comparably on the larger side than that of reported silylenes (typical values between 2–4 eV). Additionally, the measured melting point of compound **3** (122 °C) is well above the value of silepin **E** (99.2 °C), being the pre-modified version of **3**. These data validate our observations and support the hypothesis that silepin **3** indeed possesses an advanced stability after the ligand

modification, emphasizing the impact of substituent effects on the reactivity of silepins.

Conclusions

In summary, we have reported a new silepin (**3**) with a modified imine ligand based on a cyclohexyl cyclic alkyl amino carbene. The reactivity of **3** as a “masked” silylene is verified by reactivity studies with various small molecules, whereby, in great contrast to its closely related structure **E**, an inactivity of **3** towards oxidative addition of dihydrogen was observed. We assume a larger silepin silylene interconversion energy barrier in molecule **3** compared to structures **E/E'** and **G/G'**. This observation and the calculated HOMO-LUMO gap of 3.188 eV supported our theory that the ligand modification from an NHC- to a Cy-cAAC-containing imine moiety led to enhanced stability of the resulting silepin **3**, which underlines the significance of substituent effects on low-valent silicon species.

Experimental Section

Material and Methods: All manipulations were carried out under argon atmosphere using standard *Schlenk* or glovebox techniques. Glassware was heat-dried under vacuum prior to use. Unless otherwise stated, all chemicals were purchased commercially and used as received. All solvents were refluxed over sodium, distilled, and deoxygenated. Deuterated solvents were obtained commercially and were dried over 3 Å molecular sieves. All NMR samples were prepared under argon in *J. Young* PTFE tubes. Cy-cAAC and KSITMS_3 were synthesized according to procedures described in the literature.^{13,14} Carbon dioxide (5.0) and ethylene (3.5) were purchased from Westfalen AG and used as received. NMR spectra were recorded on Bruker AV-500 C or AV-400 spectrometers at ambient temperature (300 K) unless otherwise stated. ^1H , ^{13}C , and ^{29}Si NMR spectroscopic chemical shifts (δ) are reported in ppm. $\delta(^1\text{H})$ and $\delta(^{13}\text{C})$ were referenced internally to the relevant residual solvent resonances. $\delta(^{29}\text{Si})$ was referenced to the signal of tetramethylsilane (TMS) ($\delta = 0$ ppm) as the external standard. Liquid Injection Field Desorption Ionization Mass Spectrometry (LIFDI-MS) was measured directly from an inert atmosphere glovebox with a *Thermo Fisher Scientific* Exactive Plus Orbitrap equipped with an ion source from Linden CMS. Melting points were determined in sealed glass capillaries under inert gas with a *Büchi* Melting Point B-540.

Synthesis of 1: Cy-cAAC (1.34 g, 4.12 mmol, 1.0 eq.) is dissolved in toluene (20 mL), and TMSN_3 (1.37 mL, 10.3 mmol, 2.5 eq.) is added. The mixture is stirred at 90 °C for 16 h. The product is obtained upon evaporation of the solvent as an off-white solid (1.62 g, 95%). ^1H NMR (500 MHz, C_6D_6): δ [ppm] = 7.20 (dd, $J = 8.5, 6.8$ Hz, 1H, H_Ar), 7.15–7.10 (m, 2H, H_Ar), 3.16–3.04 (m, 2H, $\text{CH}(\text{CH}_2)_2$), 1.90–1.85 (m, 1H, H_Cy), 1.84 (s, 1H, CH_2), 1.79 (s, 1H, CH_2), 1.77–1.33 (m, 9H, H_Cy), 1.32–1.22 (m, 12H, CH_2), 1.19 (d, $J = 6.9$ Hz, 3H, CH_3), 1.14 (d, $J = 6.7$ Hz, 3H, CH_3), 1.02 (s, 4H, H_Me), 0.27 (s, 5H, H_Me). ^{13}C NMR (126 MHz, C_6D_6): δ [ppm] = 173.16 (C=N), 150.92 (C_Ar), 133.87 (C_Ar), 124.96 (C_Ar), 123.89 (C_Ar), 62.20 (C–N), 47.32 (N–C–C), 38.03 (C–C=N), 30.23 (C_O), 29.15 (C_O), 26.80 (C_O), 26.03 (CH_3), 23.29 (CH_3), 4.44 (TMS). ^{29}Si NMR (99 MHz, C_6D_6): δ [ppm] = –18.74. LIFDI-MS: $m/z = 412.3258$ [1]⁺. Melting point: 91.9 °C.

Synthesis of 2: Cy-cAACNTMS (1.63 g, 3.94 mmol, 1.0 eq.) is dissolved in toluene (25 mL), and SiBr_4 (0.49 mL, 3.94 mmol, 1.0 eq.) is added. The mixture is stirred at 90 °C for 16 h. The solvent is

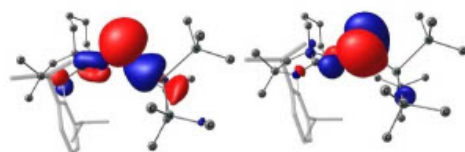


Figure 7. Visualization of the structure optimization. Calculation of HOMO and LUMO energy levels at the B3LYP/6-311+G(d,p) level of theory for the open silylene form of **3**. HOMO: 445.2797 kJ/mol (–4.615 eV), LUMO: –137.6845 kJ/mol (–1.427 eV).

Isolation of a New Silepin with an Imine Ligand Based on Cyclic Alkyl Amino Carbene

evaporated in *vacuo*. After *Whatman* filtration, the product is obtained as a powder (1.36 g, 57%). $^1\text{H NMR}$ (500 MHz, C_6D_6): δ [ppm] = 7.24–7.22 (m, 2H, H_A), 7.14 (d, $J = 1.0$ Hz, 1H, H_B), 2.89 (hept, $J = 6.8$ Hz, 2H, $\text{CH}(\text{CH}_3)_2$), 2.40–2.32 (m, 2H, CH_2), 1.71 (s, 2H, H_C), 1.66–1.50 (m, 5H, H_D), 1.46 (d, $J = 6.7$ Hz, 6H, CH_3), 1.41–1.33 (m, 1H, H_E), 1.24 (d, $J = 6.7$ Hz, 6H, CH_3), 1.21–1.10 (m, 2H, H_F), 0.95 (s, 6H, CH_3). $^{13}\text{C NMR}$ (126 MHz, C_6D_6): δ [ppm] = 172.32 (C=N), 147.62 (C_A), 130.75 (C_B), 129.05 (C_C), 124.29 (C_D), 63.50 (C=C=N), 48.81 (C=C=N), 45.65 (C=C=N), 35.21 (C_E), 29.30 (C_F), 28.95 (CH), 26.70 (C_G), 25.02 (CH_2), 23.11 (CH_3), 22.15 (CH_3). $^{29}\text{Si NMR}$ (99 MHz, C_6D_6): δ [ppm] = –107.85. LIFDI-MS: $m/z = 604.0107$ [2]⁺. Melting point: 159.5°C.

Synthesis of 3: Cy-cAAC-SiBr₃ (120 mg, 198 μmol, 1.0 eq.) and K₂SiTMS₃ (113 mg, 396 μmol, 2.0 eq.) is dissolved in toluene (3 mL) and stirred at r.t. for 1 h. After evaporation of the solvent, pentane (5 mL) is added, and the suspension is filtered through a PE syringe filter. Pentane is then removed, and the product is precipitated with MeCN (8 mL). Pure Cy-cAAC silepin is obtained after centrifugation and separation of the solvent (113 mg, 93%). $^1\text{H NMR}$ (500 MHz, C_6D_6): δ [ppm] = 6.61 (d, $J = 13.0$ Hz, 1H, H_A), 6.38 (dd, $J = 5.8$, 1.2 Hz, 1H, H_B), 6.33 (dd, $J = 13.0$, 6.1 Hz, 1H, H_C), 3.25 (hept, $J = 6.8$ Hz, 1H, $\text{CH}(\text{CH}_3)_2$), 3.04 (hept, $J = 6.7$ Hz, 1H, $\text{CH}(\text{CH}_3)_2$), 2.19–2.11 (m, 1H, CH), 2.08–2.01 (m, 1H, CH), 1.84–1.77 (m, 2H, H_D), 1.69–1.46 (m, 8H, H_E), 1.25–1.19 (m, 15H, CH_3), 1.05 (d, $J = 6.8$ Hz, 3H, CH_3), 0.41 (s, 27H, H_{Me}). $^{13}\text{C NMR}$ (126 MHz, C_6D_6): δ [ppm] = 179.53 (C=N), 146.54 (C_A), 135.61 (C_B), 133.72 (C_C), 128.93 (C_D), 123.71 (C_E), 58.28 (C=N), 52.75 (C=C=N), 42.38 (C=C=N), 37.51 (C_F), 36.79 (C_G), 33.98 (C_H), 31.17 ($\text{CH}(\text{CH}_3)_2$), 31.12 ($\text{CH}(\text{CH}_3)_2$), 29.03 (C_I), 25.96 (C_J), 24.88 (CH_3), 23.21 (CH_3), 22.99 (CH_3), 22.84 (CH_3), 22.67 (CH_3), 20.65 (CH_3), 3.36 (C_{TMS}). $^{29}\text{Si NMR}$ (99 MHz, C_6D_6): δ [ppm] = 172.5, –9.29, –135.71. LIFDI-MS: $m/z = 614.3743$ [3]⁺. Melting point: 122.4°C.

Synthesis of 4: Cy-cAAC silepin (15 mg, 24.4 μmol) is solved in C_6D_6 (0.5 mL) and filled into a PTFE *Young* tube. The solution is frozen with liquid nitrogen and degassed. Subsequently, gaseous CO_2 (1 bar) is introduced, and the tube is sealed afterward. The mixture is heated to 60°C for 16 hours. After evaporation of the solvent, the product is obtained as a pale-yellow oil (15.7 mg, 88% purity) containing compound 4 (14.7 mg, 89% yield) and SiTMS₄ (0.93 mg) as the impurity.

$^1\text{H NMR}$ (500 MHz, C_6D_6): δ [ppm] = 7.16–7.14 (m, 1H, H_A), 7.06 (d, $J = 7.3$ Hz, 2H, H_B), 2.84 (hept, $J = 6.9$ Hz, 2H, $\text{CH}(\text{CH}_3)_2$), 2.12 (td, $J = 13.1$, 3.8 Hz, 2H, C-CH₂), 1.67–1.59 (m, 5H, H_C), 1.56–1.45 (m, 5H, H_D), 1.29 (d, $J = 6.7$ Hz, 6H, CH_3), 1.16 (d, $J = 6.7$ Hz, 6H, CH_3), 0.88 (s, 6H, CH_3), 0.29 (s, 27H, H_{Me}). $^{13}\text{C NMR}$ (126 MHz, C_6D_6): δ [ppm] = 174.20 (C=N), 150.97 (C_A), 148.15 (C_B), 131.53 (C_C), 129.22 (C_D), 124.78 (C=O), 63.77 ($\text{C}(\text{CH}_3)_2$), 48.72 (C=C(CH₃)₂), 46.20 (C=C=N), 35.95 (C_E), 29.39 ($\text{CH}(\text{CH}_3)_2$), 29.29 ($\text{CH}(\text{CH}_3)_2$), 28.03 (C_F), 25.22 (C_G), 23.53 (CH_3), 22.73 (CH_3), 2.79 (C_{TMS}). $^{29}\text{Si NMR}$ (99 MHz, C_6D_6): δ [ppm] = –9.64 (TMS), –28.31 ($\text{SiO}_2\text{C=O}$), –134.20 (SiTMS₃). LIFDI-MS: $m/z = 675.3645$ [4 + H]⁺.

Synthesis of 5: Cy-cAAC silepin (15 mg, 24.4 μmol) is solved in C_6D_6 (0.5 mL) and filled into a PTFE *Young* tube. The solution is frozen with liquid nitrogen and degassed. Subsequently, gaseous ethylene (1 bar) is introduced, and the tube is sealed afterward. The mixture is heated to 90°C for 72 hours. After evaporation of the solvent, the product is obtained as a pale-yellow oil (14.3 mg, 21.3 μmol, 87%). $^1\text{H NMR}$ (500 MHz, C_6D_6): δ [ppm] = 7.21 (dd, $J = 8.4$, 6.9 Hz, 1H, H_A), 7.14 (d, $J = 8.3$ Hz, 2H, H_B), 3.01 (hept, $J = 6.7$ Hz, 2H, $\text{CH}(\text{CH}_3)_2$), 2.18 (td, $J = 13.2$, 3.6 Hz, 2H, C-CH₂), 1.77–1.46 (m, 10H, H_C), 1.32 (d, $J = 6.7$ Hz, 6H, CH_3), 1.25 (d, $J = 6.8$ Hz, 6H, CH_3), 1.19–1.12 (m, 4H, $\text{NSi}(\text{CH}_3)_2$), 1.09–1.04 (m, 2H, $\text{Si}(\text{CH}_3)_2\text{Si}$), 0.97 (s, 6H, CH_3), 0.94–0.89 (m, 2H, $\text{Si}(\text{CH}_3)_2\text{Si}$), 0.25 (s, 27H, H_{Me}). $^{13}\text{C NMR}$ (126 MHz, C_6D_6): δ [ppm] = 170.73 (C=N), 149.04 (C_A), 133.07 (C_B), 124.09 (C_C), 122.98

(C_D), 61.14 ($\text{C}(\text{CH}_3)_2$), 47.70 (C=C(CH₃)₂), 47.18 (C=C=N), 35.94 (C_E), 29.84 ($\text{CH}(\text{CH}_3)_2$), 29.37 ($\text{CH}(\text{CH}_3)_2$), 27.02 (C_F), 25.82 (C_G), 23.13 (CH_3), 22.93 (CH_3), 12.74 ($\text{NSi}(\text{CH}_3)_2$), 1.44 (C_{TMS}), 0.77 ($\text{Si}(\text{CH}_3)_2\text{Si}$). $^{29}\text{Si NMR}$ (99 MHz, C_6D_6): δ [ppm] = –13.31, –72.85, –77.03. LIFDI-MS: $m/z = 670.4366$ [5]⁺.

Synthesis of 6: Cy-cAAC silepin (15 mg, 24.4 μmol, 1.0 eq.) is solved in C_6D_6 (0.5 mL) and 2,3-dimethylbuta-1,3-diene (11.1 μL, 97.5 μmol, 4.0 eq.) is added. The mixture is filled into a *Young* PTFE tube and heated to 80°C for 16 hours. After evaporation of the solvent, the product is obtained as a white solid (15.5 mg, 22.2 μmol, 91%).

$^1\text{H NMR}$ (500 MHz, C_6D_6): δ [ppm] = 7.21–7.17 (m, 1H, H_A), 7.09 (d, $J = 7.4$ Hz, 2H, H_B), 3.05 (hept, $J = 6.8$ Hz, 2H, $\text{CH}(\text{CH}_3)_2$), 1.98 (td, $J = 13.4$, 3.7 Hz, 2H, C-CH₂), 1.80 (s, 2H, H_C), 1.72 (s, 6H, SiCH_2CH_3), 1.70–1.62 (m, 4H, SiCH_2CH_3), 1.54–1.39 (m, 4H, H_D), 1.34–1.23 (m, 4H, H_E), 1.21 (d, $J = 6.8$ Hz, 12H, CH_3), 1.00 (s, 6H, CH_3), 0.37 (s, 27H, H_{Me}). $^{13}\text{C NMR}$ (126 MHz, C_6D_6): δ [ppm] = 166.52 (C=N), 149.29 (C_A), 134.53 (C_B), 131.07 (C_C), 127.97 (C=C), 124.74 (C_D), 61.10 ($\text{C}(\text{CH}_3)_2$), 47.46 (C=C(CH₃)₂), 47.29 (C=C=N), 36.57 (C_E), 34.61 (C_F), 30.43 (SiCH_2CH_3), 28.89 ($\text{CH}(\text{CH}_3)_2$), 27.77 (CH_3), 25.50 (C_G), 24.29 (CH_3), 22.92 (CH_3), 19.40 (SiCH_2CH_3), 3.67 (C_{TMS}). $^{29}\text{Si NMR}$ (99 MHz, C_6D_6): δ [ppm] = –10.34 (TMS), –18.43 (SiCH_2CH_3), –132.75 (SiTMS₃). LIFDI-MS: $m/z = 696.4501$ [6]⁺. Melting point: 185°C.

Synthesis of 7: Cy-cAAC silepin (10 mg, 16.3 μmol, 1.0 eq.) is solved in toluene (1 mL) and *n*-butyl bromide (7.0 μL, 65.0 μmol, 4.0 eq.) or *iso*-propyl bromide (6.1 μL, 65.0 μmol, 4.0 eq.) is added. The mixture is stirred at 90°C for 24 hours. After evaporation of the solvent, the product is obtained as a yellow oil (12.1 mg, 16.6 μmol, 96% yield for reaction with *n*-butyl bromide and 11.8 mg, 15.2 μmol, 94% yield for reaction with *iso*-propyl bromide). $^1\text{H NMR}$ (400 MHz, C_6D_6): δ [ppm] = 7.15 (d, $J = 4.8$ Hz, 1H, H_A), 7.09 (d, $J = 6.6$ Hz, 2H, H_B), 2.95 (p, $J = 6.8$ Hz, 2H, $\text{CH}(\text{CH}_3)_2$), 2.81 (td, $J = 13.4$, 3.6 Hz, 2H, C-CH₂), 1.81–1.47 (m, 10H, H_C), 1.42 (d, $J = 6.7$ Hz, 6H, CH_3), 1.18 (d, $J = 6.7$ Hz, 6H, CH_3), 0.94 (s, 6H, CH_3), 0.39 (s, 27H, H_{Me}). $^{13}\text{C NMR}$ (126 MHz, C_6D_6): δ [ppm] = 173.56 (C=N), 147.70 (C_A), 132.48 (C_B), 128.60 (C_C), 124.71 (C_D), 63.52 ($\text{C}(\text{CH}_3)_2$), 49.31 (C=C(CH₃)₂), 47.23 (C=C=N), 34.78 (C_E), 29.79 (C_F), 28.76 (C_G), 28.39 ($\text{CH}(\text{CH}_3)_2$), 24.05 (CH_3), 22.44 (CH_3), 2.83 (C_{TMS}). $^{29}\text{Si NMR}$ (99 MHz, C_6D_6): δ [ppm] = –10.16 (TMS), –53.00 (SiBr₂), –101.03 (SiTMS₃). LIFDI-MS: $m/z = 697.4562$ [7–8]⁺.

Synthesis of 8: Cy-cAAC silepin (10 mg, 16.3 μmol, 1.0 eq.) is solved in C_6D_6 (0.5 mL) and diethyl silane (10.5 μL, 81.3 μmol, 5.0 eq.) is added. The mixture is filled into a *Young* PTFE tube and heated to 80°C for 16 hours. After evaporation of the solvent, the product is obtained as a white solid (11.3 mg, 16.6 μmol, 99%). $^1\text{H NMR}$ (500 MHz, C_6D_6): δ [ppm] = 7.19 (t, $J = 7.6$ Hz, 1H, H_A), 7.12 (dd, $J = 7.8$, 1.8 Hz, 1H, H_B), 7.09 (dd, $J = 7.6$, 1.8 Hz, 1H, H_C), 6.41 (d, $J = 4.1$ Hz, 1H, SiHSiHEt_2), 4.05 (qq, $J = 4.1$, 2.2 Hz, 1H, SiHSiHEt_2), 3.16–3.06 (m, $J = 6.7$ Hz, 2H, $\text{CH}(\text{CH}_3)_2$), 2.56 (m, 1H, C-CH₂), 2.47 (m, 1H, C-CH₂), 1.86 (m, 1H, H_D), 1.76–1.57 (m, 6H, H_E), 1.37 (d, $J = 6.7$ Hz, 3H, H_F), 1.29–1.20 (m, 18H, CH_3), 1.05 (s, 3H, CH_2CH_3), 1.04–0.99 (m, 1H, CH_2CH_3), 0.95 (s, 3H, CH_2CH_3), 0.94–0.78 (m, 3H, CH_2CH_3), 0.34 (s, 29H, H_{Me}). $^{13}\text{C NMR}$ (126 MHz, C_6D_6): δ [ppm] = 170.11 (C=N), 149.28 (C_A), 148.89 (C_B), 134.13 (C_C), 124.59 (C_D), 124.17 (C_E), 61.34 ($\text{C}(\text{CH}_3)_2$), 48.63 (C=C(CH₃)₂), 48.31 (C=C=N), 37.47 (C_F), 34.84 (C_G), 30.83 (C_H), 29.32 (C_I), 29.25 (C_J), 29.20 ($\text{CH}(\text{CH}_3)_2$), 29.17 ($\text{CH}(\text{CH}_3)_2$), 28.13 (CH_3), 25.72 (CH_3), 24.24 (CH_3), 23.41 (CH_3), 23.35 (CH_3), 23.15 (CH_3), 11.31 (CH_2CH_3), 10.18 (CH_2CH_3), 3.78 (C_{TMS}). $^{29}\text{Si NMR}$ (99 MHz, C_6D_6): δ [ppm] = –9.50 (TMS), –18.77 (SiHEt₂), –60.03 (SiHSiHEt₂), –130.80 (SiTMS₃). LIFDI-MS: $m/z = 702.4455$ [8]⁺. Melting point: 172.5°C.

Supporting Information

Experimental details for all newly synthesized compounds, DFT calculation details, and single crystallographic data can be found in the Supporting Information (SI). The authors have cited additional references within the SI ([20–32]).

Deposition Number(s) 2293615 (for Compound 2), 2293616 (for Compound 3), 2293619 (for Compound 4), 2293620 (for Compound 5), 2293618 (for Compound 6), 2293617 (for Compound 7) contain(s) the supplementary crystallographic data for this paper. These data are provided free of charge by the joint Cambridge Crystallographic Data Centre and Fachinformationszentrum Karlsruhe Access Structures service.

Acknowledgements

All authors want to thank Wacker Chemie AG for their scientific contributions and financial support. Furthermore, we want to express our appreciation towards Fabrizio E. Napoli for the LIFDI-MS measurements and Martin E. Doleschal for the scientific discussions. Open Access funding enabled and organized by Projekt DEAL.

Conflict of Interests

The authors declare no conflict of interest.

Data Availability Statement

The data that support the findings of this study are available in the supplementary material of this article.

Keywords: low-valent compounds · main group elements · silepins · silicon · silylenes

[1] P. Jutz, D. Kanne, C. Krüger, *Angew. Chem. Int. Ed.* 1986, 25, 164.
[2] C. Shan, S. Yao, M. Driess, *Chem. Soc. Rev.* 2020, 49, 6733.
[3] a) S. Fujimori, S. Inoue, *Commun. Chem.* 2020, 3, 175; b) D. Reiter, R. Holzner, A. Porzelt, P. Frisch, S. Inoue, *Nat. Chem.* 2020, 12, 1131; c) P. P. Power, *Nature* 2010, 463, 171; d) C. Weetman, S. Inoue, *ChemCatChem* 2018, 10, 4213; e) R. L. Melen, *Science* 2019, 363, 479.
[4] S. Fujimori, S. Inoue, *Eur. J. Inorg. Chem.* 2020, 2020, 3131.
[5] L. Wang, Y. Li, Z. Li, M. Kira, *Coord. Chem. Rev.* 2022, 457, 214413.
[6] a) A. V. Protchenko, K. H. Birjukumar, D. Dange, A. D. Schwarz, D. Vidovic, C. Jones, N. Kaltsayannis, P. Mountford, S. Aldridge, *J. Am. Chem. Soc.* 2012, 134, 6500; b) B. D. Rekker, T. M. Brown, J. C. Fettinger, H. M. Tuononen, P. P. Power, *J. Am. Chem. Soc.* 2012, 134, 6504.
[7] A. V. Protchenko, A. D. Schwarz, M. P. Blake, C. Jones, N. Kaltsayannis, P. Mountford, S. Aldridge, *Angew. Chem. Int. Ed.* 2013, 52, 568.
[8] D. Wendel, A. Porzelt, F. A. D. Herz, D. Sarkar, C. Jandl, S. Inoue, B. Rieger, *J. Am. Chem. Soc.* 2017, 139, 8134.

[9] a) D. Wendel, D. Reiter, A. Porzelt, P. J. Altmann, S. Inoue, B. Rieger, *J. Am. Chem. Soc.* 2017, 139, 17193; b) T. Eisner, A. Kostenko, F. Hanusch, S. Inoue, *Chem. Eur. J.* 2022, 28, e202202330.
[10] L. Zhu, J. Zhang, C. Cui, *Inorg. Chem.* 2019, 58, 12007.
[11] a) T. Kosai, S. Ishida, T. Iwamoto, *Angew. Chem. Int. Ed.* 2016, 55, 15554; b) T. Kosai, S. Ishida, T. Iwamoto, *Chem. Commun.* 2015, 51, 10707.
[12] a) E. Welz, J. Böhnke, R. D. Dewhurst, H. Braunschweig, B. Engels, *J. Am. Chem. Soc.* 2018, 140, 12580; b) R. Jazsar, M. Soleilhavoup, G. Bertrand, *Chem. Rev.* 2020, 120, 4141; c) Y. K. Loh, M. Melaimi, D. Murz, G. Bertrand, *J. Am. Chem. Soc.* 2023, 145, 2064; d) Y. K. Loh, M. Melaimi, M. Gemblin, D. Murz, G. Bertrand, *Nature* 2023, <https://doi.org/10.1038/s41586-023-06539-x>; e) A. Kostenko, S. Inoue, *Chem.* 2023, <https://doi.org/10.1016/j.chempr.2023.10.010>.
[13] J. T. Goettel, H. Gao, S. Dotzauer, H. Braunschweig, *Chem. Eur. J.* 2020, 26, 1136.
[14] M. W. Lu, C. Merten, M. J. Ferguson, R. McDonald, Y. Xu, E. Rivard, *Inorg. Chem.* 2015, 54, 2040.
[15] P. Jutz, D. Eikenberg, A. Möhrke, B. Neumann, H.-G. Stammer, *Organometallics* 1996, 15, 753.
[16] a) F. M. Mück, J. A. Baus, M. Nutz, C. Burschka, J. Poater, F. M. Bickelhaupt, R. Tacke, *Chem. Eur. J.* 2015, 21, 16665; b) K. Junold, M. Nutz, J. A. Baus, C. Burschka, C. Fonseca Guerra, F. M. Bickelhaupt, R. Tacke, *Chem. Eur. J.* 2014, 20, 9319.
[17] A. Sauwein, M. Nobis, S. Inoue, B. Rieger, *Inorg. Chem.* 2022, 61, 9983.
[18] D. Wendel, W. Eisenreich, C. Jandl, A. Pöthig, B. Rieger, *Organometallics* 2016, 35, 1.
[19] a) C. Marschner, *Eur. J. Inorg. Chem.* 1998, 1998, 221; b) V. Lavallo, Y. Canac, C. Präsang, B. Donnadiu, G. Bertrand, *Angew. Chem. Int. Ed.* 2005, 44, 5705; c) R. Jazsar, R. D. Dewhurst, J.-B. Bourg, B. Donnadiu, Y. Canac, G. Bertrand, *Angew. Chem. Int. Ed.* 2007, 46, 2899.
[20] APEX suite of crystallographic software, APEX 3, Version 2019–1.0, Bruker AXS Inc., Madison, Wisconsin, USA, 2019.
[21] SAINT, Version 8.40A and SADABS, Version 2016/2, Bruker AXS Inc., Madison, Wisconsin, USA, 2016/2019.
[22] G. M. Sheldrick, *Acta Crystallogr. Sect. A* 2015, 71, 3–8.
[23] G. M. Sheldrick, *Acta Crystallogr. Sect. C* 2015, 71, 3–8.
[24] C. B. Hübschle, G. M. Sheldrick, B. Dittrich, *J. Appl. Crystallogr.* 2011, 44, 1281–1284.
[25] *International Tables for Crystallography, Vol. C* (Ed.: A. J. Wilson), Kluwer Academic Publishers, Dordrecht, The Netherlands, 1992, Tables 6.1.1.4 (pp. 500–502), 4.2.6.8 (pp. 219–222), and 4.2.4.2 (pp. 193–199).
[26] C. F. Macrae, I. J. Bruno, J. A. Chisholm, P. R. Edgington, P. McCabe, E. Pidcock, L. Rodriguez-Monge, R. Taylor, J. van de Streek, P. A. Wood, *J. Appl. Crystallogr.* 2008, 41, 466–470.
[27] D. Kratzert, I. Krossing, *J. Appl. Crystallogr.* 2018, 51, 928.
[28] A. L. Spek, *Acta Crystallogr. Sect. D* 2009, 65, 148–155.
[29] C. Lee, W. Yang, R. G. Parr, *Phys. Rev. B* 1988, 37, 785–789.
[30] S. H. Vosko, L. Wilk, M. Nusair, *Can. J. Phys.* 1980, 58, 1200–1211.
[31] A. D. Becke, *J. Chem. Phys.* 1993, 98, 5648–5652.
[32] M. J. Frisch, G. W. Trucks, H. B. Schlegel, G. E. Scuseria, M. A. Robb, J. R. Cheeseman, G. Scalmani, V. Barone, G. A. Petersson, H. Nakatsuji, X. Li, M. Caricato, A. V. Marenich, J. Bloino, B. G. Janesko, R. Gomperts, B. Mennucci, H. P. Hratchian, J. V. Ortiz, A. F. Izmaylov, J. L. Sonnenberg, D. Williams-Young, F. Ding, F. Lipparini, F. Egidi, J. Goings, B. Peng, A. Petrone, T. Henderson, D. Ranasinghe, V. G. Zakrzewski, J. Gao, N. Rega, G. Zheng, W. Liang, M. Hada, M. Ehara, K. Toyota, R. Fukuda, J. Hasegawa, M. Ishida, T. Nakajima, Y. Honda, O. Kitao, H. Nakai, T. Vreven, K. Throssell, J. A. Montgomery Jr., J. E. Peralta, F. Ogliaro, M. J. Bearpark, J. J. Heyd, E. N. Brothers, K. N. Kudin, V. N. Staroverov, T. A. Keith, R. Kobayashi, J. Normand, K. Raghavachari, A. P. Rendell, J. C. Burant, S. S. Iyengar, J. Tomasi, M. Cossi, J. M. Millam, M. Mene, C. Adamo, R. Cammi, J. W. Ochterski, R. L. Martin, K. Morokuma, O. Farkas, J. B. Foresman, D. J. Fox, *Gaussian 16*; Gaussian, Inc.: Wallingford CT, 2016.

Manuscript received: September 14, 2023
Revised manuscript received: October 9, 2023
Accepted manuscript online: October 20, 2023
Version of record online: November 10, 2023

4. Isolation and Reactivity of Silepins with a Sterically Demanding Silyl Ligand

Title: "Isolation and Reactivity of Silepins with a Sterically Demanding Silyl Ligand"

Status: Research Article, first published online May 20th, 2024

Journal: European Journal of Inorganic Chemistry

Publisher: Wiley-VCH

DOI: 10.1002/ejic.202400045

Authors: Jin Yu Liu, Shigeyoshi Inoue and Bernhard Rieger

Note: J.Y. Liu planned and executed all experiments, conducted the SC-XRD measurements, and wrote the manuscript. Prof. S. Inoue contributed valuable mental input. All work was performed under the supervision of Prof. B. Rieger.

Content: The synthesis and characterization of silepins based on acyclic silylenes has led to the realization that substituent effect in such molecules is of great importance. In this work, we further investigated the impact of ligand modifications with the isolation of two new silepins with a modified silyl ligand going from $-\text{SiTMS}_3$ (hypersilyl group) to $-\text{SiTMS}_2\text{SiPh}_3$ (bis(trimethylsilyl)triphenylsilyl silyl group). Besides forming the readily known and well-investigated silacycloheptatriene structure at room temperature, we found an intramolecular C–H_{sp2} bond cleavage of the triphenyl silyl group by the silylene atom at elevated temperatures in both new silepins. Additionally, we isolated iron(0)carbonyl complexes of known and new silepins in order to further understand the impact of the silyl ligand variation. Subsequent FT-IR measurements of the complexes could shed light on their electronic properties relative to each other and thus give insight into the substituent effect in such compounds.

Isolation and Reactivity of Silepins with a Sterically Demanding Silyl Ligand



EurJIC
European Journal of Inorganic Chemistry

Research Article
doi.org/10.1002/ejic.202400045

Chemistry
Europe
European Chemical
Societies Publishing

www.eurjic.org

Isolation and Reactivity of Silepins with a Sterically Demanding Silyl Ligand

Jin Yu Liu,^[a] Shigeyoshi Inoue,^[b] and Bernhard Rieger*^[a]

Silacycloheptatriene (silepin) species are novel silicon compounds reported in recent years. The interplay between the “closed” silepin and the “open” silylene form enables an enhanced stability of the low valent species while maintaining a high reactivity towards small molecules. In this work, two new silepins of similar structures to literature known compounds bearing modified silyl ligands are reported. A unique intra-

molecular activation of an aromatic hydrogen is found, and the respective formed hydrosilanes are characterized. We further synthesized iron(0) carbonyl complexes of known and new silepins in order to investigate their electronic properties relative to each other to gain more insight into substitution effect in such compounds.

Introduction

In the past decades, a series of low-valent silicon species were isolated and reported (Figure 1). Among all newly discovered silylene compounds, acyclic silylenes are attracting major focus of main-group chemists due to the particularly small energy difference of the frontier orbitals and the sterical flexibility.^[1] These unique properties allow them to exhibit similar behavior towards small molecules, such as oxidative addition, which is reminiscent of transition metal complexes.^[2]

Intramolecular insertions in low-valent silylene species are scarcely reported to date.^[3] Usually, a steric approximation of neighboring groups within a molecule is required, as well as a highly reactive silylene atom. Due to the natural electron deficiency of the Si(II) atom,^[4] such processes are usually irreversible, leading to the final Si(VI) species, e.g. A', B', E' (Figure 2), from the respective silylene A, B, E (Figure 2).^[5]

In 2017, we described the isolation of the first silepin based on an acyclic silylene (Figure 3).^[6] The ligand applied here consists of a hypersilyl group ($-\text{Si}(\text{TMS})_3$) and a *N*-heterocyclic

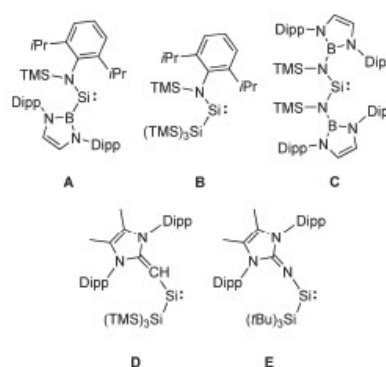


Figure 1. Selected literature known acyclic silylenes. Dipp = 2,6-Diisopropyl phenyl. TMS = Trimethylsilyl.

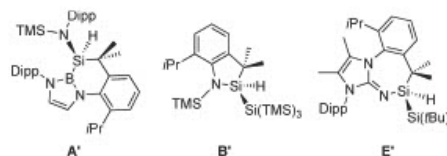


Figure 2. Literature known intramolecular insertions of Si(II) centers into the C-H bonds of attached Dipp groups.³⁻⁶

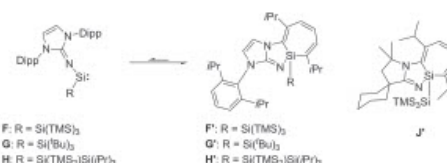


Figure 3. Selected examples of literature known silepins in equilibrium with their acyclic silylene form. *i*Pr = Isopropyl.

[a] J. Yu Liu, Prof. Dr. B. Rieger
TUM School of Natural Sciences
Department of Chemistry
Wacker Institute for Silicon Chemistry
Technical University of Munich
Lichtenbergstraße 4, 85748 Garching bei München (Germany)
E-mail: rieger@tum.de

[b] Prof. Dr. S. Inoue
TUM School of Natural Sciences
Department of Chemistry
Institute of Silicon Chemistry
Technical University of Munich
Lichtenbergstraße 4, 85748 Garching bei München (Germany)

Supporting information for this article is available on the WWW under <https://doi.org/10.1002/ejic.202400045>

© 2024 The Authors. European Journal of Inorganic Chemistry published by Wiley-VCH GmbH. This is an open access article under the terms of the Creative Commons Attribution Non-Commercial NoDerivs License, which permits use and distribution in any medium, provided the original work is properly cited, the use is non-commercial and no modifications or adaptations are made.

Isolation and Reactivity of Silepins with a Sterically Demanding Silyl Ligand

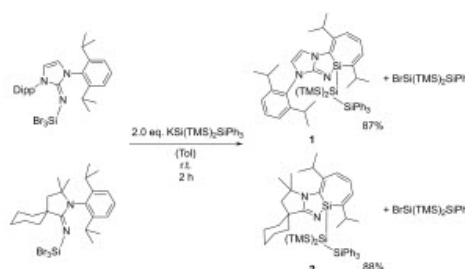
imine (NH). NHIs, conventionally based on NHCs (*N*-heterocyclic carbenes), are σ - and π -electron donating moieties with a vast variety of steric features.⁷¹ In this case, the NHI bearing a 2,6-diisopropyl phenyl (Dipp) group, derived from the ^{DBP}NHC, allows a reversible insertion of F into its aromatic framework, thus possessing a relatively high stability as a silepin (Si(IV)) while maintaining the reactivity of an acyclic silylene (Si(II)). The significant advantage of silepin structures is, therefore, the interplay between both oxidative states (II, IV) of silicon, demonstrating a key feature for potential catalytic applications. Initial studies on substituent effects in such silepin forms were performed with compound G/G' bearing a modified silyl group (-Si(^tBu)₂) as a sigma donating ligand.⁸¹ Upon exposure of F' and G' to N₂O, the respective formed silanone species (R₂Si=O) of G is found to have an enhanced stability. Additionally, silepin G' can be used as a building block in the formation of heterodinuclear Al-Si bonds resulting in the isolation of an aluminata-silene featuring an Al-Si core with a multiple bond character,⁹⁰ thus, demonstrating an interesting utilization of silepin species in the isolation of novel main-group compounds. Further investigations on silepins were conducted throughout recent years, whereby a room temperature observable equilibrium of H and H' was reported in 2022.¹⁰⁰ This was mainly achieved by the application of a sterically congested bis(trimethylsilyl)trisopropylsilylanide. H/H' shows an enhanced reactivity towards small molecules, illustrating, once again, the importance of substituent effect on such structures. Subsequently, our group reported a new silepin (J') with a modified imine ligand based on a cyclic alkyl amino carbene (cAAC).¹¹¹ This type of *N*-heterocyclic imine (NHI) based on cAAC has drawn attention in recent years.¹¹² The electronic features, as well as steric demands of cAACs relative to NHC, are distinctively different from each other, allowing effective stabilization of not only transition metal complexes but also pioneering main-group compounds.¹¹³ Structure J' is found to have an increased stability in its closed silepin form compared to its related structure F', and contemporary reported similar compounds as shown in reactivity studies and DFT calculations.

In this work, we want to present two new silepin structures contributed to the question whether we can influence the electronic properties and reactivity of the silepin with simple ligand modifications.

Results and Discussion

Synthesis of New Silepins

After our previously reported silepins F', G' and J', we intended to further investigate the impact of silyl ligand modification. For this purpose, we first isolated the silyl ligand KSi(TMS)₂SiPh₃ with comparably different electronics and steric features than the previously applied KSi(TMS)₃ following literature known procedures.¹⁴⁴ Silepins 1 and 2 (Scheme 1) are obtained analogously to our reported synthetic route with the inseparable side product BrSi(TMS)₂SiPh₃ due to their identical solubility.



Scheme 1. Last synthesis step towards the isolation of silepins 1 and 2.

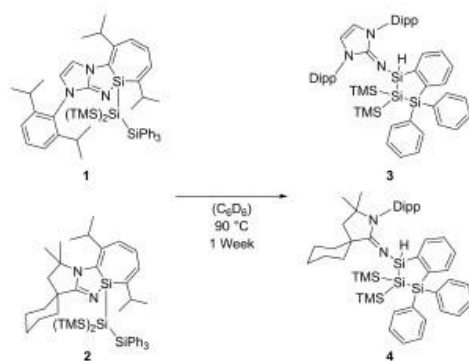
Various purification attempts were made to separate silepins 1 and 2 from their side product. Crystallization in common organic solvents (Hexane, pentane, toluene, THF, Et₂O) and PMe₃, sometimes working for compounds that don't crystallize in common solvents, did not lead to pure precipitated product nor crystals suitable for SC-XRD analysis. Washing the oily mixture consisting of silepin and side product with HMDSO (hexamethyl disiloxane) and MeCN, the latter reported by us to be able to wash out the side product during the synthesis of silepin J', only resulted in a homogeneous solution. Thus, a suitable purification method has not been found yet.

Analyzing the ¹H NMR spectrum of 1, we observed three asymmetrical aromatic protons (6.08 ppm–6.48 ppm) due to the formed silepin ring with one of the diisopropyl phenyl (Dipp) groups. Additionally, the imidazole ring protons are split into two different doublets at 5.93 ppm and 6.63 ppm with an integral of 1, which is likewise found in its related structure F' due to the asymmetric electronic environment after an intramolecular insertion of the silylene atom. Similar aromatic proton shifts are determined in the ¹H NMR spectrum of 2. The Dipp protons are split and found at 5.79 ppm–6.45 ppm, hinting at a successful intramolecular insertion. Relevant ²⁹Si NMR shifts are listed in Table 1. We will be referring the silicon atom embedded in the silepin ring as "central Si or Si_{central}" and the silicon atom bound to it as "silyl Si or Si_{silyl ligand}" for convenience. We found identical ²⁹Si shifts of the central silicon atom for related structures F' and 1 as well as J' and 2 bearing the same imine ligand motif. Thus, the shift of the central Si in the "closed" silepin form seems not to be affected by the silyl ligand modification from hypersilyl to bis(TMS)triphenylsilyl silyl ligand. Si_{silyl ligand} in 1 and 2 show typical values in the high field shifted area as a result of the electron-rich environment.

Silepin	Si(central)	Si(silyl ligand)
F'	16.1	-135.5
1	16.1	-132.6
J'	17.6	-135.7
2	17.5	-134.1

Interestingly, silepins **1** and **2** can selectively undergo a sp^2C-H activation of the aromatic proton in the triphenylsilyl moiety at elevated temperatures, forming the hydrosilane species **3** and **4**, respectively (Scheme 2). Insertions into aliphatic and aromatic $C-H$ bonds of transition metal centers have been known for decades.^[15] It is, however, rarely found regarding silylenes. Examples of aliphatic $C-H$ cleavage, inter- or intramolecularly, are reported moderately to date, while aromatic $C-H$ bonds are only cleaved intermolecularly to our knowledge.^[16] Due to the previously mentioned purification problems in the synthesis of **1** and **2**, the existing side product, $BrSi(TMS)_2SiPh_3$ could not be successfully removed from **3** and **4** either with the mentioned procedures. Even though the side product stays extensively inactive during the heating process of **1** and **2**, it causes a minor H/Br exchange reaction, forming the respective $Si-Br$ species and $HSi(TMS)_2SiPh_3$. This can be observed in the crystal structure of **4**, whereby a bromide atom with a 2% occupancy is bonding to the Si1 instead of a hydride.

1H NMR spectra show a proton shift for SiH at 5.23 ppm (**3**) and 6.56 ppm (**4**) with ^{29}Si satellites. Both signals possess an almost identical J_{SiH} coupling constant (193.0 Hz for **3**, 190.1 Hz for **4**), which is in a similar range found in related hydrosilane structures A', B', and E'. The central silicon atom adjacent to the hydrogen atom is found at a ^{29}Si NMR shift of -35.5 ppm (**3**) and -42.2 ppm (**4**), displaying, once again, particular similarity to each other. In great contrast to A', B' and E', no insertion into the *isopropyl* $C-H$ bond of the Dipp moiety was found. Thus, it is noteworthy that a bond cleavage of a sp^2C-H is preferred to the sp^3C-H in case of silepins **1** and **2**. We assume that a highly reactive silylene atom, as well as a steric approximation of an existing phenyl or aryl group bearing an ortho hydrogen, are crucial for this reactivity, which explains why A, B, and E do not display such behaviors due to the lack of suitable functional groups. The final structure of **4** is supported by SC-XRD analysis (Figure 4). We proposed a likewise structure for **3** because of the similar chemical shifts and coupling constants in the 1H and ^{29}Si NMR spectrum, as discussed above.



Scheme 2. Reaction path to hydrosilanes **3** and **4**.

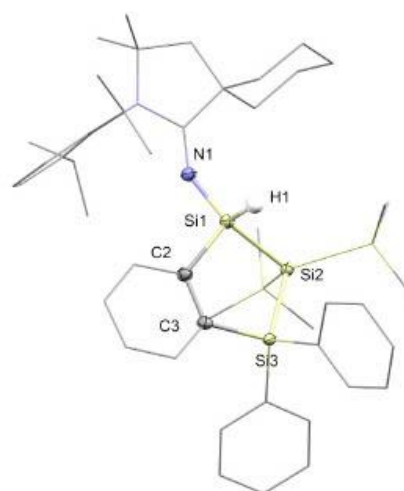


Figure 4. Molecular structure of compound **4** with ellipsoids set at the 50% probability level. The bromide atom (2% occupancy) attached to the Si1 and hydrogen atoms are omitted for clarity. Part of the ^{29}Si AAC moiety and silyl groups are simplified as wireframes. Selected bond length: Si1–H1 1.402(8) Å, Si1–N1 1.687(2) Å, Si1–Si2 2.3608(8) Å, Si2–Si3 2.3575(9) Å, Si3–C3 1.886(2) Å, C2–C3 1.405(3) Å, Si1–C2 1.891(2) Å. Selected angles: C2–Si1–Si2 99.89(7)°, Si1–Si2–Si3 88.83(3)°, C3–Si3–Si2 102.47(7)°, C2–C3–Si3 119.0(2)°, C3–C2–Si1 120.3(2)°.

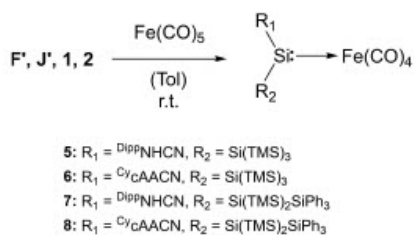
Structures **3** and **4** can be interpreted as the thermodynamically more stable product of the silepin synthesis. This phenomenon also indicates an enhanced stability of F', J' in their silepin form compared to **1**, **2** since no activity of F', J' in C_6D_6 could be determined even after heating at 90 °C for several days.

Fe(CO)₄L Complexes

As reported by our group beforehand, silepins of this type are commonly known as "masked silylenes", which are able to perform small molecule activation. Therefore, we are also interested in the electronic properties of the respective "open" silylene species of **1** and **2**. For this purpose, the respective iron(0) carbonyl complexes of all silepins (F', J', **1**, **2**) reported by our group were synthesized. We expected the formation of a dative bond, as shown in Scheme 3, due to the previously mentioned silylene reactivity.

The straightforward syntheses at room temperature yielded one sole product each as the reaction outcome (**5**, **6**, **7**, **8**). Thereby, we could successfully remove the inseparable side product ($BrSi(TMS)_2SiPh_3$) derived from the last synthesis step of **1** and **2** by precipitating the final product (**7**, **8**) in cold pentane due to the extensive insolubility of the formed iron complex. The ^{29}Si NMR spectra show a significantly downfield shifted signal for the central Si atom in all complexes (Table 2),

Isolation and Reactivity of Silepins with a Sterically Demanding Silyl Ligand



Scheme 3. Reaction of silepins *F'*, *J'*, 1, 2 with iron(0)pentacarbonyl to complexes 5–8.

Complex	Si(central)	CO vibration bands	Si1–Fe1
5	272.7	2007, 1927, 1876	2.246(1)
6	253.1	2005, 1927, 1881	2.2331(7)
7	273.1	2021, 1953, 1920, 1894	2.2345(5)
8	247.5	2027, 1954, 1926, 1900	2.2574(6)

suggesting a formation of the desired open silylene form and the presence of a dative bond. Additionally, we determined similar shifts of the $\text{Si}_{\text{central}}$ in complexes with the same imine ligand (5, 7, and 6, 8). The deviation in the values is thus solely dependent on the silyl ligand. While the difference in the ^{29}Si shifts in 5 and 7 is almost negligible, we can observe a slightly deshielded silylene atom in 6 compared to 8 under consideration of the standard deviation in ^{29}Si NMR spectra. All newly isolated iron complexes could also be characterized with SC-XRD analysis for definite proof (Figure 5). These structures also implement a successful isolation of 1 and 2.

Closer investigations of the Fe1–Si1 bond, we can determine values in the range of comparable, literature reported compounds with no deviation from the norm.^{17,18}

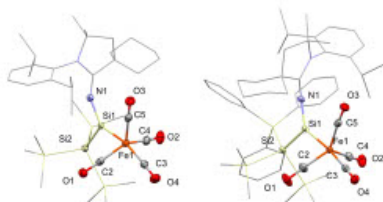


Figure 5. Molecular structure of compound 6 (left) and compound 8 (right) with ellipsoids set at the 50% probability level. Hydrogen atoms are omitted for clarity. Part of the $\text{C}^{\text{v}}\text{AAC}$ moiety and the silyl groups are simplified as wireframes. Selected bond length in structure 6: Fe1–Si1 2.2331(7) Å, Fe1–C2 1.774(2) Å, Fe1–C3 1.795(3) Å, Fe1–C4 1.779(2) Å, Fe1–C5 1.782(3) Å, Si1–Si2 2.3466(9) Å, Si1–N1 1.642(2) Å. Selected angles in structure 6: N1–Si1–Si2 112.56(7)°, Si1–Fe1–C3 165.42(8)°. Selected bond length in structure 8: Fe1–Si1 2.2574(7) Å, Fe1–C2 1.768(2) Å, Fe1–C3 1.785(2) Å, Fe1–C4 1.783(2) Å, Fe1–C5 1.800(2) Å, Si1–Si2 2.4038(6) Å, Si1–N1 1.648(2) Å. Selected angles in structure 8: N1–Si1–Si2 115.04(6)°, Si1–Fe1–C3 172.54(7)°.

To draw conclusions on the electronic properties of the $\text{Si}_{\text{central}}$ and to compare the donor strength of the silylenes to their lighter congener, we added a conventional NHC (IMe_4) to complexes 7 and 8. A ligand exchange can't be determined, thus also excluding the route to possibly obtain pure silepin 1 and 2 by releasing the silylene ligand from their iron carbonyl complexes.

Furthermore, we measured IR spectra of all FeCO_4L ($\text{L} = \text{silylene ligand}$, Scheme 3). The experimentally determined CO stretching frequencies are all within expected ranges.^{18,19} Similar C=O vibrations of complexes 5 and 6 were found, indicating that the imine ligand modification from $\text{D}^{\text{pp}}\text{NHC}$ to $\text{C}^{\text{v}}\text{AAC}$ does not seem to have a significant impact on the silylene atom. However, the increased wavenumber of complexes 7 and 8 show an overall slightly reduced donor strength of the silylene atom, most likely deriving from the altered silyl ligand (from $-\text{Si}(\text{TMS})_3$ to $-\text{Si}(\text{TMS})_2\text{SiPh}_3$). This observation is assumed to be caused by the decreased σ -donation of the silyl ligand to the silylene atom after replacing a TMS with a SiPh_3 group. The ligand modification simultaneously results in a comparably increased π -acceptance of the silylene atom (due to π -acceptor properties of the phenyl groups in SiPh_3), withdrawing electron density from the iron center, leading to higher wavenumbers.²⁰

Conclusions

In summary, we have isolated two new silepin structures 1, 2 bearing a sterically demanding silyl ligand with their inseparable side product $\text{BrSi}(\text{TMS})_2\text{SiPh}_3$ at room temperature. An intramolecular $\text{sp}^2\text{C}-\text{H}$ cleavage forming the respective hydrosilanes was found in both species at elevated temperatures, which are determined as the thermodynamically more stable product of the silepin synthesis. Furthermore, we isolated the $\text{Fe}(\text{CO})_4\text{L}$ ($\text{L} = \text{SiR}_2$) complexes of compounds *F'*, *J'*, 1, 2. Subsequent infrared spectroscopy showed an overall decreased σ -donation and increased π -acceptance of the silylene atom carrying the modified silyl ligand. The altered electronic effects of the stabilizing ligand from a hypersilyl group to a bis(trimethylsilyl)triphenylsilyl silyl group are assumed to cause the observed wavenumbers in the IR spectra. These findings, therefore, show the notable impact of small and simple ligand modifications in novel low-valent silicon compounds.

Experimental Section

All manipulations were carried out under argon atmosphere using standard *Schlenk* or glovebox techniques. Glassware was heat-dried under vacuum prior to use. Unless otherwise stated, all chemicals were purchased commercially and used as received. All solvents were refluxed over sodium, distilled, and deoxygenated prior to use. Deuterated solvents were obtained commercially and were dried over 3 Å molecular sieves prior to use. All NMR samples were prepared under argon in *J. Young* PTFE tubes. $\text{KSi}(\text{TMS})_3$, $\text{KSi}(\text{TMS})_2\text{SiPh}_3$, $\text{D}^{\text{pp}}\text{NHC}$ silepin *F'* and $\text{C}^{\text{v}}\text{AAC}$ silepin *J'* were synthesized according to procedures described in the literature.^{9,11,14} NMR spectra were recorded on Bruker AV-500C or

AV-400 spectrometers at ambient temperature (300 K) unless otherwise stated. ^1H , $^{13}\text{C}\{\text{H}\}$, and $^{29}\text{Si}\{\text{H}\}$ NMR spectroscopic chemical shifts (δ) are reported in ppm. $\delta(^1\text{H})$ and $\delta(^{13}\text{C})$ were referenced internally to the relevant residual solvent resonances. $\delta(^{29}\text{Si})$ was referenced to the signal of tetramethylsilane (TMS, $\delta = 0$ ppm) as external standard. All $^{29}\text{Si}\{\text{H}\}$ NMR spectra underwent auto baseline correction (Whittaker Smoother). FT-IR spectra were recorded on a Vertex 70 from Bruker with a Platinum ATR unit. A solution of the sample in pentane was drop-casted onto the ATR crystal and dried under a stream of nitrogen. Liquid Injection Field Desorption Ionization Mass Spectrometry (LIFDI-MS) was measured directly from an inert atmosphere glovebox with a Thermo Fisher Scientific Exactive Plus Orbitrap equipped with an ion source from Linden CMS. Melting points were determined in sealed glass capillaries under inert gas with a Büchi Melting Point B-540.

Synthesis of 1: $^{99}\text{TcNHC-SiBr}_3$ (120 mg, 198 μmol , 1.0 eq.) and $\text{KSi}(\text{TMS})_2\text{SiPh}_3$ (2.0 eq.) is dissolved in toluene (3 mL) and stirred at r.t. for 1 h. After evaporation of the solvent, pentane (5 mL) is added, and the suspension is filtered through a PE syringe filter. Pentane is then removed, and compound 1 (135 mg, 156 μmol , 87%) is obtained with its side product $\text{BrSi}(\text{TMS})_2\text{SiPh}_3$ (81 mg, 155 μmol , 87%) as a 1:1 inseparable mixture. The yield is calculated with the measured mass of the mixture (216 mg). ^1H NMR (500 MHz, C_6D_6): δ [ppm] = 7.80–7.77 (m, 7H, H_H), 7.76–7.71 (m, 8H, H_H), 7.18–7.16 (m, 15H, H_H side product), 7.16–7.15 (m, 3H, H_H), 6.63 (d, $J = 3.2$ Hz, 1H, N–C–H), 6.46 (d, $J = 12.9$ Hz, 1H, H_H), 6.43 (dd, $J = 6.5$, 1.2 Hz, 1H, H_H), 6.13–6.07 (m, 1H, H_H), 5.93 (d, $J = 2.9$ Hz, 1H, N–C–H), 3.29–3.13 (m, 2H, $\text{CH}(\text{CH}_3)_2$), 3.04–2.89 (m, 2H, $\text{CH}(\text{CH}_3)_2$), 1.39 (d, $J = 6.8$ Hz, 3H, CH_3), 1.22–1.20 (m, 8H, CH_3), 1.14 (dd, $J = 6.8$, 2.4 Hz, 4H, CH_3), 1.09 (dd, $J = 6.8$, 4.7 Hz, 6H, CH_3), 0.92 (d, $J = 6.8$ Hz, 3H, CH_3), 0.29 (s, 9H, HTMS), 0.23 (s, 9H, HTMS), 0.17 (s, 18H, HTMS side product). $^{13}\text{C}\{\text{H}\}$ NMR (126 MHz, C_6D_6): δ [ppm] = 156.81 (C=N), 148.12 (C_Ar), 147.04 (C_Ar), 144.95 (C_Ar), 137.57 (C_Ar), 137.43 (C_H), 136.75 (C_H side product), 135.00 (C_H side product), 133.68 (C_H), 130.58 (C_H), 129.99 (C_H side product), 129.45 (C_H), 129.33 (C_Ar), 129.17 (C_Ar), 128.57 (C_H side product), 128.43 (C_Ar), 125.70 (C_Ar), 124.20 (C_Ar), 124.14 (C_Ar), 117.65 (C–N), 110.12 (C–N), 32.00 ($\text{CH}(\text{CH}_3)_2$), 29.37 ($\text{CH}(\text{CH}_3)_2$), 28.81 (CH_3), 28.48 (CH_3), 26.40 (CH_3), 25.84 (CH_3), 25.40 (CH_3), 23.68 (CH_3), 23.27 (CH_3), 22.91 (CH_3), 22.66 (CH_3), 21.31 (CH_3), 3.89 (C_TMES), 3.58 (C_TMES), 0.03 (C_TMES side product). $^{29}\text{Si}\{\text{H}\}$ NMR (99 MHz, C_6D_6): δ [ppm] = 16.07 ($\text{Si}_{\text{central}}$), –8.50 (Si_{TMES}), –9.53 (Si_{TMES}), –9.55 (SiPh_3), –11.54 (Si_{TMES} side product), –20.27 (SiPh side product), –26.48 ($\text{BrSi}(\text{TMS})_2\text{SiPh}_3$), –132.58 ($\text{Si}(\text{TMS})_2\text{SiPh}_3$). LIFDI-MS: Calculated: $m/z = 863.4338$; Experimental: $m/z = 863.4311$ [1]⁺ (+ 6.65 ppm error).

Synthesis of 2: $^{99}\text{TcAAC-SiBr}_3$ (120 mg, 198 μmol , 1.0 eq.) and $\text{KSi}(\text{TMS})_2\text{SiPh}_3$ (187 mg, 396 μmol , 2.0 eq.) is dissolved in toluene (3 mL) and stirred at r.t. for 1 h. After evaporation of the solvent, pentane (5 mL) is added, and the suspension is filtered through a PE syringe filter. Pentane is then removed, and compound 2 (139 mg, 173 μmol , 88%) is obtained with its side product $\text{BrSi}(\text{TMS})_2\text{SiPh}_3$ (88.8 mg, 173 μmol , 88%) as a 1:1 inseparable mixture. The yield is calculated with the measured mass of the mixture (227 mg). ^1H NMR (500 MHz, C_6D_6): δ [ppm] = 7.86–7.70 (m, 15H, H_H side product), 7.26–7.22 (m, 6H, H_H), 7.21–7.17 (m, 5H, H_H), 7.14 (d, $J = 5.6$ Hz, 4H, H_H), 6.43 (d, $J = 13.1$ Hz, 1H, H_H), 6.31 (d, $J = 5.8$ Hz, 1H, H_H), 5.81 (dd, $J = 13.5$, 5.4 Hz, 1H, H_H), 3.26 (h, $J = 6.8$ Hz, 1H, $\text{CH}(\text{CH}_3)_2$), 2.76 (hept, $J = 7.2$, 6.7 Hz, 1H, $\text{CH}(\text{CH}_3)_2$), 2.09 (d, $J = 17.7$ Hz, 3H, H_C), 1.86–1.77 (m, 2H, CH), 1.73–1.65 (m, 2H, H_C), 1.57 (dd, $J = 13.1$, 2.4 Hz, 2H, H_C), 1.50 (s, 3H, H_C), 1.28–1.23 (m, 9H, CH_3), 1.08 (d, $J = 6.8$ Hz, 3H, CH_3), 1.01 (d, $J = 5.0$ Hz, 3H, CH_3), 1.00 (d, $J = 5.2$ Hz, 3H, CH_3), 0.34 (s, 9H, HTMS), 0.29 (s, 9H, HTMS), 0.15 (s, 18H, HTMS side product). $^{13}\text{C}\{\text{H}\}$ NMR (126 MHz, C_6D_6): δ [ppm] = 179.90 (C=N), 144.99 (C_Ar), 137.52 (C_H side product), 136.75 (C_H side product), 135.00 (C_H), 134.29 (C_H), 133.65 (C_Ar), 129.99 (C_H side product), 129.32 (C_H), 129.13 (C_H), 128.75 (C_H), 128.57 (C_Ar), 128.43 (C_H side product), 125.70 (C_Ar),

124.54 (C_Ar), 58.54 (C–N), 52.87 (C–C–N), 42.40 (C=C–N), 37.24 (C_O), 37.15 (C_O), 32.24 (C_O), 31.26 (C_O), 30.88 ($\text{CH}(\text{CH}_3)_2$), 29.20 ($\text{CH}(\text{CH}_3)_2$), 26.14 (C_O), 25.70 (CH_3), 22.97 (CH_3), 22.83 (CH_3), 22.77 (CH_3), 21.94 (CH_3), 21.30 (CH_3), 3.92 (C_TMES), 3.85 (C_TMES), 0.04 (C_TMES side product). $^{29}\text{Si}\{\text{H}\}$ NMR (99 MHz, C_6D_6): δ [ppm] = 17.53 ($\text{Si}_{\text{central}}$), –8.48 (Si_{TMES}), –8.54 (Si_{TMES}), –9.48 (SiPh), –11.54 (Si_{TMES} side product), –20.28 (Si_{TMES} side product), –26.50 ($\text{BrSi}(\text{TMS})_2\text{SiPh}_3$), –134.08 ($\text{Si}(\text{TMS})_2\text{SiPh}_3$). LIFDI-MS: Calculated: $m/z = 800.4229$; Experimental: $m/z = 800.4213$ [2]⁺ (+ 1.99 ppm error).

Synthesis of 3: A solution of a 1:1 mixture of 1 and $\text{BrSi}(\text{TMS})_2\text{SiPh}_3$ (33 mg) in C_6D_6 is heated to 90 °C for 1 week, forming the intramolecular insertion product 3 in quantitative yield. ^1H NMR (400 MHz, C_6D_6): δ [ppm] = 7.87–7.83 (m, 3H, H_H), 7.81–7.62 (m, 9H, H_H), 7.58–7.53 (m, 2H, H_H), 7.35 (td, $J = 7.4$, 1.2 Hz, 1H, H_H), 7.24–7.16 (m, 10H, H_H side product), 7.15–7.11 (m, 5H, H_H side product), 7.11–7.06 (m, 6H, H_H), 6.05 (s, 2H, N–C–H), 5.23 (s, 1H, with ^{29}Si satellites) $^1\text{J}(\text{SiH}) = 193.0$ Hz, SiH), 3.31 (hept, $J = 6.7$ Hz, 4H, $\text{CH}(\text{CH}_3)_2$), 1.31 (dd, $J = 6.8$, 1.8 Hz, 12H, CH_3), 1.19 (dd, $J = 6.9$, 2.3 Hz, 12H, CH_3), 0.16 (s, 18H, HTMS side product), 0.14 (s, 9H, HTMS), –0.14 (s, 9H, HTMS). $^{13}\text{C}\{\text{H}\}$ NMR (101 MHz, C_6D_6): δ [ppm] = 153.78 (C=N), 148.06 (C_Ar , Si_{ring}), 147.52 (C_Ar , Si_{ring}), 146.67 (C_Ar , Si_{ring}), 145.14 (C_Ar , Si_{ring}), 138.59 (C_Ar , Si_{ring}), 137.73 (C_Ar , Si_{ring}), 136.88 (H_{TMES} side product), 136.76 (C_Ar), 136.53 (C_Ar), 136.44 (C_H), 135.03 (H_{TMES} side product), 134.89 (C_H), 134.79 (C_H), 134.53 (C_H), 129.99 (H_{TMES} side product), 129.65 (C_H), 129.34 (C_H), 129.01 (C_H), 128.65 (C_H), 128.43 (H_{TMES} side product), 124.30 (C_Ar), 124.15 (C_Ar), 115.04 (C–N), 29.06 ($\text{CH}(\text{CH}_3)_2$), 29.02 ($\text{CH}(\text{CH}_3)_2$), 25.66 (CH_3), 25.11 (CH_3), 23.84 (CH_3), 23.78 (CH_3), 2.60 (C_TMES), 2.46 (C_TMES), 0.05 (C_TMES side product). $^{29}\text{Si}\{\text{H}\}$ NMR (99 MHz, C_6D_6): δ [ppm] = –4.60 (Si_{TMES}), –9.01 (Si_{TMES}), –10.11 (SiPh_3), –11.54 (Si_{TMES} side product), –20.27 (SiPh side product), –26.49 ($\text{BrSi}(\text{TMS})_2\text{SiPh}_3$), –35.48 ($\text{Si}_{\text{central}}$), –134.67 ($\text{Si}(\text{TMS})_2\text{SiPh}_3$). LIFDI-MS: Calculated: $m/z = 863.4338$; Experimental: $m/z = 863.4261$ [3]⁺ (+ 12.45 ppm error).

Synthesis of 4: A solution of a 1:1 mixture of 2 and $\text{BrSi}(\text{TMS})_2\text{SiPh}_3$ (33 mg) in C_6D_6 is heated to 90 °C for 1 week, forming the intramolecular insertion product 4 in quantitative yield. ^1H NMR (400 MHz, C_6D_6): δ [ppm] = 7.96–7.92 (m, 2H, H_H), 7.81–7.68 (m, 10H, H_H side product), 7.34 (t, $J = 7.7$ Hz, 1H, H_H), 7.27–7.22 (m, 3H, H_H side product), 7.22–7.19 (m, 2H, H_H side product), 7.19–7.16 (m, 5H, H_H), 7.15–7.01 (m, 8H, H_H), 6.92–6.88 (m, 1H, H_H), 6.56 (s, 1H, with ^{29}Si satellites) $^1\text{J}(\text{SiH}) = 190.1$ Hz, SiH), 3.14 (m, 2H, $\text{CH}(\text{CH}_3)_2$), 2.26–2.13 (m, 2H, CH_2), 2.12 (s, 1H, H_C), 1.94–1.73 (m, 3H, H_C), 1.70–1.58 (m, 4H, H_C), 1.51–1.38 (m, 2H, H_C), 1.29–1.23 (m, 10H, CH_3), 1.13 (d, $J = 6.7$ Hz, 3H, CH_3), 1.07 (d, $J = 9.6$ Hz, 6H, CH_3), 0.41 (s, 9H, HTMS), 0.16 (s, 18H, HTMS side product), 0.05 (s, 9H, HTMS). $^{13}\text{C}\{\text{H}\}$ NMR (101 MHz, C_6D_6): δ [ppm] = 169.94 (C=N), 152.56 (C_Ar , Si_{ring}), 149.60 (C_Ar , Si_{ring}), 149.12 (C_Ar , Si_{ring}), 144.10 (C_Ar , Si_{ring}), 138.83 (C_Ar , Si_{ring}), 137.33 (C_Ar , Si_{ring}), 137.01 (C_H), 136.88 (C_H), 136.76 (C_H side product), 136.42 (C_H), 135.79 (C_H), 135.03 (C_H side product), 134.45 (C_H), 134.26 (C_Ar), 129.99 (C_H side product), 129.34 (C_Ar), 129.24 (C_H), 128.88 (C_H), 128.57 (C_H side product), 125.70 (C_Ar), 124.75 (C_H), 124.62 (C_Ar), 61.00 (C–N), 48.22 (C–C–N), 47.20 (C–C–N), 36.63 (C_O), 35.96 (C_O), 30.92 (C_O), 29.47 (C_O), 29.30 ($\text{CH}(\text{CH}_3)_2$), 29.19 ($\text{CH}(\text{CH}_3)_2$), 27.95 (C_O), 26.77 (CH_3), 25.41 (CH_3), 23.84 (CH_3), 23.74 (CH_3), 22.72 (CH_3), 22.49 (CH_3), 2.81 (C_TMES), 2.78 (C_TMES), 0.05 (C_TMES side product). $^{29}\text{Si}\{\text{H}\}$ NMR (99 MHz, C_6D_6): δ [ppm] = –6.64 (Si_{TMES}), –8.94 (Si_{TMES}), –10.56 (SiPh_3), –11.54 (Si_{TMES} side product), –20.28 (SiPh side product), –26.49 ($\text{BrSi}(\text{TMS})_2\text{SiPh}_3$), –42.19 ($\text{Si}_{\text{central}}$), –129.29 ($\text{Si}(\text{TMS})_2\text{SiPh}_3$). LIFDI-MS: Calculated: $m/z = 800.4229$; Experimental: $m/z = 800.4114$ [4]⁺ (+ 14.36 ppm error).

Synthesis of 5: FeCO_2 (8.00 μL , 59.0 μmol , 2.0 eq.) was added to a solution of $^{99}\text{TcNHC}$ silepin F (20.0 mg, 29.5 μmol , 1.0 eq.) in toluene (1 mL). The mixture was stirred at r.t. for 16 h. The solvent was completely evaporated in *vacuo* to afford the product as an orange oil (18.3 mg, 73%). ^1H NMR (500 MHz, C_6D_6): δ [ppm] = 7.22–7.17 (m, 4H, H_H), 7.07 (dd, $J = 7.4$, 2.0 Hz, 2H, H_H), 6.09 (s, 2H, N–C–H), 3.85 (h, $J = 6.8$ Hz, 2H, $\text{CH}(\text{CH}_3)_2$), 2.82 (hept, $J = 6.8$ Hz, 2H, $\text{CH}(\text{CH}_3)_2$),

Isolation and Reactivity of Silepins with a Sterically Demanding Silyl Ligand

EurJIC
European Journal of Inorganic Chemistry

Research Article
doi.org/10.1002/ejic.202400045

Chemistry
Europe
European Chemical
Societies Publishing

1.57 (d, $J = 6.7$ Hz, 6H, CH₃), 1.30 (d, $J = 6.7$ Hz, 6H, CH₃), 1.11 (d, $J = 6.7$ Hz, 6H, CH₃), 0.98 (d, $J = 6.7$ Hz, 6H, CH₃), 0.22 (s, 27H, H_{TMS}). ¹³C {H} NMR (126 MHz, C₆D₆): δ [ppm] = 215.58 (CO), 152.56 (C=N), 148.33 (C_A), 146.42 (C_A), 133.53 (C_A), 130.66 (C_A), 129.33 (C_A), 125.70 (C_A), 125.14 (C_A), 124.40 (C_A), 118.19 (CH-N), 28.77 (CH₃), 28.61 (CH₃), 26.54 (CH₃), 26.27 (CH₃), 23.39 (CH₃), 23.15 (CH₃), 2.96 (C_{TMS}). ²⁹Si{H} NMR (80 MHz, C₆D₆): δ [ppm] = 272.72 (Si), -9.45 (TMS), -92.89 (Si(TMS)₃). LIFDI-MS: Calculated: $m/z = 845.3014$; Experimental: $m/z = 845.2930$ [5]⁺ (+9.93 ppm error). IR (cm⁻¹): 2958 (m), 2892 (m), 2006 (s), 1906 (s), 1875 (s), 1524 (s), 1457 (m), 1243 (s), 1034 (m), 825 (s).

Synthesis of 6: FeCO₃ (9.95 μ L, 97.5 μ mol, 2.0 eq.) was added to a solution of ⁹cAAC silepin J (30 mg, 48.7 μ mol, 1.0 eq.) in toluene (1 mL). The mixture was stirred at r.t. for 10 days. The solvent was completely evaporated in vacuo to afford the product as an orange oil (33 mg, 91%). ¹H NMR (400 MHz, C₆D₆): δ [ppm] = 7.15–7.12 (m, 2H, H_A), 6.99 (dd, $J = 5.4, 4.0$ Hz, 1H, H_A), 3.43 (hept, $J = 6.4$ Hz, 1H, CH(CH₃)₂), 2.97 (hept, $J = 6.7$ Hz, 1H, CH(CH₃)₂), 2.30 (td, $J = 13.1, 3.9$ Hz, 1H, CH₂), 2.25–2.17 (m, 1H, H_C), 1.91 (td, $J = 13.1, 3.7$ Hz, 1H, CH₂), 1.86–1.55 (m, 7H, H_C), 1.50 (d, $J = 6.6$ Hz, 3H, CH₃), 1.42–1.26 (m, 2H, H_C), 1.22 (d, $J = 6.6$ Hz, 3H, CH₃), 1.16–1.11 (m, 9H, CH₃), 0.88 (s, 3H, CH₃), 0.34 (s, 27H, H_{TMS}). ¹³C{H} NMR (101 MHz, C₆D₆): δ [ppm] = 215.11 (CO), 170.92 (C=N), 149.30 (C_A), 147.30 (C_A), 131.17 (C_A), 129.03 (C_A), 125.46 (C_A), 124.41 (C_A), 65.35 (C-N), 49.31 (C-C-N), 44.86 (C-C-N), 39.49 (C_C), 32.87 (C_C), 31.17 (C_C), 29.24 (C_C), 28.98 (CH(CH₃)₂), 28.76 (CH(CH₃)₂), 28.51 (C_C), 27.35 (CH₃), 25.11 (CH₃), 24.30 (CH₃), 23.25 (CH₃), 22.33 (CH₃), 22.02 (CH₃), 3.16 (C_{TMS}). ²⁹Si{H} NMR (99 MHz, C₆D₆): δ [ppm] = 253.11 (Si), -9.73 (Si(TMS)₃), -94.15 (Si(TMS)₃). LIFDI-MS: Calculated: $m/z = 782.2905$; Experimental: $m/z = 782.2835$ [6]⁺ (+8.94 ppm error). IR (cm⁻¹): 2950 (w), 2890 (m), 2005 (s), 1921 (s), 1881 (s), 1436 (s), 1242 (s), 824 (s).

Synthesis of 7: FeCO₃ (5.90 μ L, 43.5 μ mol, 2.0 eq.) was added to an inseparable mixture (30 mg) of ¹⁵NHC silepin-SiPh₃ 1 (18.8 mg, 21.8 μ mol, 1.0 eq.) and BrSi(TMS)₂SiPh₃ (11.2 mg) in toluene (1 mL). The mixture was stirred at r.t. for 16 h. The solvent was completely evaporated in vacuo and the remains dissolved in pentane to precipitate pure complex 7. After centrifugation and separation of the solvent, the product is dried in vacuo to afford a yellow solid (11.2 mg, 50%). ¹H NMR (500 MHz, C₆D₆): δ [ppm] = 7.82–7.79 (m, 6H, H_A), 7.24–7.16 (m, 13H, H_A), 7.05 (m, 2H, H_A), 6.10 (s, 2H, CH-N), 3.97 (hept, $J = 6.7$ Hz, 2H, CH(CH₃)₂), 2.81 (hept, $J = 6.7$ Hz, 2H, CH(CH₃)₂), 1.61 (d, $J = 6.7$ Hz, 6H, CH₃), 1.28 (d, $J = 6.7$ Hz, 6H, CH₃), 1.13 (d, $J = 6.7$ Hz, 6H, CH₃), 0.97 (d, $J = 6.6$ Hz, 6H, CH₃), 0.01 (s, 18H, H_{TMS}). ¹³C{H} NMR (126 MHz, C₆D₆): δ [ppm] = 215.42 (CO), 153.18 (C=N), 148.38 (C_A), 146.69 (C_A), 137.60 (C_A), 136.27 (C_A), 133.82 (C_A), 130.72 (C_A), 129.60 (C_A), 127.95 (C_A), 125.04 (C_A), 124.54 (C_A), 118.49 (CH-N), 28.77 (CH(CH₃)₂), 28.75 (CH(CH₃)₂), 26.69 (CH₃), 26.53 (CH₃), 23.17 (CH₃), 23.02 (CH₃), 3.48 (C_{TMS}). ²⁹Si{H} NMR (99 MHz, C₆D₆): δ [ppm] = 273.09 (Si), -8.76 (Si(TMS)₃), -9.85 (SiPh₃), -94.41 (Si(TMS)₂SiPh₃). LIFDI-MS: Calculated: $m/z = 1031.3484$; Experimental: $m/z = 1031.3546$ [7]⁺ (-6.01 ppm error). Melting point: 206.6 °C. IR (cm⁻¹): 3084 (w), 2958 (s), 2921 (s), 2021 (s), 1953 (s), 1919 (s), 1983 (s), 1548 (s), 1461 (m), 1244 (s), 1104 (s), 834 (s).

Synthesis of 8: FeCO₃ (6.10 μ L, 44.9 μ mol, 2.0 eq.) was added to an inseparable mixture (30 mg) of ⁹cAAC silepin-SiPh₃ 2 (18.0 mg, 22.5 μ mol, 1.0 eq.) and BrSi(TMS)₂SiPh₃ (12 mg) in toluene (1 mL). The mixture was stirred at r.t. for 16 h. The solvent was completely evaporated in vacuo, and the remains were dissolved in pentane to precipitate pure complex 8. After centrifugation and separation of the solvent, the product is dried in vacuo to afford a yellow solid (12.7 mg, 58%). ¹H NMR (400 MHz, C₆D₆): δ [ppm] = 7.78–7.72 (m, 6H, H_A), 7.15–7.10 (m, 9H, H_A), 7.08 (d, $J = 4.6$ Hz, 1H, H_A), 7.05 (d, $J = 7.8$ Hz, 1H, H_A), 6.73 (dd, $J = 7.4, 2.0$ Hz, 1H, H_A), 3.51 (hept, $J =$

6.2 Hz, 1H, CH(CH₃)₂), 2.61 (hept, $J = 6.9$ Hz, 1H, CH(CH₃)₂), 2.37–2.20 (m, 2H, CH₂), 1.93–1.75 (m, 4H, H_C), 1.69–1.51 (m, 6H, H_C), 1.25 (d, $J = 6.6$ Hz, 6H, CH₃), 1.07 (s, 3H, CH₃), 0.91 (d, $J = 6.8$ Hz, 3H, CH₃), 0.77 (s, 3H, CH₃), 0.37 (s, 9H, H_{TMS}), 0.30 (s, 9H, H_{TMS}). ¹³C{H} NMR (126 MHz, C₆D₆): δ [ppm] = 215.83 (CO), 171.95 (C=N), 149.22 (C_A), 147.94 (C_A), 137.79 (C_A), 137.38 (C_A), 137.16 (C_A), 131.22 (C_A), 129.69 (C_A), 129.41 (C_A), 125.29 (C_A), 124.74 (C_A), 65.83 (C-N), 49.95 (C-C-N), 44.82 (C-C-N), 38.80 (C_C), 33.30 (C_C), 31.46 (C_C), 30.08 (C_C), 29.09 (CH(CH₃)₂), 28.92 (CH(CH₃)₂), 28.03 (C_C), 27.66 (CH₃), 24.86 (CH₃), 24.39 (CH₃), 23.08 (CH₃), 22.63 (CH₃), 22.39 (CH₃), 4.36 (C_{TMS}), 3.90 (C_{TMS}). ²⁹Si{H} NMR (99 MHz, C₆D₆): δ [ppm] = 247.45 (Si), -7.41 (Si(TMS)₃), -7.79 (Si(TMS)₃), -8.35 (SiPh₃), -95.69 (Si(TMS)₂SiPh₃). LIFDI-MS: Calculated: $m/z = 968.3375$; Experimental: $m/z = 968.3386$ [8]⁺ (-1.14 ppm error). Melting point: 216.2 °C. IR (cm⁻¹): 3200–3068 (w), 2959 (s), 2927 (m), 2859 (s), 2026 (s), 1953 (s), 1925 (s), 1900 (s), 1600 (s), 1459 (m), 1428 (s), 1243 (s), 1104 (s), 833 (s), 737 (s).

Supporting Information

More experimental details for all newly synthesized compounds and single crystallographic data can be found in the Supporting Information (SI). The authors have cited additional references within the SI.^[21–28] CCDC: Deposition Numbers 2324672 (for 4), 2324673 (for 5), 2324675 (for 6), 2324674 (for 7), 2324676 (for 8) contain the supplementary crystallographic data for this paper. These data are provided free of charge by the joint Cambridge Crystallographic Data Centre and Fachinformationszentrum Karlsruhe Access Structures service.

Acknowledgements

All authors want to express their appreciation towards Franziska Hanusch for the guidance on the SC-XRD analyses and Fabrizio E. Napoli for the LIFDI-MS measurements. Furthermore, we want to thank Martin E. Doleschal for the scientific discussions. Open Access funding enabled and organized by Projekt DEAL.

Conflict of Interests

The authors declare no conflict of interest.

Data Availability Statement

The data that support the findings of this study are available from the corresponding author upon reasonable request.

Keywords: low-valent · silylenes · silepins · main group · silicon

- [1] a) S. Fujimori, S. Inoue, *Eur. J. Inorg. Chem.* 2020, 2020, 3131; b) C. Shan, S. Yao, M. Driess, *Chem. Soc. Rev.* 2020, 49, 6733; c) L. Wang, Y. Li, Z. Li, M. Kira, *Coord. Chem. Rev.* 2022, 457, 214413.
- [2] a) S. Fujimori, S. Inoue, *Commun. Chem.* 2020, 3, 175; b) D. Reiter, R. Holzner, A. Porzelt, P. Frisch, S. Inoue, *Nat. Chem.* 2020, 12, 1131; c) P. P. Power, *Nature* 2010, 463, 171; d) M. M. D. Roy, M. J. Ferguson, R.

Isolation and Reactivity of Silepins with a Sterically Demanding Silyl Ligand

- McDonald, Y. Zhou, E. Rivard, *Chem. Sci.* 2019, 10, 6476; e) M. M. D. Roy, S. R. Baird, E. Dornsiепен, L. A. Paul, L. Miao, M. J. Ferguson, Y. Zhou, I. Siewert, E. Rivard, *Chem. Eur. J.* 2021, 27, 8572.
- [3] H. Zhu, S. Fujimori, A. Kostenko, S. Inoue, *Chem. Eur. J.* 2023, 29, e202301973.
- [4] Y. Xiong, S. Yao, M. Driess, *Chem. Eur. J.* 2009, 15, 5545.
- [5] a) A. V. Protchenko, K. H. Birjukumar, D. Dange, A. D. Schwarz, D. Vidovic, C. Jones, N. Kaltsayannis, P. Mountford, S. Aldridge, *J. Am. Chem. Soc.* 2012, 134, 6500; b) A. V. Protchenko, A. D. Schwarz, M. P. Blake, C. Jones, N. Kaltsayannis, P. Mountford, S. Aldridge, *Angew. Chem. Int. Ed.* 2013, 52, 568; c) H. Zhu, A. Kostenko, D. Franz, F. Hanusch, S. Inoue, *J. Am. Chem. Soc.* 2023, 145, 1011.
- [6] D. Wendel, A. Porzelt, F. A. D. Herz, D. Sarkar, C. Jandt, S. Inoue, B. Rieger, *J. Am. Chem. Soc.* 2017, 139, 8134.
- [7] a) A. Kostenko, S. Inoue, *Chem* 2023, 9, 3022; b) T. Ochiai, D. Franz, S. Inoue, *Chem. Soc. Rev.* 2016, 45, 6327.
- [8] D. Wendel, D. Reiter, A. Porzelt, P. J. Altmann, S. Inoue, B. Rieger, *J. Am. Chem. Soc.* 2017, 139, 17193.
- [9] M. Ludwig, D. Franz, A. Espinosa Ferao, M. Bolte, F. Hanusch, S. Inoue, *Nat. Chem.* 2023, 15, 1452.
- [10] T. Eisner, A. Kostenko, F. Hanusch, S. Inoue, *Chem. Eur. J.* 2022, 28, e202202330.
- [11] J. Y. Liu, T. Eisner, S. Inoue, B. Rieger, *Eur. J. Inorg. Chem.* 2024, 27, e202300568.
- [12] a) R. Jazsar, M. Soleilhavoup, G. Bertrand, *Chem. Rev.* 2020, 120, 4141; b) J. T. Goettel, H. Gao, S. Dotzauer, H. Braunschweig, *Chem. Eur. J.* 2020, 26, 1136.
- [13] a) Y. K. Loh, M. Melaimi, M. Gembicky, D. Munz, G. Bertrand, *Nature* 2023, 623, 66; b) Y. K. Loh, M. Melaimi, D. Munz, G. Bertrand, *J. Am. Chem. Soc.* 2023, 145, 2064; c) E. Welz, J. Böhnke, R. D. Dewhurst, H. Braunschweig, B. Engels, *J. Am. Chem. Soc.* 2018, 140, 12580; d) Y. K. Loh, L. Gofjashvili, M. Melaimi, M. Gembicky, D. Munz, G. Bertrand, *Nat. Synth* 2024, 3, 727.
- [14] a) C. Kayser, R. Fischer, J. Baumgartner, C. Marschner, *Organometallics* 2002, 21, 1023; b) P. Schmidt, S. Fietze, C. Schrenk, A. Schnepf, *Z. Anorg. Allg. Chem.* 2017, 643, 1759.
- [15] a) S. Hashimoto, N. Watanabe, S. Ikegami, *Chem. Commun.* 1992, 20, 1508; b) I. Hussain, T. Singh, *Adv. Synth. Catal.* 2014, 356, 1661; c) F. Neve, M. Ghedini, A. Tiripicchio, F. Ugozzoli, *Inorg. Chem.* 1989, 28, 3084.
- [16] a) A. Jana, P. P. Samuel, G. Tavcar, H. W. Roesky, C. Schulzke, *J. Am. Chem. Soc.* 2010, 132, 10164; b) S. Takahashi, E. Bellar, A. Bacedredo, N. Saffon-Merceron, S. Massou, N. Nakata, D. Hashizume, V. Branchadell, T. Kato, *Angew. Chem. Int. Ed.* 2019, 58, 10310; c) R. H. Walker, K. A. Miller, S. L. Scott, Z. T. Cygan, J. M. Bartolin, J. W. Kampf, M. M. Banaszak Holl, *Organometallics* 2009, 28, 2744.
- [17] a) B. Blom, M. Pohl, G. Tan, D. Gallego, M. Driess, *Organometallics* 2014, 33, 5272; b) G. Dübek, F. Hanusch, S. Inoue, *Inorg. Chem.* 2019, 58, 15700; c) C. Eisenhut, T. Szilvási, G. Dübek, N. C. Breit, S. Inoue, *Inorg. Chem.* 2017, 56, 10061; d) R. S. Ghadwal, R. Azhakar, K. Pröpper, J. J. Holstein, B. Dittrich, H. W. Roesky, *Inorg. Chem.* 2011, 50, 8502; e) W. Yang, H. Fu, H. Wang, M. Chen, Y. Ding, H. W. Roesky, A. Jana, *Inorg. Chem.* 2009, 48, 5058.
- [18] A. Saurwein, T. Eisner, S. Inoue, B. Rieger, *Organometallics* 2022, 41, 3679.
- [19] a) P. Frisch, T. Szilvási, A. Porzelt, S. Inoue, *Inorg. Chem.* 2019, 58, 14931; b) D. Lutters, C. Severin, M. Schmidtman, T. Müller, *J. Am. Chem. Soc.* 2016, 138, 6061.
- [20] a) E. W. Abel, F. G. A. Stone, *Chem. Soc.* 1969, 23, 325; b) L. E. Orgel, *Inorg. Chem.* 1962, 1, 25.
- [21] APEX suite of crystallographic software, APEX 3, Version 2019-1.0, Bruker AXS Inc., Madison, Wisconsin, USA, 2019.
- [22] SAINT, Version 8.40 A and SADABS, Version 2016/2, Bruker AXS Inc., Madison, Wisconsin, USA, 2016/2019.
- [23] G. M. Sheldrick, *Acta Crystallogr. Sect. A* 2015, 71, 3.
- [24] G. M. Sheldrick, *Acta Crystallogr. Sect. C* 2015, 71, 3.
- [25] C. B. Hübschle, G. M. Sheldrick, B. Dittrich, *J. Appl. Crystallogr.* 2011, 44, 1281–1284.
- [26] *International Tables for Crystallography, Vol. C* (Ed.: A. J. Wilson), Kluwer Academic Publishers, Dordrecht, The Netherlands, 1992, Tables 6.1.1.4 (pp. 500–502), 4.2.6.8 (pp. 219–222), and 4.2.4.2 (pp. 193–199).
- [27] C. F. Macrae, I. J. Bruno, J. A. Chisholm, P. R. Edgington, P. McCabe, E. Pidcock, L. Rodriguez-Monge, R. Taylor, J. van de Streek, P. A. Wood, *J. Appl. Crystallogr.* 2008, 41, 466.
- [28] A. L. Spek, *Acta Crystallogr. Sect. D* 2009, 65, 148.

Manuscript received: January 23, 2024
Revised manuscript received: May 16, 2024
Accepted manuscript online: May 20, 2024
Version of record online: June 28, 2024

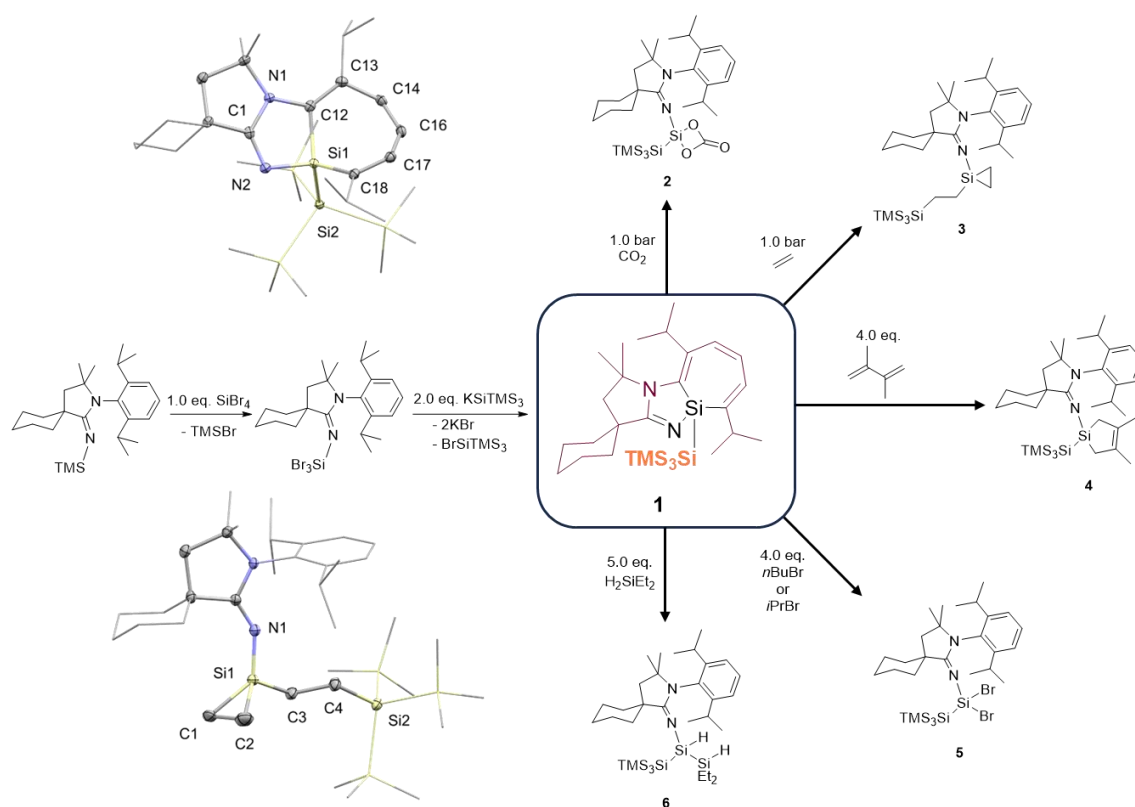
5. Summary and Outlook

Low valent main-group compounds have so far outlined diverse catalytic applications and can be considered potential candidates to replace transition metal-based catalysts. Amongst all novel structures, organosilicon compounds attracted the major focus of research due to their high abundance and non-toxic nature. Silylenes, being a class of low valent and low coordinate silicon-containing structures, were first discovered by *Jutzi* in 1986, marking a milestone in modern main-group chemistry. Genuine, non-transient acyclic silylenes, on the other hand, were to follow about 20 years later and opened up new pathways to possibly substitute transition metal (TM) centers in catalysis: Due to the oxidative flexibility, small HOMO-LUMO gap and open coordination site, acyclic silylenes were quickly regarded as greener alternatives to TMs. During extensive research, a new species based on acyclic silylenes was reported a few years ago: Silepins based on acyclic silylenes, which show an interplay between both oxidative states (+II, +IV) of the silicon center. This unique observation motivates further investigations of silepins regarding the substituent effect and its potential application as a molecular catalyst.

As shown in Scheme 16, a new silepin structure (**1**) is prepared and isolated in the first step. The literature unknown imine ligand bearing a ^{Cyc}AAc moiety, derived from the originally applied NHI containing the ^{Dipp}NHC group, was synthesized analogously to reported procedures. Subsequently, two equivalents of KSiTMS₃ are added to achieve a substitution and a reduction simultaneously. This step also introduces the second ligand to effectively stabilize the resulting silylene atom. After successful intramolecular insertion, ^{Cyc}AAc silepin (**1**) is formed. It acts, as expected, as a “masked” silylene and can engage in small molecule activations. However, in contrast to its directly structurally related silepin **L-49**, **1** is not able to cleave the strong non-polar bond of dihydrogen, suggesting an enhanced stability of **1** in its silepin form. Regarding this matter, DFT calculations have revealed a HOMO-LUMO gap of 3.188 eV, being on the larger side of literature-reported values for acyclic silylenes. Moreover, the experimentally determined melting point of **1** of 122 °C is also well above that of **L-49** (99.2 °C). This study shows that the modification from

Summary and Outlook

a ^{Dipp}NHC to a ^{CycAAC} moiety led to a notable change in the stability and, thus, reactivity of the resulting silepin and demonstrated the impact of substituent effect in these unique species.

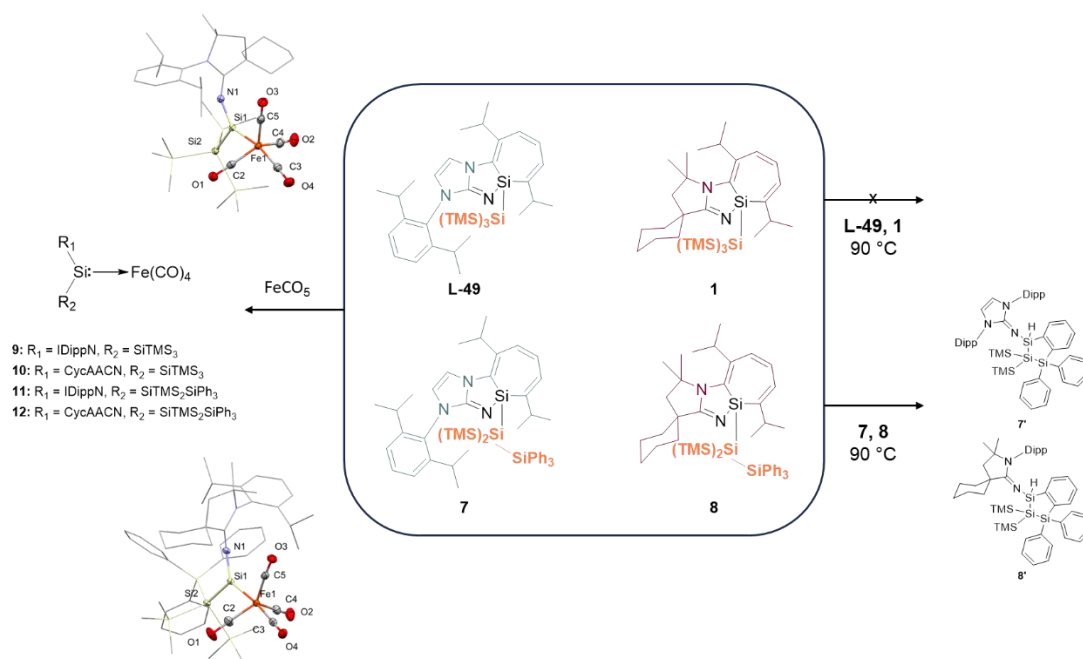


Scheme 16: Isolation of ^{CycAAC} silepin (**1**) and its reactivity towards small molecules.

After the above-mentioned imine ligand modification, it is beneficial to investigate silyl ligand variation due to scarce reports in the literature. Therefore, the respective potassium silanide is changed from KSiTMS₃ to KSiTMS₂SiPh₃, swapping one trimethyl silyl with a triphenyl silyl group, the latter possessing altered electronic and steric properties. Combined with either NHI (^{Dipp}NHC- or ^{CycAAC}-based) as the second ligand, two new silepins (**7,8**) could be obtained following literature-reported procedures. However, the side product of the reaction, BrSiTMS₂SiPh₃, cannot be removed from the main compounds **7** and **8** after various unsuccessful attempts. Upon elevating the temperatures to 90 °C, silepins **7** and **8** show a unique intramolecular insertion into the *ortho* C–H bond of the triphenyl silyl moiety forming **7'** and **8'**, which is determined as the thermodynamically more stable

Summary and Outlook

product of the silepin synthesis. Interestingly, this phenomenon is not observed for other silepins based on acyclic silylenes, e.g., their direct structural analogs **L-49** and **1**. It is assumed that the silyl ligand modification from $-\text{SiTMS}_3$ to $-\text{SiTMS}_2\text{SiPh}_3$ enabled this new reactivity due to the steric proximity of the aromatic groups bearing *o*-hydrogen.



Scheme 17: Isolated silepins with modified silyl ligand and their reactivity.

In order to gain further insight into the influence of both imine and silyl ligand variations, iron(0)carbonyl complexes of the silepins shown in Scheme 17 is synthesized. SC-XRD analyses revealed adduct formations in structures **9-12**. Subsequent FT-IR measurements showed a shift in the CO vibration bands: While complexes bearing the identical silyl ligand (**9,10** and **11,12**) express very similar values in comparison, the measured wavenumbers go higher from compound **9** to **11** and **10** to **12**, respectively. This observation suggests that the silylene atom in complexes **11** and **12** possesses a comparably reduced σ -donation and increased π -acceptance, thus leading to the higher wavenumbers.

Summary and Outlook

In summary, this doctoral thesis pursued the major goal of further investigating novel silepin structures based on acyclic silylenes. Different ligand modifications shed light on the impact of substituents resulting in altered chemical and physical properties in silepins, which led to new interesting reactivities. Furthermore, the equilibrium between Si(II) and Si(IV), being a crucial aspect for potential catalysis, is heavily influenced by both the imine and the silyl ligand, as shown in reported reactivity studies opening up new possibilities and opportunities of a metal-free, silicon mediated catalysis.

6. Appendix

6.1 Supporting Information for Chapter 3

European Journal of Inorganic Chemistry

Supporting Information

Isolation of a New Silepin with an Imine Ligand Based on Cyclic Alkyl Amino Carbene

Jin Yu Liu, Teresa Eisner, Shigeyoshi Inoue, and Bernhard Rieger*

Appendix

1. Experimental Procedures

A) General Methods and Instrumentation

All manipulations were carried out under argon atmosphere using standard *Schlenk* or glovebox techniques. Glassware was heat-dried under vacuum prior to use. Unless otherwise stated, all chemicals were purchased commercially and used as received. All solvents were refluxed over sodium, distilled, and deoxygenated prior to use. Deuterated solvents were obtained commercially and were dried over 3 Å molecular sieves prior to use. All NMR samples were prepared under argon in *J. Young* PTFE tubes. Cy-cAAC and KSiTMS₃ were synthesized according to procedures described in the literature.^[1]

Carbon dioxide (5.0) and ethylene (3.5) were purchased from Westfalen AG and used as received. NMR spectra were recorded on Bruker AV-500C or AV-400 spectrometers at ambient temperature (300 K), unless otherwise stated. ¹H, ¹³C and ²⁹Si NMR spectroscopic chemical shifts (δ) are reported in ppm. $\delta(^1\text{H})$ and $\delta(^{13}\text{C})$ were referenced internally to the relevant residual solvent resonances. $\delta(^{29}\text{Si})$ was referenced to the signal of tetramethylsilane (TMS) ($\delta = 0$ ppm) as external standard.

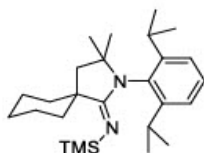
Liquid Injection Field Desorption Ionization Mass Spectrometry (LIFDI-MS) was measured directly from an inert atmosphere glovebox with a *Thermo Fisher Scientific* Exactive Plus Orbitrap equipped with an ion source from Linden CMS.

Melting points were determined in sealed glass capillaries under inert gas with a *Büchi* Melting Point B-540.

Appendix

B) Synthesis and Characterization of New Compounds

Cy-cAACN-TMS (Compound 1)



Cy-cAAC (1.34 g, 4.12 mmol, 1.0 eq.) is dissolved in toluene (20 mL) and TMSN_3 (1.37 mL, 10.3 mmol, 2.5 eq.) is added. The mixture is stirred at 90 °C for 16 h. The product is obtained upon evaporation of the solvent as an off-white solid (1.62 g, 95%).

$^1\text{H NMR}$ (500 MHz, C_6D_6): δ [ppm] = 7.20 (dd, $J = 8.5, 6.8$ Hz, 1H, H_{Ar}), 7.15 – 7.10 (m, 2H, H_{Ar}), 3.16 – 3.04 (m, 2H, $\text{CH}(\text{CH}_3)_2$), 1.90 – 1.85 (m, 1H, H_{Cy}), 1.84 (s, 1H, CH_2), 1.79 (s, 1H, CH_2), 1.77 – 1.33 (m, 9H, H_{Cy}), 1.32 – 1.22 (m, 12H, CH_3), 1.19 (d, $J = 6.9$ Hz, 3H, CH_3), 1.14 (d, $J = 6.7$ Hz, 3H, CH_3), 1.02 (s, 4H, H_{TMS}), 0.27 (s, 5H, H_{TMS}).

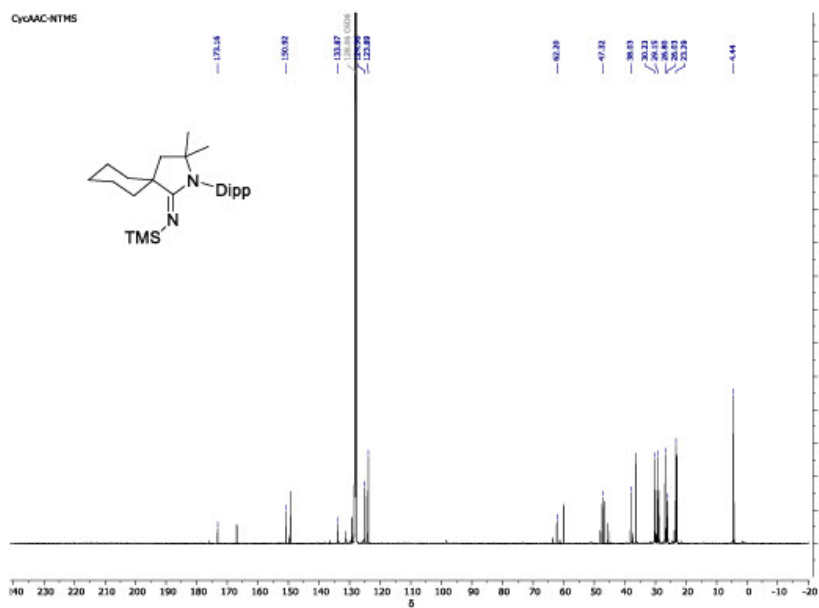
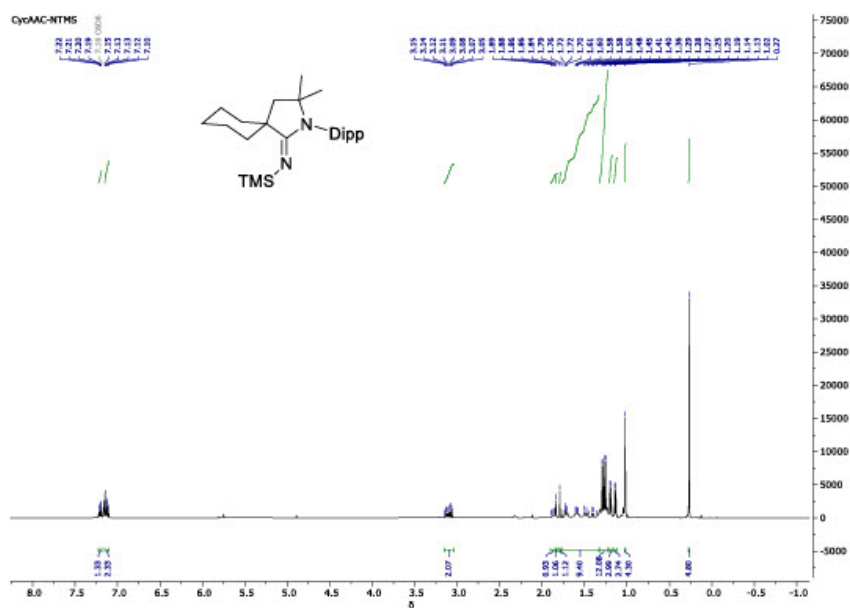
$^{13}\text{C NMR}$ (126 MHz, C_6D_6): δ [ppm] = 173.16 (C=N), 150.92 (C_{Ar}), 133.87 (C_{Ar}), 124.96 (C_{Ar}), 123.89 (C_{Ar}), 62.20 (C-N), 47.32 (N-C-C), 38.03 (C-C=N), 30.23 (C_{Cy}), 29.15 (C_{Cy}), 26.80 (C_{Cy}), 26.03 (CH_3), 23.29 (CH_3), 4.44 (TMS).

$^{29}\text{Si NMR}$ (99 MHz, C_6D_6): δ [ppm] = -18.74.

LIFDI-MS: $m/z = 412.3258$ [1] $^+$.

Melting point: 91.9 °C

Appendix



Appendix

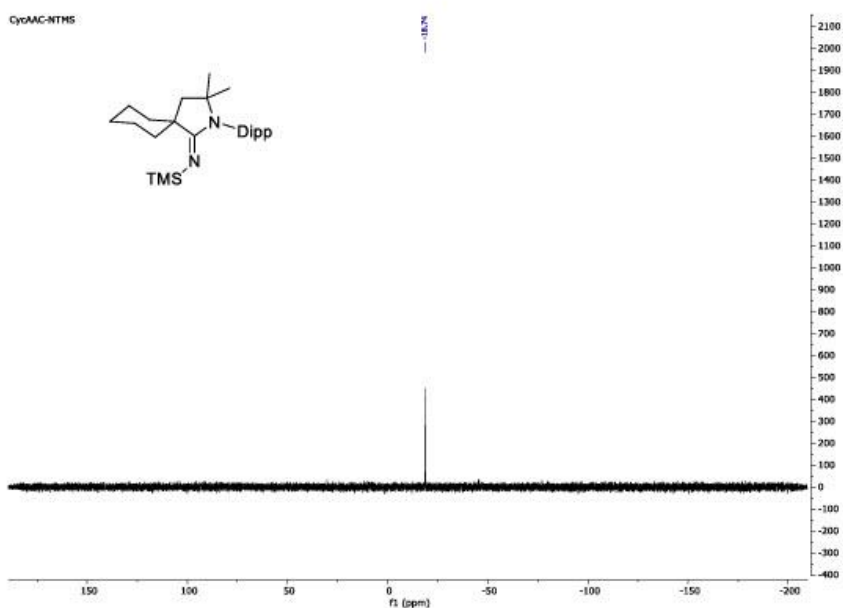
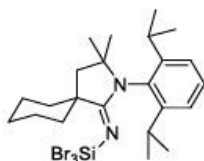


Figure 3: ^{29}Si NMR of compound 1.

Cy-cAACN-SiBr₃ (Compound 2)



Cy-cAACNTMS (1.63 g, 3.94 mmol, 1.0 eq.) is dissolved in toluene (25 mL) and SiBr₄ (0.49 mL, 3.94 mmol, 1.0 eq.) is added. The mixture is stirred at 90 °C for 16 h. The solvent is evaporated *in vacuo*. After *Whatman* filtration, the product is obtained as a powder (1.36 g, 57%).

^1H NMR (500 MHz, C_6D_6): δ [ppm] = 7.24 – 7.22 (m, 2H, H_{Ar}), 7.14 (d, J = 1.0 Hz, 1H, H_{Ar}), 2.89 (hept, J = 6.8 Hz, 2H, $\text{CH}(\text{CH}_3)_2$), 2.40 – 2.32 (m, 2H, CH_2), 1.71 (s, 2H, H_{Cy}), 1.66 – 1.50 (m, 5H, H_{Cy}), 1.46 (d, J = 6.7 Hz, 6H, CH_3), 1.41 – 1.33 (m, 1H, H_{Cy}), 1.24 (d, J = 6.7 Hz, 6H, CH_3), 1.21 – 1.10 (m, 2H, H_{Cy}), 0.95 (s, 6H, CH_3).

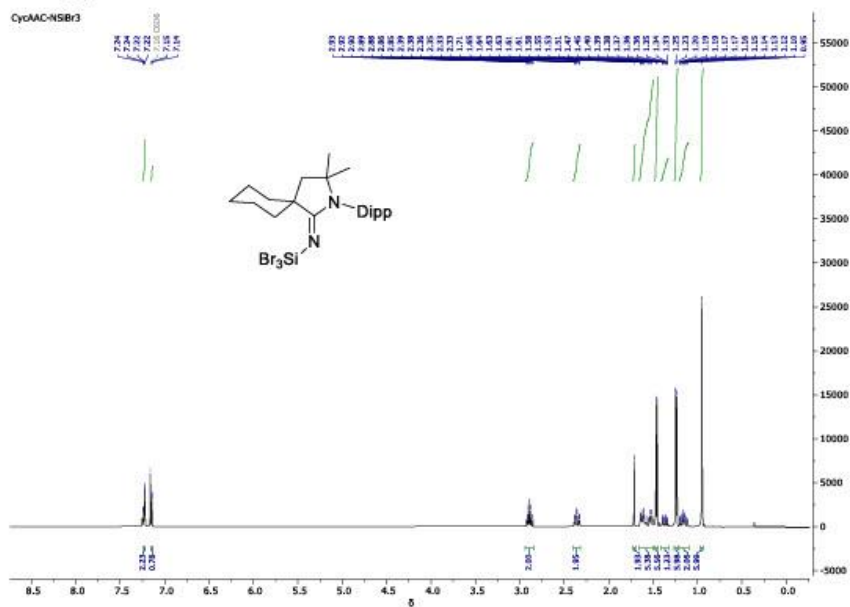
^{13}C NMR (126 MHz, C_6D_6): δ [ppm] = 172.32 (C=N), 147.62 (C_{Ar}), 130.75 (C_{Ar}), 129.05 (C_{Ar}), 124.29 (C_{Ar}), 63.50 (C-C-N), 48.81 (C-C-N), 45.65 (C-C=N), 35.21 (C_{Cy}), 29.30 (C_{Cy}), 28.95 (CH), 26.70 (C_{Cy}), 25.02 (CH_3), 23.11 (CH_3), 22.15 (CH_3).

Appendix

^{29}Si NMR (99 MHz, C_6D_6): δ [ppm] = -107.85.

LIFDI-MS: $m/z = 604.0107$ [2] $^+$.

Melting point: 159.5 $^\circ\text{C}$



Appendix

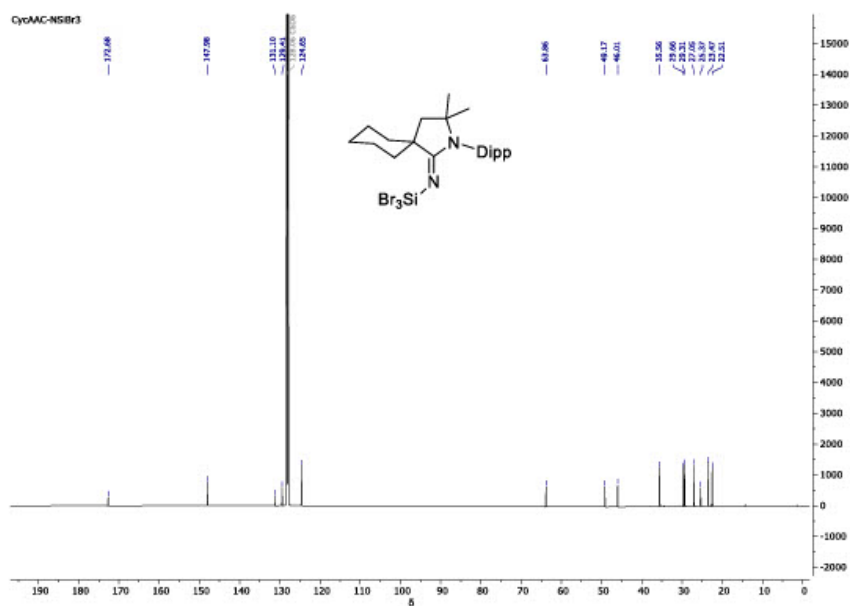


Figure 5: ^{13}C NMR of compound 2.

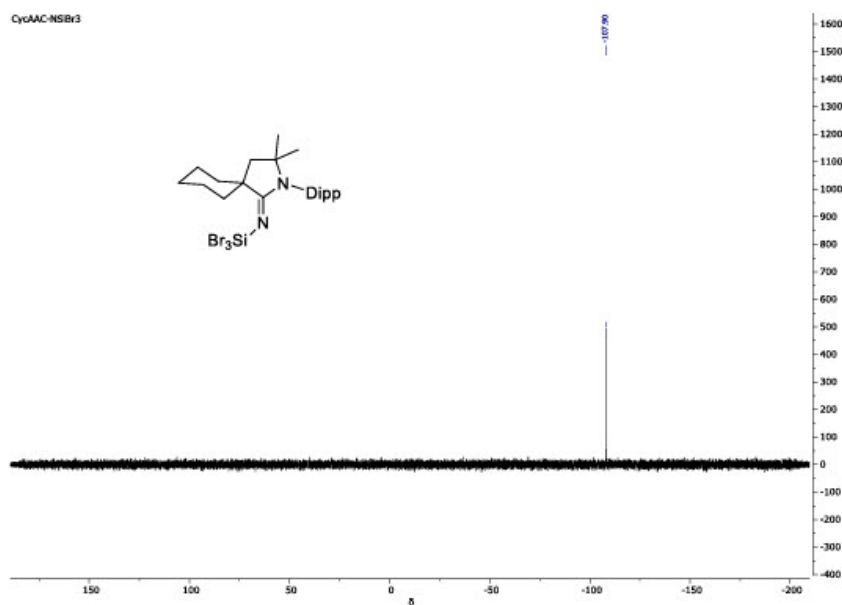
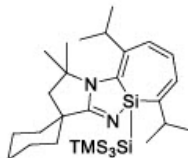


Figure 6: ^{29}Si NMR of compound 2.

Appendix

Cy-cAAC silepin (Compound 3)



Cy-cAAC-SiBr₃ (120 mg, 198 mmol, 1.0 eq.) and KSiTMS₃ (113 mg, 396 mmol, 2.0 eq.) is dissolved in toluene (3 mL) and stirred at r.t. for 1 h. After evaporation of the solvent, pentane (5 mL) is added and the suspension is filtered through a PE syringe filter. Pentane is then removed and the product is precipitated with MeCN (8 mL). Pure Cy-cAAC silepin is obtained after centrifugation and separation of the solvent (113 mg, 93%).

¹H NMR (500 MHz, C₆D₆): δ [ppm] = 6.61 (d, *J* = 13.0 Hz, 1H, H_{Az}), 6.38 (dd, *J* = 5.8, 1.2 Hz, 1H, H_{Az}), 6.33 (dd, *J* = 13.0, 6.1 Hz, 1H, H_{Az}), 3.25 (hept, *J* = 6.8 Hz, 1H, CH(CH₃)₂), 3.04 (hept, *J* = 6.7 Hz, 1H, CH(CH₃)₂), 2.19 – 2.11 (m, 1H, CH), 2.08 – 2.01 (m, 1H, CH), 1.84 – 1.77 (m, 2H, H_{Cy}), 1.69 – 1.46 (m, 8H, H_{Cy}), 1.25 – 1.19 (m, 15H, CH₃), 1.05 (d, *J* = 6.8 Hz, 3H, CH₃), 0.41 (s, 27H, H_{TMS}).

¹³C NMR (126 MHz, C₆D₆): δ [ppm] = 179.53 (C=N), 146.54 (C_{Az}), 135.61 (C_{Az}), 133.72 (C_{Az}), 128.93 (C_{Az}), 123.71 (C_{Az}), 58.28 (C-N), 52.75 (C-C-N), 42.38 (C-C=N), 37.51 (C_{Cy}), 36.79 (C_{Cy}), 33.98 (C_{Cy}), 31.17 (CH(CH₃)₂), 31.12 (CH(CH₃)₂), 29.03 (C_{Cy}), 25.96 (C_{Cy}), 24.88 (CH₃), 23.21 (CH₃), 22.99 (CH₃), 22.84 (CH₃), 22.67 (CH₃), 20.65 (CH₃), 3.36 (C_{TMS}).

²⁹Si NMR (99 MHz, C₆D₆): δ [ppm] = 17.25, -9.29, -135.71.

LIFDI-MS: *m/z* = 614.3743 [3]⁺.

Melting point: 122.4 °C

Appendix

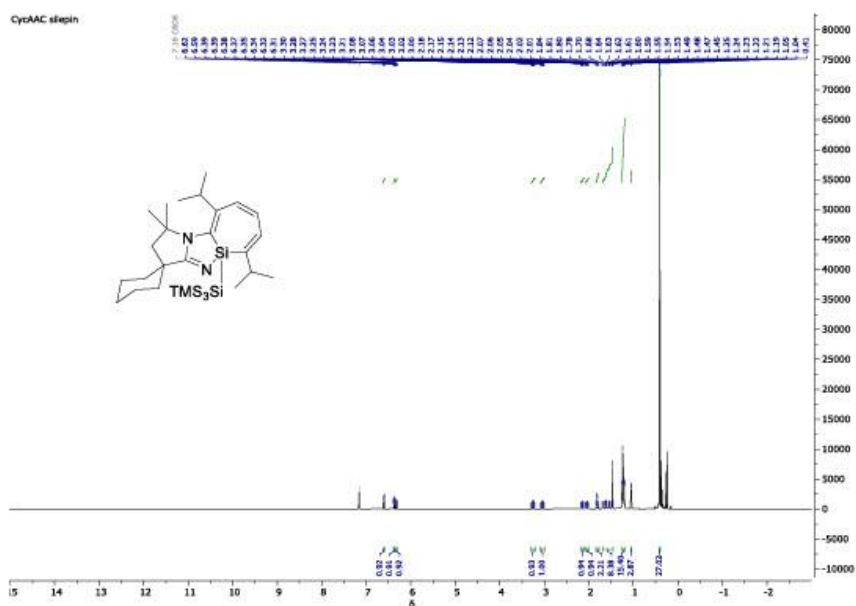


Figure 7: ¹H NMR of compound 3.

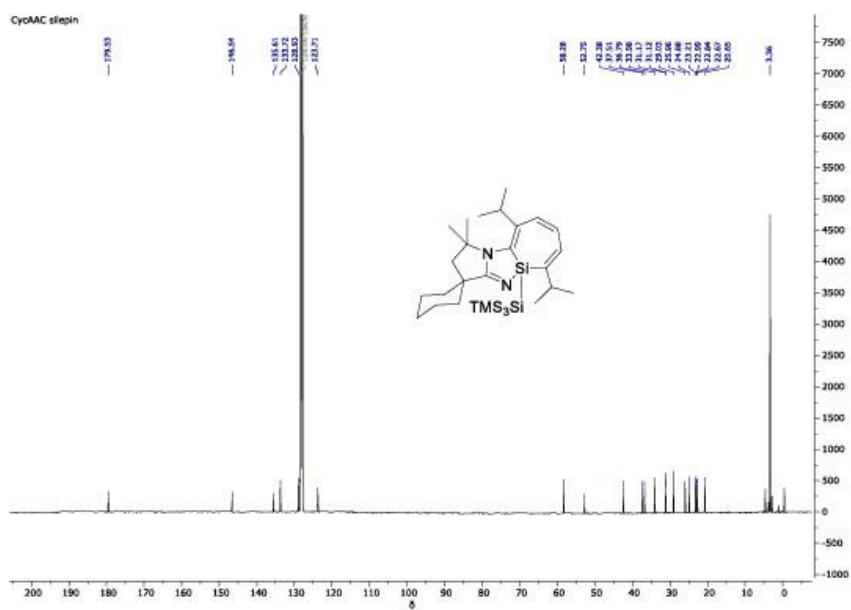


Figure 8: ¹³C NMR of compound 3.

Appendix

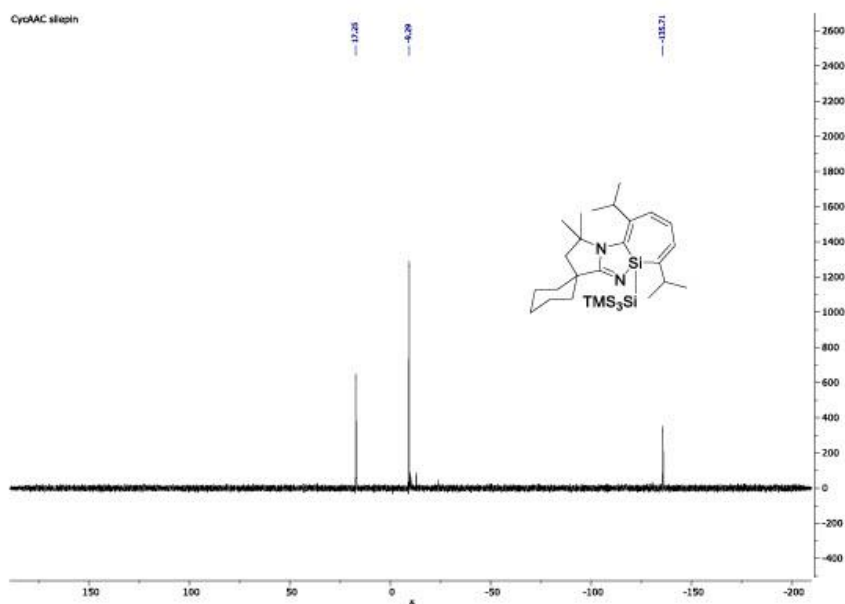
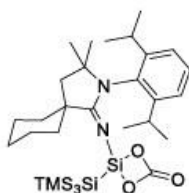


Figure 9: ²⁹Si NMR of compound 3.

Cy-cAAC silepin CO₂ adduct (Compound 4) NMR experiment



Cy-cAAC silepin (15 mg, 24.4 μ mol) is solved in C₆D₆ (0.5 mL) and filled into a PTFE *J*Young tube. The solution is frozen with liquid nitrogen and degassed. Subsequently, gaseous CO₂ (1 bar) is introduced, and the tube is sealed afterwards. The mixture is heated to 60 °C for 16 hours. After evaporation of the solvent, the product is obtained as a pale-yellow oil (15.7 mg, 88% purity) containing compound 4 (14.7 mg, 89% yield) and SiTMS₄ (0.93 mg) as the impurity.

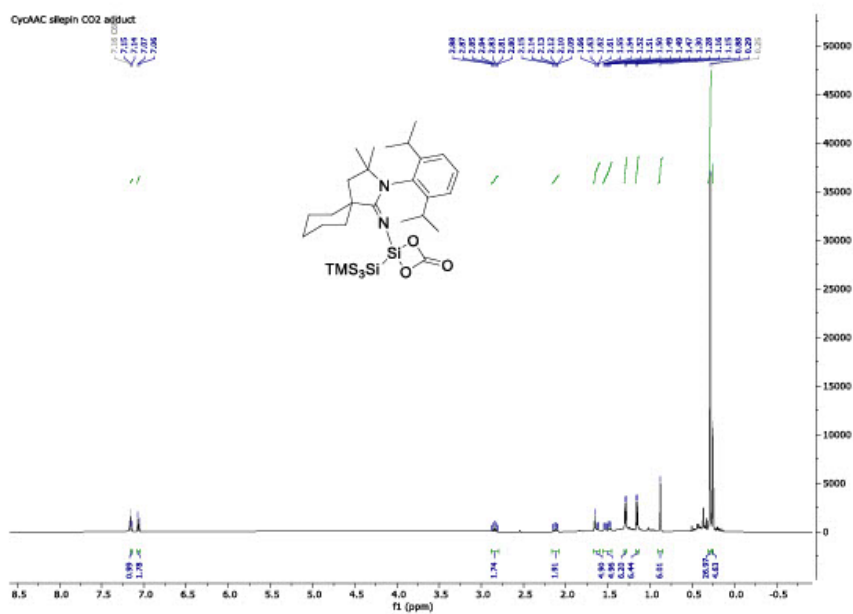
¹H NMR (500 MHz, C₆D₆): δ [ppm] = 7.16 – 7.14 (m, 1H, H_{A1}), 7.06 (d, J = 7.3 Hz, 2H, H_{A2}), 2.84 (hept, J = 6.9 Hz, 2H, CH(CH₃)₂), 2.12 (td, J = 13.1, 3.8 Hz, 2H, C-CH₂), 1.67 – 1.59 (m, 5H, H_{C7}), 1.56 – 1.45 (m, 5H, H_{C7}), 1.29 (d, J = 6.7 Hz, 6H, CH₃), 1.16 (d, J = 6.7 Hz, 6H, CH₃), 0.88 (s, 6H, CH₃), 0.29 (s, 27H, H_{TMS}).

Appendix

^{13}C NMR (126 MHz, C_6D_6): δ [ppm] = 174.20 (C=N), 150.97 (C_{Ar}), 148.15 (C_{Ar}), 131.53 (C_{Ar}), 129.22 (C_{Ar}), 124.78 (C=O), 63.77 ($\text{C}(\text{CH}_3)_2$), 48.72 ($\text{C}-\text{C}(\text{CH}_3)_2$), 46.20 (C-C=N), 35.95 (C_{C_7}), 29.39 ($\text{CH}(\text{CH}_3)_2$), 29.29 ($\text{CH}(\text{CH}_3)_2$), 28.03 (C_{C_7}), 25.22 (C_{C_7}), 23.53 (CH_3), 22.73 (CH_3), 2.79 (C_{TMS}).

^{29}Si NMR (99 MHz, C_6D_6): δ [ppm] = -9.64 (TMS), -28.31 ($\text{SiO}_2\text{C}=\text{O}$), -134.20 (SiTMS_3).

LIFDI-MS: $m/z = 675.3645 [4 + \text{H}]^+$.



Appendix

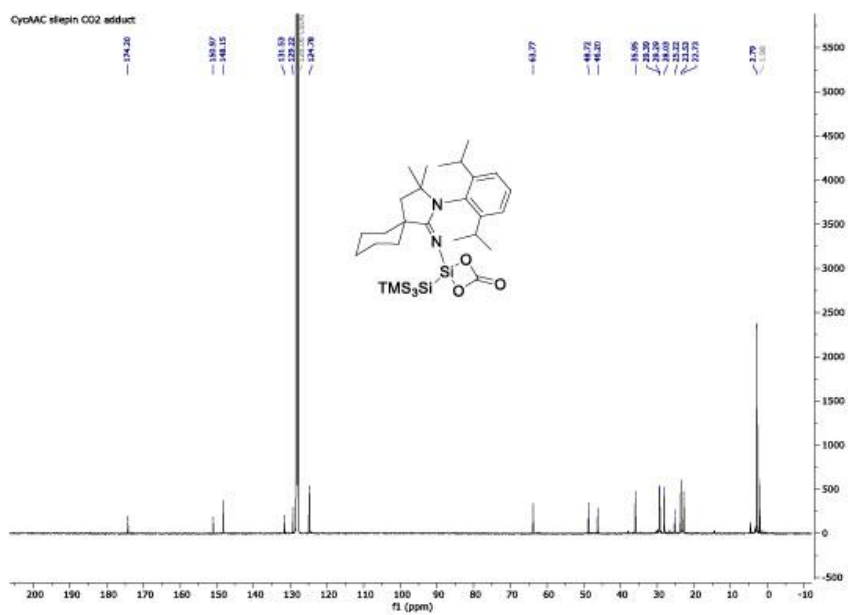


Figure 11: ^{13}C NMR of compound 4.

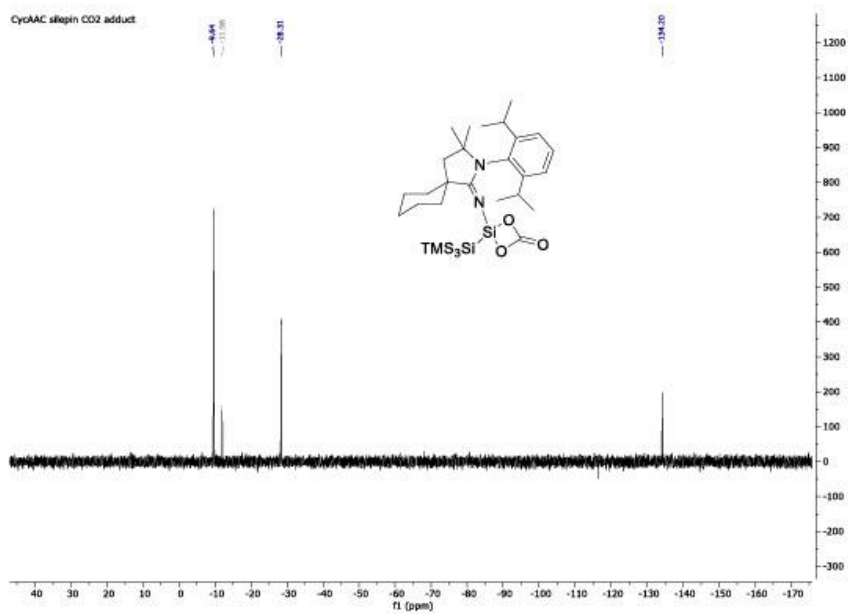
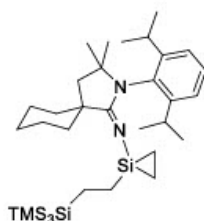


Figure 12: ^{29}Si NMR of compound 4.

Appendix

Cy-cAAC silepin ethylene insertion product (Compound 5) NMR experiment



Cy-cAAC silepin (15 mg, 24.4 μmol) is solved in C_6D_6 (0.5 mL) and filled into a PTFE *J*Young tube. The solution is frozen with liquid nitrogen and degassed. Subsequently, gaseous ethylene (1 bar) is introduced, and the tube is sealed afterwards. The mixture is heated to 90 $^\circ\text{C}$ for 72 hours. After evaporation of the solvent, the product is obtained as a pale-yellow oil (14.3 mg, 21.3 μmol , 87%).

^1H NMR (500 MHz, C_6D_6): δ [ppm] = 7.21 (dd, J = 8.4, 6.9 Hz, 1H, H_{Ar}), 7.14 (d, J = 8.3 Hz, 2H, H_{Ar}), 3.01 (hept, J = 6.7 Hz, 2H, $\text{CH}(\text{CH}_3)_2$), 2.18 (td, J = 13.2, 3.6 Hz, 2H, C- CH_2), 1.77 – 1.46 (m, 10H, H_{C_7}), 1.32 (d, J = 6.7 Hz, 6H, CH_3), 1.25 (d, J = 6.8 Hz, 6H, CH_3), 1.19 – 1.12 (m, 4H, $\text{NSi}(\text{CH}_2)_2$), 1.09 – 1.04 (m, 2H, $\text{Si}(\text{CH}_2)_2\text{Si}$), 0.97 (s, 6H, CH_3), 0.94 – 0.89 (m, 2H, $\text{Si}(\text{CH}_2)_2\text{Si}$), 0.25 (s, 27H, H_{TMS}).

^{13}C NMR (126 MHz, C_6D_6): δ [ppm] = 170.73 (C=N), 149.04 (C_{Ar}), 133.07 (C_{Ar}), 124.09 (C_{Ar}), 122.98 (C_{Ar}), 61.14 (C(CH_3) $_2$), 47.70 (C-C(CH_3) $_2$), 47.18 (C-C=N), 35.94 (C_{C_7}), 29.84 (CH(CH_3) $_2$), 29.37 (CH(CH_3) $_2$), 27.02 (C_{C_7}), 25.82 (C_{C_7}), 23.13 (CH_3), 22.93 (CH_3), 12.74 ($\text{NSi}(\text{CH}_2)_2$), 1.44 (C_{TMS}), 0.77 ($\text{Si}(\text{CH}_2)_2\text{Si}$).

^{29}Si NMR (99 MHz, C_6D_6): δ [ppm] = -13.31, -72.85, -77.03.

LIFDI-MS: m/z = 670.4366 [5] $^+$.

Appendix

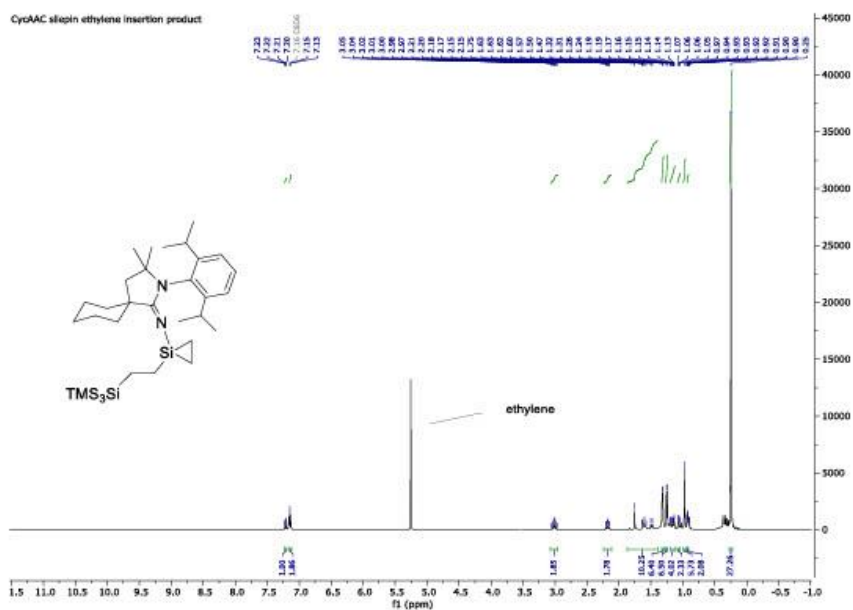


Figure 13: ¹H NMR of compound 5.

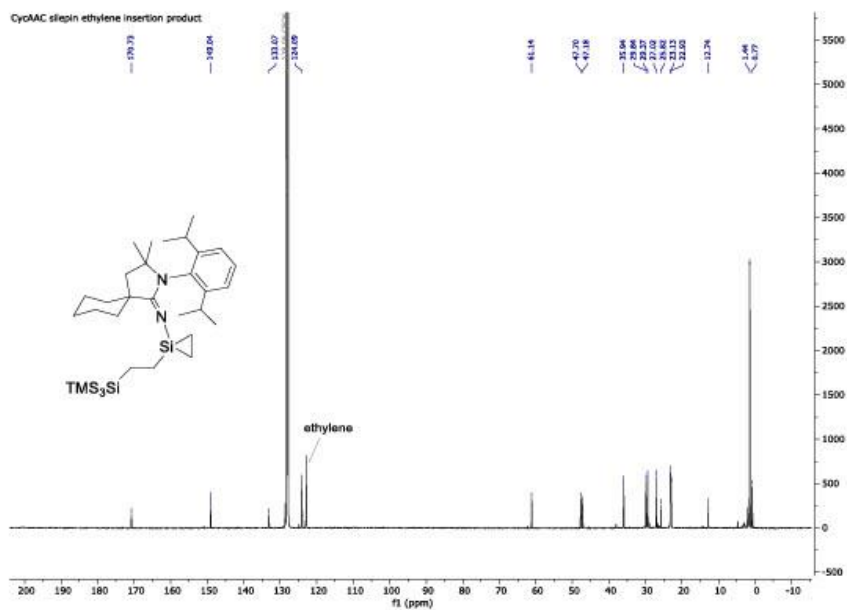


Figure 14: ¹³C NMR of compound 5.

Appendix

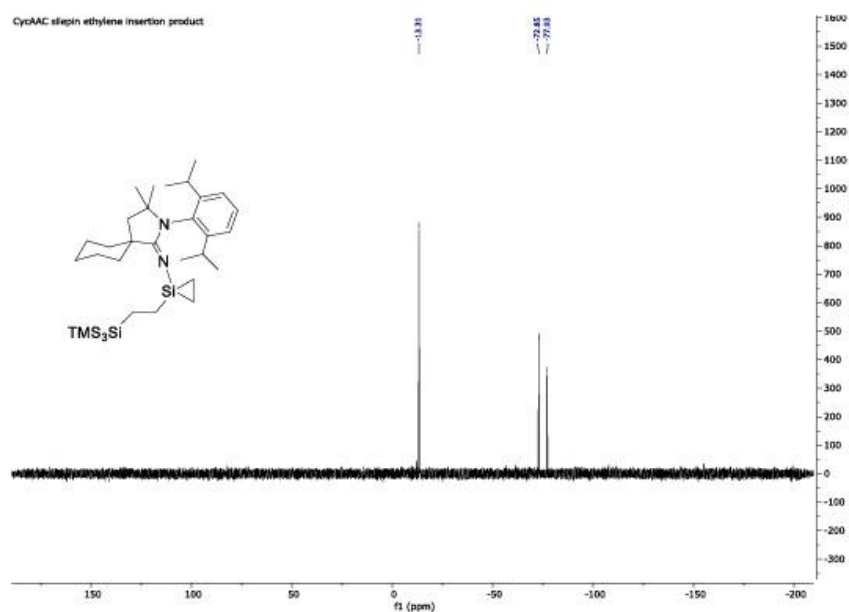
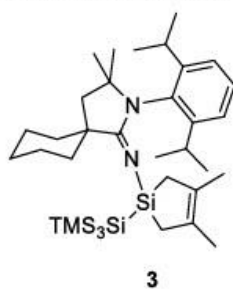


Figure 15: ^{29}Si NMR of compound 5.

Cy-cAAC silepin 2,3-Dimethyl-1,3-butadien adduct (Compound 6) NMR experiment



Cy-cAAC silepin (15 mg, 24.4 μmol , 1.0 eq.) is solved in C_6D_6 (0.5 mL) and 2,3-dimethylbuta-1,3-diene (11.1 μL , 97.5 μmol , 4.0 eq.) is added. The mixture is filled into a *JYoung* PTFE tube and heated to 80 $^\circ\text{C}$ for 16 hours. After evaporation of the solvent, the product is obtained as a white solid (15.5 mg, 22.2 μmol , 91%).

^1H NMR (500 MHz, C_6D_6): δ [ppm] = 7.21 – 7.17 (m, 1H, H_{Ar}), 7.09 (d, $J = 7.4$ Hz, 2H, H_{Ar}), 3.05 (hept, $J = 6.8$ Hz, 2H, $\text{CH}(\text{CH}_3)_2$), 1.98 (td, $J = 13.4, 3.7$ Hz, 2H, C- CH_2), 1.80 (s, 2H, H_{Cy}), 1.72 (s, 6H, SiCH_2CH_3), 1.70 – 1.62 (m, 4H, SiCH_2CH_3), 1.54 – 1.39 (m, 4H, H_{Cy}), 1.34 – 1.23 (m, 4H, H_{Cy}), 1.21 (d, $J = 6.8$ Hz, 12H, CH_3), 1.00 (s, 6H, CH_3), 0.37 (s, 27H, H_{TMS}).

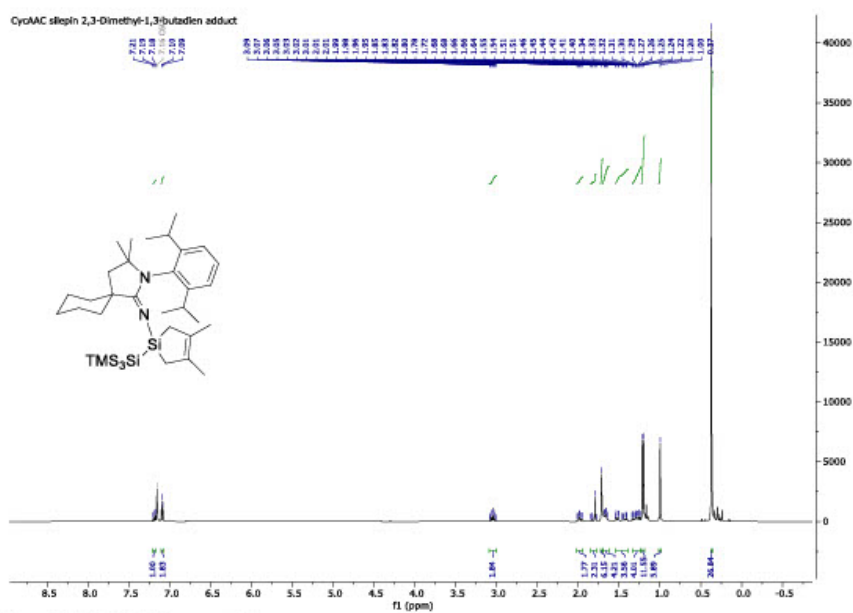
Appendix

^{13}C NMR (126 MHz, C_6D_6): δ [ppm] = 166.52 (C=N), 149.29 (C_{Ar}), 134.53 (C_{Ar}), 131.07 (C_{Ar}), 127.97 (C=C), 124.74 (C_{Ar}), 61.10 (C(CH $_3$) $_2$), 47.46 (C-C(CH $_3$) $_2$), 47.29 (C-C=N), 36.57 (C_{C_7}), 34.61 (C_{C_7}), 30.43 (SiCH $_2$ CH $_3$), 28.89 (CH(CH $_3$) $_2$), 27.77 (CH $_3$), 25.50 (C_{C_7}), 24.29 (CH $_3$), 22.92 (CH $_3$), 19.40 (SiCH $_2$ CH $_3$), 3.67 (C_{TMS}).

^{29}Si NMR (99 MHz, C_6D_6): δ [ppm] = -10.34 (TMS), -18.43 (SiCH $_2$ CH $_3$), -132.75 (SiTMS $_3$).

LIFDI-MS: m/z = 696.4501 [6] $^+$.

Melting point: 185 $^\circ\text{C}$



Appendix

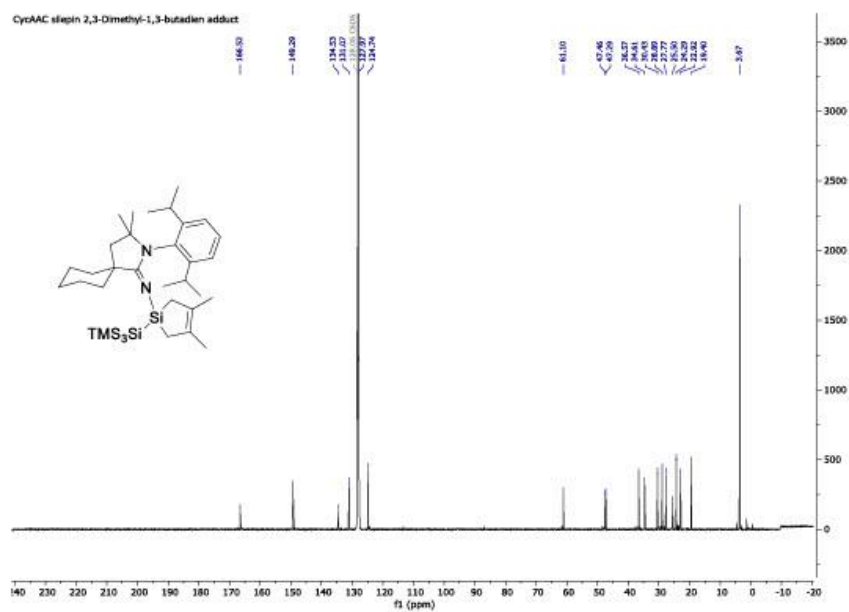


Figure 17: ^{13}C NMR of compound 6.

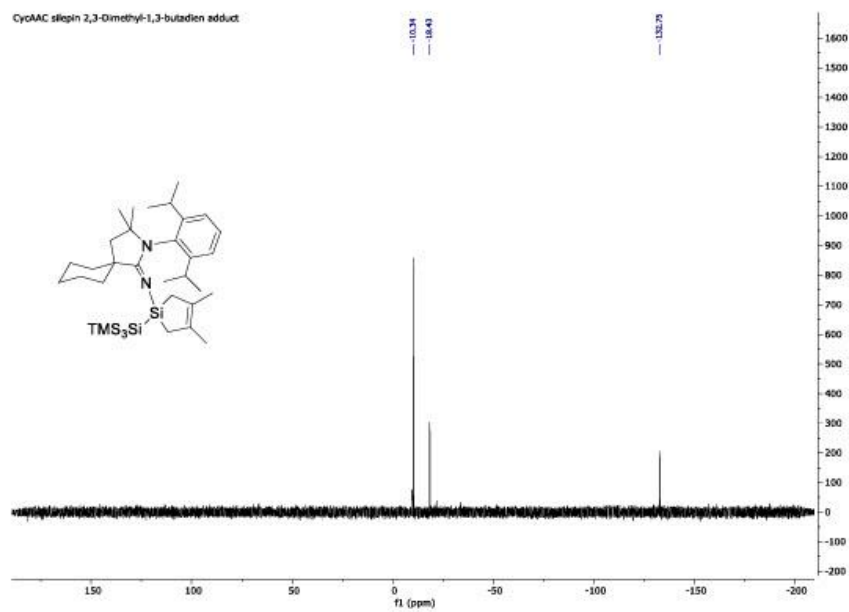
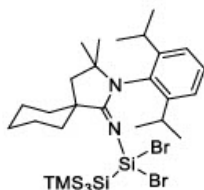


Figure 18: ^{29}Si NMR of compound 6.

Appendix

Cy-cAAC silepin dibromide (Compound 7) NMR experiment



Cy-cAAC silepin (10 mg, 16.3 μmol , 1.0 eq.) is solved in toluene (1 mL) and *n*-butylbromide (7.0 μL , 65.0 μmol , 4.0 eq.) or isopropyl bromide (6.1 μL , 65.0 μmol , 4.0 eq.) is added. The mixture is stirred at 90 $^{\circ}\text{C}$ for 24 hours. After evaporation of the solvent, the product is obtained as a yellow oil (12.1 mg, 16.6 μmol , 96% yield for reaction with *n*-butylbromide and 11.8 mg, 15.2 μmol , 94% for reaction with *iso*-propyl bromide).

^1H NMR (400 MHz, C_6D_6): δ [ppm] = 7.15 (d, J = 4.8 Hz, 1H, H_{Ar}), 7.09 (d, J = 6.6 Hz, 2H, H_{Ar}), 2.95 (p, J = 6.8 Hz, 2H, $\text{CH}(\text{CH}_3)_2$), 2.81 (td, J = 13.4, 3.6 Hz, 2H, C- CH_2), 1.81 – 1.47 (m, 10H, H_{Cy}), 1.42 (d, J = 6.7 Hz, 6H, CH_3), 1.18 (d, J = 6.7 Hz, 6H, CH_3), 0.94 (s, 6H, CH_3), 0.39 (s, 27H, H_{TMS}).

^{13}C NMR (126 MHz, C_6D_6): δ [ppm] = 173.56 (C=N), 147.70 (C_{Ar}), 132.48 (C_{Ar}), 128.60 (C_{Ar}), 124.71 (C_{Ar}), 63.52 (C(CH_3) $_2$), 49.31 (C-C(CH_3) $_2$), 47.23 (C-C=N), 34.78 (C_{Cy}), 29.79 (C_{Cy}), 28.76 (C_{Cy}), 28.39 (CH(CH_3) $_2$), 24.05 (CH_3), 22.44 (CH_3), 2.83 (C_{TMS}).

^{29}Si NMR (99 MHz, C_6D_6): δ [ppm] = -10.16 (TMS), -53.00 (SiBr_2), -101.03 (SiTMS_3).

LIFDI-MS: m/z = 697.4562 [7-Br] $^+$.

Appendix

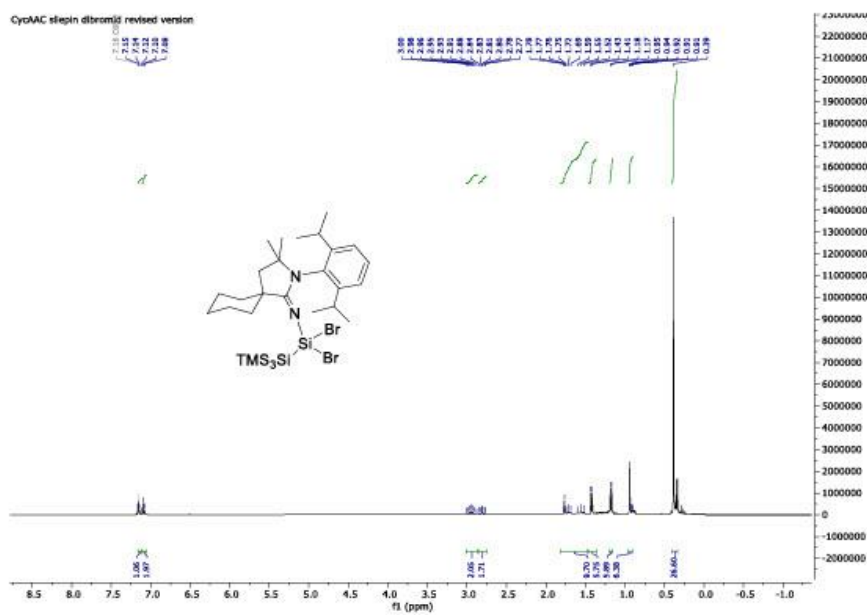


Figure 19: ^1H NMR of compound 7.

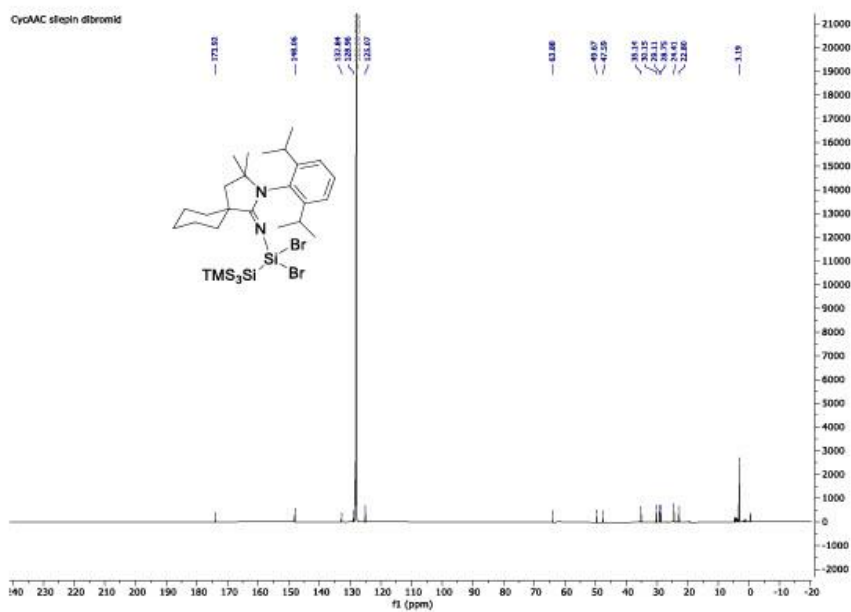


Figure 20: ^{13}C NMR of compound 7.

Appendix

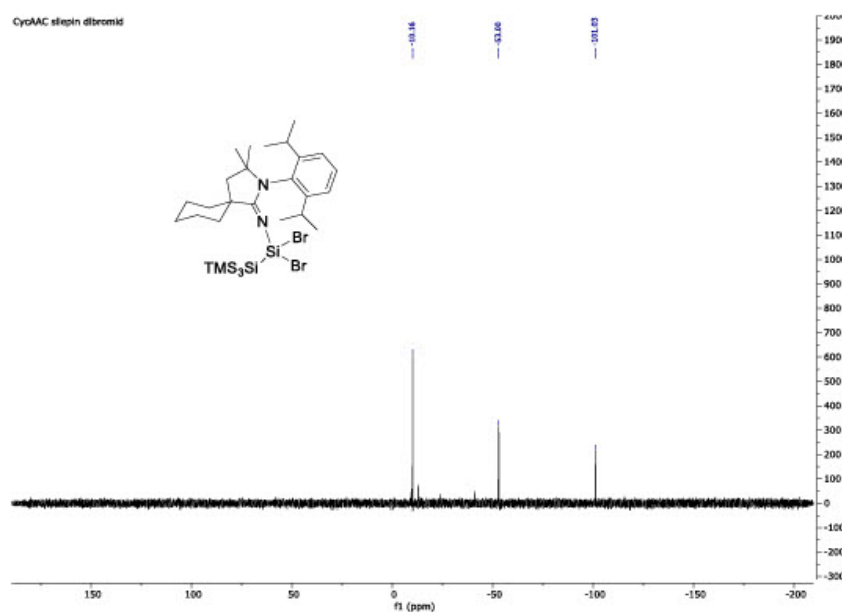
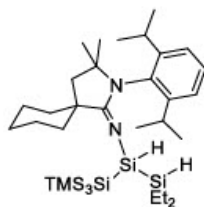


Figure 21: ^{29}Si NMR of compound 7.

Cy-cAAC silepin diethylsilane adduct (Compound 8) NMR experiment



Cy-cAAC silepin (10 mg, 16.3 μmol , 1.0 eq.) is solved in C_6D_6 (0.5 mL) and diethyl silane (10.5 μL , 81.3 μmol , 5.0 eq.) is added. The mixture is filled into a *JYoung* PTFE tube and heated to 80 $^\circ\text{C}$ for 16 hours. After evaporation of the solvent, the product is obtained as a white solid (11.3 mg, 16.6 μmol , 99%).

^1H NMR (500 MHz, C_6D_6): δ [ppm] = 7.19 (t, $J = 7.6$ Hz, 1H, H_{Ar}), 7.12 (dd, $J = 7.8, 1.8$ Hz, 1H, H_{Ar}), 7.09 (dd, $J = 7.6, 1.8$ Hz, 1H, H_{Ar}), 6.41 (d, $J = 4.1$ Hz, 1H, SiHSiHEt_2), 4.05 (qq, $J = 4.1, 2.2$ Hz, 1H, SiHSiHEt_2), 3.16 – 3.06 (m, $J = 6.7$ Hz, 2H, $\text{CH}(\text{CH}_3)_2$), 2.56 (m, 1H, C- CH_2), 2.47 (m, 1H, C- CH_2), 1.86 (m, 1H, H_{C7}), 1.76 – 1.57 (m, 6H, H_{C7}), 1.37 (d, $J = 6.7$ Hz, 3H, H_{C7}), 1.29 – 1.20 (m, 18H, CH_3).

Appendix

1.05 (s, 3H, CH₂CH₃), 1.04 – 0.99 (m, 1H, CH₂CH₃), 0.95 (s, 3H, CH₂CH₃), 0.94 – 0.78 (m, 3H, CH₂CH₃), 0.34 (s, 29H, H_{TMS}).

¹³C NMR (126 MHz, C₆D₆): δ [ppm] = 170.11 (C=N), 149.28 (C_{Az}), 148.89 (C_{Az}), 134.13 (C_{Az}), 124.59 (C_{Az}), 124.17 (C_{Az}), 61.34 (C(CH₃)₂), 48.63 (C-C(CH₃)₂), 48.31 (C-C=N), 37.47 (C_{Cy}), 34.84 (C_{Cy}), 30.83 (C_{Cy}), 29.32 (C_{Cy}), 29.25 (C_{Cy}), 29.20 (CH(CH₃)₂), 29.17 (CH(CH₃)₂), 28.13 (CH₃), 25.72 (CH₃), 24.24 (CH₃), 23.41 (CH₃), 23.35 (CH₃), 23.15 (CH₃), 11.31 (CH₂CH₃), 10.18 (CH₂CH₃), 3.78 (C_{TMS}).

²⁹Si NMR (99 MHz, C₆D₆): δ [ppm] = -9.50 (TMS), -18.77 (SiHEt₂), -60.03 (SiHSiHEt₂), -130.80 (SiTMS₃).

LIFDI-MS: m/z = 702.4455 [8]⁺.

Melting point: 172.5 °C

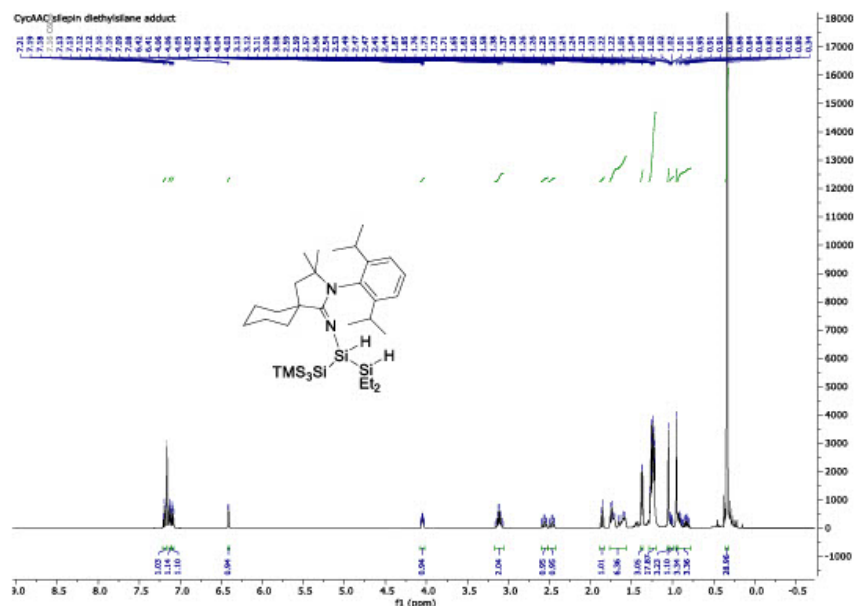


Figure 22: ¹H NMR of compound 8.

Appendix

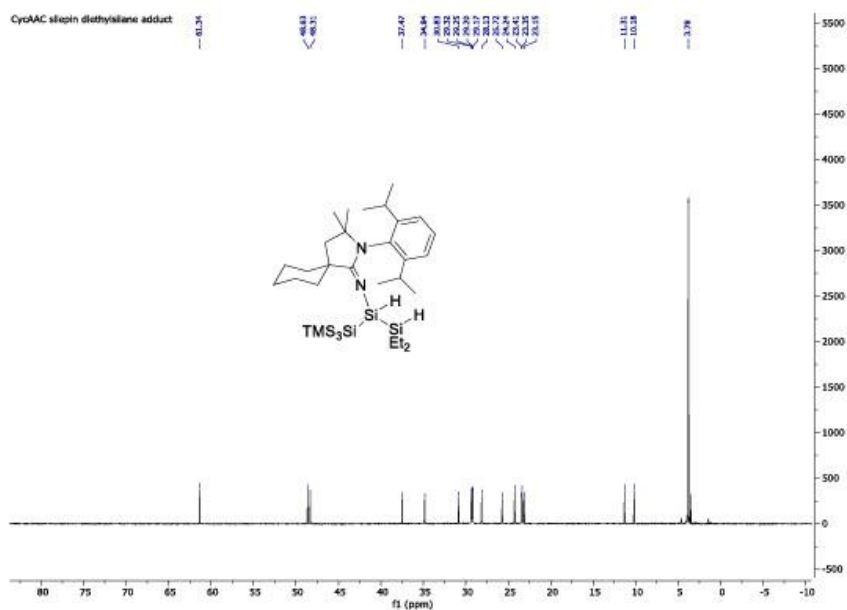


Figure 23: ¹³C NMR of compound 8.

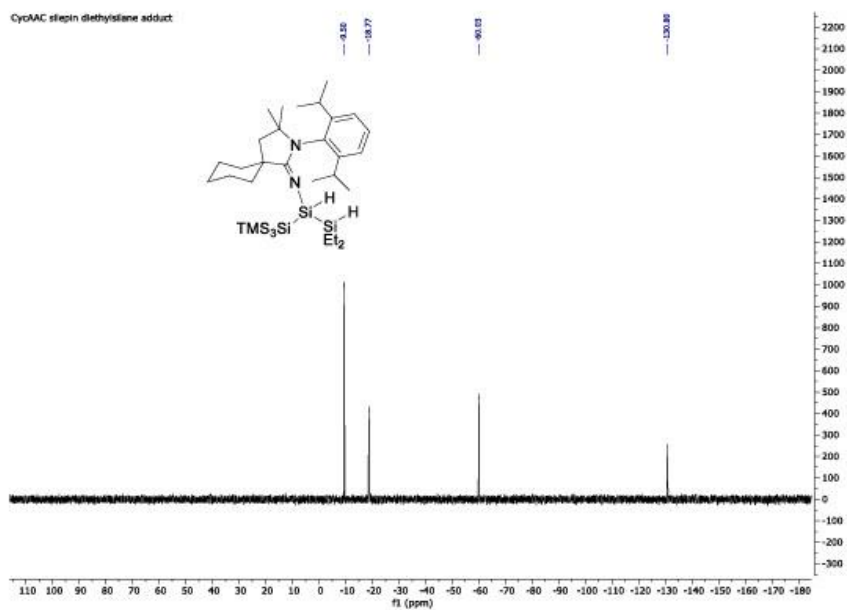


Figure 24: ²⁹Si NMR of compound 8.

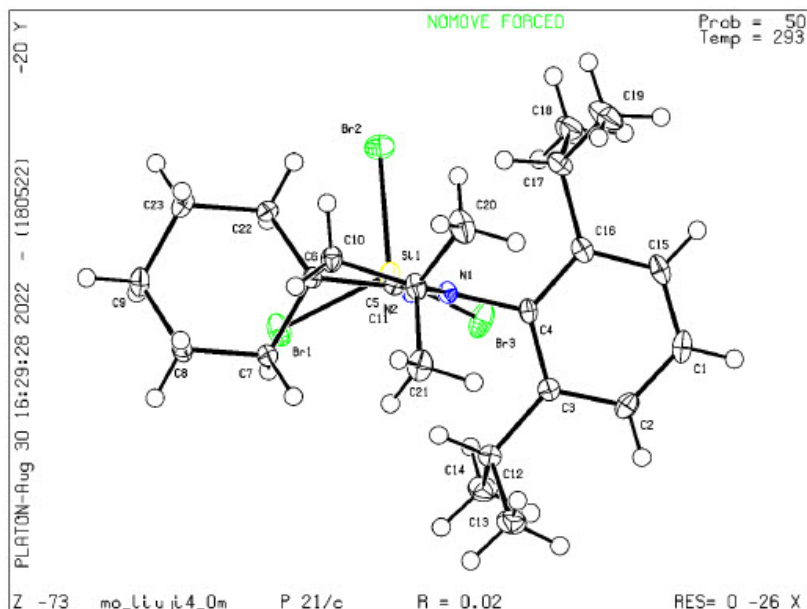
2. X-Ray Crystallographic Data

A) General

Data were collected on a single crystal X-ray diffractometer equipped with a CPAD detector (Bruker Photon-II), an IMS microsource or a TXS rotating anode with MoK α radiation ($\lambda = 0.71073$ Å) and a Helios optic using the APEX4 software package.^[2] The crystal was fixed on the top of a kapton micro sampler with perfluorinated ether and transferred to the diffractometer and frozen under a stream of cold nitrogen. A matrix scan was used to determine the initial lattice parameters. Reflections were corrected for Lorentz and polarisation effects, scan speed, and background using SAINT.^[3] Absorption correction, including odd and even ordered spherical harmonics was performed using SADABS.^[4] Space group assignment was based upon systematic absences, E statistics, and successful refinement of the structure. The structures were solved using SHELXT with the aid of successive difference Fourier maps and were refined against all data using SHELXL in conjunction with SHELXLE.^[4,5,6] Hydrogen atoms (except on heteroatoms) were calculated in ideal positions as follows: Methyl hydrogen atoms were refined as part of rigid rotating groups, with a C–H distance of 0.98 Å and $U_{iso}(H) = 1.5 \cdot U_{eq}(C)$. Non-methyl H atoms were placed in calculated positions and refined using a riding model with methylene, aromatic, and other C–H distances of 0.99 Å, 0.95 Å, and 1.00 Å, respectively, and $U_{iso}(H) = 1.2 \cdot U_{eq}(C)$. Non-hydrogen atoms were refined with anisotropic displacement parameters. Full-matrix least-squares refinements were carried out by minimizing $\sum w(F_o - F_c)^2$ with the SHELXL weighting scheme. Neutral atom scattering factors for all atoms and anomalous dispersion corrections for the non-hydrogen atoms were taken from International Tables for Crystallography.^[7] Co-crystallized pentane was disordered and modeled using free variables in conjunction with ISOR, SIMU, RIGU, SADI, and SAME restraints as implemented in the DSR plugin in SHELXLE.^[8,9] Images of the crystal structure were generated with Mercury and PLATON.^[8,10] Deposition Number 2293615–2293620 contains the supplementary crystallographic data for this paper. These data are provided free of charge by the joint Cambridge Crystallographic Data Centre and Fachinformationszentrum Karlsruhe. Access Structures service www.ccdc.cam.ac.uk/structures.

Appendix

Cy-cAACNSiBr₃ (Compound 2, CCDC 2293615)



Diffractometer operator Jinyu Liu

scanspeed 10s per frame dx 40mm

1464 frames measured in 4 data sets

phi-scans with delta_phi = 0.5

omega-scans with delta_omega = 0.5

shutterless mode

Crystal data

C₂₃H₃₅Br₃N₂Si

$M_r = 607.32$

Monoclinic, $P2_1/c$

Hall symbol: -P 2ybc

$a = 15.6717 (5) \text{ \AA}$

$b = 10.1334 (3) \text{ \AA}$

$c = 17.3758 (6) \text{ \AA}$

$D_x = 1.556 \text{ Mg m}^{-3}$

Melting point: ? K

Mo $K\alpha$ radiation, $\lambda = 0.71073 \text{ \AA}$

Cell parameters from 9900 reflections

$\theta = 2.5\text{--}26.4^\circ$

$\mu = 4.73 \text{ mm}^{-1}$

Appendix

$\beta = 110.005 (1)^\circ$ $T = 293 \text{ K}$
 $V = 2592.91 (15) \text{ \AA}^3$ **Fragment, colorless**
 $Z = 4$ $0.44 \times 0.27 \times 0.15 \text{ mm}$
 $F(000) = 1224$

Data collection

Bruker D8 Venture **5305 independent reflections**
diffractometer
Radiation source: IMS microsource **4865 reflections with $I > 2\sigma(I)$**
Helios optic monochromator $R_{\text{int}} = 0.028$
Detector resolution: $7.5 \text{ pixels mm}^{-1}$ $\theta_{\text{max}} = 26.4^\circ$, $\theta_{\text{min}} = 2.4^\circ$
phi- and ω -rotation scans $h = -19 \text{ } 19$
Absorption correction: multi-scan $k = -11 \text{ } 12$
SADABS 2016/2, Bruker, 2016
 $T_{\text{min}} = 0.596$, $T_{\text{max}} = 0.745$ $l = -21 \text{ } 21$
49401 measured reflections

Refinement

Refinement on F^2 **Secondary atom site location: difference Fourier**
map
Least-squares matrix: full **Hydrogen site location: inferred from**
neighbouring sites
 $R[F^2 > 2\sigma(F^2)] = 0.016$ **H-atom parameters constrained**
 $wR(F^2) = 0.039$ $W = 1/[\Sigma^2(FO^2) + (0.0144P)^2 + 1.7724P]$
WHERE $P = (FO^2 + 2FC^2)/3$
 $S = 1.04$ $(\Delta/\sigma)_{\text{max}} = 0.002$
5305 reflections $\Delta\rho_{\text{max}} = 0.45 \text{ e \AA}^{-3}$
268 parameters $\Delta\rho_{\text{min}} = -0.41 \text{ e \AA}^{-3}$
0 restraints **Extinction correction: none**

Appendix

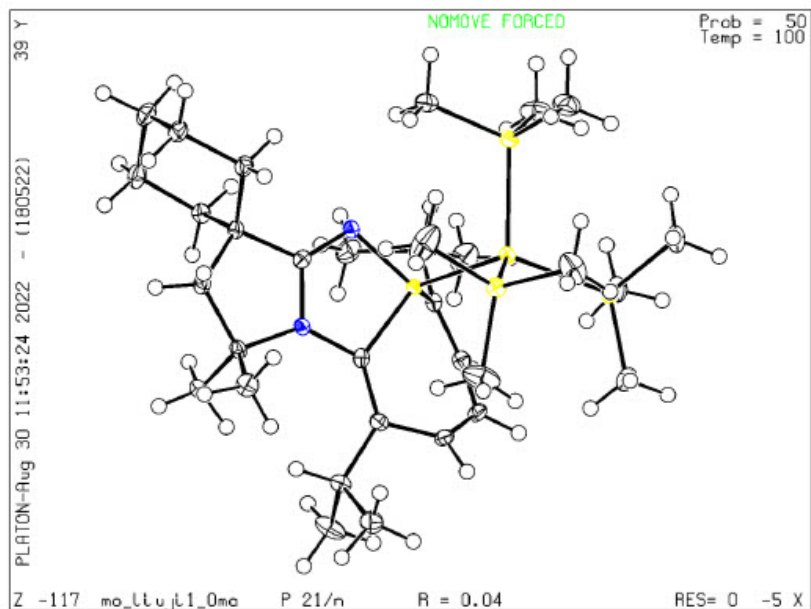
- constraints

Extinction coefficient: -

Primary atom site location: iterative

Appendix

Cy-cAAC silepin (Compound 3, CCDC 2293616)



Diffractometer operator Jinyu Liu

scanspeed 5s per frame

dx 38mm

1650 frames measured in 6 data sets

phi-scans with delta_phi = 0.5

omega-scans with delta_omega = 0.5

shutterless mode

Crystal data

$C_{32}H_{62}N_2Si_5$

$M_r = 615.29$

Monoclinic, $P2_1/n$

Hall symbol: $-P 2_1n$

$a = 9.5236 (7) \text{ \AA}$

$b = 42.212 (3) \text{ \AA}$

$D_x = 1.084 \text{ Mg m}^{-3}$

Melting point: ? K

Mo $K\alpha$ radiation, $\lambda = 0.71073 \text{ \AA}$

Cell parameters from 9936 reflections

$\theta = 2.2\text{--}27.4^\circ$

Appendix

$c = 9.5536 (6) \text{ \AA}$ $\mu = 0.21 \text{ mm}^{-1}$
 $\beta = 101.056 (2)^\circ$ $T = 100 \text{ K}$
 $V = 3769.4 (5) \text{ \AA}^3$ Fragment, colorless
 $Z = 4$ $0.19 \times 0.12 \times 0.02 \text{ mm}$
 $F(000) = 1352$

Data collection

Bruker D8 Venture diffractometer 7707 independent reflections
 Radiation source: IMS microsource 6464 reflections with $I > 2\sigma(I)$
 Helios optic monochromator $R_{\text{int}} = 0.066$
 Detector resolution: $7.5 \text{ pixels mm}^{-1}$ $\theta_{\text{max}} = 26.4^\circ$, $\theta_{\text{min}} = 1.9^\circ$
 phi- and ω -rotation scans $h = -11 \ 11$
 Absorption correction: multi-scan $k = -52 \ 52$
SADABS 2016/2, Bruker, 2016
 $T_{\text{min}} = 0.714$, $T_{\text{max}} = 0.746$ $l = -11 \ 11$
 47480 measured reflections

Refinement

Refinement on F^2 Secondary atom site location: difference Fourier map
 Least-squares matrix: full Hydrogen site location: inferred from neighbouring sites
 $R[F^2 > 2\sigma(F^2)] = 0.043$ H-atom parameters constrained
 $wR(F^2) = 0.092$ $W = 1/[\Sigma^2(FO^2) + (0.0254P)^2 + 2.9789P]$
 $S = 1.08$ WHERE $P = (FO^2 + 2FC^2)/3$
 7707 reflections $(\Delta/\sigma)_{\text{max}} = 0.001$
 367 parameters $\Delta\rho_{\text{max}} = 0.37 \text{ e \AA}^{-3}$
 $\Delta\rho_{\text{min}} = -0.30 \text{ e \AA}^{-3}$

Appendix

0 restraints

Extinction correction: none

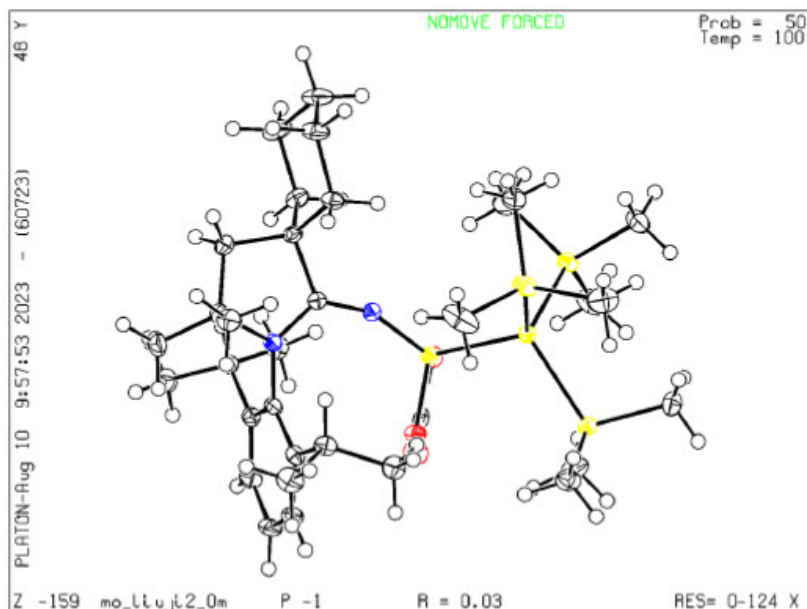
0 constraints

Extinction coefficient: -

Primary atom site location: iterative

Appendix

Cy-cAAC silepin CO₂ adduct (Compound 4, CCDC 2293619)



Diffractometer operator Jinyu Liu

scanspeed 5s per frame dx 38mm

2035 frames measured in 12 data sets

phi-scans with delta_phi = 0.5

omega-scans with delta_omega = 0.5

shutterless mode

Crystal data

C₃₃H₆₂N₂O₃Si₅

$F(000) = 736$

$M_r = 675.30$

Triclinic, *P*

$D_x = 1.126 \text{ Mg m}^{-3}$

Hall symbol: -*P* 1

Melting point: ? K

$a = 11.0094 (10) \text{ \AA}$

Mo $K\alpha$ radiation, $\lambda = 0.71073 \text{ \AA}$

$b = 11.9760 (12) \text{ \AA}$

Cell parameters from 9322 reflections

$c = 15.9693 (16) \text{ \AA}$

$\theta = 2.3\text{--}25.7^\circ$

Appendix

$\alpha = 84.306 (4)^\circ$	$\mu = 0.21 \text{ mm}^{-1}$
$\beta = 87.974 (4)^\circ$	$T = 100 \text{ K}$
$\gamma = 71.952 (3)^\circ$	Fragment, colorless
$V = 1992.0 (3) \text{ \AA}^3$	$0.26 \times 0.25 \times 0.19 \text{ mm}$
$Z = 2$	

Data collection

Bruker D8 Venture diffractometer	7606 independent reflections
Radiation source: IMS microsource	7173 reflections with $I > 2\sigma(I)$
Helios optic monochromator	$R_{\text{int}} = 0.027$
Detector resolution: $7.5 \text{ pixels mm}^{-1}$	$\theta_{\text{max}} = 25.7^\circ$, $\theta_{\text{min}} = 2.1^\circ$
phi- and ω -rotation scans	$h = -13 \text{ } 13$
Absorption correction: multi-scan SADABS 2016/2, Bruker, 2016	$k = -14 \text{ } 14$
$T_{\text{min}} = 0.715$, $T_{\text{max}} = 0.745$	$l = -19 \text{ } 19$
59425 measured reflections	

Refinement

Refinement on F^2	Secondary atom site location: difference Fourier map
Least-squares matrix: full	Hydrogen site location: inferred from neighbouring sites
$R[F^2 > 2\sigma(F^2)] = 0.027$	H-atom parameters constrained
$wR(F^2) = 0.072$	$W = 1/[\Sigma^2(FO^2) + (0.0392P)^2 + 1.2997P]$ WHERE $P = (FO^2 + 2FC^2)/3$
$S = 0.90$	$(\Delta/\sigma)_{\text{max}} = 0.001$
7606 reflections	$\Delta\rho_{\text{max}} = 0.39 \text{ e \AA}^{-3}$
403 parameters	$\Delta\rho_{\text{min}} = -0.21 \text{ e \AA}^{-3}$

Appendix

0 restraints

- constraints

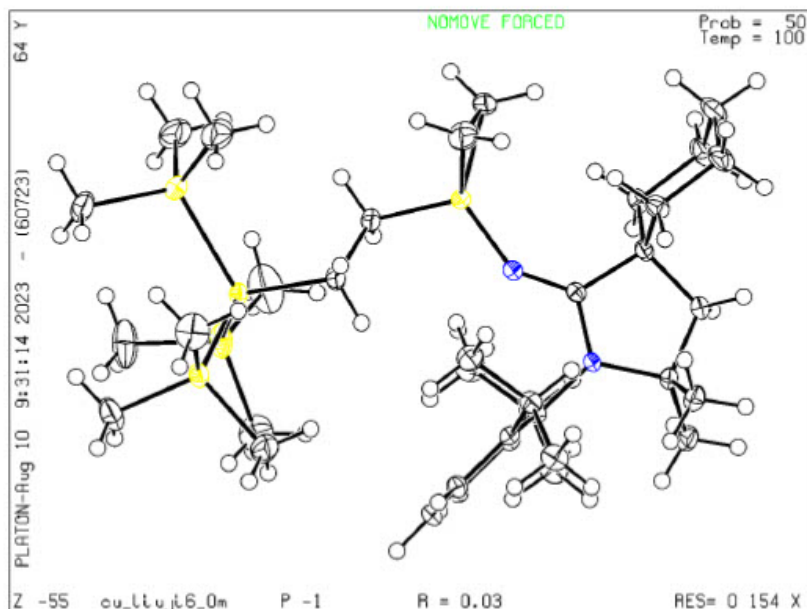
Primary atom site location: iterative

Extinction correction: none

Extinction coefficient: -

Appendix

Cy-cAAC silepin ethylene insertion product (5, CCDC 2293620)



Diffractometer operator Jinyu Liu

scanspeed 10s per frame dx 38mm

6698 frames measured in 39 data sets

phi-scans with $\Delta\phi = 0.5$

omega-scans with $\Delta\omega = 0.5$

shutterless mode

Crystal data

$C_{36}H_{70}N_2Si_5$

$F(000) = 740$

$M_r = 671.39$

Triclinic, P

$D_x = 1.044 \text{ Mg m}^{-3}$

Hall symbol: $-P 1$

Melting point: ? K

$a = 9.383 (3) \text{ \AA}$

Cu $K\alpha$ radiation, $\lambda = 1.54178 \text{ \AA}$

$b = 14.196 (3) \text{ \AA}$

Cell parameters from 9003 reflections

$c = 16.747 (3) \text{ \AA}$

$\theta = 3.2\text{--}72.2^\circ$

Appendix

$\alpha = 94.650 (12)^\circ$	$\mu = 1.73 \text{ mm}^{-1}$
$\beta = 93.87 (2)^\circ$	$T = 100 \text{ K}$
$\gamma = 105.183 (18)^\circ$	Fragment, colorless
$V = 2136.6 (9) \text{ \AA}^3$	$0.29 \times 0.28 \times 0.10 \text{ mm}$
$Z = 2$	

Data collection

Bruker D8 Venture diffractometer	7807 independent reflections
Radiation source: IMS microsource	7334 reflections with $I > 2\sigma(I)$
Helios optic monochromator	$R_{\text{int}} = 0.029$
Detector resolution: $7.5 \text{ pixels mm}^{-1}$	$\theta_{\text{max}} = 68.4^\circ$, $\theta_{\text{min}} = 2.7^\circ$
phi- and ω -rotation scans	$h = -11 \ 11$
Absorption correction: multi-scan SADABS 2016/2, Bruker, 2016	$k = -17 \ 17$
$T_{\text{min}} = 0.619$, $T_{\text{max}} = 0.754$	$l = -20 \ 20$
87797 measured reflections	

Refinement

Refinement on F^2	Secondary atom site location: difference Fourier map
Least-squares matrix: full	Hydrogen site location: inferred from neighbouring sites
$R[F^2 > 2\sigma(F^2)] = 0.028$	H-atom parameters constrained
$wR(F^2) = 0.078$	$W = 1/[\Sigma^2(FO^2) + (0.0387P)^2 + 0.9518P]$ WHERE $P = (FO^2 + 2FC^2)/3$
$S = 1.04$	$(\Delta/\sigma)_{\text{max}} = 0.001$
7807 reflections	$\Delta\rho_{\text{max}} = 0.32 \text{ e \AA}^{-3}$
403 parameters	$\Delta\rho_{\text{min}} = -0.28 \text{ e \AA}^{-3}$

Appendix

0 restraints

- constraints

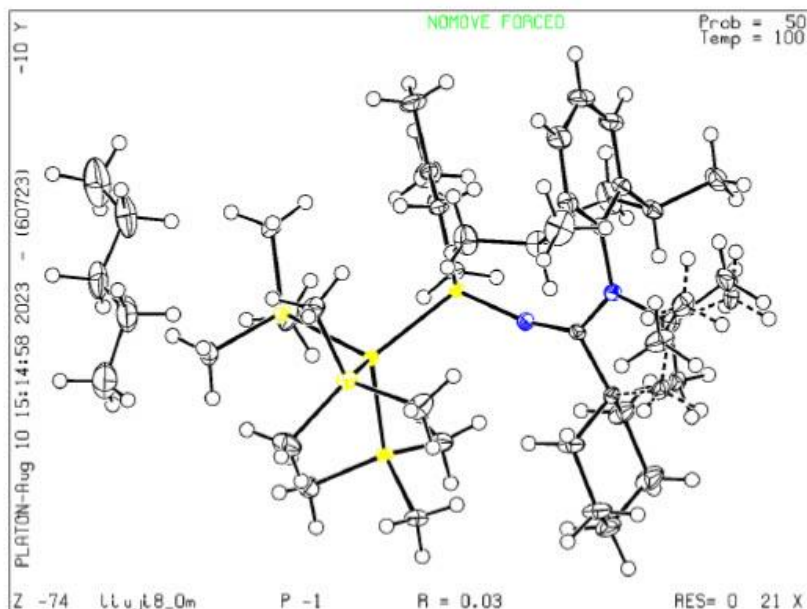
Primary atom site location: iterative

Extinction correction: none

Extinction coefficient: -

Appendix

Cy-cAAC silepin 2,3-Dimethyl-1,3-butadien adduct (Compound 6, CCDC 2293618)



Diffractometer operator Jinyu Liu

scanspeed 10s per frame dx 38mm

2634 frames measured in 12 data sets

phi-scans with $\Delta\phi = 0.5$

omega-scans with $\Delta\omega = 0.5$

shutterless mode

Crystal data

$C_{38}H_{72}N_2Si_5 \cdot 0.501(C_5H_{12})$

$F(000) = 810$

$M_r = 733.57$

Triclinic, P

$D_x = 1.062 \text{ Mg m}^{-3}$

Hall symbol: $-P 1$

Melting point: ? K

$a = 11.7541 (11) \text{ \AA}$

Mo $K\alpha$ radiation, $\lambda = 0.71073 \text{ \AA}$

$b = 12.3619 (13) \text{ \AA}$

Cell parameters from 9427 reflections

$c = 16.7898 (17) \text{ \AA}$

$\theta = 2.9\text{--}28.4^\circ$

Appendix

$\alpha = 89.906 (4)^\circ$	$\mu = 0.18 \text{ mm}^{-1}$
$\beta = 86.126 (3)^\circ$	$T = 100 \text{ K}$
$\gamma = 70.561 (3)^\circ$	Fragment, colorless
$V = 2294.7 (4) \text{ \AA}^3$	$0.38 \times 0.27 \times 0.22 \text{ mm}$
$Z = 2$	

Data collection

Bruker D8 Venture diffractometer	9729 independent reflections
Radiation source: IMS microsource	9099 reflections with $I > 2\sigma(I)$
Helios optic monochromator	$R_{\text{int}} = 0.046$
Detector resolution: $7.5 \text{ pixels mm}^{-1}$	$\theta_{\text{max}} = 26.7^\circ$, $\theta_{\text{min}} = 2.4^\circ$
phi- and ω -rotation scans	$h = -14 \ 14$
Absorption correction: multi-scan <i>SADABS</i> 2016/2, Bruker, 2016	$k = -15 \ 15$
$T_{\text{min}} = 0.684$, $T_{\text{max}} = 0.746$	$l = -21 \ 21$
98708 measured reflections	

Refinement

Refinement on F^2	Secondary atom site location: difference Fourier map
Least-squares matrix: full	Hydrogen site location: inferred from neighbouring sites
$R[F^2 > 2\sigma(F^2)] = 0.030$	H-atom parameters constrained
$wR(F^2) = 0.079$	$W = 1/[\Sigma^2(FO^2) + (0.0338P)^2 + 1.0839P]$ WHERE $P = (FO^2 + 2FC^2)/3$
$S = 1.06$	$(\Delta/\sigma)_{\text{max}} = 0.001$
9729 reflections	$\Delta\rho_{\text{max}} = 0.33 \text{ e \AA}^{-3}$
502 parameters	$\Delta\rho_{\text{min}} = -0.27 \text{ e \AA}^{-3}$

Appendix

175 restraints

- constraints

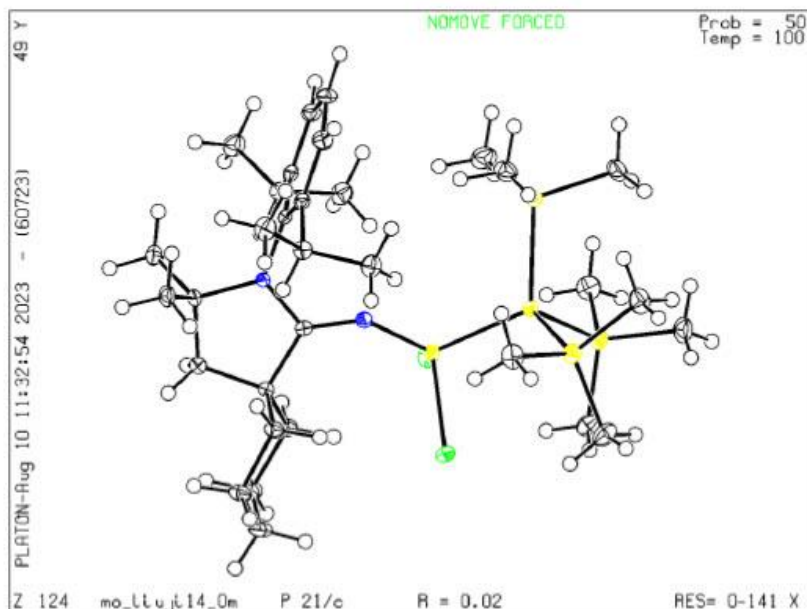
Primary atom site location: iterative

Extinction correction: none

Extinction coefficient: -

Appendix

Cy-cAAC silepin alkylbromide adduct (7, CCDC 2293617)



Diffractometer operator Jinyu Liu

scanspeed 8s per frame dx 38mm

2482 frames measured in 7 data sets

phi-scans with delta_phi = 0.5

omega-scans with delta_omega = 0.5

shutterless mode

Crystal data

$C_{32}H_{62}Br_2N_2Si_5$

$M_r = 775.09$

Monoclinic, $P2_1/c$

Hall symbol: $-P 2ybc$

$a = 9.4470 (5) \text{ \AA}$

$b = 37.200 (2) \text{ \AA}$

$c = 11.4682 (7) \text{ \AA}$

$D_x = 1.296 \text{ Mg m}^{-3}$

Melting point: ? K

Mo $K\alpha$ radiation, $\lambda = 0.71073 \text{ \AA}$

Cell parameters from 9604 reflections

$\theta = 2.4\text{--}26.4^\circ$

$\mu = 2.21 \text{ mm}^{-1}$

Appendix

$\beta = 99.656 (2)^\circ$ $T = 100 \text{ K}$
 $V = 3973.2 (4) \text{ \AA}^3$ Fragment, colorless
 $Z = 4$ $0.25 \times 0.25 \times 0.14 \text{ mm}$
 $F(000) = 1632$

Data collection

Bruker Photon CMOS diffractometer 8134 independent reflections
 Radiation source: TXS rotating anode 7689 reflections with $I > 2\sigma(I)$
 Helios optic monochromator $R_{\text{int}} = 0.039$
 Detector resolution: 16 pixels mm^{-1} $\theta_{\text{max}} = 26.4^\circ$, $\theta_{\text{min}} = 1.9^\circ$
 phi- and ω -rotation scans $h = -11 \text{ } 11$
 Absorption correction: multi-scan $k = -46 \text{ } 46$
SADABS 2016/2, Bruker, 2016
 $T_{\text{min}} = 0.638$, $T_{\text{max}} = 0.745$ $l = -14 \text{ } 14$
 148738 measured reflections

Refinement

Refinement on F^2 Secondary atom site location: difference Fourier map
 Least-squares matrix: full Hydrogen site location: inferred from neighbouring sites
 $R[F^2 > 2\sigma(F^2)] = 0.024$ H-atom parameters constrained
 $wR(F^2) = 0.067$ $W = 1/[\Sigma^2(FO^2) + (0.0353P)^2 + 3.133P]$ WHERE $P = (FO^2 + 2FC^2)/3$
 $S = 1.07$ $(\Delta/\sigma)_{\text{max}} = 0.002$
 8134 reflections $\Delta\rho_{\text{max}} = 0.44 \text{ e \AA}^{-3}$
 385 parameters $\Delta\rho_{\text{min}} = -0.53 \text{ e \AA}^{-3}$
 0 restraints Extinction correction: none

Appendix

- constraints

Extinction coefficient: -

Primary atom site location: iterative

3. Computational Calculations

Calculations were performed at the B3LYP/6-311+G(d)¹¹⁻¹³ level of theory using Gaussian 16.8¹⁴. Geometry optimization was carried out using the respective silylene fragment of the crystal structure of compound 7 as a base model. The optimized geometry was verified as minima by analytical frequency calculation.

Table 1: Energies (E^h) (E – electronic energy; H – total enthalpy; G – Gibbs energy) of the calculated compound.

Compound	E	H	G
3	-2813.89834271	-2812.961972	-2813.056539

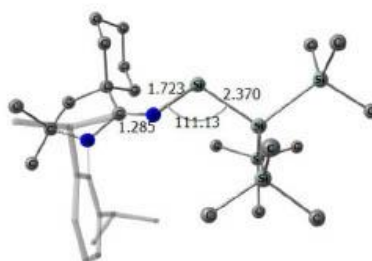
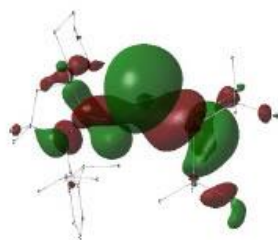
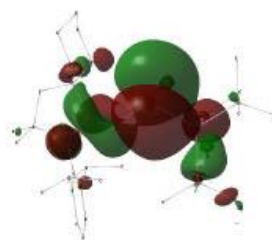


Figure 25: Visualization of the calculated structure of compound 3.



HOMO: -4.228 eV, Si lone pair



LUMO: -1.913eV, empty Si_{3p}

Figure 26: Visualization of HOMO and LUMO of compound 3.

4. References

- [S1] a) C. Marschner, *Eur. J. Inorg. Chem.* **1998**, *1998*, 221; b) V. Lavallo, Y. Canac, C. Präsang, B. Donnadiou, G. Bertrand, *Angew. Chem. Int. Ed.* **2005**, *44*, 5705; c) R. Jazzar, R. D. Dewhurst, J.-B. Bourg, B. Donnadiou, Y. Canac, G. Bertrand, *Angew. Chem. Int. Ed.* **2007**, *46*, 2899.
- [S2] *APEX suite of crystallographic software*, APEX 3, Version 2019-1.0, Bruker AXS Inc., Madison, Wisconsin, USA, 2019.
- [S3] *SAINT*, Version 8.40A and *SADABS*, Version 2016/2, Bruker AXS Inc., Madison, Wisconsin, USA, 2016/2019.
- [S4] G. M. Sheldrick, *Acta Crystallogr. Sect. A* **2015**, *71*, 3–8.
- [S5] G. M. Sheldrick, *Acta Crystallogr. Sect. C* **2015**, *71*, 3–8.
- [S6] C. B. Hübschle, G. M. Sheldrick, B. Dittrich, *J. Appl. Cryst.* **2011**, *44*, 1281–1284
- [S7] *International Tables for Crystallography, Vol. C* (Ed.: A. J. Wilson), Kluwer Academic Publishers, Dordrecht, The Netherlands, **1992**, Tables 6.1.1.4 (pp. 500–502), 4.2.6.8 (pp. 219–222), and 4.2.4.2 (pp. 193–199).
- [S8] C. F. Macrae, I. J. Bruno, J. A. Chisholm, P. R. Edgington, P. McCabe, E. Pidcock, L. Rodriguez-Monge, R. Taylor, J. van de Streek, P. A. Wood, *J. Appl. Cryst.* **2008**, *41*, 466–470.
- [S9] D. Kratzert, I. Krossing, *J. Appl. Crystallogr.* **2018**, *51*, 928.
- [S10] A. L. Spek, *Acta Crystallogr. Sect. D* **2009**, *65*, 148–155.
- [S11] Lee; Yang, *Phys. Rev. B* **1988**, *37*, 785–789.
- [S12] Vosko, S. H.; Wilk, L.; Nusair, *Can. J. Phys.* **1980**, *58*, 1200–1211.
- [S13] Becke, A. D., *J. Chem. Phys.* **1993**, *98*, 5648–5652.
- [S14] M. J. Frisch, G. W. Trucks, H. B. Schlegel, G. E. Scuseria, M. A. Robb, J. R. Cheeseman, G. Scalmani, V. Barone, G. A. Petersson, H. Nakatsuji, X. Li, M. Caricato, A. V. Marenich, J. Bloino, B. G. Janesko, R. Gomperts, B. Mennucci, H. P. Hratchian, J. V. Ortiz, A. F. Izmaylov, J. L. Sonnenberg, D. Williams-Young, F. Ding, F. Lipparini, F. Egidi, J. Goings, B. Peng, A. Petrone, T. Henderson, D. Ranasinghe, V. G. Zakrzewski, J. Gao, N. Rega, G. Zheng, W. Liang, M. Hada, M. Ehara, K. Toyota, R. Fukuda, J. Hasegawa, M. Ishida, T. Nakajima, Y. Honda, O. Kitao, H. Nakai, T. Vreven, K. Throssell, J. A. Montgomery, Jr., J. E. Peralta, F. Ogliaro, M. J. Bearpark, J. J. Heyd, E. N. Brothers, K. N. Kudin, V. N. Staroverov, T. A. Keith, R. Kobayashi, J. Normand, K. Raghavachari, A. P. Rendell, J. C. Burant, S. S. Iyengar, J. Tomasi, M. Cossi, J. M. Millam, M. Klene, C. Adamo, R. Cammi, J. W. Ochterski, R. L. Martin, K. Morokuma, O. Farkas, J. B. Foresman, and D. J. Fox. *Gaussian 16*; Gaussian, Inc.: Wallingford CT, 2016.

6.2 Supporting Information for Chapter 4

European Journal of Inorganic Chemistry

Supporting Information

Isolation and Reactivity of Silepins with a Sterically Demanding Silyl Ligand

Jin Yu Liu, Shigeyoshi Inoue, and Bernhard Rieger*

Appendix

Isolation and Reactivity of Silepins with a Sterically Demanding Silyl Ligand

Supporting Information

1. Experimental Procedures

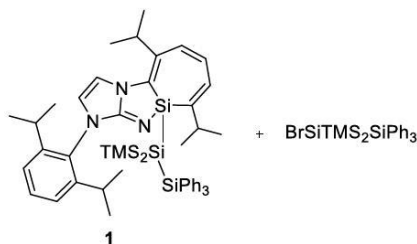
A) General Methods and Instrumentation

All manipulations were carried out under argon atmosphere using standard *Schlenk* or glovebox techniques. Glassware was heat-dried under vacuum prior to use. Unless otherwise stated, all chemicals were purchased commercially and used as received. All solvents were refluxed over sodium, distilled, and deoxygenated prior to use. Deuterated solvents were obtained commercially and were dried over 3 Å molecular sieves prior to use. All NMR samples were prepared under argon in *J. Young* PTFE tubes. KSiTMS_3 , $\text{KSiTMS}_2\text{SiPh}_3$, $^{\text{CycAAC}}$ silepin and $^{\text{DippNHC}}$ silepin were synthesized according to procedures described in the literature.^[51] NMR spectra were recorded on Bruker AV-500C or AV-400 spectrometers at ambient temperature (300 K) unless otherwise stated. ^1H , ^{13}C and $^{29}\text{Si}_{\text{ig}}$ NMR spectroscopic chemical shifts (δ) are reported in ppm. $\delta(^1\text{H})$ and $\delta(^{13}\text{C})$ were referenced internally to the relevant residual solvent resonances. $\delta(^{29}\text{Si})$ was referenced to the signal of tetramethylsilane (TMS) ($\delta = 0$ ppm) as external standard. All $^{29}\text{Si}_{\text{ig}}$ NMR spectra underwent auto baseline correction (*Whittaker Smoother*). FT-IR spectra were recorded on a Vertex 70 from Bruker with a Platinum ATR unit. A solution of the sample in pentane was drop-casted onto the ATR crystal and dried under a stream of nitrogen. Liquid Injection Field Desorption Ionization Mass Spectrometry (LIFDI-MS) was measured directly from an inert atmosphere glovebox with a *Thermo Fisher Scientific* Exactive Plus Orbitrap equipped with an ion source from *Linden CMS*. Melting points were determined in sealed glass capillaries under inert gas with a *Büchi* Melting Point B-540.

Appendix

B) Synthesis and Characterization of New Compounds

DippNHC silepin-SiPh₃ (Compound **1**) + Side product



Dipp-NHC-SiBr₃ (120 mg, 198 μmol, 1.0 eq.) and KSiTMS₂SiPh₃ (2.0 eq.) are dissolved in toluene (3 mL) and stirred at r.t. for 1 h. After evaporation of the solvent, pentane (5 mL) is added, and the suspension is filtered through a PE syringe filter. Pentane is then removed, and compound **1** (135 mg, 156 μmol, 87%) is obtained with its side product BrSiTMS₂SiPh₃ (81 mg, 155 μmol, 87%) as a 1:1 inseparable mixture. The yield is calculated with the measured mass of the mixture (216 mg).

Purification attempts were made by crystallization in common organic solvents (Hexane, pentane, toluene, THF, Et₂O) and PMe₃ did not lead to pure precipitated product nor crystals suitable for SC-XRD. Washing the mixture with HMDSO and MeCN solely resulted in homogeneous solutions.

¹H NMR (500 MHz, C₆D₆): δ [ppm] = 7.80 – 7.77 (m, 7H, H_{Ph}), 7.76 – 7.71 (m, 8H, H_{Ph}), 7.18 – 7.16 (m, 15H, H_{Ph} sideproduct), 7.16 – 7.15 (m, 3H, H_{Ar}), 6.63 (d, *J* = 3.2 Hz, 1H, N-C-H), 6.46 (d, *J* = 12.9 Hz, 1H, H_{Ar}), 6.43 (dd, *J* = 6.5, 1.2 Hz, 1H, H_{Ar}), 6.13 – 6.07 (m, 1H, H_{Ar}), 5.93 (d, *J* = 2.9 Hz, 1H, N-C-H), 3.29 – 3.13 (m, 2H, CH(CH₃)₂), 3.04 – 2.89 (m, 2H, CH(CH₃)₂), 1.39 (d, *J* = 6.8 Hz, 3H, CH₃), 1.22 – 1.20 (m, 8H, CH₃), 1.14 (dd, *J* = 6.8, 2.4 Hz, 4H, CH₃), 1.09 (dd, *J* = 6.8, 4.7 Hz, 6H, CH₃), 0.92 (d, *J* = 6.8 Hz, 3H, CH₃), 0.29 (s, 9H, H_{TMS}), 0.23 (s, 9H, H_{TMS}), 0.17 (s, 18H, H_{TMS} sideproduct).

¹³C{¹H} NMR (126 MHz, C₆D₆): δ [ppm] = 156.81 (C=N), 148.12 (C_{Ar}), 147.04 (C_{Ar}), 144.95 (C_{Ar}), 137.57 (C_{Ar}), 137.43 (C_{Ph}), 136.75 (C_{Ph} sideproduct), 135.00 (C_{Ph} sideproduct), 133.68 (C_{Ph}), 130.58 (C_{Ph}), 129.99 (C_{Ph} sideproduct), 129.45 (C_{Ph}), 129.33 (C_{Ar}), 129.17 (C_{Ar}), 128.57 (C_{Ph} sideproduct), 128.43 (C_{Ar}), 125.70 (C_{Ar}), 124.20 (C_{Ar}), 124.14 (C_{Ar}), 117.65 (C-N), 110.12 (C-N), 32.00 (CH(CH₃)₂), 29.37 (CH(CH₃)₂), 28.81 (CH₃), 28.48 (CH₃), 26.40 (CH₃), 25.84 (CH₃), 25.40 (CH₃), 23.68 (CH₃), 23.27 (CH₃), 22.91 (CH₃), 22.66 (CH₃), 21.31 (CH₃), 3.89 (C_{TMS}), 3.58 (C_{TMS}), 0.03 (C_{TMS} sideproduct).

Appendix

$^{29}\text{Si}\{\text{H}\}$ NMR (99 MHz, C_6D_6): δ [ppm] = 16.07 ($\text{Si}_{\text{central}}$), -8.50 (Si_{TMS}), -9.53 (Si_{TMS}), -9.55 (SiPh_3), -11.54 (Si_{TMS} sideproduct), -20.27 (SiPh sideproduct), -26.48 ($\text{BrSiTMS}_2\text{SiPh}_3$), -132.58 ($\text{SiTMS}_2\text{SiPh}_3$).

LIFDI-MS: Calculated: $m/z = 863.4338$; Experimental: $m/z = 863.4311$ [$\mathbf{1}$] $^+$ (+ 6.65 ppm error).

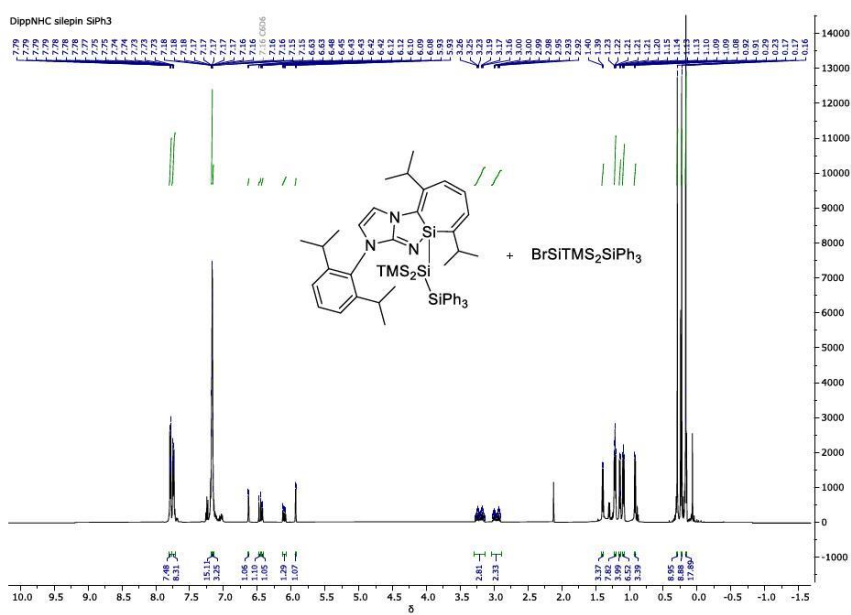


Figure S1: ^1H NMR of **1**.

Appendix

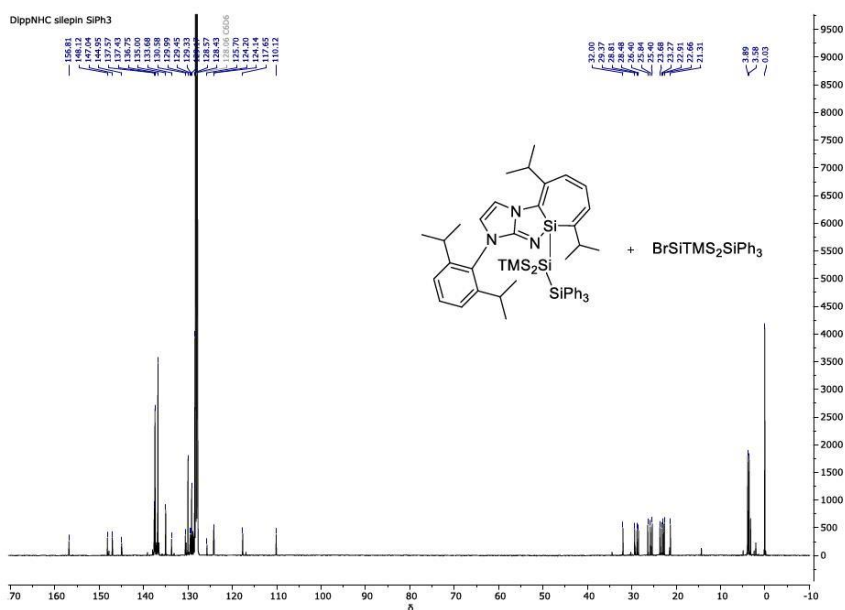


Figure S2: ¹³C NMR of **1**.

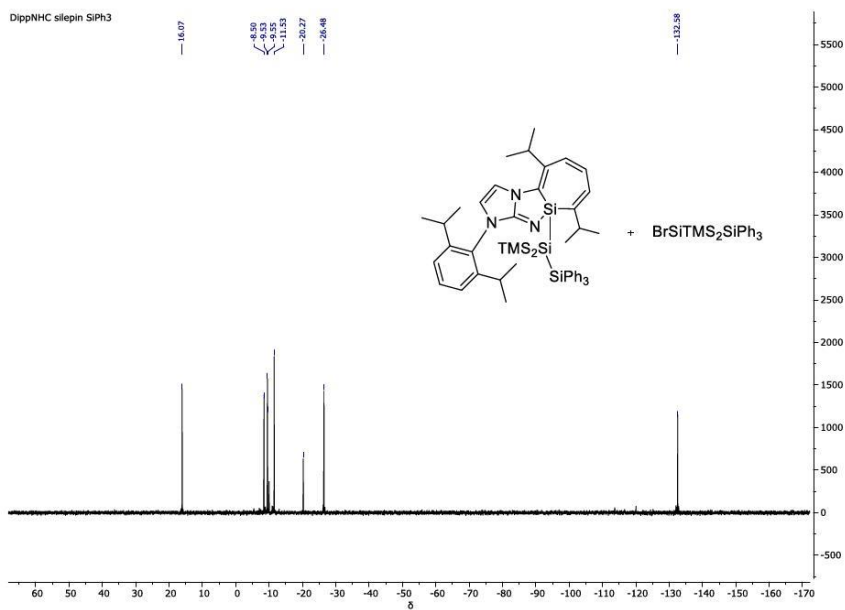
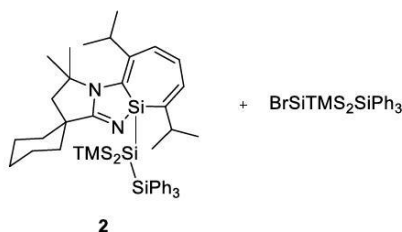


Figure S3: ²⁹Si NMR of **1**.

Appendix

CycAAC silepin-SiPh₃ (Compound **2**) + Side product



CycAAC-SiBr₃ (120 mg, 198 μmol, 1.0 eq.) and KSiTMS₂SiPh₃ (187 mg, 396 μmol, 2.0 eq.) are dissolved in toluene (3 mL) and stirred at r.t. for 1 h. After evaporation of the solvent, pentane (5 mL) is added, and the suspension is filtered through a PE syringe filter. Pentane is then removed, and compound **2** (139 mg, 173 μmol, 88%) is obtained with its side product BrSiTMS₂SiPh₃ (88.8 mg, 173 μmol, 88%) as a 1:1 inseparable mixture. The yield is calculated with the measured mass of the mixture (227 mg).

Purification attempts were made by crystallization in common organic solvents (Hexane, pentane, toluene, THF, Et₂O) and PMe₃ did not lead to pure precipitated product nor crystals suitable for SC-XRD. Washing the mixture with HMDSO and MeCN solely resulted in homogeneous solutions.

¹H NMR (500 MHz, C₆D₆): δ [ppm] = 7.86 – 7.70 (m, 15H, H_{Ph} sideproduct), 7.26 – 7.22 (m, 6H, H_{Ph}), 7.21 – 7.17 (m, 5H, H_{Ph}), 7.14 (d, *J* = 5.6 Hz, 4H, H_{Ph}), 6.43 (d, *J* = 13.1 Hz, 1H, H_{Ar}), 6.31 (d, *J* = 5.8 Hz, 1H, H_{Ar}), 5.81 (dd, *J* = 13.5, 5.4 Hz, 1H, H_{Ar}), 3.26 (h, *J* = 6.8 Hz, 1H, CH(CH₃)₂), 2.76 (hept, *J* = 7.2, 6.7 Hz, 1H, CH(CH₃)₂), 2.09 (d, *J* = 17.7 Hz, 3H, H_{Cy}), 1.86 – 1.77 (m, 2H, CH), 1.73 – 1.65 (m, 2H, H_{Cy}), 1.57 (dd, *J* = 13.1, 2.4 Hz, 2H, H_{Cy}), 1.50 (s, 3H, H_{Cy}), 1.28 – 1.23 (m, 9H, CH₃), 1.08 (d, *J* = 6.8 Hz, 3H, CH₃), 1.01 (d, *J* = 5.0 Hz, 3H, CH₃), 1.00 (d, *J* = 5.2 Hz, 3H, CH₃), 0.34 (s, 9H, H_{TMS}), 0.29 (s, 9H, H_{TMS}), 0.15 (s, 18H, H_{TMS} sideproduct).

¹³C{¹H} NMR (126 MHz, C₆D₆): δ [ppm] = 179.90 (C=N), 144.99 (C_{Ar}), 137.52 (C_{Ph} sideproduct), 136.75 (C_{Ph} sideproduct), 135.00 (C_{Ph}), 134.29 (C_{Ph}), 133.65 (C_{Ar}), 129.99 (C_{Ph} sideproduct), 129.32 (C_{Ph}), 129.13 (C_{Ph}), 128.75 (C_{Ph}), 128.57 (C_{Ar}), 128.43 (C_{Ph} sideproduct), 125.70 (C_{Ar}), 124.54 (C_{Ar}), 58.54 (C-N), 52.87 (C-C-N), 42.40 (C-C=N), 37.24 (C_{Cy}), 37.15 (C_{Cy}), 32.24 (C_{Cy}), 31.26 (C_{Cy}), 30.88 (CH(CH₃)₂), 29.20 (CH(CH₃)₂), 26.14 (C_{Cy}), 25.70 (CH₃), 22.97 (CH₃), 22.83 (CH₃), 22.77 (CH₃), 21.94 (CH₃), 21.30 (CH₃), 3.92 (C_{TMS}), 3.85 (C_{TMS}), 0.04 (C_{TMS} sideproduct).

²⁹Si{¹H} NMR (99 MHz, C₆D₆): δ [ppm] = 17.53 (Si_{central}), -8.48 (Si_{TMS}), -8.54 (Si_{TMS}), -9.48 (Si_{Ph}), -11.54 (Si_{TMS} sideproduct), -20.28 (Si_{Ph} sideproduct), -26.50 (BrSiTMS₂SiPh₃), -134.08 (SiTMS₂SiPh₃).

Appendix

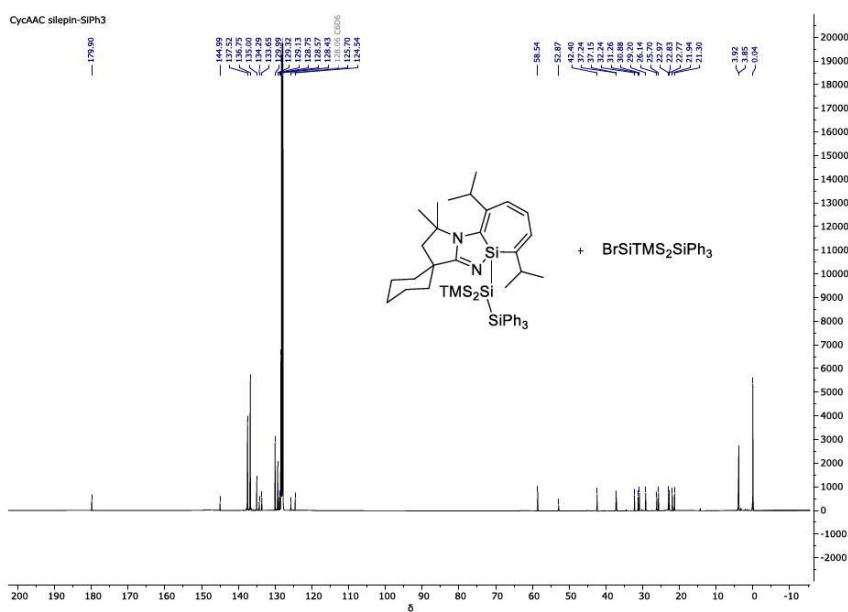


Figure S5: ¹³C NMR of **2**.

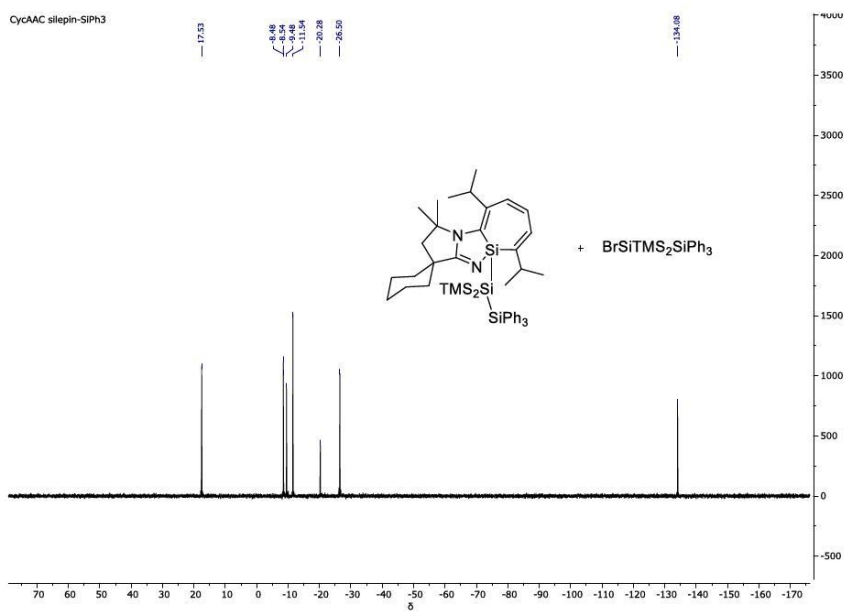
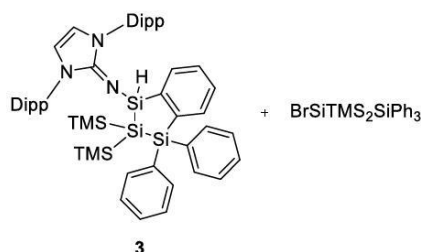


Figure S6: ²⁹Si of **2**.

Appendix

Sp²CH activation product Dipp-NHC silepin (Compound **3**) + Side product



A solution of a 1:1 mixture of **1** and BrSiTMS₂SiPh₃ (33 mg) in C₆D₆ is heated to 90 °C for 1 week forming the intramolecular insertion product **3**.

Purification attempts were made by crystallization in common organic solvents (Hexane, pentane, toluene, THF, Et₂O) and PMe₃ did not lead to pure precipitated product nor crystals suitable for SC-XRD. Washing the mixture with HMDSO and MeCN solely resulted in homogeneous solutions.

Since a 2% occupancy by a bromide atom instead of the hydrid atom could be determined in the crystal structure of **4** suggesting a minor H/Br exchange with the side product during heating, we also assume a likewise reactivity for compound **3**.

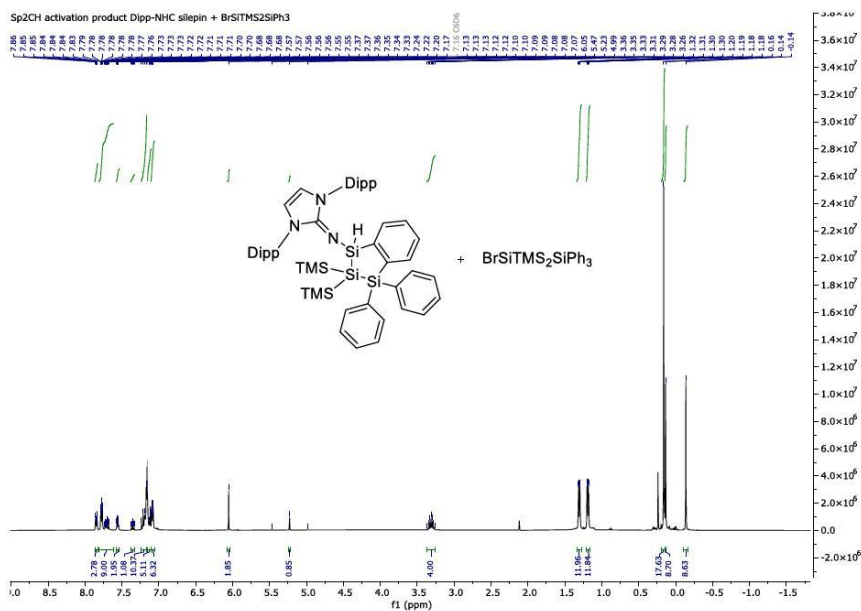
¹H NMR (400 MHz, C₆D₆) δ 7.87 – 7.83 (m, 3H, H_{Ar}), 7.81 – 7.62 (m, 9H, H_{Ph}), 7.58 – 7.53 (m, 2H, H_{Ar}), 7.35 (td, *J* = 7.4, 1.2 Hz, 1H, H_{Ar}), 7.24 – 7.16 (m, 10H, H_{Ph} sideproduct), 7.15 – 7.11 (m, 5H, H_{Ph} sideproduct), 7.11 – 7.06 (m, 6H, H_{Ph}), 6.05 (s, 2H, N-C-H), 5.23 (s, 1H, with ²⁹Si satellites ¹*J*(SiH) = 193.0 Hz, SiH), 3.31 (hept, *J* = 6.7 Hz, 4H, CH(CH₃)₂), 1.31 (dd, *J* = 6.8, 1.8 Hz, 12H, CH₃), 1.19 (dd, *J* = 6.9, 2.3 Hz, 12H, CH₃), 0.16 (s, 18H, H_{TMS} sideproduct), 0.14 (s, 9H, H_{TMS}), -0.14 (s, 9H, H_{TMS}).

¹³C{¹H} NMR (101 MHz, C₆D₆): δ [ppm] = 153.78 (C=N), 148.06 (C_{Ar}, Si-ring), 147.52 (C_{Ar}, Si-ring), 146.67 (C_{Ar}, Si-ring), 145.14 (C_{Ar}, Si-ring), 138.59 (C_{Ar}, Si-ring), 137.73 (C_{Ar}, Si-ring), 136.88 (H_{Ph} sideproduct), 136.76 (C_{Ar}), 136.53 (C_{Ar}), 136.44 (C_{Ph}), 135.03 (H_{Ph} sideproduct), 134.89 (C_{Ph}), 134.79 (C_{Ph}), 134.53 (C_{Ph}), 129.99 (H_{Ph} sideproduct), 129.65 (C_{Ph}), 129.34 (C_{Ph}), 129.01 (C_{Ph}), 128.65 (C_{Ph}), 128.43 (H_{Ph} sideproduct), 124.30 (C_{Ar}), 124.15 (C_{Ar}), 115.04 (C-N), 29.06 (CH(CH₃)₂), 29.02 (CH(CH₃)₂), 25.66 (CH₃), 25.11 (CH₃), 23.84 (CH₃), 23.78 (CH₃), 2.60 (C_{TMS}), 2.46 (C_{TMS}), 0.05 (C_{TMS} sideproduct).

²⁹Si{¹H} NMR (99 MHz, C₆D₆): δ [ppm] = -4.60 (Si_{TMS}), -9.01 (Si_{TMS}), -10.11 (SiPh₃), -11.54 (Si_{TMS} sideproduct), -20.27 (Si_{Ph} sideproduct), -26.49 (BrSiTMS₂SiPh₃), -35.48 (Si_{central}), -134.67 (SiTMS₂SiPh₃).

Appendix

LIFDI-MS: Calculated: $m/z = 863.4338$; Experimental: $m/z = 863.4261$ [3]⁺ (+ 12.45 ppm error).



Appendix

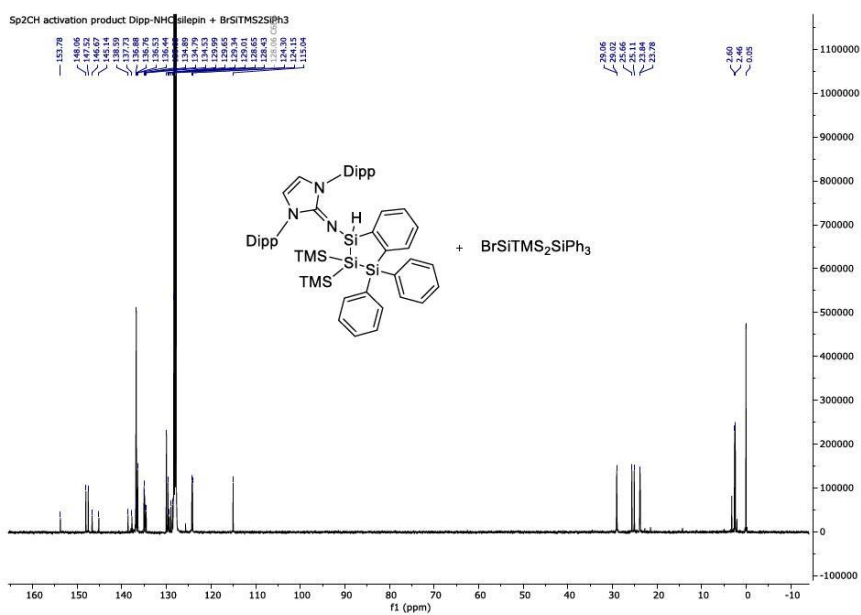


Figure S8: ¹³C NMR of **3**.

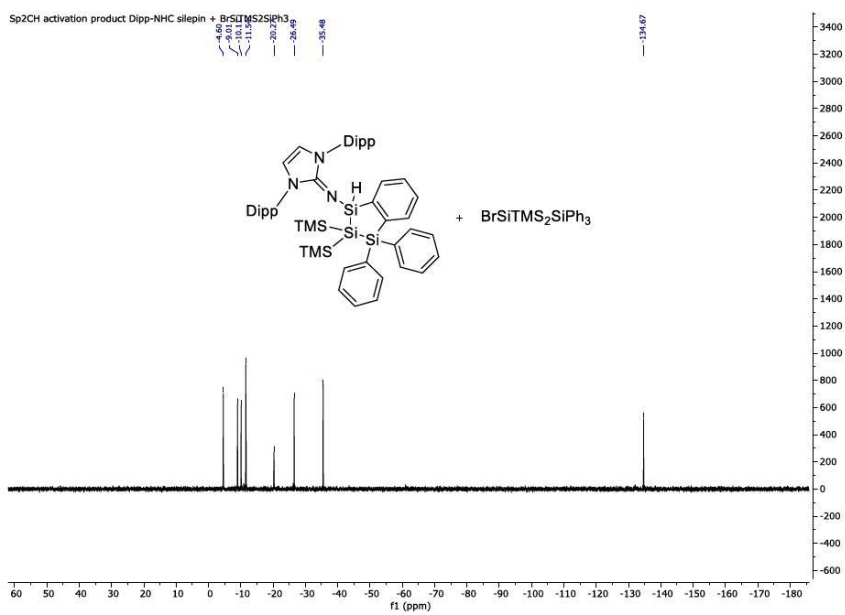
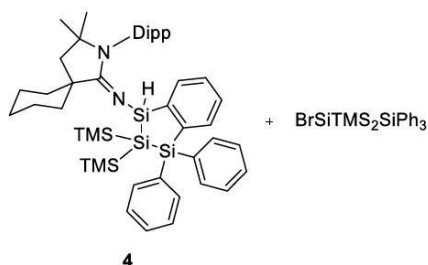


Figure S9: ²⁹Si NMR of **3**.

Appendix

Sp²CH activation product CycAAC silepin (Compound **4**) + BrSiTMS₂SiPh₃



A solution of a 1:1 mixture of **2** and BrSiTMS₂SiPh₃ (33 mg) in C₆D₆ is heated to 90 °C for 1 week forming the intramolecular insertion product **4**.

Purification attempts were made by crystallization in common organic solvents (Hexane, pentane, toluene, THF, Et₂O) and PMe₃ did not lead to pure precipitated product. Washing the mixture with HMDSO and MeCN solely resulted in homogeneous solutions. Crystals suitable for SC-XRD analysis could be obtained from crystallization in cold pentane, which is however, not reproducible in various other attempts made for this compound (**4**) and also compound **1**, **2** or **3**.

A 2% occupancy by a bromide atom instead of the hydrid atom could be determined in the crystal structure of **4** suggesting a minor H/Br exchange with the side product during heating.

¹H NMR (400 MHz, C₆D₆): δ [ppm] = 7.96 – 7.92 (m, 2H, H_{Ar}), 7.81 – 7.68 (m, 10H, H_{Ph, sideproduct}), 7.34 (t, J = 7.7 Hz, 1H, H_{Ar}), 7.27 – 7.22 (m, 3H, H_{Ph, sideproduct}), 7.22 – 7.19 (m, 2H, H_{Ph, sideproduct}), 7.19 – 7.16 (m, 5H, H_{Ph}), 7.15 – 7.01 (m, 8H, H_{Ph}), 6.92 – 6.88 (m, 1H, H_{Ph}), 6.56 (s, 1H, with ²⁹Si satellites ¹J(SiH) = 190.1 Hz, SiH), 3.14 (m, 2H, CH(CH₃)₂), 2.26 – 2.13 (m, 2H, CH₂), 2.12 (s, 1H, H_{Cy}), 1.94 – 1.73 (m, 3H, H_{Cy}), 1.70 – 1.58 (m, 4H, H_{Cy}), 1.51 – 1.38 (m, 2H, H_{Cy}), 1.29 – 1.23 (m, 10H, CH₃), 1.13 (d, J = 6.7 Hz, 3H, CH₃), 1.07 (d, J = 9.6 Hz, 6H, CH₃), 0.41 (s, 9H, H_{TMS}), 0.16 (s, 18H, H_{TMS sideproduct}), 0.05 (s, 9H, H_{TMS}).

¹³C{¹H} NMR (101 MHz, C₆D₆): δ [ppm] = 169.94 (C=N), 152.56 (C_{Ar, Si-ring}), 149.60 (C_{Ar, Si-ring}), 149.12 (C_{Ar, Si-ring}), 144.10 (C_{Ar, Si-ring}), 138.83 (C_{Ar, Si-ring}), 137.33 (C_{Ar, Si-ring}), 137.01 (C_{Ph}), 136.88 (C_{Ph}), 136.76 (C_{Ph sideproduct}), 136.42 (C_{Ph}), 135.79 (C_{Ph}), 135.03 (C_{Ph sideproduct}), 134.45 (C_{Ph}), 134.26 (C_{Ar}), 129.99 (C_{Ph sideproduct}), 129.34 (C_{Ar}), 129.24 (C_{Ph}), 128.88 (C_{Ph}), 128.57 (C_{Ph sideproduct}), 125.70 (C_{Ar}), 124.75 (C_{Ph}), 124.62 (C_{Ar}), 61.00 (C-N), 48.22 (C-C-N), 47.20 (C-C=N), 36.63 (C_{Cy}), 35.96 (C_{Cy}), 30.92 (C_{Cy}), 29.47 (C_{Cy}), 29.30 (CH(CH₃)₂), 29.19 (CH(CH₃)₂), 27.95 (C_{Cy}), 26.77 (CH₃), 25.41 (CH₃), 23.84 (CH₃), 23.74 (CH₃), 22.72 (CH₃), 22.49 (CH₃), 2.81 (C_{TMS}), 2.78 (C_{TMS}), 0.05 (C_{TMS sideproduct}).

Appendix

$^{29}\text{Si}\{\text{H}\}$ NMR (99 MHz, C_6D_6): δ [ppm] = -6.64 (Si_{TMS}), -8.94 (Si_{TMS}), -10.56 (SiPh_3), -11.54 (Si_{TMS} sideproduct), -20.28 (SiPh sideproduct), -26.49 ($\text{BrSiTMS}_2\text{SiPh}_3$), -42.19 ($\text{Si}_{\text{central}}$), -129.29 ($\text{SiTMS}_2\text{SiPh}_3$).

LIFDI-MS: Calculated: $m/z = 800.4229$; Experimental: $m/z = 800.4114$ [**4**]⁺ (+ 14.36 ppm error).

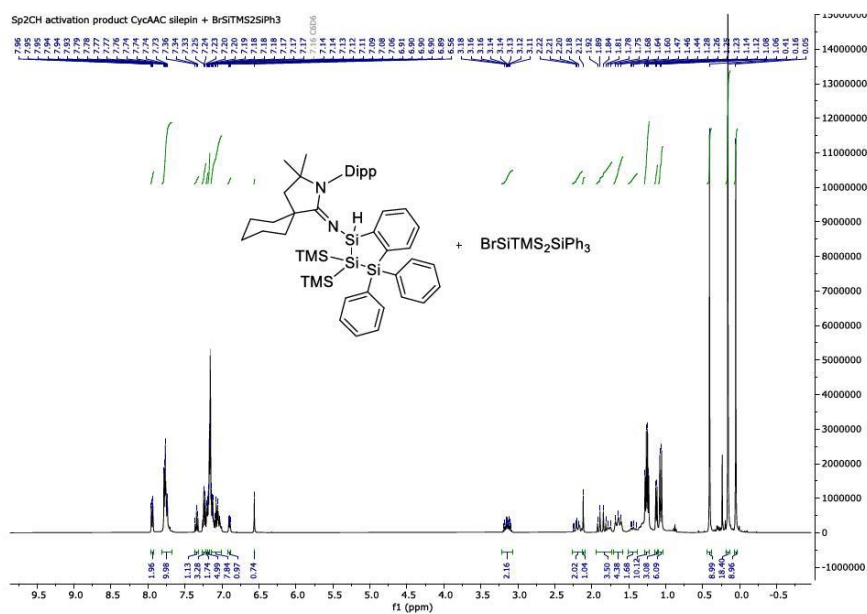


Figure S10: ^1H NMR of **4**.

Appendix

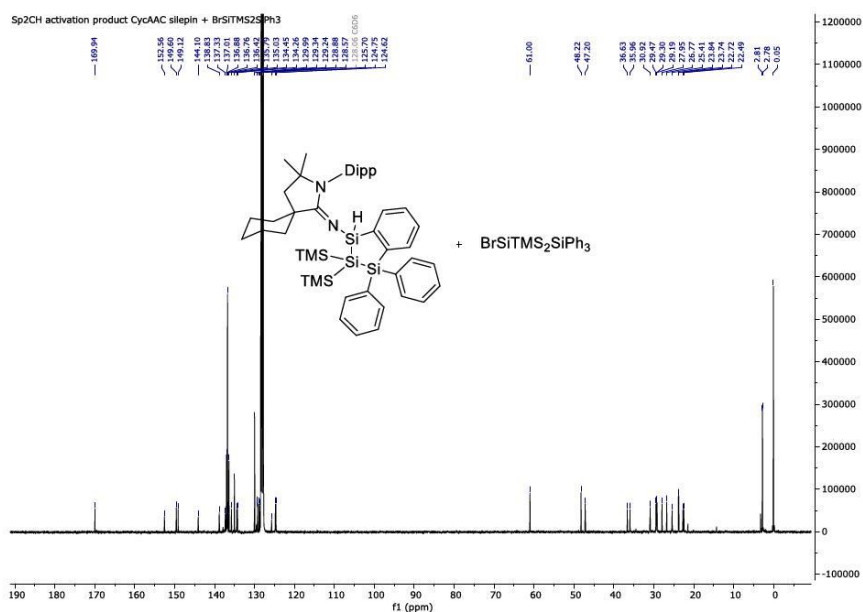


Figure S11: ¹³C NMR of 4.

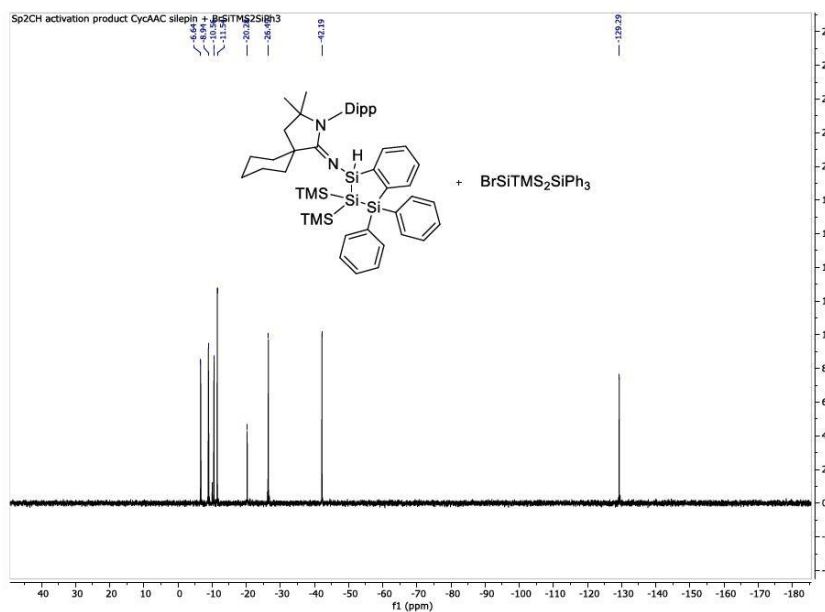
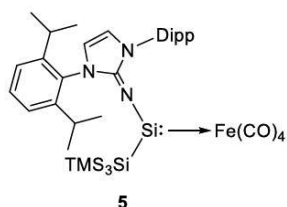


Figure S12: ²⁹Si NMR of 4.

Appendix

DippNHC silepin iron carbonyl complex (Compound **5**)



FeCO_5 (8.00 μL , 59.0 μmol , 2.0 eq.) was added to a solution of DippNHC silepin **F**^{*} (20.0 mg, 29.5 μmol , 1.0 eq.) in toluene (1 mL). The mixture was stirred at r.t. for 16 h. The solvent was completely evaporated in *vacuo* to afford the product (**5**) as an orange oil (18.3 mg, 73%).

^1H NMR (500 MHz, C_6D_6): δ [ppm] = 7.22 – 7.17 (m, 4H, H_{Ar}), 7.07 (dd, $J = 7.4, 2.0$ Hz, 2H, H_{Ar}), 6.09 (s, 2H, N-C-H), 3.85 (h, $J = 6.8$ Hz, 2H, $\text{CH}(\text{CH}_3)_2$), 2.82 (hept, $J = 6.8$ Hz, 2H, $\text{CH}(\text{CH}_3)_2$), 1.57 (d, $J = 6.7$ Hz, 6H, CH_3), 1.30 (d, $J = 6.7$ Hz, 6H, CH_3), 1.11 (d, $J = 6.7$ Hz, 6H, CH_3), 0.98 (d, $J = 6.7$ Hz, 6H, CH_3), 0.22 (s, 27H, H_{TMS}).

$^{13}\text{C}\{\text{H}\}$ NMR (126 MHz, C_6D_6): δ [ppm] = 215.58 (CO), 152.56 (C=N), 148.33 (C_{Ar}), 146.42 (C_{Ar}), 133.53 (C_{Ar}), 130.66 (C_{Ar}), 129.33 (C_{Ar}), 125.70 (C_{Ar}), 125.14 (C_{Ar}), 124.40 (C_{Ar}), 118.19 (CH-N), 28.77 (CH_3), 28.61 (CH_3), 26.54 (CH_3), 26.27 (CH_3), 23.39 (CH_3), 23.15 (CH_3), 2.96 (C_{TMS}).

$^{29}\text{Si}\{\text{H}\}$ NMR (80 MHz, C_6D_6): δ = 272.72 (Si:), -9.45 (TMS), -92.89 (SiTMS₃).

LIFDI-MS: Calculated: $m/z = 845.3014$; Experimental: $m/z = 845.2930$ [**5**]⁺ (+ 9.93 ppm error).

IR (cm^{-1}): 2958 (m), 2892 (m), 2006 (s), 1906 (s), 1875 (s), 1524 (s), 1457 (m), 1243 (s), 1034 (m), 825 (s).

Appendix

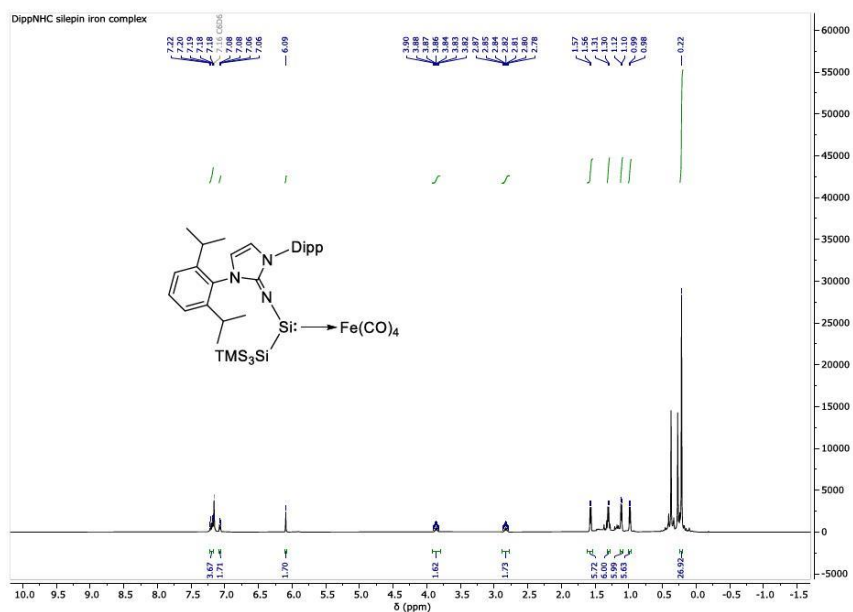


Figure S13: ^1H NMR of **5**.

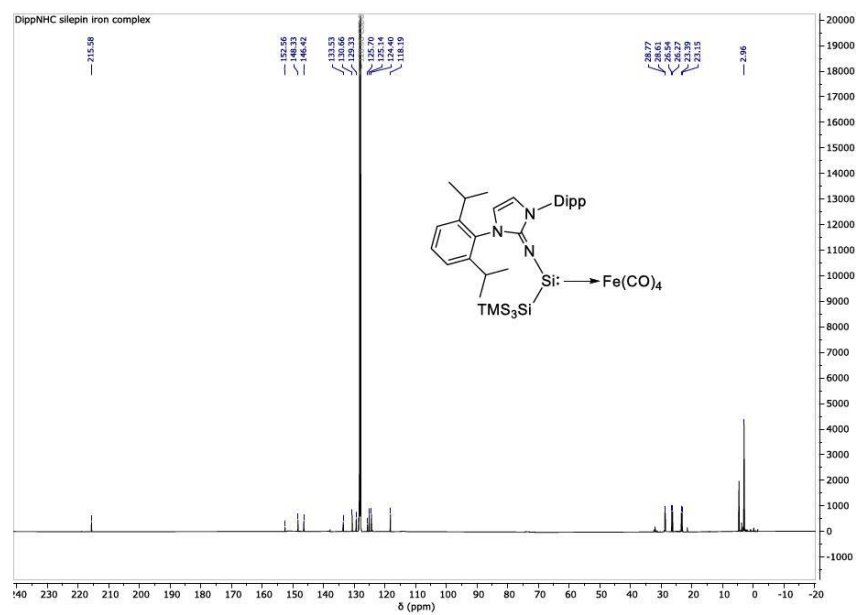


Figure S14: ^{13}C NMR of **5**.

Appendix

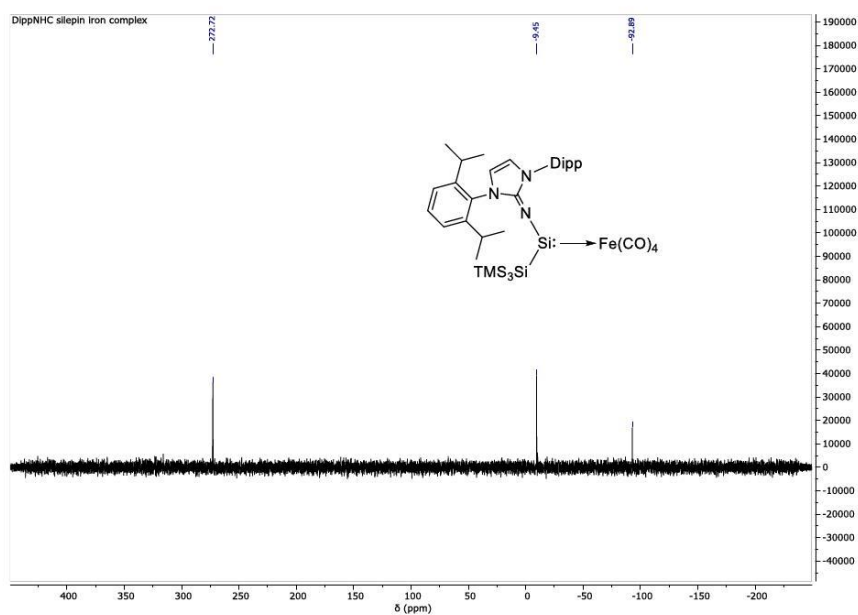


Figure S15: ²⁹Si NMR of **5**.

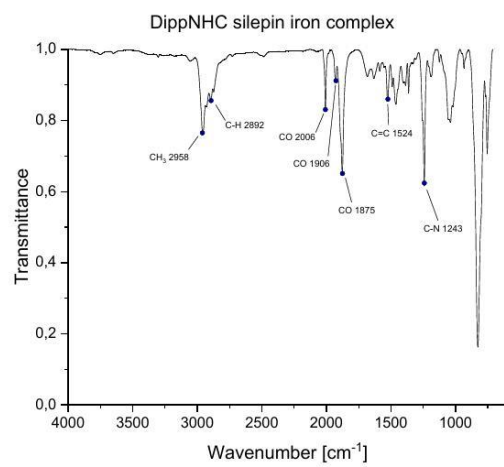
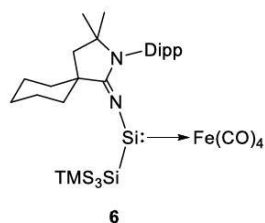


Figure S16: IR spectrum of **5**.

Appendix

CycAAC silepin iron carbonyl complex (Compound 6)



FeCO_5 (9.95 μL , 97.5 μmol , 2.0 eq.) was added to a solution of CycAAC silepin **J** (30 mg, 48.7 μmol , 1.0 eq.) in toluene (1 mL). The mixture was stirred at r.t. for 10 days. The solvent was completely evaporated in *vacuo* to afford the product (**6**) as an orange oil (33 mg, 91%).

$^1\text{H NMR}$ (400 MHz, C_6D_6) δ [ppm] = 7.15 – 7.12 (m, 2H, H_{Ar}), 6.99 (dd, $J = 5.4, 4.0$ Hz, 1H, H_{Ar}), 3.43 (hept, $J = 6.4$ Hz, 1H, $\text{CH}(\text{CH}_3)_2$), 2.97 (hept, $J = 6.7$ Hz, 1H, $\text{CH}(\text{CH}_3)_2$), 2.30 (td, $J = 13.1, 3.9$ Hz, 1H, CH_2), 2.25 – 2.17 (m, 1H, H_{Cy}), 1.91 (td, $J = 13.1, 3.7$ Hz, 1H, CH_2), 1.86 – 1.55 (m, 7H, H_{Cy}), 1.50 (d, $J = 6.6$ Hz, 3H, CH_3), 1.42 – 1.26 (m, 2H, H_{Cy}), 1.22 (d, $J = 6.6$ Hz, 3H, CH_3), 1.16 – 1.11 (m, 9H, CH_3), 0.88 (s, 3H, CH_3), 0.34 (s, 27H, H_{TMS}).

$^{13}\text{C}\{\text{H}\}$ NMR (101 MHz, C_6D_6): δ [ppm] = 215.11 (CO), 170.92 (C=N), 149.30 (C_{Ar}), 147.30 (C_{Ar}), 131.17 (C_{Ar}), 129.03 (C_{Ar}), 125.46 (C_{Ar}), 124.41 (C_{Ar}), 65.35 (C-N), 49.31 (C-C-N), 44.86 (C-C=N), 39.49 (C_{Cy}), 32.87 (C_{Cy}), 31.17 (C_{Cy}), 29.24 (C_{Cy}), 28.98 ($\text{CH}(\text{CH}_3)_2$), 28.76 ($\text{CH}(\text{CH}_3)_2$), 28.51 (C_{Cy}), 27.35 (CH_3), 25.11 (CH_3), 24.30 (CH_3), 23.25 (CH_3), 22.33 (CH_3), 22.02 (CH_3), 3.16 (C_{TMS}).

$^{29}\text{Si}\{\text{H}\}$ NMR (99 MHz, C_6D_6) δ [ppm] = 253.11 (Si:), -9.73 (Si_{TMS}), -94.15 (SiTMS_3).

LIFDI-MS: Calculated: $m/z = 782.2905$; Experimental: $m/z = 782.2835$ [**6**]⁺ (+ 8.94 ppm error).

IR (cm^{-1}): 2950 (w), 2890 (m), 2005 (s), 1921 (s), 1881 (s), 1436 (s), 1242 (s), 824 (s).

Appendix

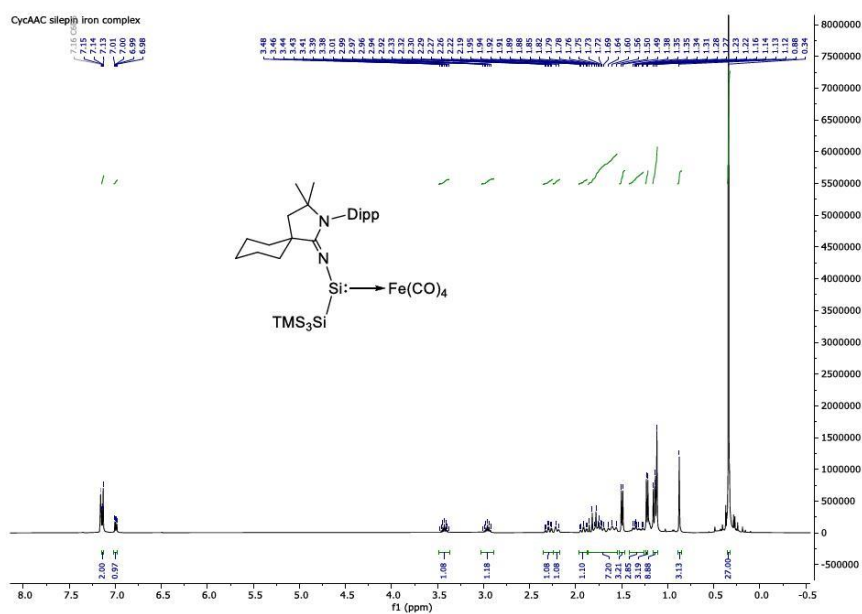


Figure S17: ¹H NMR of **6**.

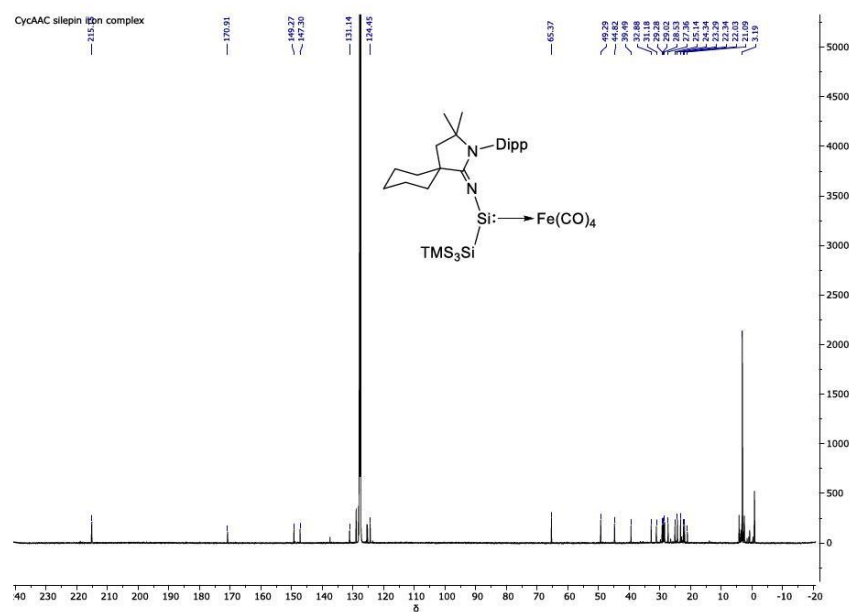


Figure S18: ¹³C NMR of **6**.

Appendix

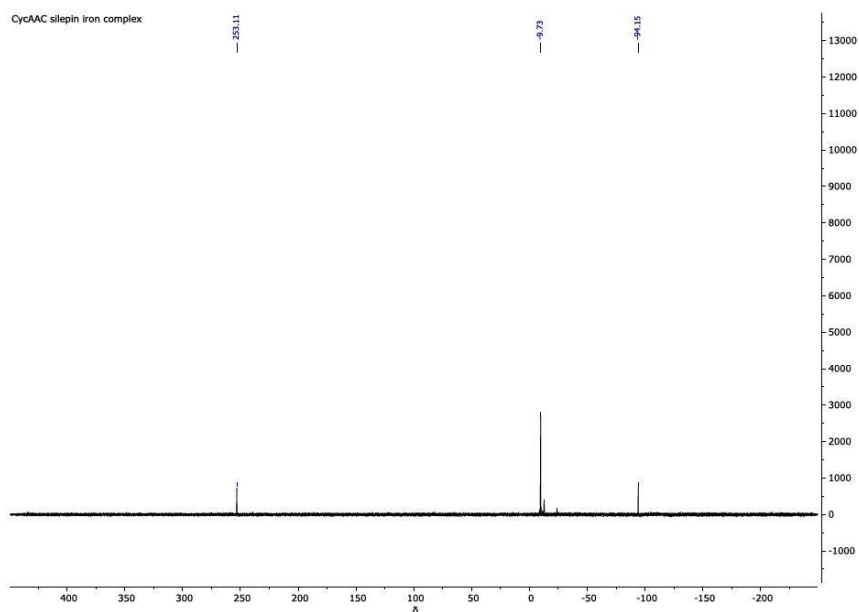


Figure S19: ^{29}Si NMR of **6**.

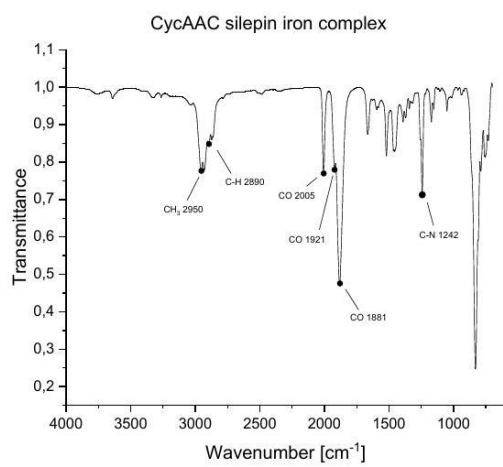
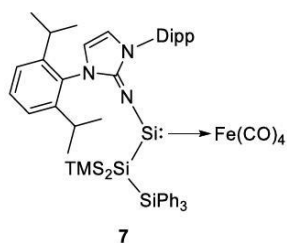


Figure S20: IR spectrum of **6**.

Appendix

DippNHC silepin-SiPh₃ iron carbonyl complex (Compound 7)



FeCO₅ (5.90 μL, 43.5 μmol, 2.0 eq.) was added to an inseparable mixture (30 mg) of IDipp-NHC silepin-SiPh₃ **1** (18.8 mg, 21.8 μmol, 1.0 eq.) and BrSiTMS₂SiPh₃ (11.2 mg) in toluene (1 mL). The mixture was stirred at r.t. for 16 h. The solvent was completely evaporated in *vacuo* and the remains dissolved in pentane to precipitate pure complex **7**. After centrifugation and separation of the solvent, the product is dried in *vacuo* to afford a yellow solid (11.2 mg, 50%).

¹H NMR (500 MHz, C₆D₆): δ [ppm] = 7.82 – 7.79 (m, 6H, H_{Ar}), 7.24 – 7.16 (m, 13H, H_{Ph}), 7.05 (m, 2H, H_{Ph}), 6.10 (s, 2H, CH-N), 3.97 (hept, *J* = 6.7 Hz, 2H, CH(CH₃)₂), 2.81 (hept, *J* = 6.7 Hz, 2H, CH(CH₃)₂), 1.61 (d, *J* = 6.7 Hz, 6H, CH₃), 1.28 (d, *J* = 6.7 Hz, 6H, CH₃), 1.13 (d, *J* = 6.7 Hz, 6H, CH₃), 0.97 (d, *J* = 6.6 Hz, 6H, CH₃), 0.01 (s, 18H, H_{TMS}).

¹³C{¹H} NMR (126 MHz, C₆D₆): δ [ppm] = 215.42 (CO), 153.18 (C=N), 148.38 (C_{Ar}), 146.69 (C_{Ar}), 137.60 (C_{Ar}), 136.27 (C_{Ar}), 133.82 (C_{Ar}), 130.72 (C_{Ar}), 129.60 (C_{Ph}), 127.95 (C_{Ph}), 125.04 (C_{Ph}), 124.54 (C_{Ph}), 118.49 (CH-N), 28.77 (CH(CH₃)₂), 28.75 ((CH(CH₃)₂), 26.69 (CH₃), 26.53 (CH₃), 23.17 (CH₃), 23.02 (CH₃), 3.48 (C_{TMS}).

²⁹Si{¹H} NMR (99 MHz, C₆D₆): δ [ppm] = 273.09 (Si:), -8.76 (Si_{TMS}), -9.85 (SiPh₃), -94.41 (SiTMS₂SiPh₃).

LIFDI-MS: Calculated: *m/z* = 1031.3484; Experimental: *m/z* = 1031.3546 [**7**]⁺ (– 6.01 ppm error).

Melting point: 206.6 °C

IR (cm⁻¹): 3084 (w), 2958 (s), 2921 (s), 2021 (s), 1953 (s), 1919 (s), 1983 (s), 1548 (s), 1461 (m), 1244 (s), 1104 (s), 834 (s).

Appendix

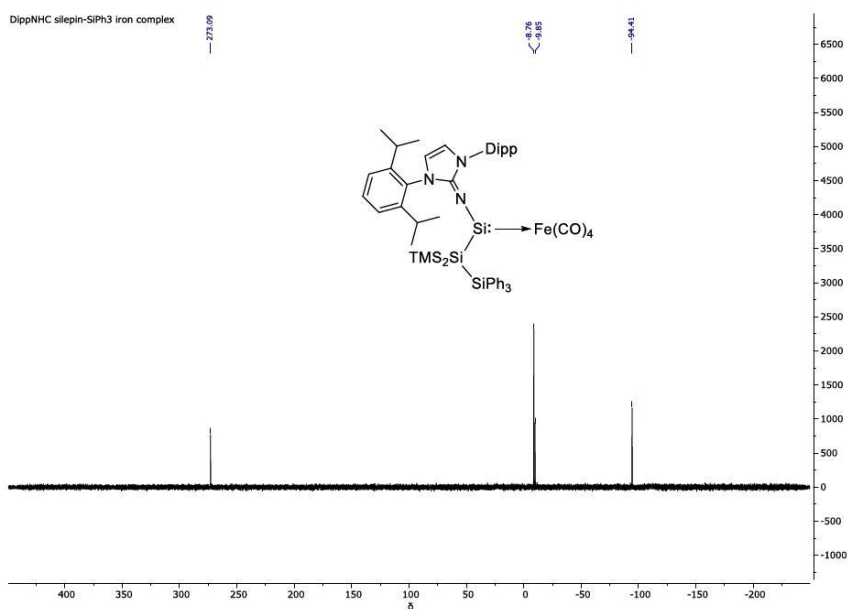


Figure S23: ²⁹Si NMR of 7.

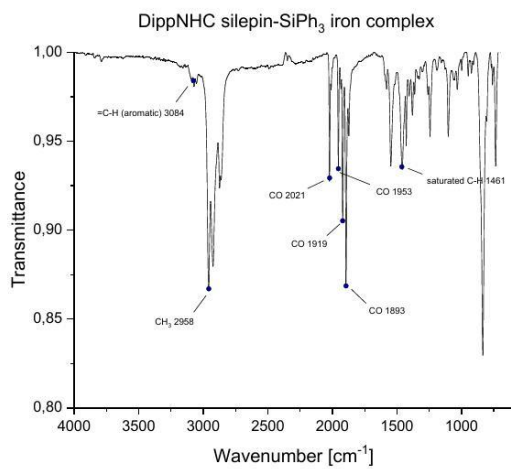
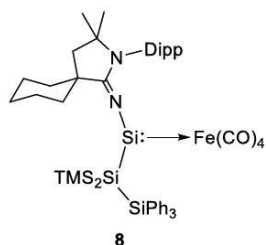


Figure S24: IR spectrum of 7.

Appendix

CycAAC silepin-SiPh₃ iron carbonyl complex (Compound **8**)



FeCO₅ (6.10 μ L, 44.9 μ mol, 2.0 eq.) was added to an inseparable mixture (30 mg) of CycAAC silepin-SiPh₃ **2** (18.0 mg, 22.5 μ mol, 1.0 eq.) and BrSiTMS₂SiPh₃ (12 mg) in toluene (1 mL). The mixture was stirred at r.t. for 16 h. The solvent was completely evaporated in *vacuo*, and the remains were dissolved in pentane to precipitate pure complex **8**. After centrifugation and separation of the solvent, the product is dried in *vacuo* to afford a yellow solid (12.7 mg, 58%).

¹H NMR (400 MHz, C₆D₆): δ [ppm] = 7.78 – 7.72 (m, 6H, H_{Ph}), 7.15 – 7.10 (m, 9H, H_{Ph}), 7.08 (d, J = 4.6 Hz, 1H, H_{Ar}), 7.05 (d, J = 7.8 Hz, 1H, H_{Ar}), 6.73 (dd, J = 7.4, 2.0 Hz, 1H, H_{Ar}), 3.51 (hept, J = 6.2 Hz, 1H, CH(CH₃)₂), 2.61 (hept, J = 6.9 Hz, 1H, CH(CH₃)₂), 2.37 – 2.20 (m, 2H, CH₂), 1.93 – 1.75 (m, 4H, H_{Cy}), 1.69 – 1.51 (m, 6H, H_{Cy}), 1.25 (d, J = 6.6 Hz, 6H, CH₃), 1.07 (s, 3H, CH₃), 0.91 (d, J = 6.8 Hz, 3H, CH₃), 0.77 (s, 3H, CH₃), 0.37 (s, 9H, H_{TMS}), 0.30 (s, 9H, H_{TMS}).

¹³C{¹H} NMR (126 MHz, C₆D₆): δ [ppm] = 215.83 (CO), 171.95 (C=N), 149.22 (C_{Ar}), 147.94 (C_{Ar}), 137.79 (C_{Ar}), 137.38 (C_{Ar}), 137.16 (C_{Ar}), 131.22 (C_{Ar}), 129.69 (C_{Ph}), 129.41 (C_{Ph}), 125.29 (C_{Ph}), 124.74 (C_{Ph}), 65.83 (C-N), 49.95 (C-C-N), 44.82 (C-C=N), 38.80 (C_{Cy}), 33.30 (C_{Cy}), 31.46 (C_{Cy}), 30.08 (C_{Cy}), 29.09 (CH(CH₃)₂), 28.92 (CH(CH₃)₂), 28.03 (C_{Cy}), 27.66 (CH₃), 24.86 (CH₃), 24.39 (CH₃), 23.08 (CH₃), 22.63 (CH₃), 22.39 (CH₃), 4.36 (C_{TMS}), 3.90 (C_{TMS}).

²⁹Si{¹H} NMR (99 MHz, C₆D₆): δ [ppm] = 247.45 (Si), -7.41 (Si_{TMS}), -7.79 (Si_{TMS}), -8.35 (SiPh₃), -95.69 (SiTMS₂SiPh₃).

LIFDI-MS: Calculated: m/z = 968.3375; Experimental: m/z = 968.3386 [**8**]⁺ (- 1.14 ppm error).

Melting point: 216.2 °C

Appendix

IR (cm⁻¹): 3200-3068 (w), 2959 (s), 2927 (m), 2859 (s), 2026 (s), 1953 (s), 1925 (s), 1900 (s), 1600 (s), 1459 (m), 1428 (s), 1243 (s), 1104 (s), 833 (s), 737 (s).

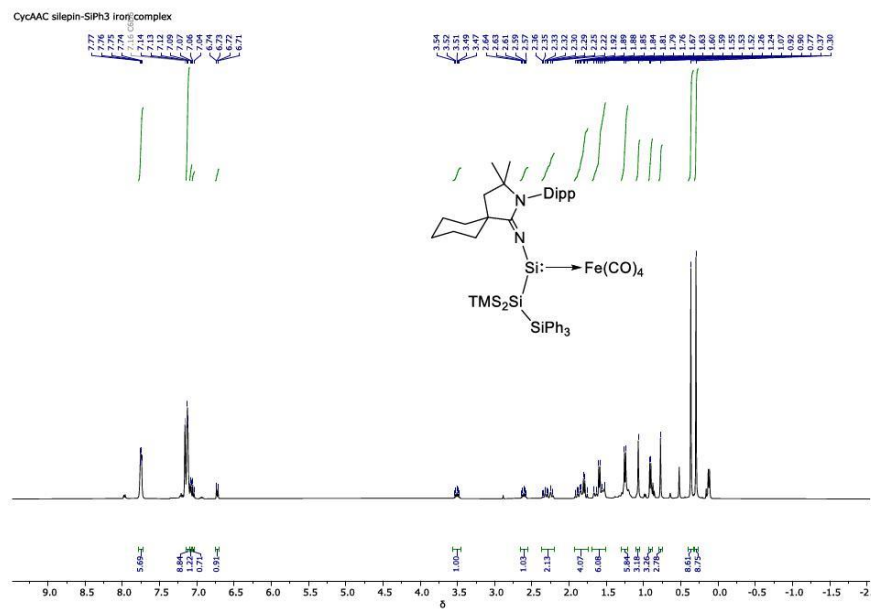


Figure S25: ¹H NMR of **8**.

Appendix

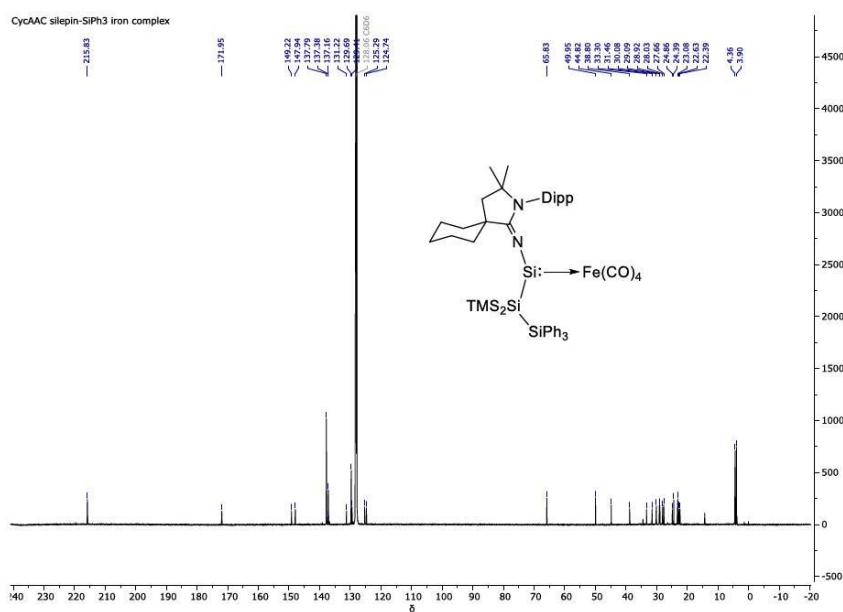


Figure S26: ¹³C NMR of **8**.

Appendix

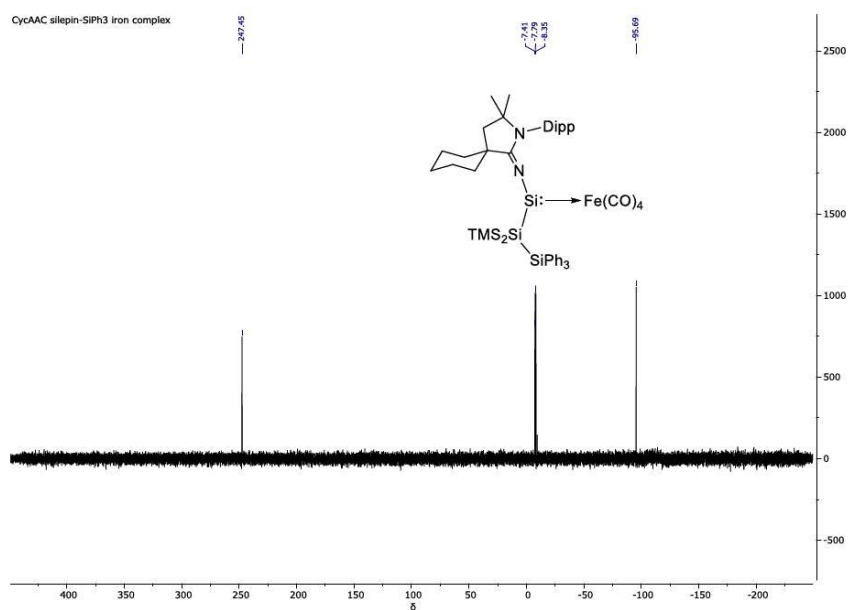


Figure S27: ²⁹Si NMR of **8**.

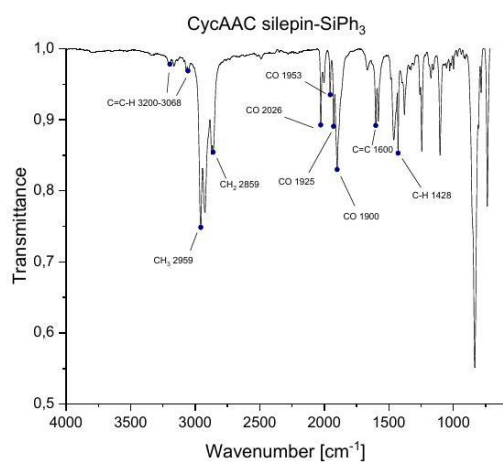


Figure S28: IR spectrum of **8**.

2. X-Ray Crystallographic Data

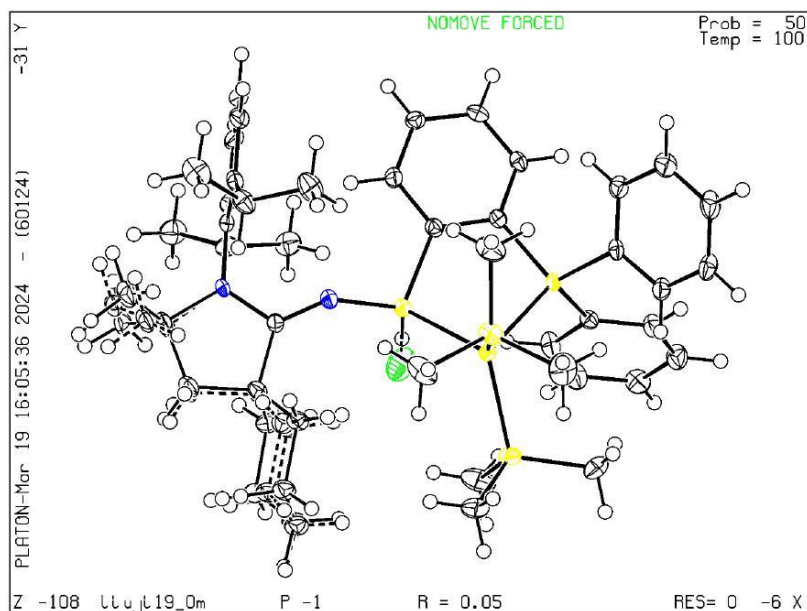
A) General

Data were collected on a single crystal X-ray diffractometer equipped with a CPAD detector (Bruker Photon-II), a TXS rotating anode with MoK α radiation ($\lambda = 0.71073 \text{ \AA}$) and a Helios optic using the APEX4 software package.^[2] The crystal was fixed on the top of a kapton micro sampler with perfluorinated ether and transferred to the diffractometer, and frozen under a stream of cold nitrogen. A matrix scan was used to determine the initial lattice parameters. Reflections were corrected for Lorentz and polarisation effects, scan speed, and background using SAINT.^[3] Absorption correction, including odd and even ordered spherical harmonics was performed using SADABS.^[4] Space group assignment was based upon systematic absences, E statistics, and successful refinement of the structure. The structures were solved using SHELXT with the aid of successive difference Fourier maps and were refined against all data using SHELXL in conjunction with SHELXLE.^[4,5,6] Hydrogen atoms (except on heteroatoms) were calculated in ideal positions as follows: Methyl hydrogen atoms were refined as part of rigid rotating groups, with a C–H distance of 0.98 \AA and $U_{\text{iso(H)}} = 1.5 \cdot U_{\text{eq(C)}}$. Non-methyl H atoms were placed in calculated positions and refined using a riding model with methylene, aromatic, and other C–H distances of 0.99 \AA , 0.95 \AA , and 1.00 \AA , respectively, and $U_{\text{iso(H)}} = 1.2 \cdot U_{\text{eq(C)}}$. Non-hydrogen atoms were refined with anisotropic displacement parameters. Full-matrix least-squares refinements were carried out by minimizing $\Sigma w(F_o^2 - F_c^2)^2$ with the SHELXL weighting scheme. Neutral atom scattering factors for all atoms and anomalous dispersion corrections for the non-hydrogen atoms were taken from International Tables for Crystallography.^[7] Disorders were modelled using free variables in conjunction with restraints in SHELXLE and is mentioned in detail below the crystal images of every compound.^[8] Images of the crystal structure were generated with Mercury and PLATON.^[8,10] Deposition Number 2324672-2324676 contains the supplementary crystallographic data for this paper. These data are provided free of charge by the joint Cambridge Crystallographic Data Centre and Fachinformationszentrum Karlsruhe Access Structures service www.ccdc.cam.ac.uk/structures.

Appendix

B) Crystallographic Details

Compound **4** (CCDC 2324672)



Part of the CycAAC moiety was disordered and modelled as a two-part disorder in conjunction with SIMU and SAME restraints. A DFIX for the H1-Si1 bond was applied for the hydride hydrogen H1.

Diffractometer operator Jinyu Liu
scanspeed 8s per frame dx 38 mm
1962 frames measured in 6 data sets
phi-scans with delta phi = 0.5
omega-scans with delta omega = 0.5
shutterless mode

Crystal data

$C_{47}H_{68}Br_{0.02}N_2Si_5$

$M_r = 803.08$

Triclinic, *P*

Hall symbol: *-P 1*

$a = 11.7588$ (7) Å

$b = 12.8498$ (8) Å

$c = 17.8955$ (11) Å

$F(000) = 869$

$D_x = 1.129$ Mg m⁻³

Mo $K\alpha$ radiation, $\lambda = 0.71073$ Å

Cell parameters from 9828 reflections

$\theta = 2.4\text{--}26.3^\circ$

Appendix

$\alpha = 98.300 (2)^\circ$
 $\beta = 106.769 (2)^\circ$
 $\gamma = 108.945 (2)^\circ$
 $V = 2362.7 (3) \text{ \AA}^3$
 $Z = 2$

$\mu = 0.20 \text{ mm}^{-1}$
 $T = 100 \text{ K}$
Fragment, orange
 $0.80 \times 0.41 \times 0.40 \text{ mm}$

Data collection

Bruker Photon CMOS
diffractometer 9521 independent reflections

Radiation source: TXS rotating anode 9127 reflections with $I > 2\sigma(I)$

Helios optic monochromator $R_{\text{int}} = 0.040$

Detector resolution: 16 pixels mm⁻¹ $\theta_{\text{max}} = 26.4^\circ$, $\theta_{\text{min}} = 2.0^\circ$

phi- and omega-rotation scans $h = -14 \quad 13$

Absorption correction: multi-scan
SADABS 2016/2, Bruker, 2016 $k = -16 \quad 16$

$T_{\text{min}} = 0.693$, $T_{\text{max}} = 0.745$ $l = -22 \quad 22$

57511 measured reflections

Refinement

Refinement on F^2 Secondary atom site location: difference Fourier map

Least-squares matrix: full Hydrogen site location: mixed

$R[F^2 > 2\sigma(F^2)] = 0.048$ H atoms treated by a mixture of independent and constrained refinement

$wR(F^2) = 0.129$ $W = 1/[\Sigma^2(F_o^2) + (0.0548P)^2 + 2.7126P]$

$S = 1.07$ WHERE $P = (F_o^2 + 2F_c^2)/3$

9521 reflections $(\Delta/\sigma)_{\text{max}} = 0.001$

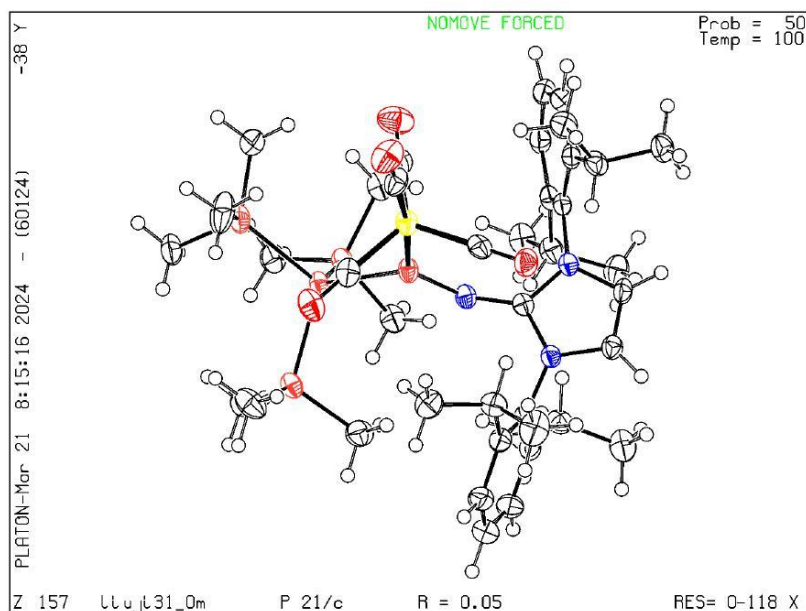
605 parameters $\Delta\rho_{\text{max}} = 1.72 \text{ e \AA}^{-3}$

323 restraints $\Delta\rho_{\text{min}} = -0.66 \text{ e \AA}^{-3}$

Primary atom site location: iterative Extinction correction: none

Appendix

Compound 5 (CCDC 2324673)



For this compound, no suitable twin law could be found with platon and the twin tool embedded in Shelxle. Thus, a treatment according to standard merohedral procedure were performed.

Diffractometer operator Jinyu Liu
scanspeed 10s per frame dx 45mm
1970 frames measured in 6 data sets
phi-scans with delta phi = 0.5
omega-scans with delta omega = 0.5
shutterless mode

Crystal data

$C_{40}H_{63}FeN_2O_4Si_5$

$M_r = 846.23$

Monoclinic, $P2_1/c$

Hall symbol: $-P 2_1/c$

$a = 19.1813 (15) \text{ \AA}$

$b = 12.8994 (10) \text{ \AA}$

$c = 20.0740 (16) \text{ \AA}$

$D_x = 1.198 \text{ Mg m}^{-3}$

Mo $K\alpha$ radiation, $\lambda = 0.71073 \text{ \AA}$

Cell parameters from 9878 reflections

$\theta = 2.4\text{--}25.3^\circ$

$\mu = 0.49 \text{ mm}^{-1}$

Appendix

$\beta = 109.135 (3)^\circ$
 $V = 4692.4 (6) \text{ \AA}^3$
 $Z = 4$
 $F(000) = 1808$

$T = 100 \text{ K}$
Fragment, orange
 $0.17 \times 0.14 \times 0.11 \text{ mm}$

Data collection

Bruker Photon CMOS
diffractometer 8632 independent reflections

Radiation source: TXS rotating anode 6387 reflections with $I > 2\sigma(I)$

Helios optic monochromator $R_{\text{int}} = 0.075$

Detector resolution: $16 \text{ pixels mm}^{-1}$ $\theta_{\text{max}} = 25.4^\circ$, $\theta_{\text{min}} = 1.9^\circ$

phi- and omega-rotation scans $h = -23 \ 22$

Absorption correction: multi-scan
SADABS 2016/2, Bruker, 2016 $k = -15 \ 15$

$T_{\text{min}} = 0.628$, $T_{\text{max}} = 0.745$ $l = -24 \ 24$

80637 measured reflections

Refinement

Refinement on F^2 Secondary atom site location: difference Fourier
map

Least-squares matrix: full Hydrogen site location: inferred from
neighbouring sites

$R[F^2 > 2\sigma(F^2)] = 0.050$ H-atom parameters constrained

$wR(F^2) = 0.159$ $W = 1/[\Sigma^2(F_o^2) + (0.0743P)^2 + 7.3359P]$
WHERE $P = (F_o^2 + 2F_c^2)/3$

$S = 1.10$ $(\Delta/\sigma)_{\text{max}} < 0.001$

8632 reflections $\Delta\rho_{\text{max}} = 0.49 \text{ e \AA}^{-3}$

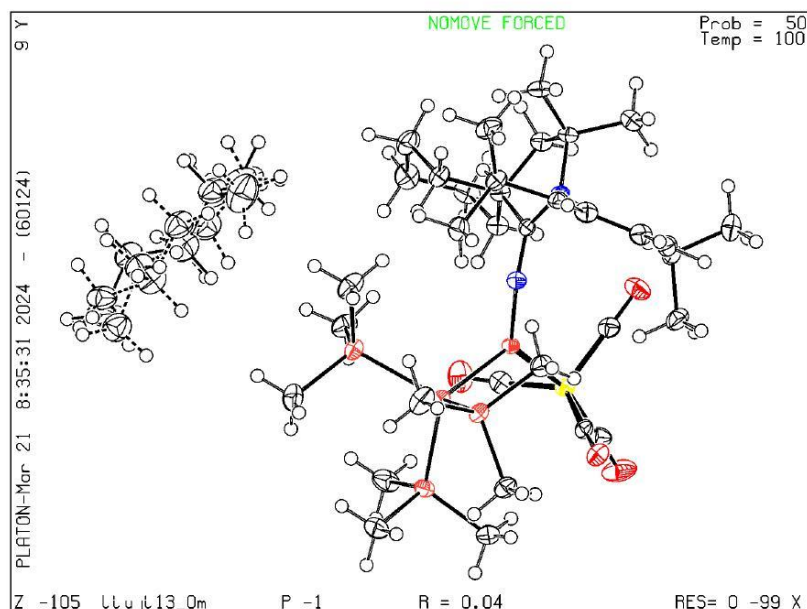
496 parameters $\Delta\rho_{\text{min}} = -0.53 \text{ e \AA}^{-3}$

0 restraints Extinction correction: none

Primary atom site location: iterative

Appendix

Compound 6 (CCDC 2324675)



A three-part disorder model was applied for the disordered solvent molecule pentane in conjunction with SIMU and SAME restraints. The variables were allowed to refine freely with the SUMP command. Subsequently, the values are added to each part. A one time adjustment of the last digit of one of the variables were carried out to achieve a full atomic number of 1.

Diffractometer operator Jinyu Liu
scanspeed 8s per frame dx 38mm
1962 frames measured in 6 data sets
phi-scans with delta phi = 0.5
omega-scans with delta omega = 0.5
shutterless mode

Crystal data

$C_{36}H_{62}FeN_2O_4Si_5 \cdot C_5H_{12}$

$M_r = 855.32$

Triclinic, P

Hall symbol: $-P\ 1$

$a = 11.7516(8) \text{ \AA}$

$F(000) = 924$

$D_x = 1.171 \text{ Mg m}^{-3}$

Mo $K\alpha$ radiation, $\lambda = 0.71073 \text{ \AA}$

Appendix

$b = 15.1478 (9) \text{ \AA}$	Cell parameters from <u>9690</u> reflections
$c = 15.1698 (9) \text{ \AA}$	$\theta = 2.7\text{--}26.4^\circ$
$\alpha = 82.963 (2)^\circ$	$\mu = 0.47 \text{ mm}^{-1}$
$\beta = 71.122 (2)^\circ$	$T = 100 \text{ K}$
$\gamma = 71.818 (2)^\circ$	<u>Fragment, orange</u>
$V = 2426.9 (3) \text{ \AA}^3$	$0.37 \times 0.25 \times 0.25 \text{ mm}$
$Z = 2$	

Data collection

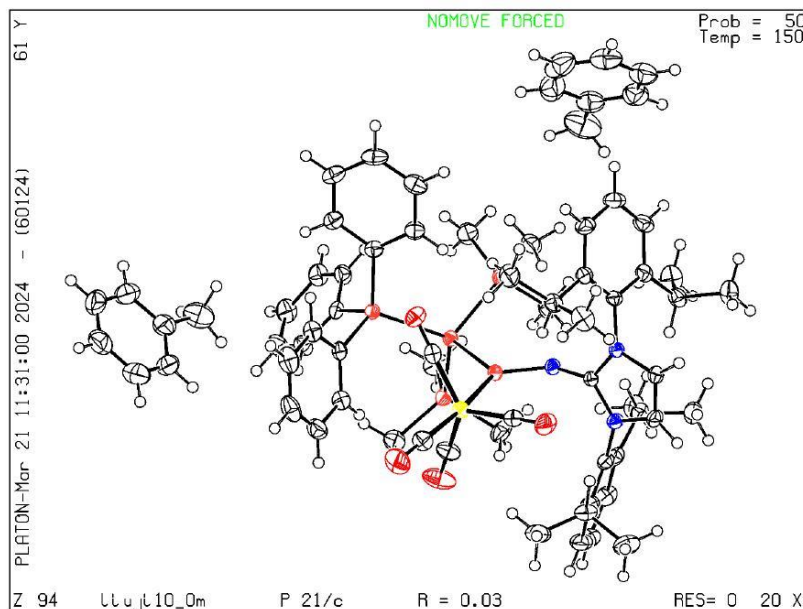
<u>Bruker Photon CMOS</u> diffractometer	<u>9839</u> independent reflections
Radiation source: <u>TXS rotating anode</u>	<u>8343</u> reflections with $I > 2\sigma(I)$
<u>Helios optic monochromator</u>	$R_{\text{int}} = 0.082$
Detector resolution: <u>16 pixels mm⁻¹</u>	$\theta_{\text{max}} = 26.4^\circ$, $\theta_{\text{min}} = 1.9^\circ$
<u>phi- and omega-rotation scans</u>	$h = -14 \text{ } 14$
Absorption correction: <u>multi-scan</u> <u>SADABS 2016/2, Bruker, 2016</u>	$k = -18 \text{ } 18$
$T_{\text{min}} = 0.632$, $T_{\text{max}} = 0.745$	$l = -18 \text{ } 18$
<u>77881</u> measured reflections	

Refinement

Refinement on F^2	Secondary atom site location: <u>difference Fourier map</u>
Least-squares matrix: <u>full</u>	Hydrogen site location: <u>inferred from neighbouring sites</u>
$R[F^2 > 2\sigma(F^2)] = 0.040$	<u>H-atom parameters constrained</u>
$wR(F^2) = 0.104$	$W = 1/[\Sigma^2(F_o^2) + (0.0349P)^2 + 2.5381P]$ <u>WHERE $P = (F_o^2 + 2F_c^2)/3$</u>
$S = 1.10$	$(\Delta/\sigma)_{\text{max}} = 0.001$
<u>9839</u> reflections	$\Delta\rho_{\text{max}} = 0.41 \text{ e \AA}^{-3}$
<u>589</u> parameters	$\Delta\rho_{\text{min}} = -0.70 \text{ e \AA}^{-3}$
<u>315</u> restraints	Extinction correction: <u>none</u>
Primary atom site location: <u>iterative</u>	

Appendix

Compound 7 (CCDC 2324674)



Diffractometer operator Jinyu Liu
 scanspeed 8s per frame dx 38mm
 2019 frames measured in 6 data sets
 phi-scans with delta_phi = 0.5
 omega-scans with delta_omega = 0.5
 shutterless mode

Crystal data

C₅₅H₆₉FeN₃O₄Si₅·2(C₇H₈)

$M_r = 1216.70$

$D_x = 1.202 \text{ Mg m}^{-3}$

Monoclinic, $P2_1/c$

Hall symbol: -P 2ybc

Mo $K\alpha$ radiation, $\lambda = 0.71073 \text{ \AA}$

$a = 12.0163 (5) \text{ \AA}$

Cell parameters from 9944 reflections

$b = 19.0809 (8) \text{ \AA}$

$\theta = 2.3\text{--}26.4^\circ$

$c = 29.6727 (12) \text{ \AA}$

$\mu = 0.36 \text{ mm}^{-1}$

$\beta = 98.664 (2)^\circ$

$T = 150 \text{ K}$

$V = 6725.8 (5) \text{ \AA}^3$

Fragment, orange

$Z = 4$

$0.49 \times 0.31 \times 0.17 \text{ mm}$

Appendix

$F(000) = 2592$

Data collection

Bruker Photon CMOS
diffractometer 13224 independent reflections

Radiation source: TXS rotating anode 11935 reflections with $I > 2\sigma(I)$

Helios optic monochromator $R_{\text{int}} = 0.063$

Detector resolution: 16 pixels mm⁻¹ $\theta_{\text{max}} = 26.0^\circ$, $\theta_{\text{min}} = 2.2^\circ$

phi- and omega-rotation scans $h = -14 \ 14$

Absorption correction: multi-scan
SADABS 2016/2, Bruker, 2016 $k = -23 \ 23$

$T_{\text{min}} = 0.691$, $T_{\text{max}} = 0.745$ $l = -36 \ 36$

215693 measured reflections

Refinement

Refinement on F^2 Secondary atom site location: difference Fourier map

Least-squares matrix: full Hydrogen site location: inferred from neighbouring sites

$R[F^2 > 2\sigma(F^2)] = 0.028$ H-atom parameters constrained

$wR(F^2) = 0.079$ $W = 1/[\Sigma^2(FO^2) + (0.0381P)^2 + 2.5358P]$
WHERE $P = (FO^2 + 2FC^2)/3$

$S = 1.06$ $(\Delta/\sigma)_{\text{max}} = 0.004$

13224 reflections $\Delta\rho_{\text{max}} = 0.31 \text{ e } \text{\AA}^{-3}$

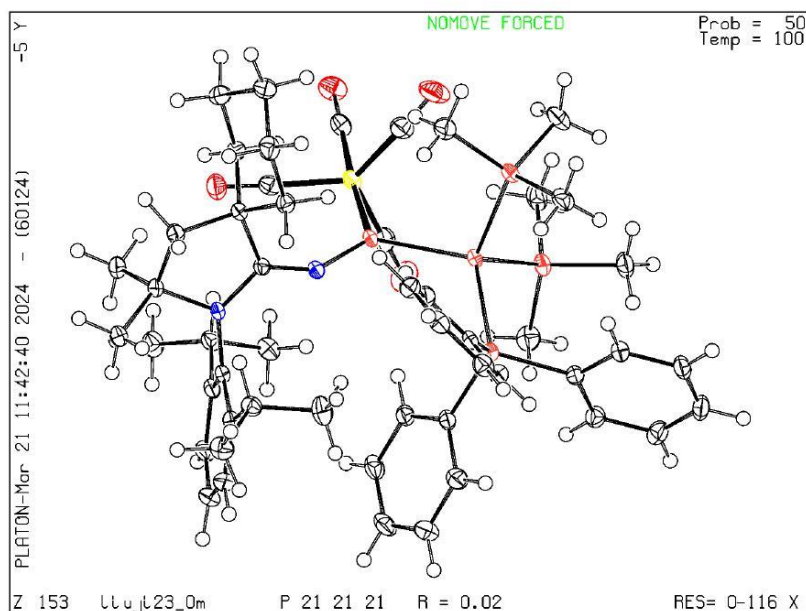
755 parameters $\Delta\rho_{\text{min}} = -0.27 \text{ e } \text{\AA}^{-3}$

0 restraints Extinction correction: none

Primary atom site location: iterative

Appendix

Compound **8** (CCDC 2324676)



The crystal structure of **8** was treated with the merohedral twin law found in Shelxle. A few reflections caused errors in the most disagreeable reflections, which mainly comes from the crystals intense scattering leading to cutted reflections. The scan time could not be greatly reduced in order to prevent this issue, thus, they were omitted.

Diffractometer operator Jinyu Liu
scanspeed 2s per frame dx 38mm
2691 frames measured in 7 data sets
phi-scans with delta_phi = 0.5
omega-scans with delta_omega = 0.5
shutterless mode

Crystal data

$C_{51}H_{68}FeN_2O_4Si_5$

$M_r = 969.37$

Orthorhombic, $P2_12_12_1$

Hall symbol: $P\ 2ac\ 2ab$

$a = 13.5273(6)\ \text{\AA}$

$D_x = 1.250\ \text{Mg m}^{-3}$

Mo $K\alpha$ radiation, $\lambda = 0.71073\ \text{\AA}$

Cell parameters from 9984 reflections

Appendix

$b = 19.2163 (9) \text{ \AA}$
 $c = 19.8185 (10) \text{ \AA}$
 $V = 5151.7 (4) \text{ \AA}^3$
 $Z = 4$
 $F(000) = 2064$

$\theta = 3.3\text{--}26.4^\circ$
 $\mu = 0.45 \text{ mm}^{-1}$
 $T = 100 \text{ K}$
Fragment, orange
 $0.24 \times 0.20 \times 0.18 \text{ mm}$

Data collection

Bruker Photon CMOS
diffractometer 10489 independent reflections

Radiation source: TXS rotating anode 10285 reflections with $I > 2\sigma(I)$

Helios optic monochromator $R_{\text{int}} = 0.045$

Detector resolution: $16 \text{ pixels mm}^{-1}$ $\theta_{\text{max}} = 26.4^\circ$, $\theta_{\text{min}} = 2.1^\circ$

ϕ - and ω -rotation scans $h = -16 \ 16$

Absorption correction: multi-scan
SADABS 2016/2, Bruker, 2016 $k = -24 \ 24$

$T_{\text{min}} = 0.673$, $T_{\text{max}} = 0.745$ $l = -24 \ 24$

169893 measured reflections

Refinement

Refinement on F^2 Hydrogen site location: inferred from neighbouring sites

Least-squares matrix: full H-atom parameters constrained

$R[F^2 > 2\sigma(F^2)] = 0.021$ $W = 1/[\Sigma^2(F_o^2) + (0.0317P)^2 + 1.1129P]$
WHERE $P = (F_o^2 + 2F_c^2)/3$

$wR(F^2) = 0.056$ $(\Delta/\sigma)_{\text{max}} = 0.002$

$S = 1.06$ $\Delta\rho_{\text{max}} = 0.33 \text{ e \AA}^{-3}$

10489 reflections $\Delta\rho_{\text{min}} = -0.32 \text{ e \AA}^{-3}$

581 parameters Extinction correction: none

Primary atom site location: iterative Absolute structure: Flack (1983)

Secondary atom site location: difference Fourier map Absolute structure parameter: 0.018 (9)

Appendix

3. References

- [S1] a) C. Kayser, R. Fischer, J. Baumgartner, C. Marschner, *Organometallics* **2002**, *21*, 1023; b) P. Schmidt, S. Fietze, C. Schrenk, A. Schnepf, *Z. Anorg. Allg. Chem.* **2017**, *643*, 1759; c) D. Wendel, A. Porzelt, F. A. D. Herz, D. Sarkar, C. Jandl, S. Inoue, B. Rieger, *J. Am. Chem. Soc.* **2017**, *139*, 8134.; d) J. Y. Liu, T. Eisner, S. Inoue, B. Rieger, *Eur. J. Inorg. Chem.* **2023**.
- [S2] *APEX suite of crystallographic software*, APEX 3, Version 2019-1.0, Bruker AXS Inc., Madison, Wisconsin, USA, 2019.
- [S3] *SAINT*, Version 8.40A and *SADABS*, Version 2016/2, Bruker AXS Inc., Madison, Wisconsin, USA, 2016/2019.
- [S4] G. M. Sheldrick, *Acta Crystallogr. Sect. A* **2015**, *71*, 3–8.
- [S5] G. M. Sheldrick, *Acta Crystallogr. Sect. C* **2015**, *71*, 3–8.
- [S6] C. B. Hübschle, G. M. Sheldrick, B. Dittrich, *J. Appl. Cryst.* **2011**, *44*, 1281–1284.
- [S7] *International Tables for Crystallography, Vol. C* (Ed.: A. J. Wilson), Kluwer Academic Publishers, Dordrecht, The Netherlands, **1992**, Tables 6.1.1.4 (pp. 500–502), 4.2.6.8 (pp. 219–222), and 4.2.4.2 (pp. 193–199).
- [S8] C. F. Macrae, I. J. Bruno, J. A. Chisholm, P. R. Edgington, P. McCabe, E. Pidcock, L. Rodriguez-Monge, R. Taylor, J. van de Streek, P. A. Wood, *J. Appl. Cryst.* **2008**, *41*, 466–470.
- [S9] A. L. Spek, *Acta Crystallogr. Sect. D* **2009**, *65*, 148–155.

6.3 Licenses

Appendix


25.07.24, 14:04

RightsLink Printable License

JOHN WILEY AND SONS LICENSE TERMS AND CONDITIONS Jul 25, 2024

This Agreement between Jin Yu Liu ("You") and John Wiley and Sons ("John Wiley and Sons") consists of your license details and the terms and conditions provided by John Wiley and Sons and Copyright Clearance Center.

License Number	5835900883036
License date	Jul 25, 2024
Licensed Content Publisher	John Wiley and Sons
Licensed Content Publication	European Journal of Inorganic Chemistry
Licensed Content Title	Isolation of a New Silepin with an Imine Ligand Based on Cyclic Alkyl Amino Carbene
Licensed Content Author	Jin Yu Liu, Teresa Eisner, Shigeyoshi Inoue, et al
Licensed Content Date	Nov 10, 2023
Licensed Content Volume	27
Licensed Content Issue	1
Licensed Content Pages	6
Type of use	Dissertation/Thesis
Requestor type	Author of this Wiley article
Format	Print and electronic
Portion	Full article
Will you be translating?	No
Title of new work	New Silepins - Structure and Reactivity
Institution name	Technical University of Munich (TUM)
Expected presentation date	Sep 2024
The Requesting Person / Organization to Appear on the License	Jin Yu Liu

Ms. Jin Yu Liu


Requestor Location


Attn: Ms. Jin Yu Liu

Publisher Tax ID	EU826007151
Total	0.00 EUR
Terms and Conditions	

TERMS AND CONDITIONS

This copyrighted material is owned by or exclusively licensed to John Wiley & Sons, Inc. or one of its group companies (each a "Wiley Company") or handled on behalf of a society with which a Wiley Company has exclusive publishing rights in relation to a particular work (collectively "WILEY"). By clicking "accept" in connection with completing this licensing transaction, you agree that the following terms and conditions apply to this transaction (along with the billing and payment terms and conditions established by the Copyright Clearance Center Inc., ("CCC's Billing and Payment terms and conditions"), at the time that you opened your RightsLink account (these are available at any time at <http://myaccount.copyright.com>).

<https://s100.copyright.com/CustomAdmin/PLF.jsp?ref=7dd52339-a577-4e9c-ab26-95c7897da224>

1/5

Terms and Conditions

- The materials you have requested permission to reproduce or reuse (the "Wiley Materials") are protected by copyright.
- You are hereby granted a personal, non-exclusive, non-sub licensable (on a stand-alone basis), non-transferable, worldwide, limited license to reproduce the Wiley Materials for the purpose specified in the licensing process. This license, **and any CONTENT (PDF or image file) purchased as part of your order**, is for a one-time use only and limited to any maximum distribution number specified in the license. The first instance of republication or reuse granted by this license must be completed within two years of the date of the grant of this license (although copies prepared before the end date may be distributed thereafter). The Wiley Materials shall not be used in any other manner or for any other purpose, beyond what is granted in the license. Permission is granted subject to an appropriate acknowledgement given to the author, title of the material/book/journal and the publisher. You shall also duplicate the copyright notice that appears in the Wiley publication in your use of the Wiley Material. Permission is also granted on the understanding that nowhere in the text is a previously published source acknowledged for all or part of this Wiley Material. Any third party content is expressly excluded from this permission.
- With respect to the Wiley Materials, all rights are reserved. Except as expressly granted by the terms of the license, no part of the Wiley Materials may be copied, modified, adapted (except for minor reformatting required by the new Publication), translated, reproduced, transferred or distributed, in any form or by any means, and no derivative works may be made based on the Wiley Materials without the prior permission of the respective copyright owner. **For STM Signatory Publishers clearing permission under the terms of the [STM Permissions Guidelines](#) only, the terms of the license are extended to include subsequent editions and for editions in other languages, provided such editions are for the work as a whole in situ and does not involve the separate exploitation of the permitted figures or extracts**, You may not alter, remove or suppress in any manner any copyright, trademark or other notices displayed by the Wiley Materials. You may not license, rent, sell, loan, lease, pledge, offer as security, transfer or assign the Wiley Materials on a stand-alone basis, or any of the rights granted to you hereunder to any other person.
- The Wiley Materials and all of the intellectual property rights therein shall at all times remain the exclusive property of John Wiley & Sons Inc, the Wiley Companies, or their respective licensors, and your interest therein is only that of having possession of and the right to reproduce the Wiley Materials pursuant to Section 2 herein during the continuance of this Agreement. You agree that you own no right, title or interest in or to the Wiley Materials or any of the intellectual property rights therein. You shall have no rights hereunder other than the license as provided for above in Section 2. No right, license or interest to any trademark, trade name, service mark or other branding ("Marks") of WILEY or its licensors is granted hereunder, and you agree that you shall not assert any such right, license or interest with respect thereto
- NEITHER WILEY NOR ITS LICENSORS MAKES ANY WARRANTY OR REPRESENTATION OF ANY KIND TO YOU OR ANY THIRD PARTY, EXPRESS, IMPLIED OR STATUTORY, WITH RESPECT TO THE MATERIALS OR THE ACCURACY OF ANY INFORMATION CONTAINED IN THE MATERIALS, INCLUDING, WITHOUT LIMITATION, ANY IMPLIED WARRANTY OF MERCHANTABILITY, ACCURACY, SATISFACTORY QUALITY, FITNESS FOR A PARTICULAR PURPOSE, USABILITY,

Appendix

25.07.24, 14:04

RightsLink Printable License

INTEGRATION OR NON-INFRINGEMENT AND ALL SUCH WARRANTIES ARE HEREBY EXCLUDED BY WILEY AND ITS LICENSORS AND WAIVED BY YOU.

- WILEY shall have the right to terminate this Agreement immediately upon breach of this Agreement by you.
- You shall indemnify, defend and hold harmless WILEY, its Licensors and their respective directors, officers, agents and employees, from and against any actual or threatened claims, demands, causes of action or proceedings arising from any breach of this Agreement by you.
- IN NO EVENT SHALL WILEY OR ITS LICENSORS BE LIABLE TO YOU OR ANY OTHER PARTY OR ANY OTHER PERSON OR ENTITY FOR ANY SPECIAL, CONSEQUENTIAL, INCIDENTAL, INDIRECT, EXEMPLARY OR PUNITIVE DAMAGES, HOWEVER CAUSED, ARISING OUT OF OR IN CONNECTION WITH THE DOWNLOADING, PROVISIONING, VIEWING OR USE OF THE MATERIALS REGARDLESS OF THE FORM OF ACTION, WHETHER FOR BREACH OF CONTRACT, BREACH OF WARRANTY, TORT, NEGLIGENCE, INFRINGEMENT OR OTHERWISE (INCLUDING, WITHOUT LIMITATION, DAMAGES BASED ON LOSS OF PROFITS, DATA, FILES, USE, BUSINESS OPPORTUNITY OR CLAIMS OF THIRD PARTIES), AND WHETHER OR NOT THE PARTY HAS BEEN ADVISED OF THE POSSIBILITY OF SUCH DAMAGES. THIS LIMITATION SHALL APPLY NOTWITHSTANDING ANY FAILURE OF ESSENTIAL PURPOSE OF ANY LIMITED REMEDY PROVIDED HEREIN.
- Should any provision of this Agreement be held by a court of competent jurisdiction to be illegal, invalid, or unenforceable, that provision shall be deemed amended to achieve as nearly as possible the same economic effect as the original provision, and the legality, validity and enforceability of the remaining provisions of this Agreement shall not be affected or impaired thereby.
- The failure of either party to enforce any term or condition of this Agreement shall not constitute a waiver of either party's right to enforce each and every term and condition of this Agreement. No breach under this agreement shall be deemed waived or excused by either party unless such waiver or consent is in writing signed by the party granting such waiver or consent. The waiver by or consent of a party to a breach of any provision of this Agreement shall not operate or be construed as a waiver of or consent to any other or subsequent breach by such other party.
- This Agreement may not be assigned (including by operation of law or otherwise) by you without WILEY's prior written consent.
- Any fee required for this permission shall be non-refundable after thirty (30) days from receipt by the CCC.
- These terms and conditions together with CCC's Billing and Payment terms and conditions (which are incorporated herein) form the entire agreement between you and WILEY concerning this licensing transaction and (in the absence of fraud) supersedes all prior agreements and representations of the parties, oral or written. This Agreement may not be amended except in writing signed by both parties. This Agreement shall be binding upon and inure to the benefit of the parties' successors, legal representatives, and authorized assigns.
- In the event of any conflict between your obligations established by these terms and conditions and those established by CCC's Billing and Payment terms and

<https://s100.copyright.com/CustomAdmin/PLF.jsp?ref=7dd52339-a577-4e9c-ab26-95c7897da224>

3/5

Appendix

25.07.24, 14:04

RightsLink Printable License

conditions, these terms and conditions shall prevail.

- WILEY expressly reserves all rights not specifically granted in the combination of (i) the license details provided by you and accepted in the course of this licensing transaction, (ii) these terms and conditions and (iii) CCC's Billing and Payment terms and conditions.
- This Agreement will be void if the Type of Use, Format, Circulation, or Requestor Type was misrepresented during the licensing process.
- This Agreement shall be governed by and construed in accordance with the laws of the State of New York, USA, without regards to such state's conflict of law rules. Any legal action, suit or proceeding arising out of or relating to these Terms and Conditions or the breach thereof shall be instituted in a court of competent jurisdiction in New York County in the State of New York in the United States of America and each party hereby consents and submits to the personal jurisdiction of such court, waives any objection to venue in such court and consents to service of process by registered or certified mail, return receipt requested, at the last known address of such party.

WILEY OPEN ACCESS TERMS AND CONDITIONS

Wiley Publishes Open Access Articles in fully Open Access Journals and in Subscription journals offering Online Open. Although most of the fully Open Access journals publish open access articles under the terms of the Creative Commons Attribution (CC BY) License only, the subscription journals and a few of the Open Access Journals offer a choice of Creative Commons Licenses. The license type is clearly identified on the article.

The Creative Commons Attribution License

The [Creative Commons Attribution License \(CC-BY\)](#) allows users to copy, distribute and transmit an article, adapt the article and make commercial use of the article. The CC-BY license permits commercial and non-

Creative Commons Attribution Non-Commercial License

The [Creative Commons Attribution Non-Commercial \(CC-BY-NC\) License](#) permits use, distribution and reproduction in any medium, provided the original work is properly cited and is not used for commercial purposes.(see below)

Creative Commons Attribution-Non-Commercial-NoDerivs License

The [Creative Commons Attribution Non-Commercial-NoDerivs License \(CC-BY-NC-ND\)](#) permits use, distribution and reproduction in any medium, provided the original work is properly cited, is not used for commercial purposes and no modifications or adaptations are made. (see below)

Use by commercial "for-profit" organizations

Use of Wiley Open Access articles for commercial, promotional, or marketing purposes requires further explicit permission from Wiley and will be subject to a fee.

Further details can be found on Wiley Online Library <http://olabout.wiley.com/WileyCDA/Section/id-410895.html>

<https://s100.copyright.com/CustomAdmin/PLF.jsp?ref=7dd52339-a577-4e9c-ab26-95c7897da224>

4/5

Appendix

25.07.24, 14:04

RightsLink Printable License

Other Terms and Conditions:

v1.10 Last updated September 2015

Questions? customercare@copyright.com.

Appendix

25.07.24, 14:03

RightsLink Printable License

JOHN WILEY AND SONS LICENSE TERMS AND CONDITIONS Jul 25, 2024

This Agreement between Jin Yu Liu ("You") and John Wiley and Sons ("John Wiley and Sons") consists of your license details and the terms and conditions provided by John Wiley and Sons and Copyright Clearance Center.

License Number	5835900818877
License date	Jul 25, 2024
Licensed Content Publisher	John Wiley and Sons
Licensed Content Publication	European Journal of Inorganic Chemistry
Licensed Content Title	Isolation and Reactivity of Silepins with a Sterically Demanding Silyl Ligand
Licensed Content Author	Bernhard Rieger, Shigeyoshi Inoue, Jin Yu Liu
Licensed Content Date	Jun 28, 2024
Licensed Content Volume	27
Licensed Content Issue	21
Licensed Content Pages	7
Type of use	Dissertation/Thesis
Requestor type	Author of this Wiley article
Format	Print and electronic
Portion	Full article
Will you be translating?	No
Title of new work	New Silepins - Structure and Reactivity
Institution name	Technical University of Munich (TUM)
Expected presentation date	Sep 2024
The Requesting Person / Organization to Appear on the License	Jin Yu Liu Ms. Jin Yu Liu [REDACTED]
Requestor Location	[REDACTED] Attn: Ms. Jin Yu Liu
Publisher Tax ID	EU826007151
Total	0.00 EUR
Terms and Conditions	

TERMS AND CONDITIONS

This copyrighted material is owned by or exclusively licensed to John Wiley & Sons, Inc. or one of its group companies (each a "Wiley Company") or handled on behalf of a society with which a Wiley Company has exclusive publishing rights in relation to a particular work (collectively "WILEY"). By clicking "accept" in connection with completing this licensing transaction, you agree that the following terms and conditions apply to this transaction (along with the billing and payment terms and conditions established by the Copyright Clearance Center Inc., ("CCC's Billing and Payment terms and conditions"), at the time that you opened your RightsLink account (these are available at any time at <http://myaccount.copyright.com>).

<https://s100.copyright.com/CustomAdmin/PLF.jsp?ref=e59948ae-ba5d-47e1-81cb-636ba9fda19d>

1/5

Terms and Conditions

- The materials you have requested permission to reproduce or reuse (the "Wiley Materials") are protected by copyright.
- You are hereby granted a personal, non-exclusive, non-sub licensable (on a stand-alone basis), non-transferable, worldwide, limited license to reproduce the Wiley Materials for the purpose specified in the licensing process. This license, **and any CONTENT (PDF or image file) purchased as part of your order**, is for a one-time use only and limited to any maximum distribution number specified in the license. The first instance of republication or reuse granted by this license must be completed within two years of the date of the grant of this license (although copies prepared before the end date may be distributed thereafter). The Wiley Materials shall not be used in any other manner or for any other purpose, beyond what is granted in the license. Permission is granted subject to an appropriate acknowledgement given to the author, title of the material/book/journal and the publisher. You shall also duplicate the copyright notice that appears in the Wiley publication in your use of the Wiley Material. Permission is also granted on the understanding that nowhere in the text is a previously published source acknowledged for all or part of this Wiley Material. Any third party content is expressly excluded from this permission.
- With respect to the Wiley Materials, all rights are reserved. Except as expressly granted by the terms of the license, no part of the Wiley Materials may be copied, modified, adapted (except for minor reformatting required by the new Publication), translated, reproduced, transferred or distributed, in any form or by any means, and no derivative works may be made based on the Wiley Materials without the prior permission of the respective copyright owner. **For STM Signatory Publishers clearing permission under the terms of the [STM Permissions Guidelines](#) only, the terms of the license are extended to include subsequent editions and for editions in other languages, provided such editions are for the work as a whole in situ and does not involve the separate exploitation of the permitted figures or extracts**, You may not alter, remove or suppress in any manner any copyright, trademark or other notices displayed by the Wiley Materials. You may not license, rent, sell, loan, lease, pledge, offer as security, transfer or assign the Wiley Materials on a stand-alone basis, or any of the rights granted to you hereunder to any other person.
- The Wiley Materials and all of the intellectual property rights therein shall at all times remain the exclusive property of John Wiley & Sons Inc, the Wiley Companies, or their respective licensors, and your interest therein is only that of having possession of and the right to reproduce the Wiley Materials pursuant to Section 2 herein during the continuance of this Agreement. You agree that you own no right, title or interest in or to the Wiley Materials or any of the intellectual property rights therein. You shall have no rights hereunder other than the license as provided for above in Section 2. No right, license or interest to any trademark, trade name, service mark or other branding ("Marks") of WILEY or its licensors is granted hereunder, and you agree that you shall not assert any such right, license or interest with respect thereto
- NEITHER WILEY NOR ITS LICENSORS MAKES ANY WARRANTY OR REPRESENTATION OF ANY KIND TO YOU OR ANY THIRD PARTY, EXPRESS, IMPLIED OR STATUTORY, WITH RESPECT TO THE MATERIALS OR THE ACCURACY OF ANY INFORMATION CONTAINED IN THE MATERIALS, INCLUDING, WITHOUT LIMITATION, ANY IMPLIED WARRANTY OF MERCHANTABILITY, ACCURACY, SATISFACTORY QUALITY, FITNESS FOR A PARTICULAR PURPOSE, USABILITY,

Appendix

25.07.24, 14:03

RightsLink Printable License

INTEGRATION OR NON-INFRINGEMENT AND ALL SUCH WARRANTIES ARE HEREBY EXCLUDED BY WILEY AND ITS LICENSORS AND WAIVED BY YOU.

- WILEY shall have the right to terminate this Agreement immediately upon breach of this Agreement by you.
- You shall indemnify, defend and hold harmless WILEY, its Licensors and their respective directors, officers, agents and employees, from and against any actual or threatened claims, demands, causes of action or proceedings arising from any breach of this Agreement by you.
- IN NO EVENT SHALL WILEY OR ITS LICENSORS BE LIABLE TO YOU OR ANY OTHER PARTY OR ANY OTHER PERSON OR ENTITY FOR ANY SPECIAL, CONSEQUENTIAL, INCIDENTAL, INDIRECT, EXEMPLARY OR PUNITIVE DAMAGES, HOWEVER CAUSED, ARISING OUT OF OR IN CONNECTION WITH THE DOWNLOADING, PROVISIONING, VIEWING OR USE OF THE MATERIALS REGARDLESS OF THE FORM OF ACTION, WHETHER FOR BREACH OF CONTRACT, BREACH OF WARRANTY, TORT, NEGLIGENCE, INFRINGEMENT OR OTHERWISE (INCLUDING, WITHOUT LIMITATION, DAMAGES BASED ON LOSS OF PROFITS, DATA, FILES, USE, BUSINESS OPPORTUNITY OR CLAIMS OF THIRD PARTIES), AND WHETHER OR NOT THE PARTY HAS BEEN ADVISED OF THE POSSIBILITY OF SUCH DAMAGES. THIS LIMITATION SHALL APPLY NOTWITHSTANDING ANY FAILURE OF ESSENTIAL PURPOSE OF ANY LIMITED REMEDY PROVIDED HEREIN.
- Should any provision of this Agreement be held by a court of competent jurisdiction to be illegal, invalid, or unenforceable, that provision shall be deemed amended to achieve as nearly as possible the same economic effect as the original provision, and the legality, validity and enforceability of the remaining provisions of this Agreement shall not be affected or impaired thereby.
- The failure of either party to enforce any term or condition of this Agreement shall not constitute a waiver of either party's right to enforce each and every term and condition of this Agreement. No breach under this agreement shall be deemed waived or excused by either party unless such waiver or consent is in writing signed by the party granting such waiver or consent. The waiver by or consent of a party to a breach of any provision of this Agreement shall not operate or be construed as a waiver of or consent to any other or subsequent breach by such other party.
- This Agreement may not be assigned (including by operation of law or otherwise) by you without WILEY's prior written consent.
- Any fee required for this permission shall be non-refundable after thirty (30) days from receipt by the CCC.
- These terms and conditions together with CCC's Billing and Payment terms and conditions (which are incorporated herein) form the entire agreement between you and WILEY concerning this licensing transaction and (in the absence of fraud) supersedes all prior agreements and representations of the parties, oral or written. This Agreement may not be amended except in writing signed by both parties. This Agreement shall be binding upon and inure to the benefit of the parties' successors, legal representatives, and authorized assigns.
- In the event of any conflict between your obligations established by these terms and conditions and those established by CCC's Billing and Payment terms and

<https://s100.copyright.com/CustomAdmin/PLF.jsp?ref=e59948ae-ba5d-47e1-81cb-636ba9fda19d>

3/5

Appendix

25.07.24, 14:03

RightsLink Printable License

conditions, these terms and conditions shall prevail.

- WILEY expressly reserves all rights not specifically granted in the combination of (i) the license details provided by you and accepted in the course of this licensing transaction, (ii) these terms and conditions and (iii) CCC's Billing and Payment terms and conditions.
- This Agreement will be void if the Type of Use, Format, Circulation, or Requestor Type was misrepresented during the licensing process.
- This Agreement shall be governed by and construed in accordance with the laws of the State of New York, USA, without regards to such state's conflict of law rules. Any legal action, suit or proceeding arising out of or relating to these Terms and Conditions or the breach thereof shall be instituted in a court of competent jurisdiction in New York County in the State of New York in the United States of America and each party hereby consents and submits to the personal jurisdiction of such court, waives any objection to venue in such court and consents to service of process by registered or certified mail, return receipt requested, at the last known address of such party.

WILEY OPEN ACCESS TERMS AND CONDITIONS

Wiley Publishes Open Access Articles in fully Open Access Journals and in Subscription journals offering Online Open. Although most of the fully Open Access journals publish open access articles under the terms of the Creative Commons Attribution (CC BY) License only, the subscription journals and a few of the Open Access Journals offer a choice of Creative Commons Licenses. The license type is clearly identified on the article.

The Creative Commons Attribution License

The [Creative Commons Attribution License \(CC-BY\)](#) allows users to copy, distribute and transmit an article, adapt the article and make commercial use of the article. The CC-BY license permits commercial and non-

Creative Commons Attribution Non-Commercial License

The [Creative Commons Attribution Non-Commercial \(CC-BY-NC\) License](#) permits use, distribution and reproduction in any medium, provided the original work is properly cited and is not used for commercial purposes.(see below)

Creative Commons Attribution-Non-Commercial-NoDerivs License

The [Creative Commons Attribution Non-Commercial-NoDerivs License \(CC-BY-NC-ND\)](#) permits use, distribution and reproduction in any medium, provided the original work is properly cited, is not used for commercial purposes and no modifications or adaptations are made. (see below)

Use by commercial "for-profit" organizations

Use of Wiley Open Access articles for commercial, promotional, or marketing purposes requires further explicit permission from Wiley and will be subject to a fee.

Further details can be found on Wiley Online Library <http://olabout.wiley.com/WileyCDA/Section/id-410895.html>

<https://s100.copyright.com/CustomAdmin/PLF.jsp?ref=e59948ae-ba5d-47e1-81cb-636ba9fda19d>

4/5

Appendix

25.07.24, 14:03

RightsLink Printable License

Other Terms and Conditions:

v1.10 Last updated September 2015

Questions? customercare@copyright.com.

7. References

- [1] M. L. Crawley, B. M. Trost (Eds.) *Applications of Transition Metal Catalysis in Drug Discovery and Development*, Wiley, **2012**.
- [2] P. Anastas, N. Eghbali, *ChemCatChem* **2010**, *39*, 301.
- [3] C. A. Busacca, D. R. Fandrick, J. J. Song, C. H. Senanayake in *Applications of Transition Metal Catalysis in Drug Discovery and Development* (Eds.: M. L. Crawley, B. M. Trost), Wiley, **2012**, pp. 1–24.
- [4] F. K. Crundwell, M. S. Moats, V. Ramachandran, T. G. Robinson, W. G. Davenport in *Extractive Metallurgy of Nickel, Cobalt and Platinum Group Metals*, Elsevier, **2011**, pp. 395–409.
- [5] a) C. Trueman in *Encyclopedia of Analytical Science*, Elsevier, **2005**, pp. 171–181; b) F. R. Hartley, *Chemistry of the Platinum Group Metals. Recent Developments*, Elsevier Science, Amsterdam, **2014**.
- [6] P. P. Power, *Chem. Rev.* **1999**, *99*, 3463.
- [7] Y. Mizuhata, T. Sasamori, N. Tokitoh, *Chem. Rev.* **2009**, *109*, 3479.
- [8] G. Linti, H. Schnöckel, *Coord. Chem. Rev.* **2000**, *206-207*, 285.
- [9] a) R. G. Hicks, *OBC* **2007**, *5*, 1321; b) V. Y. Lee, M. Nakamoto, A. Sekiguchi, *Chem. Lett.* **2008**, *37*, 128; c) P. P. Power, *Chem. Rev.* **2003**, *103*, 789.
- [10] P. P. Power, *Nature* **2010**, *463*, 171.
- [11] a) "Covalent Radius of the Elements", can be found under <https://periodictable.com/Properties/A/CovalentRadius.v.log.html>; b) W. Kutzelnigg, *Angew. Chem. Int. Ed.* **1984**, *23*, 272.
- [12] a) D. E. Goldberg, D. H. Harris, M. F. Lappert, K. M. Thomas, *Chem. Commun.* **1976**, 261; b) D. E. Goldberg, P. B. Hitchcock, M. F. Lappert, K. M. Thomas, A. J. Thorne, T. Fjeldberg, A. Haaland, B. E. R. Schilling, *Dalton Trans.* **1986**, 2387.
- [13] R. West, M. J. Fink, J. Michl, *Science* **1981**, *214*, 1343.
- [14] N. Wiberg, H. Schuster, A. Simon, K. Peters, *Angew. Chem. Int. Ed.* **1986**, *25*, 79.
- [15] M. Stürmann, M. Weidenbruch, K. W. Klinkhammer, F. Lissner, H. Marsmann, *Organometallics* **1998**, *17*, 4425.
- [16] R. S. Grev in *Advances in Organometallic Chemistry*, Elsevier, **1991**, pp. 125–170.
- [17] a) R. F. W. Bader, *Can. J. Chem.* **1962**, *40*, 1164; b) R. G. Pearson, *J. Am. Chem. Soc.* **1969**, *91*, 4947.
- [18] A.-V. Mudring in *Inorganic Chemistry in Focus III* (Eds.: G. Meyer, D. Naumann, L. Wesemann), Wiley, **2006**, pp. 15–28.
- [19] F. Hanusch, L. Groll, S. Inoue, *Chem. Sci* **2020**, *12*, 2001.
- [20] P. B. Hitchcock, M. F. Lappert, S. J. Miles, A. J. Thorne, *Chem. Commun.* **1984**, 480.
- [21] V. Y. Lee, *CheM* **2012**, *2*, 35.
- [22] V. Y. Lee, T. Fukawa, M. Nakamoto, A. Sekiguchi, B. L. Tumanskii, M. Karni, Y. Apeloig, *J. Am. Chem. Soc.* **2006**, *128*, 11643.

References

- [23] V. Y. Lee, K. McNeice, Y. Ito, A. Sekiguchi, *Chem. Commun.* **2011**, 47, 3272.
- [24] V. Y. Lee, K. McNiece, Y. Ito, A. Sekiguchi, N. Geinik, J. Y. Becker, *Heteroatom Chemistry* **2014**, 25, 313.
- [25] R. Bashkurov, N. Fridman, D. Bravo-Zhivotovskii, Y. Apeloig, *Chem. Eur. J.* **2023**, 29, e202302678.
- [26] G. H. Spikes, J. C. Fettinger, P. P. Power, *J. Am. Chem. Soc.* **2005**, 127, 12232.
- [27] S. Wang, T. J. Sherbow, L. A. Berben, P. P. Power, *J. Am. Chem. Soc.* **2018**, 140, 590.
- [28] T. Sugahara, J.-D. Guo, T. Sasamori, Y. Karatsu, Y. Furukawa, A. E. Ferao, S. Nagase, N. Tokitoh, *Bull. Chem. Soc. Jpn.* **2016**, 89, 1375.
- [29] T. Sugahara, J.-D. Guo, T. Sasamori, S. Nagase, N. Tokitoh, *Angew. Chem. Int. Ed.* **2018**, 57, 3499.
- [30] a) M. Weidenbruch, *Organometallics* **2003**, 22, 4348; b) M. Weidenbruch, *J. Organomet. Chem.* **2002**, 646, 39.
- [31] M. Driess, H. Grützmacher, *Angew. Chem. Int. Ed.* **1996**, 35, 828.
- [32] a) T. J. Hadlington, M. Driess, C. Jones, *Chem. Soc. Rev.* **2018**, 47, 4176; b) A. V. Protchenko, J. I. Bates, L. M. A. Saleh, M. P. Blake, A. D. Schwarz, E. L. Kolychev, A. L. Thompson, C. Jones, P. Mountford, S. Aldridge, *J. Am. Chem. Soc.* **2016**, 138, 4555.
- [33] J. W. Dube, C. M. E. Graham, C. L. B. Macdonald, Z. D. Brown, P. P. Power, P. J. Ragona, *Chem. Eur. J.* **2014**, 20, 6739.
- [34] D. Sarkar, C. Weetman, D. Munz, S. Inoue, *Angew. Chem. Int. Ed.* **2021**, 60, 3519.
- [35] T. J. Hadlington, M. Hermann, G. Frenking, C. Jones, *J. Am. Chem. Soc.* **2014**, 136, 3028.
- [36] T. J. Hadlington, C. E. Kefalidis, L. Maron, C. Jones, *ACS Catal.* **2017**, 7, 1853.
- [37] T. J. Hadlington, M. Hermann, G. Frenking, C. Jones, *Chem. Sci.* **2015**, 6, 7249.
- [38] a) O. Köhl, P. Lönnecke, J. Heinicke, *Polyhedron* **2001**, 20, 2215; b) H. Braunschweig, B. Gehrhus, P. B. Hitchcock, M. F. Lappert, *Z. Anorg. Allg. Chem.* **1995**, 621, 1922.
- [39] R. Dasgupta, S. Das, S. Hiwase, S. K. Pati, S. Khan, *Organometallics* **2019**, 38, 1429.
- [40] F. S. Tschernuth, A. Kostenko, S. Stigler, A. Gradenegger, S. Inoue, *Dalton Trans.* **2023**, 53, 74.
- [41] D. Sarkar, L. Groll, D. Munz, F. Hanusch, S. Inoue, *ChemCatChem* **2022**, 14.
- [42] G. B. Gerber, A. Léonard, *Mutation research* **1997**, 387, 141.
- [43] S. G. Schäfer, U. Femfert, *Regulatory toxicology and pharmacology : RTP* **1984**, 4, 57.
- [44] a) S. Pizzini, *Solar Energy Materials and Solar Cells* **2010**, 94, 1528; b) S. Pizzini, C. Calligarich, *J. Electrochem. Soc.* **1984**, 131, 2128.
- [45] C. Ramírez-Márquez, M. Martín in *Sustainable Design for Renewable Processes*, Elsevier, **2022**, pp. 397–439.
- [46] A. Goodrich, P. Hacke, Q. Wang, B. Sopori, R. Margolis, T. L. James, M. Woodhouse, *Solar Energy Materials and Solar Cells* **2013**, 114, 110.
- [47] a) A. D. Gordon, B. J. Hinch, D. R. Strongin, *Catal. Lett.* **2009**, 133, 14; b) T. J. Wessel, D. G. Rethwisch, *J. Catal.* **1996**, 161, 861.
- [48] Y. Zhang, J. Li, H. Liu, Y. Ji, Z. Zhong, F. Su, *ChemCatChem* **2019**, 11, 2757.
- [49] E. Yilgör, I. Yilgör, *Prog. Polym. Sci.* **2014**, 39, 1165.

References

- [50] RSC Periodic Table, "Silicon", can be found under <https://www.rsc.org/periodic-table/element/14/silicon>, **2024**.
- [51] A. G. Brook, F. Abdesaken, B. Gutekunst, G. Gutekunst, R. K. Kallury, *Chem. Commun.* **1981**, 191.
- [52] M. Kira, *Proceedings of the Japan Academy. Series B, Physical and biological sciences* **2012**, *88*, 167.
- [53] A. Baceiredo, T. Kato in *Organosilicon Compounds*, Elsevier, **2017**, pp. 533–618.
- [54] D. Wendel, T. Szilvási, C. Jandl, S. Inoue, B. Rieger, *J. Am. Chem. Soc.* **2017**, *139*, 9156.
- [55] a) S. Boomgaarden, W. Saak, M. Weidenbruch, H. Marsmann, *Z. Anorg. Allg. Chem.* **2001**, *627*, 349; b) S. L. McOnie, G. A. Özpınar, J. L. Bourque, T. Müller, K. M. Baines, *Dalton Trans.* **2021**, *50*, 17734; c) A. Meltzer, M. Majumdar, A. J. P. White, V. Huch, D. Scheschkewitz, *Organometallics* **2013**, *32*, 6844; d) Z. M. Sharif, G. A. Özpınar, S. L. McOnie, P. D. Boyle, T. Müller, K. M. Baines, *Chem. Eur. J.* **2023**, *29*, e202301003.
- [56] D. Wendel, T. Szilvási, D. Henschel, P. J. Altmann, C. Jandl, S. Inoue, B. Rieger, *Angew. Chem. Int. Ed.* **2018**, *57*, 14575.
- [57] R. Holzner, A. Porzelt, U. S. Karaca, F. Kiefer, P. Frisch, D. Wendel, M. C. Holthausen, S. Inoue, *Dalton Trans.* **2021**, *50*, 8785.
- [58] a) C. Marschner, *Eur. J. Inorg. Chem.* **2015**, *2015*, 3805; b) M. W. Stanford, J. I. Schweizer, M. Menche, G. S. Nichol, M. C. Holthausen, M. J. Cowley, *Angew. Chem. Int. Ed.* **2019**, *58*, 1329.
- [59] T. Kosai, T. Iwamoto, *J. Am. Chem. Soc.* **2017**, *139*, 18146.
- [60] a) S. Khan, R. Michel, D. Koley, H. W. Roesky, D. Stalke, *Inorg. Chem.* **2011**, *50*, 10878; b) M. Majumdar, I. Omlor, C. B. Yildiz, A. Azizoglu, V. Huch, D. Scheschkewitz, *Angew. Chem. Int. Ed.* **2015**, *54*, 8746; c) N. Wiberg, W. Niedermayer, K. Polborn, P. Mayer, *Chem. Eur. J.* **2002**, *8*, 2730.
- [61] J. S. Han, T. Sasamori, Y. Mizuhata, N. Tokitoh, *J. Am. Chem. Soc.* **2010**, *132*, 2546.
- [62] a) T. Sugahara, J.-D. Guo, D. Hashizume, T. Sasamori, S. Nagase, N. Tokitoh, *Dalton Trans.* **2018**, *47*, 13318; b) T. Sugahara, T. Sasamori, N. Tokitoh, *Dalton Trans.* **2019**, *48*, 9053.
- [63] R. Kinjo, M. Ichinohe, A. Sekiguchi, N. Takagi, M. Sumimoto, S. Nagase, *J. Am. Chem. Soc.* **2007**, *129*, 7766.
- [64] Y. Ding, Y. Li, J. Zhang, C. Cui, *Angew. Chem. Int. Ed.* **2022**, *61*, e202205785.
- [65] Y. Ding, J. Zhang, Y. Li, C. Cui, *J. Am. Chem. Soc.* **2022**, *144*, 20566.
- [66] P. Jutzi, D. Kanne, C. Krüger, *Angew. Chem. Int. Ed.* **1986**, *25*, 164.
- [67] a) M. Denk, R. Lennon, R. Hayashi, R. West, A. V. Belyakov, H. P. Verne, A. Haaland, M. Wagner, N. Metzler, *J. Am. Chem. Soc.* **1994**, *116*, 2691; b) D. Gau, T. Kato, N. Saffon-Merceron, F. P. Cossío, A. Baceiredo, *J. Am. Chem. Soc.* **2009**, *131*, 8762; c) M. Kira, S. Ishida, T. Iwamoto, C. Kabuto, *J. Am. Chem. Soc.* **1999**, *121*, 9722; d) C.-W. So, H. W. Roesky, J. Magull, R. B. Oswald, *Angew. Chem. Int. Ed.* **2006**, *45*, 3948.
- [68] A. V. Protchenko, K. H. Birj Kumar, D. Dange, A. D. Schwarz, D. Vidovic, C. Jones, N. Kaltsoyannis, P. Mountford, S. Aldridge, *J. Am. Chem. Soc.* **2012**, *134*, 6500.

References

- [69] B. D. Rekker, T. M. Brown, J. C. Fettinger, H. M. Tuononen, P. P. Power, *J. Am. Chem. Soc.* **2012**, *134*, 6504.
- [70] B. D. Rekker, T. M. Brown, J. C. Fettinger, F. Lips, H. M. Tuononen, R. H. Herber, P. P. Power, *J. Am. Chem. Soc.* **2013**, *135*, 10134.
- [71] A. V. Protchenko, A. D. Schwarz, M. P. Blake, C. Jones, N. Kaltsoyannis, P. Mountford, S. Aldridge, *Angew. Chem. Int. Ed.* **2013**, *52*, 568.
- [72] S. Inoue, K. Leszczyńska, *Angew. Chem. Int. Ed.* **2012**, *51*, 8589.
- [73] A. Saurwein, M. Nobis, S. Inoue, B. Rieger, *Inorg. Chem.* **2022**, *61*, 9983.
- [74] M. M. D. Roy, M. J. Ferguson, R. McDonald, Y. Zhou, E. Rivard, *Chem. Sci.* **2019**, *10*, 6476.
- [75] D. Reiter, R. Holzner, A. Porzelt, P. J. Altmann, P. Frisch, S. Inoue, *J. Am. Chem. Soc.* **2019**, *141*, 13536.
- [76] N. Tokitoh, H. Suzuki, R. Okazaki, K. Ogawa, *J. Am. Chem. Soc.* **1993**, *115*, 10428.
- [77] F. Lips, J. C. Fettinger, A. Mansikkamäki, H. M. Tuononen, P. P. Power, *J. Am. Chem. Soc.* **2014**, *136*, 634.
- [78] D. Wendel, W. Eisenreich, C. Jandl, A. Pöthig, B. Rieger, *Organometallics* **2016**, *35*, 1.
- [79] a) H. Werner, *Angew. Chem. Int. Ed.* **1990**, *29*, 1077; b) W. A. Herrmann, *J. Organomet. Chem.* **1990**, *383*, 21.
- [80] a) X.-F. Wu, X. Fang, L. Wu, R. Jackstell, H. Neumann, M. Beller, *Acc. Chem. Res.* **2014**, *47*, 1041; b) C. W. Bird, *Chem. Rev.* **1962**, *62*, 283.
- [81] D. Reiter, R. Holzner, A. Porzelt, P. Frisch, S. Inoue, *Nat. Chem* **2020**, *12*, 1131.
- [82] V. P. Boyarskiy, N. A. Bokach, K. V. Luzyanin, V. Y. Kukushkin, *Chem. Rev.* **2015**, *115*, 2698.
- [83] C. Ganesamoorthy, J. Schoening, C. Wölper, L. Song, P. R. Schreiner, S. Schulz, *Nat. Chem* **2020**, *12*, 608.
- [84] a) T. Kosai, S. Ishida, T. Iwamoto, *Angew. Chem. Int. Ed.* **2016**, *55*, 15554; b) T. Kosai, S. Ishida, T. Iwamoto, *Chem. Commun.* **2015**, *51*, 10707; c) H. Gilman, S. G. Cottis, W. H. Atwell, *J. Am. Chem. Soc.* **1964**, *86*, 5584.
- [85] D. Wendel, A. Porzelt, F. A. D. Herz, D. Sarkar, C. Jandl, S. Inoue, B. Rieger, *J. Am. Chem. Soc.* **2017**, *139*, 8134.
- [86] L. Zhu, J. Zhang, C. Cui, *Inorg. Chem.* **2019**, *58*, 12007.
- [87] D. Wendel, D. Reiter, A. Porzelt, P. J. Altmann, S. Inoue, B. Rieger, *J. Am. Chem. Soc.* **2017**, *139*, 17193.
- [88] T. Eisner, A. Kostenko, F. Hanusch, S. Inoue, *Chem. Eur. J.* **2022**, *28*, e202202330.